INTERACTING EFFECTS OF SUNLIGHT, DISSOLVED ORGANIC MATTER AND REACTIVE OXYGEN SPECIES ON *ESCHERICHIA COLI* AND *ENTEROCOCCUS FAECALIS* SURVIVAL

by

ADELUMOLA ADEOYE OLADEINDE

(Under the Direction of Erin K. Lipp)

ABSTRACT

The studies presented in this dissertation show the interacting effects of agriculturally derived DOM, sunlight, and reactive oxygen species (ROS) on *Escherichia coli* (C3000) and *Enterococcus faecalis* (ATCC 29212) survival. Cattle feces was collected from a commercial farm in northeast Georgia and made into a filter-sterilized extract referred to as “cattle fecal extract (CFE)”. CFE was diluted to represent DOM concentrations in water resulting from low to high fecal input, and exposed to artificial sunlight for 12 h. Irradiated spiked water (I-DOMW), non-irradiated spiked water (N-DOMW) and phosphate buffered water microcosms were inoculated with mid-logarithmic phase aliquots of individual bacterial strain cultures (~10^3 - 10^6 colony forming unit (CFU) mL^{-1}), in monoculture or as co-culture. Microcosms were monitored periodically in the dark for bacterial concentration, nutrient loss/uptake, ROS, transcriptomic changes and metabolite production.

Singlet oxygen, hydrogen peroxide (HOOH) and superoxide radicals were detected during 12 h of irradiation. In the presence of *E. coli* only, extracellular HOOH dropped from ~15μM to <MDL (500nM) after 6 h of dark incubation. However, in the presence of *Ent. faecalis,* extracellular HOOH increased significantly, with a 140% increase after 6 h of dark incubation. DOM irradiation resulted in a 1-log reduction in *Ent. faecalis* concentrations.

When *E. coli* and *Ent. faecalis* were incubated as co-culture in I-DOMW and N-DOMW, the growth rate of *Ent. faecalis* significantly increased. Further, extracellular HOOH in I-DOMW decreased gradually for 24 h while the expression of catalase and peroxidase genes increased for up to 12 h for *E. coli*. However, in N-DOMW, *Ent. faecalis* showed a ~3-log die-off within 3 h of incubation. In addition, there was an increase in production of HOOH and a significant increase in expression of the peroxidase and thioredoxin transcripts for *Ent. faecalis* (>3-FC).

Most importantly, we observed a form of “exploitative competition” between these strains in DOMW microcosms, where chorismate and arginine/ornithine served as shared public goods for the biosynthesis of enterobactin and polyamines. For this cooperative competition to be efficient, both bacteria increased the expression of genetic networks associated with oxidative stress, bacteriophage activation, non-ribosomal peptide production, plasmid loss and virulence, toxin-antitoxin systems, quorum sensing, biofilm formation and antimicrobial resistance. We provide for the first time evidence of such cooperation between two distantly related species of bacteria.

KEY WORDS: Sunlight, Dissolved organic matter, Reactive oxygen species, Hydrogen peroxide, *Escherichia coli*, *Enterococcus faecalis*

INTERACTING EFFECTS OF SUNLIGHT, DISSOLVED ORGANIC MATTER AND REACTIVE OXYGEN SPECIES ON *ESCHERICHIA COLI* AND *ENTEROCOCCUS FAECALIS* SURVIVAL

By

ADELUMOLA ADEOYE OLADEINDE

B.S., University of Lagos, Nigeria, 2008

MPH., University of Georgia, 2010

A Dissertation Submitted to the Graduate Faculty of The University of Georgia in Partial Fulfillment of the Requirements for the Degree

DOCTOR OF PHILOSOPHY

ATHENS, GEORGIA

2017

INTERACTING EFFECTS OF SUNLIGHT, DISSOLVED ORGANIC MATTER AND REACTIVE OXYGEN SPECIES ON *ESCHERICHIA COLI* AND *ENTEROCOCCUS FAECALIS* SURVIVAL

By

ADELUMOLA ADEOYE OLADEINDE

Major Professor: Erin K. Lipp

Committee: Marirosa Molina

Travis Glenn

Mussie Y. Habteselassie

Richard Muirhead

Electronic Version Approved:

Suzanne Barbour

Dean of the Graduate School

The University of Georgia

May 2017

DEDICATION

I would like to dedicate this dissertation to my mom for working so hard for me to achieve my dreams, and for never giving up on me.

ACKNOWLEDGMENTS

I would like to express my sincere gratitude to my wife for her support and love. For being my first reviewer all through the writing of this dissertation. To our dogs (Izzy and Olive) and the trail behind Oglethorpe elementary School, for the inspiration during my walks and run. I would also like to acknowledge my mentor and advisor, Dr. Marirosa Molina and Dr. Erin Lipp for the guidance, advice and direction they have provided me over the past years. Special thanks to Dr. Richard Muirhead for his support and suggestions, and for his availability for meetings even though the time difference was a pain.

Finally, I would love to thank my family and friends for their support. I am eternally grateful to all the folks at EPA ORD and Region IV for their help and support throughout my time at EPA.

TABLE OF CONTENTS

LIST OF TABLES

LIST OF FIGURES

CHAPTER 1

INTRODUCTION

The major cause of stream impairment in the United States is due to elevated levels of fecal indicator bacteria (FIB) with agriculture as the primary source of contamination[1-3] (Oladeinde, McCrary and USEPA). Manure run-off from land application and pasture during storm events have been reported as a significant source of these high concentrations of FIB[4-6]. FIB were selected as water quality standards due to their correlation with incidence of gastrointestinal illnesses in epidemiological studies conducted at recreational beaches in the early 1980's[7, 8]. However, one of the shortcomings of FIB is that all warm-blooded animals carry them, thus one cannot differentiate bacteria coming from humans or animals including birds[9]. Further, observed increases have been associated with the ability of FIB to grow extra-intestinally[3, 10, 11]. Consequently, regulators and water resource managers are left to consider the risk of illness to be the same for all water bodies regardless of the source of contamination[9].

Despite these confounding factors that hinders our ability to adequately quantify the relationship between FIB, zoonotic pathogens and the risk of illness, an understanding of the factors that influence bacteria fate in the environment is needed and is critical in developing control/adaptation strategies to minimize pathogen transfer[12, 13]. Moreover, the health risks these pathogens pose to water and food resources are highly dependent on their fate and transport in the environment.

A significant amount of work has been done to elucidate the environmental factors that determine the survival of zoonotic microorganisms. Most of these studies have focused on the die-off of pathogens in water microcosms, irrigation water, manure amended soils/compost manure and intact cattle feces[14-16]. However, no study has investigated the effect of the interaction between dissolved organic matter (DOM), reactive oxygen species (ROS) and competition on FIB survival. DOM represents a vital source of nutrients for bacteria in diverse environments and DOM transformations mediated by biotic and abiotic processes controls the bioavailability of these nutrients[17]. For example, high molecular weight compounds in DOM can be degraded by sunlight to low molecular labile compounds such as ammonium which can then be used as a nitrogen source. In addition, DOM can also be photo-degraded to produce sub-lethal concentrations of ROS such as hydrogen peroxide (HOOH) which have the potential to cause bacterial DNA damage[18, 19].

To understand the role of photo-produced ROS and competition on the survival of *E. coli* and *Ent. faecalis*, we attempted to isolate the effect of ROS using controlled microcosms of phosphate buffered water and natural stream water spiked with extracts derived from cattle feces that were irradiated prior to inoculation with bacteria. In the third chapter of this dissertation I demonstrate that HOOH is the most important ROS affecting fecal bacteria growth dynamics. The fourth chapter investigates the transcriptomic response of fecal bacteria to DOM photo-degradation, showing *E. coli* uses oxy-R controlled genes to efficiently scavenge exogenous HOOH, while *E. faecalis* produces HOOH from glycerol metabolism. In the fifth chapter, I used metabolomics and RNA-seq to investigate the role of competition on the survival of *E. coli* and *Ent.*

faecalis in co-culture experiments. I show that *Ent. faecalis* growth increases in the presence of *E. coli* and photo-produced HOOH, and overall survival was dependent on exploitative and cooperative competition between the two of them. Together, these findings suggest that *E. coli* has a greater capability to remove photo-produced HOOH and overall, a higher regrowth potential than *Ent*. *faecalis*.

REFERENCES

1. USEPA, National water quality inventory: report to congress, 2004 reporting cycle. EPA/841/R-08/001 In Washington DC, 2009.

2. Oladeinde, A.; Bohrmann, T.; Wong, K.; Purucker, S.; Bradshaw, K.; Brown, R.; Snyder, B.; Molina, M., Decay of Fecal Indicator Bacterial Populations and Bovine-Associated Source-Tracking Markers in Freshly Deposited Cow Pats. *Applied and environmental microbiology* **2014,** *80*, (1), 110-118.

3. McCrary, K. J.; Case, C. L. H.; Gentry, T. J.; Aitkenhead-Peterson, J. A., Escherichia coli regrowth in disinfected sewage effluent: Effect of DOC and nutrients on regrowth in laboratory incubations and urban streams. *Water, Air, & Soil Pollution* **2013,** *224*, (2), 1-11.

4. Whelan, G.; Kim, K.; Pelton, M. A.; Soller, J. A.; Castleton, K. J.; Molina, M.; Pachepsky, Y.; Zepp, R., An integrated environmental modeling framework for performing Quantitative Microbial Risk Assessments. *Environmental Modelling & Software* **2014,** *55*, 77-91.

5. Soupir, M. L.; Mostaghimi, S.; Dillaha, T., Attachment of Escherichia coli and enterococci to particles in runoff. *Journal of Environmental Quality* **2010,** *39*, (3), 1019-1027.

6. Edwards, D. R., Coyne, M. S., Vendrell, P. F., Daniel, T. C., Moore, P. r., Murdoch, J. F., Fecal coliform and streptococcus concentrations in runoff from grazed pastures in northwest Arkansas. *ournal Of The American Water Resources Association* **1997,** *33*, (2), 413-422.

7. Dufour, A. P.; Ballantine, P., Bacteriological Ambient Water Quality Criteria for Marine and Freshwater Recreational Waters. *U.S. Environmental Protection Agency* **1986**, EPA 440/5-84-002.

8. Cabelli, V. J., A.P. Dufour, and L.J. McCabe, Swimming associated gastrointestinal illness and water quality. *American journal of Epidemiology* **1982,** *115*, 606-616.

9. Dufour, A.; Wade, T. J.; Kay, D., Epidemiological studies on swimmer health effects associated with potential exposure to zoonotic pathogens in bathing beach water–a review. *Animal Waste, Water Quality and Human Health* **2012**.

10. Giannakis, S.; Darakas, E.; Escalas-Canellas, A.; Pulgarin, C., Elucidating bacterial regrowth: Effect of disinfection conditions in dark storage of solar treated secondary effluent. *J Photoch Photobio A* **2014,** *290*, 43-53.

11. Derry, C.; Attwater, R., Regrowth of enterococci indicator in an open recycled-water impoundment. *Sci Total Environ* **2014,** *468*, 63-67.

12. Bradford, S. A.; Schijven, J.; Harter, T., Microbial Transport and Fate in the Subsurface Environment: Introduction to the Special Section. *Journal of environmental quality* **2015,** *44*, (5), 1333-1337.

13. Bradford, S. A.; Morales, V. L.; Zhang, W.; W., H. R.; Packman, A. I.; Mohanram, A.; Welty, C., Transport and Fate of Microbial Pathogens in Agricultural Settings. *Critical Reviews in Environmental Science & Technology* **2013,** *43*, (8), 775-893.

14. Rogers, S. W.; Donnelly, M.; Peed, L.; Kelty, C. A.; Mondal, S.; Zhong, Z.; Shanks, O. C., Decay of bacterial pathogens, fecal indicators, and real-time quantitative PCR genetic markers in manure-amended soils. *Appl Environ Microbiol* **2011,** *77*, (14), 4839-48.

15. Muirhead, R. W.; Littleljohn, R. P., Die-off of Escherichia coli in intact and disrupted cowpats. *Soil Use & Management* **2009,** *25*, (4), 389-394.

16. Sokolova, E.; Astrom, J.; Pettersson, T. J.; Bergstedt, O.; Hermansson, M., Decay of Bacteroidales genetic markers in relation to traditional fecal indicators for water quality modeling of drinking water sources. *Environ Sci Technol* **2012,** *46*, (2), 892-900.

17. Meyer, J., The microbial loop in flowing waters. *Microbial Ecology* **1994,** *28*, (2), 195-199.

18. Mostofa, K. M.; Yoshioka, T.; Mottaleb, A.; Vione, D., *Photobiogeochemistry of organic matter: principles and practices in water environments*. Springer Science & Business Media: 2012.

19. Mostofa, K. M.; Liu, C.-q.; Sakugawa, H.; Vione, D.; Minakata, D.; Wu, F., Photoinduced and microbial generation of hydrogen peroxide and organic peroxides in natural waters. In *Photobiogeochemistry of Organic Matter*, Springer: 2013; pp 139-207

CHAPTER 2

LITERATURE REVIEW

OVERVIEW

Fecal indicator bacteria are a group of coliform bacteria once thought to only inhabit the gastrointestinal tracts of warm-blooded animals. Initially, FIB included the 4 genera of Gram-negative bacteria belonging to the family Enterobacteriaceae and were called total coliforms. The total coliform limit was developed from two studies published in 1951, showing the predictability of salmonellosis from Salmonella population in bathing waters and microbiological surveys conducted at Connecticut beaches [1-3]. Based on these studies, a guideline of 1000/100mL was set for recreational waters. However, in 1951 Stevenson's et al. conducted a series of epidemiological studies at the Great Lakes (Michigan) and the Inland River (Ohio) and showed an epidemiologically detectable health effect at levels of 2300 to 2400 coliforms /100mL [4, 5]. Based on this result and sanitary surveys completed along the Ohio lakes, 18% of total coliforms were found to be fecal derived. Therefore, the National Technical Advisory Committee (NTAC) recommended a fecal coliform guideline of 200 coliforms per 100mL. Several stakeholders argued that the rationale for using the Stevenson's studies, as a guideline was not justified citing deficiencies in the analysis of the data, and in the interpretation of the results [2, 4].

In response to the suggested weaknesses in the existing health effects guidelines and standards for recreational waters, EPA initiated a program to re-examine

the entire question of health effects associated with swimming in wastewater-polluted waters. A series of epidemiological studies were conducted in marine beaches in New York, Massachusetts and Louisiana to investigate the health effects of participants to recreational water exposure [4, 6, 7]. Several potential indicator bacteria were measured including *E. coli*, enterococci, fecal coliforms, total coliforms and *Clostridrium perfringens*. The results showed that Enterococci was the best predictor of gastrointestinal illnesses in participants with high credible gastrointestinal illness (HCGI), while *E. coli* was the second-best predictor and fecal coliforms had the weakest correlation. Based on these studies, the current standards require the geometric mean of 4 samplings in one month not to exceed: 126 CFU /100ml of *E. coli* or 33 CFU /100mL of enterococci in fresh water and 35 CFU /100mL enterococci in marine waters. EPA estimated in 1986 that the predicted level of illness associated with the criteria was 8 HCGI per 1,000 primary contact recreators in fresh water and 19 HCGI per 1,000 primary contact recreators in marine waters [8].

E. coli are gram negative, rod-shaped, facultative anaerobes of the genus *Escherichia*. They are versatile microorganisms, having the capability to withstand several adverse environmental conditions, and survive on a wide variety of substrates. Their optimum growth is at 37^{o}C but growth can still be achieved under a wide range of temperatures. They are mostly non-pathogenic but several serotypes with pathogenicity islands have been isolated. They are bounded by a cell wall and a lipid outer membrane which is its major structural defense. Recommended methods for measuring *E. coli* are culture based including EPA Method 1603 [9] that uses membrane filtration on a selective media to grow the bacteria. The methods are based on the use of bacterial specific

substrate which results in a color change at a set temperature. Most probable number (MPN) methods like Colilert have also been adopted for quantifying *E. coli* [10].

Enterococcus represents a large group of lactic-acid bacteria. They are gram-positive, cocci, facultative anaerobes and can tolerate a wide range of environmental conditions. There are several species represented in this genus, however only 5 are often reported in water or environmental matrices [11]. They include *E. faecalis, E. casseliflavus, E. gallinarum, E. hirae and E. faecium.* They possess a cell wall composed of >90% peptidoglycan that constitutes their major structural barrier from unwanted compounds or metabolites. They are measured via culture (EPA method 1600) and MPN (Enterolert) based techniques [12].

The adoption of these two groups of bacteria as fecal indicators poses several unaddressed shortcomings. First, FIB are harbored by all warm-blooded animals, thus one cannot differentiate bacteria coming from humans or animals including birds [13, 14]. As a consequence, regulators and water resource managers are left to consider the risk of illness to be the same for all water bodies regardless of the source of contamination [15]. A few epidemiological studies that have tried to investigate the risk of illness associated with recreational waters contaminated with animal and bird fecal wastes have reported little or no association between FIB and risk of GI illness [13, 15-19]. In a review [15], the authors suggested that the reported lack of association in these studies could be attributed to the water quality standard in use. The water quality standards at the selected sites were based on data gathered from the 1980's human epidemiological studies - at sites impacted by human sewage. In the 2012 revised EPA recreational criteria, section 6.2.2. was included to serve as a guidance for stakeholders interested

in adopting an alternative indicator that are site-specific to address non-point sources of pollutants [20, 21].

More recently, DNA/RNA based source tracking technologies have been developed to identify the fecal source of contamination and to make quantitative designations to different sources [22-24]. However, none of the methods developed so far have been shown to be 100% specific. Moreover, the methods are not sensitive enough to adequately characterize the source of fecal contamination in recreational and surface waters [25-28].

Despite the confounding factors that hinders our ability to adequately quantify the relationship between zoonotic pathogens and the risk of illness, an understanding of the factors that influence pathogen fate in agricultural settings is needed and is critical in developing control/adaptation strategies to minimize pathogen transfer. Moreover, the health risks these pathogens pose to water and food resources are highly dependent on their fate in the environment [29].

FACTORS CONTRIBUTING TO FIB SURVIVAL

Sunlight. The role of sunlight as an inactivating agent has been well documented. Ultraviolet radiation from sunlight causes DNA lesions in bacteria, thereby killing them. Sunlight mediated inactivation of FIB has been reported in water, soil and fecal matrices [30-34]. However, die-off rates typically differ between *E. coli* and Enterococci. In studies that have investigated the impact of the different wavelengths of UV on FIB, *E. coli* always showed a faster die-off than Enterococci under UV-B exposure [35-38]. *Enterococcus* ability to survive longer has been attributed to its thick peptidoglycan cell

wall [39, 40]. In addition, strains that carry carotenoid pigments (e.g. *E. casseliflavus*), have been shown to be more prevalent during sunlit conditions [41].

Furthermore, the potential for sunlight inactivation is controlled by several factors including depth and turbidity of the water column [42, 43]. For example, in highly turbid or high absorbance water, one would expect a very limited penetration of UV and thus a lower inactivation of FIB. On the hand, in clear waters, UVR can penetrate up 30 meters, thus allowing for a higher potential for FIB inactivation [43].

Dissolved Organic Matter (DOM). The survival or growth of fecal bacteria in extra-intestinal environments is determined by the availability of nutrients or substrates for uptake. DOM represents a major resource for all forms of life in surface waters. The sources of DOM in aquatic ecosystems are diverse and spatially variable. More importantly, in watersheds dominated by agriculture, livestock farms or lagoon ponds are a major non-point source of DOM via runoff related processes [44-46]. This form of DOM is of fecal origin and has been broken down by the gut microbiome of warm blooded animals, making them bioavailable for use by extra-intestinal microbes. Dead microbiota can also serve as a new pool of bioavailable DOM [47-49]. Microorganisms that can readily utilize this source of nutrients for growth maybe at an advantage. Moreover, elevated levels of FIB in streams and rivers have been attributed to these non-point sources of pollution (USEPA, 2014).

Sunlight DOM interaction. The colored fraction of DOM (CDOM) is primarily responsible for the absorption of UV-R [50]. CDOM can be degraded into a variety of photoproducts that stimulate the growth and activity of microorganisms in aquatic environments. Bushaw and Zepp [51] demonstrated that ammonium is among the

nitrogenous compounds released and is produced most efficiently by ultraviolet wavelengths. Other studies have demonstrated an increase in total bacterial population after amending unfiltered stream or lake water samples with sunlight irradiated filtered water [52-54]. Photo-degradation and biodegradation of DOM can lead to the conversion of DOM to inorganic compounds and its subsequent loss from the water column, and to the alteration of DOM chemical composition [48]. No study to date has demonstrated the effect of photodegraded DOM on FIB.

Photodegradation of DOM has also been observed to elicit an inhibitory response in bacterial populations exposed to them [32, 52, 55-57]. This response has been attributed to the photoproduction of reactive oxygen species (ROS) from DOM photo-sensitization[52]. ROS are reactive molecules and free radicals derived from reactions with molecular oxygen. They include singlet oxygen ($^1O_2$), hydroxyl radicals ($OH^{\cdot}$), superoxide radicals (O_2^{-}) and hydrogen peroxide (HOOH), which all have the potential to cause bacterial DNA lesions [58, 59]. Singlet oxygen has a half-life on the order of microseconds, making its diffusion to potential cellular targets highly restricted [60, 61]. Gram-positive bacteria have been reported to be more sensitive to $^1O_2$ than gram-negative bacteria [62, 63]. However, studies that have shown an increase in FIB inactivation rate from $^1O_2$ exposure have used high steady states concentration that are not environmentally relevant or representative [38, 57].

On the other hand, the high reactivity and charge of the radicals limit their potential to cross cell barriers and affect vital cell functions [64]. Superoxide radicals cannot cross the lipid bilayers at neutral pH, moreover they are immediately scavenged by superoxide dismutase and reductase enzymes produced by many species of

bacteria and cyanobacteria [58]. Hydroxyl radicals is the neutral form of hydroxide ion and it is short-lived. They are formed in a series of fenton reactions involving iron, HOOH and O_2^- as reactants. Hydroxyl radicals are the most damaging of all ROS, and can cause nucleic acid mutations, lipid peroxidation and amino-acid and protein oxidative damage [65-67]. However, the low concentrations (10^{-19} – 10^{-16} M) observed in surface waters suggest they may not play a direct role in fecal bacteria survival [68]. For example, Maraccini, Wenk and Boehm [57] reported no correlation between measured exogenous $OH^{\cdot}$ and fecal bacteria inactivation rates in a laboratory controlled experiment. Further, the lack of an ideal method of measurement in-situ has hampered our success in understanding the role of $OH^{\cdot}$.

Hydrogen peroxide (unlike the radicals) is an uncharged species that can penetrate the bacterial membrane. In addition, the lifetime of HOOH in natural waters have been reported to range from several hours to days [69, 70]. Hydrogen peroxide is mutagenic and can directly oxidize unincorporated intracellular ferrous iron in bacteria, some of which are associated with DNA. This series of reactions with iron (fenton reaction) generates the more damaging $OH^{\cdot}$ and also inactivates a family of dehydratases [65, 67]. Approximately, one micromolar of intracellular HOOH is sufficient to cause crippling levels of DNA damage in *E. coli* [58]. Anesio, Granéli, Aiken, Kieber and Mopper [52] showed that the suppression of bacterial carbon production was highly correlated with the concentration of photochemically formed HOOH and concluded that extracellular HOOH concentrations of about 2μM to 3μM were inhibitory for bacteria. The concentration of HOOH varies on a diel cycle, with peak concentrations at noontime and low concentrations at night [71, 72]. This day light increase was recently

shown to correlate with significant expression of bacterial genes encoding HOOH degrading enzymes including catalases and peroxidases [73].

It is important to note that ROS can also be produced endogenously by bacteria (Figure. 2.1). For example, *E. coli* produces HOOH at 15μM/s when saturated with oxygen in Luria Bertani media [74]. Enterococci on the other hand, excretes large doses of HOOH from the metabolism of glycerol and lactic acid via glycerol, pyruvate and lactate oxidases [58]. This form of dark production is quite dominant in surface waters [69, 75].

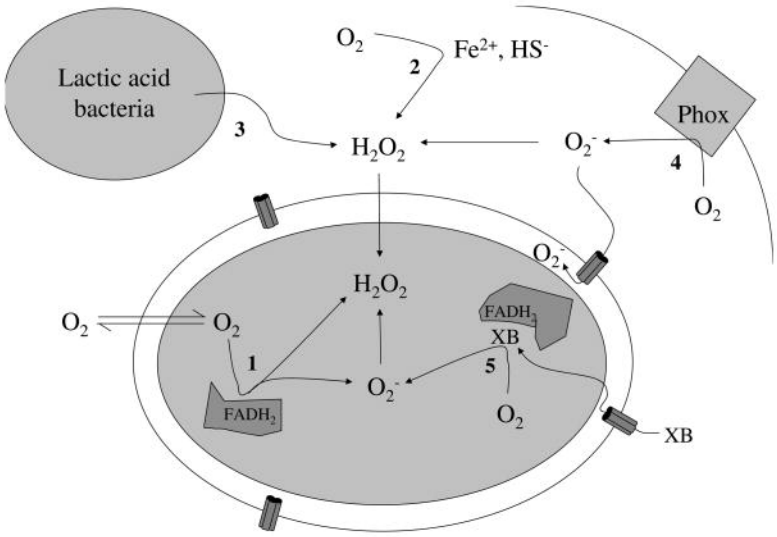

Figure 2.1. Schematic for intracellular and extracellular production of reactive oxygen species (ROS). Figure adopted from Imlay [58].

Competition. Bacteria do not live in isolation but communicate with other strains and species as a community. This interaction can lead to competition for scarce resources and limited space, a bottom up control of bacterial populations. A bacterial strain is defined to be competitive if they cause a decrease in fitness of another competitor

strain, and if the observed interaction evolved as a result of a biotic process rather than predation or parasitism [49].

Bacteria can compete indirectly by consuming the limited nutrients and restricting its availability to other competitors. This form of competition is called exploitative or passive competition [49]. This could occur by increasing the uptake of nutrients, consequently generating higher growth rates than their competitors [76]. In contrast, direct or interference competition occurs when individual bacteria cells damage one another – a form of chemical warfare. This could occur via the secretion of secondary metabolites, toxins, bacteriocins, antibiotics or siderophores (iron-scavenging molecules).

Competition is widespread in natural environments and it has been suggested to be a favored survival mechanism for bacteria under three scenarios: (i) when strains or species of bacteria coexisting have similar or overlapping resource requirements (ii) when cells of different strains are spatially mixed, and where resources and secretions are shared, and (iii) when bacterial population density is high relative to available nutrients [49]. These three different scenarios are influenced by several environmental conditions including nutrient complexity, microbial diversity, environmental disturbances, and cell motility. For example, species of bacteria that are distantly related (e.g. Gram-positive vs Gram-negative) and with no overlap in nutrient requirement will be weak competitors of one another and possibly coexist with minimal negative consequences [77]. In contrast, strains with similar metabolic niches and low nutrient complexity are more likely to compete for resources and space. Although there is a wide consensus on the importance of competition on FIB survival, the estimated effect seems to vary by bacteria or habitat [78, 79]. For instance, Wanjugi and Harwood [79] reported that competition

had much greater effect on *E. coli* than *E. faecalis* in water and sediment micro and mesocosms .

Understanding the role of competition in the structuring of FIB communities will require more studies on an ecological and evolutionary time scale. Competition is predicted to result in ecological stability – a situation where less competitive strains could go extinct while others dominate the community, or strains can continue to coexist by cooperation (e.g. occupying different metabolic roles) [49, 77]. However, the question on the time scale and microbial diversity required to drive such stable communities or environment warrants more studies.

Predation. Bacteria do not only interact with one another but also with other micro and macro-organisms such as bacteriophages and protists. This form of interaction results in a top down control of bacterial populations below levels supportable by resources alone [80]. Predation is an important evolutionary force, favoring the selection of more effective predators and more resistant prey. The predator-prey theory predicts that when prey are numerous, the numbers of predators will increase and vice- versa [81]. In laboratory studies, it has been shown that such predator-prey systems might be unstable - as predator runs out of prey or become selective of their prey [82]. Nevertheless, in aquatic ecosystems where spatial heterogeneity is a controlling factor, one will expect some prey to persist in niches or pockets (e.g. sediments) where they escape predation [83]. Prey can fuel a new population of bacteria once predators decline and upon nutrient availability. It has been suggested that such relationships stabilize predator-prey systems in nature [84] .

Bacteriophages and ciliates differ in their mechanism used for predation. While phages are typically host – specific, ciliate grazers select their preys based on relatively non-specific features [85, 86]. In addition, a single protist can consume multiple prey bacteria before reproducing, whereas a single infection of a bacterium by a lytic bacteriophage can produce millions of progenies [85]. That said, bacteria have developed several mechanisms to ward of predators including phage resistance for bacteriophages and oversized morphology and toxin secretion for protozoans [85, 87].

The effects of predation on FIB population is an area of current research interest. Recent studies have shown predation to be a significant factor in controlling *E. coli* and *E. faecalis* population in outdoor mesocosm studies [33, 79, 88, 89]. However, the fraction of observed die-off attributable to predation or competition is still an open question. Moreover, most of these studies use Cylcoheximide (CHM) to stop protein synthesis in ciliates/protozoans. The use of this compound may confound the results reported in these studies, since CHM has been observed to inhibit bacterial growth at a dose of 50mg liter $^{-1}$ [90]. Tremaine and Mills [90] concluded that using CHM in grazing experiments violated the assumption of selective inhibition of heterotrophic eukaryotes and suggested its use should be avoided. In another experiment, CHM was found to be effective in eliminating fungi from sheep and goat dry matter but also resulted in an increase in bacterial population after 72 h of incubation [91].

Collectively, untangling the effects of predation or competition on FIB survival dynamics still poses several challenges and requires further study.

Temperature, pH and salinity. Numerous abiotic factors influence the survival of FIB in secondary habitats in addition to the ones described previously. Temperature has been

documented to lower bacteria survival as it increases [92-96], while the effect of salinity has been described to be bacteria dependent [97-99]. In addition, these variables can have an interacting role on other biotic and abiotic processes. For example, ROS steady state concentrations measured in surface waters is pH dependent and HOOH seem to increase as salinity increases [100]. On the other hand, several studies have suggested a positive correlation between predation and temperature. As temperature increases, so does protozoan grazing rates [101, 102].

RESEARCH GOALS AND OBJECTIVES

The goal of this dissertation is to provide a better understanding on the role of sunlight and agriculturally derived DOM on fecal bacteria survival dynamics. To achieve this goal, I had 4 objectives: (1) Determine if HOOH production from photo-degradation of cattle derived DOM will have any significant negative effect on fecal bacteria survival (2) provide an understanding on the mechanism used by fecal bacteria for the removal and production of HOOH (3) Determine the role of competition in HOOH production and (4) determine the synergistic effect of direct sunlight, HOOH photoproduction and competition on FIB survival dynamics.

REFERENCES

1. Scott, W. J., Sanitary Study of Shore Bathing Waters. *Connecticut health bulletin* **1951,** *65*, (3), 74-85.

2. Cabelli, V. J.; Dufour, A. P.; McCabe, L.; Levin, M., A marine recreational water quality criterion consistent with indicator concepts and risk analysis. *Journal (Water Pollution Control Federation)* **1983**, 1306-1314.

3. Streeter, H., Bacterial quality objectives for the Ohio River: A guide for the evaluation of sanitary conditions of waters used for potable supplies and recreational uses. *Cincinnati, Ohio River Valley Water Sanitation Commission* **1951**.

4. Dufour, A. P., Bacterial indicators of recreational water quality. *Canadian Journal of Public Health/Revue Canadienne de Sante'e Publique* **1984,** *75*, (1), 49-56.

5. Stevenson, A. H., Studies of bathing water quality and health*. *American Journal of Public Health and the Nations Health* **1953,** *43*, (5_Pt_1), 529-538.

6. Dufour, A. P.; Cabelli, V. J., Ambient water quality criteria for bacteria. *U.S. Environmental Protection Agency* **1998**, EPA-A440/5-84-002.

7. Cabelli, V. J., A.P. Dufour, and L.J. McCabe, Swimming associated gastrointestinal illness and water quality. *American journal of Epidemiology* **1982,** *115*, 606-616.

8. Dufour, A.; Ballentine, R., *Ambient water quality criteria for bacteria, 1986: bacteriological ambient water quality criteria for marine and fresh recreational waters*. National Technical Information Service, Department of Commerce, US: 1986.

9. USEPA, E. *Method 1603: Escherichia coli (E. coli) in water by membrane filtration using modified membrane-thermotolerant Escherichia coli agar (modified mTEC)*; EPA 821-R-02-023, US Environmental Protection Agency, Washington [DC]: 2002.

10. Crane, R.; Jackson, C. B.; Sedlacek, R.; Walker, D., EPA approves new test procedures for the analysis of microbiological pollutants in wastewater and sludge. *Loveland, CO: Hach Company. Available online at* http://www/. *hach. com/fmmimghach* **2006**.

11. Boehm, A. B.; Sassoubre, L. M., Enterococci as indicators of environmental fecal contamination. **2014**.

12. Ferguson, D. M.; Griffith, J. F.; McGee, C. D.; Weisberg, S. B.; Hagedorn, C., Comparison of Enterococcus species diversity in marine water and wastewater using Enterolert and EPA Method 1600. *Journal of environmental and public health* **2013,** *2013*.

13. Dorevitch, S.; Ashbolt, N. J.; Ferguson, C. M.; Fujioka, R.; McGee, C. G.; Soller, J. A.; Whitman, R. L., Meeting report: knowledge and gaps in developing microbial criteria for inland recreational waters. *Environmental Health Perspectives* **2010,** *118*, (6), 871.

14. Schwab, K. J., Are existing bacterial indicators adequate for determining recreational water illness in waters impacted by nonpoint pollution? *Epidemiology* **2007,** *18*, (1), 21-22.

15. Dufour, A.; Wade, T. J.; Kay, D., Epidemiological studies on swimmer health effects associated with potential exposure to zoonotic pathogens in bathing beach water–a review. *Animal Waste, Water Quality and Human Health* **2012**.

16. Cheung, W.; Chang, K.; Hung, R.; Kleevens, J., Health effects of beach water pollution in Hong Kong. *Epidemiology and infection* **1990,** *105*, (01), 139-162.

17. Colford Jr, J. M.; Wade, T. J.; Schiff, K. C.; Wright, C. C.; Griffith, J. F.; Sandhu, S. K.; Burns, S.; Sobsey, M.; Lovelace, G.; Weisberg, S. B., Water quality indicators and the risk of illness at beaches with nonpoint sources of fecal contamination. *Epidemiology* **2007,** *18*, (1), 27-35.

18. Sinigalliano, C. D.; Fleisher, J. M.; Gidley, M. L.; Solo-Gabriele, H. M.; Shibata, T.; Plano, L. R.; Elmir, S. M.; Wanless, D.; Bartkowiak, J.; Boiteau, R., Traditional and molecular analyses for fecal indicator bacteria in non-point source subtropical recreational marine waters. *Water research* **2010,** *44*, (13), 3763-3772.

19. Soller, J. A.; Bartrand, T.; Ashbolt, N. J.; Ravenscroft, J.; Wade, T. J., Estimating the primary etiologic agents in recreational freshwaters impacted by human sources of faecal contamination. *Water Research* **2010,** *44*, (16), 4736-4747.

20. Fujioka, R. S.; Solo-Gabriele, H. M.; Byappanahalli, M. N.; Kirs, M., US Recreational Water Quality Criteria: A Vision for the Future. *International journal of environmental research and public health* **2015,** *12*, (7), 7752-7776.

21. USEPA, Recreational Water Quality Criteria. In Water, O. o.; Agency, U. S. E. P., Eds. Washington, D.C., 2012.

22. Shanks, O. C.; Domingo, J. W.; Lu, J.; Kelty, C. A.; Graham, J. E., Identification of bacterial DNA markers for the detection of human fecal pollution in water. *Appl Environ Microbiol* **2007,** *73*, (8), 2416-22.

23. Haugland, R. A.; Varma, M.; Sivaganesan, M.; Kelty, C.; Peed, L.; Shanks, O. C., Evaluation of genetic markers from the 16S rRNA gene V2 region for use in quantitative detection of selected Bacteroidales species and human fecal waste by qPCR. *Syst Appl Microbiol* **2010,** *33*, (6), 348-57.

24. Mieszkin, S.; Yala, J. F.; Joubrel, R.; Gourmelon, M., Phylogenetic analysis of Bacteroidales 16S rRNA gene sequences from human and animal effluents and assessment of ruminant faecal pollution by real-time PCR. *J Appl Microbiol* **2010,** *108*, (3), 974-84.

25. Shanks, O. C.; White, K.; Kelty, C. A.; Hayes, S.; Sivaganesan, M.; Jenkins, M.; Varma, M.; Haugland, R. A., Performance assessment PCR-based assays targeting bacteroidales genetic markers of bovine fecal pollution. *Appl Environ Microbiol* **2010,** *76*, (5), 1359-66.

26. Shanks, O. C.; White, K.; Kelty, C. A.; Sivaganesan, M.; Blannon, J.; Meckes, M.; Varma, M.; Haugland, R. A., Performance of PCR-based assays targeting Bacteroidales genetic markers of human fecal pollution in sewage and fecal samples. In *Environ Sci Technol*, 2010/08/14 ed.; 2010; Vol. 44, pp 6281-8.

27. Harwood, V. J.; Staley, C.; Badgley, B. D.; Borges, K.; Korajkic, A., Microbial source tracking markers for detection of fecal contamination in environmental waters: relationships between pathogens and human health outcomes. *FEMS microbiology reviews* **2014,** *38*, (1), 1-40.

28. Boehm, A. B.; Van De Werfhorst, L. C.; Griffith, J. F.; Holden, P. A.; Jay, J. A.; Shanks, O. C.; Wang, D.; Weisberg, S. B., Performance of forty-one microbial source tracking methods: a twenty-seven lab evaluation study. *Water research* **2013,** *47*, (18), 6812-6828.

29. Bradford, S. A.; Morales, V. L.; Zhang, W.; W., H. R.; Packman, A. I.; Mohanram, A.; Welty, C., Transport and Fate of Microbial Pathogens in Agricultural Settings. *Critical Reviews in Environmental Science & Technology* **2013,** *43*, (8), 775-893.

30. Bolton, N. F.; Cromar, N. J.; Hallsworth, P.; Fallowfield, H. J., A review of the factors affecting sunlight inactivation of micro-organisms in waste stabilisation ponds: preliminary results for enterococci. *Water Science & Technology* **2010,** *61*, (4), 885-890.

31. Davies-Colley, R.; Donnison, A.; Speed, D.; Ross, C.; Nagels, J. a., Inactivation of faecal indicator micro-organisms in waste stabilisation ponds: interactions of environmental factors with sunlight. *Water Research* **1999,** *33*, (5), 1220-1230.

32. Kadir, K.; Nelson, K. L., Sunlight mediated inactivation mechanisms of Enterococcus faecalis and Escherichia coli in clear water versus waste stabilization pond water. *Water research* **2014,** *50*, 307-317.

33. Korajkic, A.; McMinn, B. R.; Shanks, O. C.; Sivaganesan, M.; Fout, G. S.; Ashbolt, N. J., Biotic interactions and sunlight affect persistence of fecal indicator bacteria and microbial source tracking genetic markers in the upper Mississippi river. *Applied and environmental microbiology* **2014,** *80*, (13), 3952-3961.

34. Nguyen, M. T.; Jasper, J. T.; Boehm, A. B.; Nelson, K. L., Sunlight inactivation of fecal indicator bacteria in open-water unit process treatment wetlands: Modeling endogenous and exogenous inactivation rates. *Water research* **2015,** *83*, 282-292.

35. Deller, S.; Mascher, F.; Platzer, S.; Reinthaler, F. F.; Marth, E., EFFECT OF SOLAR RADIATION ON SURVIVAL OF INDICATOR BACTERIA IN BATHING WATERS. *Central European Journal of Public Health* **2006,** *14*, (3), 133-137.

36. Oladeinde, A.; Bohrmann, T.; Wong, K.; Purucker, S.; Bradshaw, K.; Brown, R.; Snyder, B.; Molina, M., Decay of Fecal Indicator Bacterial Populations and Bovine-Associated Source-Tracking Markers in Freshly Deposited Cow Pats. *Applied and environmental microbiology* **2014,** *80*, (1), 110-118.

37. Hijnen, W. A. M.; Beerendonk, E. F.; Medema, G. J., Review: Inactivation credit of UV radiation for viruses, bacteria and protozoan (oo)cysts in water: A review. *Water Research* **2006,** *40*, 3-22.

38. Maraccini, P. A.; Wenk, J.; Boehm, A. B., Exogenous Indirect Photoinactivation of Bacterial Pathogens and Indicators in Water with Natural and Synthetic Photosensitizers in Simulated Sunlight With Reduced UVB. *Journal of applied microbiology* **2016**.

39. Arima, H.; Ibrahim, H. R.; Kinoshita, T.; Kato, A., Bactericidal action of lysozymes attached with various sizes of hydrophobic peptides to the C-terminal using genetic modification. *FEBS Letters* **1997,** *415*, (1), 114-118.

40. Peng, L.; Wenli, D.; Qisui, W.; Xi, L., The damage of outer membrane of Escherichia coli in the presence of TiO2 combined with UV light. *Colloids and Surfaces B: Biointerfaces* **2010**

, *78*, 171-176.

41. Maraccini, P. A.; Ferguson, D. M.; Boehm, A. B., Diurnal variation in Enterococcus species composition in polluted ocean water and a potential role for the enterococcal carotenoid in protection against photoinactivation. *Applied and environmental microbiology* **2012,** *78*, (2), 305-310.

42. Maraccini, P. A.; Mattioli, M. C. M.; Sassoubre, L. M.; Cao, Y.; Griffith, J. F.; Ervin, J. S.; Van De Werfhorst, L. C.; Boehm, A. B., Solar Inactivation of Enterococci and Escherichia coli in Natural Waters: Effects of Water Absorbance and Depth. *Environ Sci Technol* **2016,** *50*, (10), 5068-5076.

43. Hargreaves, B. R., Water column optics and penetration of UVR. *UV effects in aquatic organisms and ecosystems* **2003,** *1*, 59-108.

44. Graeber, D.; Boëchat, I. G.; Encina-Montoya, F.; Esse, C.; Gelbrecht, J.; Goyenola, G.; Gücker, B.; Heinz, M.; Kronvang, B.; Meerhoff, M., Global effects of agriculture on fluvial dissolved organic matter. *Scientific reports* **2015,** *5*.

45. Heinz, M.; Graeber, D.; Zak, D.; Zwirnmann, E.; Gelbrecht, J.; Pusch, M. T., Comparison of organic matter composition in agricultural versus forest affected headwaters with special emphasis on organic nitrogen. *Environ Sci Technol* **2015,** *49*, (4), 2081-2090.

46. Bida, M. R.; Tyler, A. C.; Pagano, T., Quantity and composition of stream dissolved organic matter in the watershed of Conesus Lake, New York. *Journal of Great Lakes Research* **2015,** *41*, (3), 730-742.

47. Logue, J. B.; Stedmon, C. A.; Kellerman, A. M.; Nielsen, N. J.; Andersson, A. F.; Laudon, H.; Lindström, E. S.; Kritzberg, E. S., Experimental insights into the importance of aquatic bacterial community composition to the degradation of dissolved organic matter. *The ISME journal* **2016,** *10*, (3), 533-545.

48. Hansen, A. M.; Kraus, T. E.; Pellerin, B. A.; Fleck, J. A.; Downing, B. D.; Bergamaschi, B. A., Optical properties of dissolved organic matter (DOM): Effects of biological and photolytic degradation. *Limnology and Oceanography* **2016,** *61*, (3), 1015-1032.

49. Ghoul, M.; Mitri, S., The Ecology and Evolution of Microbial Competition. *Trends in microbiology* **2016,** *24*, (10), 833-845.

50. Häder, D.-P.; Helbling, E.; Williamson, C.; Worrest, R., Effects of UV radiation on aquatic ecosystems and interactions with climate change. *Photochemical & Photobiological Sciences* **2011,** *10*, (2), 242-260.

51. Bushaw, K. L.; Zepp, R. G., Photochemical release of biologically available nitrogen from aquatic dissolved organic matter. *Nature* **1996,** *381*, (6581), 404.

52. Anesio, A. M.; Granéli, W.; Aiken, G. R.; Kieber, D. J.; Mopper, K., Effect of humic substance photodegradation on bacterial growth and respiration in lake water. *Applied and environmental microbiology* **2005,** *71*, (10), 6267-6275.

53. Tranvik, L. J.; Bertilsson, S., Contrasting effects of solar UV radiation on dissolved organic sources for bacterial growth. *Ecology Letters* **2001,** *4*, (5), 458-463.

54. Lindell, M. J.; Granéli, W.; Tranvik, L. J., Enhanced bacterial growth in response to photochemical transformation of dissolved organic matter. *Limnology and Oceanography* **1995,** *40*, (1), 195-199.

55. Scully, N. M.; Cooper, W. J.; Tranvik, L. J., Photochemical effects on microbial activity in natural waters: the interaction of reactive oxygen species and dissolved organic matter. *FEMS microbiology ecology* **2003,** *46*, (3), 353-357.

56. Pullin, M. J.; Bertilsson, S.; Goldstone, J. V.; Voelker, B. M., Effects of sunlight and hydroxyl radical on dissolved organic matter: Bacterial growth efficiency and production of carboxylic acids and other substrates. *Limnology and Oceanography* **2004,** *49*, (6), 2011-2022.

57. Maraccini, P. A.; Wenk, J.; Boehm, A. B., Photoinactivation of eight health-relevant bacterial species: determining the importance of the exogenous indirect mechanism. *Environ Sci Technol* **2016,** *50*, (10), 5050-5059.

58. Imlay, J. A., Cellular defenses against superoxide and hydrogen peroxide. *Annu Rev Biochem* **2008,** *77*, 755-76.

59. Imlay, J. A.; Linn, S., Mutagenesis and stress responses induced in Escherichia coli by hydrogen peroxide. *Journal of Bacteriology* **1987,** *169*, (7), 2967-2976.

60. Dahl, T., Examining the role of singlet oxygen in photosensitized cytotoxicity. In CRC Press, Boca Raton: 1994; pp 241-258.

61. Haag, W. R.; Hoigne, J., Singlet oxygen in surface waters. 3. Photochemical formation and steady-state concentrations in various types of waters. *Environ Sci Technol* **1986,** *20*, (4), 341-348.

62. Dahl, T. A.; Midden, W.; Hartman, P. E., Comparison of killing of gram-negative and gram-positive bacteria by pure singlet oxygen. *Journal of bacteriology* **1989,** *171*, (4), 2188-2194.

63. Glaeser, S. P.; Berghoff, B. A.; Stratmann, V.; Grossart, H.-P.; Glaeser, J., Contrasting effects of singlet oxygen and hydrogen peroxide on bacterial community composition in a humic lake. *PloS one* **2014,** *9*, (3).

64. Kieber, D. J.; Peake, B. M.; Scully, N. M., Reactive oxygen species in aquatic ecosystems. *UV effects in aquatic organisms and ecosystems. Royal Society of Chemistry* **2003**, 251-288.

65. Imlay, J. A., The molecular mechanisms and physiological consequences of oxidative stress: lessons from a model bacterium. *Nature Reviews Microbiology* **2013,** *11*, (7), 443-454.

66. Imlay, J. A., Transcription Factors That Defend Bacteria Against Reactive Oxygen Species. *Annual Review of Microbiology* **2015,** *69*, (1).

67. Imlay, J. A., Diagnosing oxidative stress in bacteria: not as easy as you might think. *Current opinion in microbiology* **2015,** *24*, 124-131.

68. Gligorovski, S.; Strekowski, R.; Barbati, S.; Vione, D., Environmental implications of hydroxyl radicals (• OH). *Chemical reviews* **2015,** *115*, (24), 13051-13092.

69. Mostofa, K. M.; Liu, C.-q.; Sakugawa, H.; Vione, D.; Minakata, D.; Wu, F., Photoinduced and microbial generation of hydrogen peroxide and organic peroxides in natural waters. In *Photobiogeochemistry of Organic Matter*, Springer: 2013; pp 139-207.

70. Mostofa, K. M.; Sakugawa, H., Spatial and temporal variations and factors controlling the concentrations of hydrogen peroxide and organic peroxides in rivers. *Environmental Chemistry* **2009,** *6*, (6), 524-534.

71. Clark, C. D.; De Bruyn, W. J.; Hirsch, C. M.; Jakubowski, S. D., Hydrogen peroxide measurements in recreational marine bathing waters in Southern California, USA. *Water research* **2010,** *44*, (7), 2203-2210.

72. Cooper, W. J.; Lean, D. R., Hydrogen peroxide concentration in a northern lake: photochemical formation and diel variability. *Environ Sci Technol* **1989,** *23*, (11), 1425-1428.

73. Morris, J. J.; Johnson, Z. I.; Wilhelm, S. W.; Zinser, E. R., Diel regulation of hydrogen peroxide defenses by open ocean microbial communities. *Journal of Plankton Research* **2016**, fbw016.

74. Seaver, L. C.; Imlay, J. A., Are respiratory enzymes the primary sources of intracellular hydrogen peroxide? *Journal of Biological Chemistry* **2004,** *279*, (47), 48742-48750.

75. Marsico, R. M.; Schneider, R. J.; Voelker, B. M.; Zhang, T.; Diaz, J. M.; Hansel, C. M.; Ushijima, S., Spatial and temporal variability of widespread dark production and decay of hydrogen peroxide in freshwater. *Aquatic Sciences* **2015,** *77*, (4), 523-533.

76. MacLean, R. C.; Gudelj, I., Resource competition and social conflict in experimental populations of yeast. *Nature* **2006,** *441*, (7092), 498-501.

77. Mitri, S.; Richard Foster, K., The genotypic view of social interactions in microbial communities. *Annual Review of Genetics* **2013,** *47*, 247-273.

78. Feng, F.; Goto, D.; Yan, T., Effects of autochthonous microbial community on the die-off of fecal indicators in tropical beach sand. *FEMS microbiology ecology* **2010,** *74*, (1), 214-225.

79. Wanjugi, P.; Harwood, V. J., The influence of predation and competition on the survival of commensal and pathogenic fecal bacteria in aquatic habitats. *Environmental microbiology* **2013,** *15*, (2), 517-526.

80. Pace, M.; Cole, J., Comparative and experimental approaches to top-down and bottom-up regulation of bacteria. *Microbial Ecology* **1994,** *28*, (2), 181-193.

81. Berryman, A. A., The Orgins and Evolution of Predator-Prey Theory. *Ecology* **1992,** *73*, (5), 1530-1535.

82. Friman, V.-P.; Dupont, A.; Bass, D.; Murrell, D. J.; Bell, T., Relative importance of evolutionary dynamics depends on the composition of microbial predator–prey community. *The ISME journal* **2016,** *10*, (6), 1352-1362.

83. Hilborn, R., The effect of spatial heterogeneity on the persistence of predator-prey interactions. *Theoretical population biology* **1975,** *8*, (3), 346-355.

84. Abrams, P. A., The evolution of predator-prey interactions: theory and evidence. *Annual Review of Ecology and Systematics* **2000**, 79-105.

85. Örmälä-Odegrip, A.-M.; Ojala, V.; Hiltunen, T.; Zhang, J.; Bamford, J. K.; Laakso, J., Protist predation can select for bacteria with lowered susceptibility to infection by lytic phages. *BMC evolutionary biology* **2015,** *15*, (1), 1.

86. Gonzalez, J. M.; Sherr, E. B.; Sherr, B. F., Size-selective grazing on bacteria by natural assemblages of estuarine flagellates and ciliates. *Applied and Environmental Microbiology* **1990,** *56*, (3), 583-589.

87. Matz, C.; Kjelleberg, S., Off the hook–how bacteria survive protozoan grazing. *Trends in microbiology* **2005,** *13*, (7), 302-307.

88. Korajkic, A.; Wanjugi, P.; Harwood, V. J., Indigenous microbiota and habitat influence Escherichia coli survival more than sunlight in simulated aquatic environments. *Applied and environmental microbiology* **2013,** *79*, (17), 5329-5337.

89. Ravva, S. V.; Sarreal, C. Z.; Mandrell, R. E., Strain differences in fitness of Escherichia coli O157: H7 to resist protozoan predation and survival in soil. **2014**.

90. Tremaine, S. C.; Mills, A. L., Inadequacy of the eucaryote inhibitor cycloheximide in studies of protozoan grazing on bacteria at the freshwater-sediment interface. *Applied and environmental microbiology* **1987,** *53*, (8), 1969-1972.

91. Li, D.; Hou, X., Effect of fungal elimination on bacteria and protozoa populations and degradation of straw dry matter in the rumen of sheep and goats. *ASIAN AUSTRALASIAN JOURNAL OF ANIMAL SCIENCES* **2007,** *20*, (1), 70.

92. Garcia, R.; Baelum, J.; Fredslund, L.; Santorum, P.; Jacobsen, C. S., Influence of temperature and predation on survival of Salmonella enterica serovar Typhimurium and expression of invA in soil and manure-amended soil. *Appl Environ Microbiol* **2010,** *76*, (15), 5025-31.

93. Marti, R.; Mieszkin, S.; Solecki, O.; Pourcher, A. M.; Hervio-Heath, D.; Gourmelon, M., Effect of oxygen and temperature on the dynamic of the dominant bacterial populations of pig manure and on the persistence of pig-associated genetic markers, assessed in river water microcosms. *Journal Of Applied Microbiology* **2011,** *111*, (5), 1159-1175.

94. Okabe, S.; Shimazu, Y., Persistence of host-specific Bacteroides-Prevotella 16S rRNA genetic markers in environmental waters: effects of temperature and salinity. *Appl Microbiol Biotechnol* **2007,** *76*, (4), 935-44.

95. Oliver, D. M.; Bird, C.; Burd, E.; Wyman, M., Quantitative PCR profiling of E. coli in livestock faeces reveals increased population resilience relative to culturable counts under temperature extremes. *Environ Sci Technol* **2016**.

96. Schulz, C. J.; Childers, G. W., Fecal bacteroidales diversity and decay in response to variations in temperature and salinity. *Appl Environ Microbiol* **2011,** *77*, (8), 2563-72.

97. Davies, C. M.; Long, J. A.; Donald, M.; Ashbolt, N. J., Survival of fecal microorganisms in marine and freshwater sediments. *Applied and Environmental Microbiology* **1995,** *61*, (5), 1888-1896.

98. Anderson, K. L.; Whitlock, J. E.; Harwood, V. J., Persistence and differential survival of fecal indicator bacteria in subtropical waters and sediments. *Applied and environmental microbiology* **2005,** *71*, (6), 3041-3048.

99. Byappanahalli, M. N.; Roll, B. M.; Fujioka, R. S., Evidence for occurrence, persistence, and growth potential of Escherichia coli and enterococci in Hawaii's soil environments. *Microbes and Environments* **2012,** *27*, (2), 164-170.

100. Mostofa, K. M.; Yoshioka, T.; Mottaleb, A.; Vione, D., *Photobiogeochemistry of organic matter: principles and practices in water environments*. Springer Science & Business Media: 2012.

101. Sherr, B. F.; Sherr, E. B.; Rassoulzadegan, F., Rates of digestion of bacteria by marine phagotrophic protozoa: temperature dependence. *Applied and Environmental Microbiology* **1988,** *54*, (5), 1091-1095.

102. Barcina, I.; Ayo, B.; Muela, A.; Egea, L.; Iriberri, J., Predation rates of flagellate and ciliated protozoa on bacterioplankton in a river. *FEMS Microbiology Letters* **1991,** *85*, (2), 141-149.

CHAPTER 3

PHOTO-PRODUCED HYDROGEN PEROXIDE CONTROLS FECAL INDICATOR BACTERIA AND *E. COLI* O157:H7 GROWTH DYNAMICS

Oladeinde, A., Erin Lipp, Chia-Ying Chen and Marirosa Molina

Submitted to Applied and Environmental Microbiology, 01/11/2017

ABSTRACT

The response of fecal bacteria to the presence of metabolites derived from the photodegradation of organic matter is not well characterized. In this study, we investigated the effect of photochemical production of reactive oxygen species (ROS) on the survival of fecal bacteria. We compared the survival dynamics of *Enterococcus faecalis*, *Escherichia coli* and *Escherichia coli* O157:H7 after inoculation into aqueous treatments containing sunlight-irradiated dissolved organic matter (DOM) derived from cattle feces. Fecal bacteria population grew by several orders of magnitude in the dark following addition into irradiated and non-irradiated spiked water. At low dissolved organic carbon (~2- 3 mg L^{-1} C), *E. faecalis* showed no signs of growth, while *E. coli* and *E. coli* O157:H7 exhibited ~ 2-log increase in concentration after 24 h of incubation at 25^{o}C. Sunlight irradiation of DOM before bacterial inoculation resulted in a significant decrease in *E. faecalis* concentration (1-log reduction) and in limited expression in genes associated with peroxidase and catalase activity (<2-fold change (FC)). Further, in the presence of *E. faecalis*, extracellular peroxide (HOOH) increased 170% after 6 h of dark incubation. In treatments containing *E. coli* or *E. coli* O157:H7, irradiation of DOM resulted in an increase in expression of HOOH scavenging genes (3.65 - 5.62 FC) and >95% reduction in extracellular HOOH. Our study suggests that fecal bacteria differ in their response to the presence of HOOH produced from the photodegradation of DOM. While *E. coli* is able to quickly activate an efficient HOOH scavenging mechanisms, *E. faecalis* struggles to grow under high HOOH concentrations, which may result in limiting regrowth potential in environments with high ROS production.

IMPORTANCE

Hydrogen peroxide (HOOH) is an uncharged form of reactive oxygen species that is omnipresent in surface waters. The concentration and mechanism of production of HOOH present in water resources is determined by microbial metabolism of dissolved organic matter (DOM) and DOM degradation by sunlight. Here, we show that HOOH generated from sunlight degradation of cattle manure derived DOM can cause significant inhibition of growth in fecal bacterial populations. We also demonstrate that the removal of exogenous HOOH by catalase and peroxidase genes was critical for efficient fecal bacterial growth.

Keywords: Cattle Fecal Extract, Dissolved Organic Matter, Sunlight, Hydrogen Peroxide, Oxidative Stress, Fecal Indicator Bacteria, *E. coli* O157:H7

INTRODUCTION

Elevated levels of fecal bacteria is one of the major causes of stream impairment in the United States, with agricultural activities considered the primary source of contamination [1, 2]. The attributable increase from agriculture stems from runoff contaminated with fecal microorganisms originating from crop and pastureland receiving manure applications [3]. In addition, An FIB increase in environmental matrices could occur due to regrowth. Recent studies have shown that commensal *E. coli* has the capacity to grow and flourish in surface waters under diverse environmental conditions [4-6]. Bradford, et al. [7] termed such behavior “regrowth” - the growth in the environment of nonindigenous bacteria of public health interest when optimal growth conditions are met.

The potential for regrowth is dependent on several environmental factors, particularly, resource availability [7-9]. Dissolved organic matter (DOM) represents a major

resource for all forms of life in surface waters. The sources of DOM are diverse and spatially variable [10-12]. One important fraction of DOM is the colored fraction (CDOM), which is responsible for absorbing UV light, and can lead to the photo-production of labile nutrients and/or reactive oxygen species (ROS) [13-17].

We have previously reported significant regrowth of *E. coli* under sunlight exposure compared to the growth dynamic observed in shaded controls in a study investigating the die-off of FIB in cattle feces under sunlight exposure [1]. A follow-up controlled experiment was conducted (unpublished data) in which a cattle fecal slurry was irradiated under a solar simulator for 9 h. To our surprise, we observed a 3-log increase in the *E. coli* population, while enterococci experienced a significant die-off. The results from the two studies suggested that while photo-production of labile nutrients could stimulate some bacterial growth, it could also result in the production of inhibitory agents responsible for bacterial die-off. We hypothesized that the latter could be attributed to the photo-production of ROS including, hydrogen peroxide (HOOH), hydroxyl radicals (.OH) and/or singlet oxygen ($^1O_2$), which have been shown to cause bacterial DNA damage [18, 19.]

Our objective in the current study was to understand the dynamic between photodegradation of DOM derived from agricultural sources and fecal bacteria survival. We used cattle fecal extract (CFE) as a DOM source to investigate the growth and survival of *Escherichia coli* O157:H7 strain B6914 (a surrogate pathogen that does not produce shiga-like toxins I or II) [20], and FIB including *Escherichia coli* C3000 (American Type Culture Collection (ATCC) strain 15597) and *Enterococcus faecalis* (ATCC 29212). We show that the production of HOOH from DOM photodegradation inhibited FIB growth. Removal of extracellular HOOH and expression of catalase and peroxidase genes were required for optimal growth.

MATERIALS AND METHODS

Cattle Fecal Extract Preparation. Fresh fecal samples were collected from 5 individual cows from a commercial farm in northeast Georgia on July 13, 2013. Fecal samples were composited, homogenized and made into 1:10 fecal slurry in 0.85% KCl and mixed for 1 h in a hand wrist shaker. The resulting fecal slurry was then centrifuged twice at 4000 x g for 10 min and the resulting supernatant was saved and referred to as cattle fecal extract (CFE). CFE was sequentially filtered through 1.2µm, 0.45µm and 0.2µm pore –sized polycarbonate membrane filters. CFE was then spiked into autoclaved phosphate buffered water (PBW) to concentrations mimicking high (1:10) and low (1:140) DOM inputs from agricultural runoff into streams. The absence of bacteria and lytic phages in CFE was confirmed by culturing 100µl of CFE in Brain Heart Infusion (BHI) broth and phage double agar overlay assay [21], respectively. For the overlay assay, bacteria strains used in the present study were used as phage hosts. Thereafter, CFE spiked water was divided into two volumes with one receiving solar radiation (Irradiated DOM-Spiked Water (I-DOMW)) and the other as a dark control (Non-irradiated DOM-Spiked Water (N-DOMW)).

Solar Irradiation. Sunlight irradiations were performed in an Atlas SunTest CPS/CPS+ solar simulator (Atlas Materials Testing Technology, Chicago, IL) equipped with a 1kW xenon arc lamp. Irradiance of the simulator in the UV spectral region was similar to mid-summer, midday natural sunlight at 33.95^{o}N, 83.33^{o}W (Athens, GA, USA) (Supp. Mat. Fig 3S1). Irradiation was carried out in 25ml quartz tubes for 12 h. Throughout irradiation, tubes were maintained at 20^{o}C in a NESLAB recirculating water bath. Spectral irradiance at the surface of the tubes was measured using an Optronic Laboratories OL756 Spectroradiometer. Incident irradiance at the tube surface, summed from 290 to 700 nm,

was 0.065 Wcm^{-2} [22]. After irradiation, the content of individual quartz tubes containing I-DOMW was combined and homogenized in a sterile beaker.

Inoculum Preparation. Overnight cultures of *E. coli* C3000 (ATCC 15597) - hereafter referred to as *E. coli*, *Enterococcus faecalis* (ATCC 29212) and *Escherichia coli* O157:H7 B6914-hereafter referred to as *E. coli* O157:H7 were harvested, washed and grown for an additional1.5 h to mid-logarithm phase (OD_{600} of 0.1) in BHI broth. Each culture was centrifuged at 4000 x g for 5 min and washed twice in phosphate buffered water (PBW). Thereafter, serial dilutions were made to the desired concentrations.

Microbiological Analysis. Following irradiation, I-DOMW, N-DOMW and PBW controls were separately inoculated with mid-logarithmic phase of each bacterium to a final concentration of 10^2-10^3 colony forming unit (CFU) ml^{-1}. Twenty milliliters of each treatment were dispensed into sterile 50ml centrifuge tubes and incubated in the dark at 25^oC in a refrigerated incubator shaker (150 rpm) (Innova 4230, New Brunswick Scientific, Edison, NJ). Triplicate samples per bacterium and treatment (18 biological replicates per treatment) were selected at random for analysis at 0.5, 6, 12, 24, 48 and 72 h (Fig. 3.1). *E. coli, E. faecalis* and *E. coli* O157:H7 were quantified by culture method using modified mTEC agar (EPA method 1603), mEI agar (EPA method 1600) and MUG *E. coli* O157:H7 agar supplemented with 100µg ml^{-1} ampicillin (Sigma Aldrich), respectively (Fig. 3.1).

Reactive Oxygen Species (ROS) Measurement. The production and concentration of singlet oxygen ($^1O_2$) and hydroxyl radicals (.OH) were determined separately as described by Chen and Jafvert [23]. $^1O_2$ was monitored via the loss of furfuryl alcohol (FFA) and the pseudo-state concentration of $^1O_2$ was determined. To detect OH, *p*-chlorobenzoic acid (pCBA), an OH scavenger, was added. *p*CBA was added at a low concentration (2µM)

allowing the pseudo-steady-state concentration of OH to be calculated. HOOH production was measured by the copper-DMP (2,9 –dimethyl-1, 10-phenanthroline) spectrophotometric method. A more complete description of the methods used to detect and quantify ROS is provided in the Supplemental Material.

RNA Isolation. For transcriptional studies, a similar experimental design (Fig. 3.1) was adopted but with an increase in the starting concentration of bacteria (10^6 CFU mL^{-1}) and volume (50mL) to aid in recovery of adequate concentrations for RT-qPCR. For more information on the modified experimental design and RNA isolation method, see the Supplemental Material.

RT-qPCR. Total RNA (100ng) from each bacterial culture was reverse transcribed with 100U of high capacity cDNA reverse transcription kit (Life Technologies, Grand Island, NY) per manufacturer's instructions. Primers were synthesized by Integrated DNA Technologies (Coralville, IA) (Suppl. Mat. Table 3S1). Real-time qPCR was performed on an ABI Prism 7500HT Fast Sequence Detection System (Applied Biosystems, Foster City, CA) with 40 amplification cycles using Fast SYBR Green PCR Master Mix as signal reporter. Each reaction was composed of 2µl of cDNA, 1µM sense and antisense primers for a total volume of 20µl. RT-qPCR was run in a Fast 96-well microtiter PCR plate using the following amplification conditions: 1 cycle for 10 min at 95°C; and 40 two-step cycles at 95°C for 15 seconds and 60°C for 60 seconds. Specificity of primer pairs was verified by melting curve analysis. qPCR efficiency was tested with serial dilutions of cDNA samples, and all ranged between 72% and 107%. To assess for reagent and genomic DNA contamination, no-template and no-reverse-transcriptase controls were included.

Expression of HOOH Scavenging Genes. Expression levels of *idnT*, *cysG*, *hcaT*, *gyrB* and *gapA* [24-26] were evaluated as possible reference controls for the normalization of *E.*

coli HOOH scavenging gene expression. The constitutive genes were carefully considered to identify the optimal normalization gene among the set of candidates by geNorm finder algorithm available under the Python library-Eleven [27]. Data were analyzed using the $2^{-\Delta\Delta CT}$ method described by Livak and Schmittgen [28]. For each gene, the ratio of expression in I-DOMW compared to that in N-DOMW was normalized to the expression of the top two ranked constitutive genes in *E. coli* (*gapA* and *gyrB*). For *E. faecalis,* this ratio was normalized to the expression of *rpoB* and *gyrB* [29].

Nutrient Analysis. To determine the rate of removal of nutrients between bacteria in I-DOMW and N-DOMW, samples collected at each time point were filtered through 0.2µm pore size filters and the filtrates were analyzed for nitrate (NO_3), ammonium (NH_4), orthophosphate (PO_4^3) and dissolved organic carbon (DOC). [NH_4^+] and [PO_4^{3-}] were determined by colorimetric methods and [NO_3^-] was analyzed as described by Crumpton, et al. [30] using the second-derivative spectroscopy method. DOC was determined using a total organic carbon analyzer (TOC-V_{CPH}, Shimadzu, Kyoto, Japan) equipped with auto samplers. Due to the low concentration of nutrients (below methods limit of detection) in 1:140 DOM dilution, nutrient concentrations were not determined.

Statistical Analysis. The growth curve for each pathogen under the two conditions tested was fitted using the Gompertz growth model [31] (equation 1). The model is available under the grofit package in R [32]. The model describes the number of organisms (N) or the logarithm of the number of organisms [log (N)] as a function of time.

$$\text{Equation 1} \quad Y = A \exp\{-\exp[\mu^e/A\,(\lambda - t) + 1]$$

Where the maximum specific growth rate, µ, is defined as the tangent in the inflection point; the lag time, λ, is defined as the x-axis intercept of this tangent; and the asymptote

[$A = \ln (N_\infty/N_O)$] is the maximal value reached. Since bacteria grow exponentially, it is useful to plot the logarithm of the relative population size [$y = \ln (N/N_0)$] against time (t).

A profile analysis was performed to compare bacteria growth rates (μ_6 vs. $\mu_{0.5}$, μ_{12} vs. μ_6, μ_{24} vs. μ_{12}, μ_{48} vs. μ_{24}, μ_{72} vs. μ_{48}) between treatments, after which a multivariate analysis of variance (MANOVA) was used to test for significant differences between bacteria incubated in I-DOMW and N-DOMW microcosm. We do recognize that low sample size can affect the power and the homogeneity of the variance test, however, profile analysis still provides us more power than univariate tests[33]. Graphs were plotted in SigmaPlot (Systat Software, San Jose, CA)

RESULTS

Bacterial Regrowth Potential. The regrowth potential of *E. coli, E. coli* O157:H7 and *E. faecalis* was monitored for 72 h in the dark at two levels of dilution. In addition, the effect of DOM photodegradation on overall bacterial growth was investigated. All three bacteria showed a faster growth rate and higher yield in 1:10 DOM dilutions than 1:140 ($P< 0.05$), with *E. faecalis* showing no signs of growth in 1:140 (Table 3.1, Fig. 3.2). *E. coli* and *E. coli* O157:H7 showed similar growth rates at all conditions with maximum growth rates after 12 h; however, *E. coli* consistently had a higher final concentration. Sunlight irradiation of DOM spiked water before inoculation did not result in a significant higher growth rate for any of the bacteria tested, however we observed a significantly lower growth rate after 6 and 12 h of incubation in 1:10 I-DOMW for *E. coli* O157:H7 ($P<0.01$) (Fig. 3.2c). For *E. faecalis*, maximum growth rate in I-DOMW was not possible until 24 h while in N-DOMW maximum growth rate was achieved after 6 h. Our results suggest that photodegradation of DOM resulted in a significantly reduced growth rate for *E. faecalis* after 6, 12, 24, 48 h of dark incubation ($P<0.05$) (Fig. 3.2a).

Nutrient Loss. The average (± standard error (SE)) starting concentration of ammonium, nitrate, DOC and orthophosphate were 0.68 ± 0.07 mg L^{-1}, 0.55 ± 0.04 mg L^{-1}, 32.48±1.52 mg L^{-1} and 8.14 ± 0.48 mg L^{-1}, respectively, for I-DOMW, and 0.73 ± 0.07 mg L^{-1}, 0.44 ± 0.03 mg L^{-1}, 41 ± 4.53 mg L^{-1}, 8.50 ± 0.72 mg L^{-1}, respectively, for N-DOMW. Nutrient loss differed between bacteria but overall, there was a decline in nutrient concentration with time, except for orthophosphate which did not change during the length of the study (Supp. Mat. Fig. 3S4-7). There were gains and losses relative to the starting nutrient concentrations before bacteria inoculation, suggesting immobilization and mineralization between the two-nitrogen species (NH_4-N, NO_3-N) and DOC. For more on nutrient results see supplemental material.

ROS Production from DOM Photo-degradation. ROS production including $^1O_2$ and HOOH was observed during 12 h of irradiation previous to bacterial inoculation. No hydroxyl radicals (.OH) were detected. Sunlight irradiation of 1:10 I-DOMW resulted in the photo-production of $^1O_2$ at a steady state of 2.32^{-13}M and HOOH at a concentration of 15.38±0.81μM.

Extracellular HOOH Concentrations during Dark Incubation. In a separate experiment, we monitored the removal of extracellular HOOH during dark incubation in 1:10 I-DOMW using higher starting bacterium inoculum. *E. coli* and *E. coli* O157:H7 had HOOH concentrations below our method's limit of detection (<0.5μM) after 6 h of dark incubation (Fig. 3.3 b and c). In contrast, HOOH concentrations increased by 170% in *E. faecalis* after 6 h and by the end of the experiment, the overall concentration had increased by 140%. There was no noticeable overall decline in HOOH concentrations in I-DOMW controls (no bacteria inoculated) during the experiment (Fig. 3S2).

Expression of Oxidative Stress Genes during Dark Incubation. Bacterial cells recovered at 0.5, 6, 12, 24 and 48 h in I-DOMW showed an increase in expression of selected oxidative stress genes in comparison with N-DOMW grown cells (Fig. 3.4a-c) and the expression of these genes varied between bacteria.

E. coli showed an immediate increase in expression in 3 of 4 oxidative stress genes following inoculation into I-DOMW (3.65 - 5.62-fold change (FC)). These genes remained upregulated for up to 48 h (0.01- 2.11-FC) except *katG* which was downregulated at 12 and 24 h (0.12- 0.22-FC) and *ahpF* which was downregulated at 24 h (0.8-FC) (Fig. 3.4c). In contrast, *E. coli* O157:H7 showed an immediate increase in all 4 genes following inoculation (0.2 - 6.35-FC); however, after 6 h of incubation there was a downregulation in 3 of 4 genes (0.08 - 1.17-FC) except *oxyS*, which remained upregulated for 48 h (0.53 - 1.64-FC) (Fig. 3.4c).

In contrast to *E. coli*, *E. faecalis* showed minimal expression of oxidative stress genes following inoculation into I-DOMW (0.15 -1.55-FC) (Fig. 4a). NADH peroxidase (*npr*) and thiol peroxidase (*tpx*) genes were upregulated and downregulated, respectively, at each time point investigated (0.15 -1.09-FC). Catalase (*katA*) gene was only upregulated after 6 h while *ahpC* gene was upregulated at time point 6, 12, and 24 h (0.12 - 0.63-FC). The *oxyR* and *fur* regulator was upregulated and downregulated, respectively, (0.22 – 1.55-FC) except at 6 h when *oxyR* was downregulated (Fig. 3.4a).

Although these results represent the expression of genes at a high bacterial starting concentration (~10^6 CFU mL^{-1}; see supplemental material), a similar expression pattern was seen with lower inocula (~10^3 CFU mL^{-1}). For example, upregulation of HOOH scavenging genes in *E. coli* and *E. coli* O157:H7 was observed for up to 12 h (0.27- 4.37-FC), while the expression of these genes was only observed for up to 6 h for *E. faecalis*

(0.2 - 0.86- FC) (data not shown). However, due to poor RNA recovery at lower inocula, genomic RNA was pooled from triplicate samples and normalized, resulting in a sample size (n) of 1, and precluding us from conducting further statistical analysis.

Significant Factors for Regrowth. The effects of nutrients and sunlight irradiation of DOM on culturable bacterial concentrations (CFU) were determined by univariate analysis of variance (GLM model) with sunlight irradiation of DOM and nutrient as fixed factors. There was no significant interaction between irradiation of DOM and nutrient concentrations. Overall, irradiation of DOM before bacterial inoculation did not result in a significant higher growth rate for any of the fecal bacteria. However, we observed significant effects on bacterial concentrations at different time points. For example, irradiation resulted in a significantly lower *E. coli* O157:H7 concentration after 6 h of incubation ($p<0.01$) (Fig. 3.2c) but significantly higher concentrations of *E. coli* after 48 and 72 h of incubation ($P<0.01$) (Fig. 3.2b). On the other hand, irradiation of DOM resulted in a significantly lower *E. faecalis* concentrations at all time points except 0.5 h (Fig. 3.2a).

DISCUSSION

The survival of bacteria is dependent not only on DOM availability but also on the effect of potential DOM transformations in the environment, In this study, we are particularly interested in DOM transformations mediated by abiotic factors, such as sunlight [34, 35]. We determined the growth potential of *E. coli* and *E. faecalis*, commensal bacteria in warm-blooded animals and *E. coli* O157: H7, a pathogen of public health importance, using cattle fecal extracts as DOM source. Our aim was to gain a better understanding of the indirect role of sunlight by measuring the photochemical release of nitrogen-rich compounds and ROS from CDOM. Our results show that all three bacteria can grow up to several logs in water spiked with DOM derived from cattle manure. Both *E.*

coli and *E. coli* O157: H7 showed a dose response where the higher the concentration of DOM, the higher the growth potential and yield. Similar results, where *E. coli* concentration in the water column increased by two orders of magnitude in response to nutrient spikes from cow manure slurries have been observed [36]. The lower growth potential shown by *E. faecalis* in our study suggests that *E. faecalis* may have a higher or different nutrient requirement compared to *E. coli* [4, 37]. For instance, del Mar Lleo et al.[37] showed that oligotrophy was the main parameter inhibiting divisional capability and activating survival strategies in *E. faecalis*, *E. faecium* and *E. hirae*.

Further, many studies have demonstrated enhanced microbial production after amending filtered stream or lake water samples with sunlight irradiated DOM substrates [38-41]. These studies focused on the total bacterial concentration increase and not a bacterium-specific response. At high DOM (1:10; 31- 45 mg L^{-1} C), photodegraded DOM did not result in significant bacterial growth for any of the bacteria used in this study. This suggests that the majority of the DOM extracted from cattle manure used in our study is readily bioavailable for uptake by bacteria and photodegradration did not significantly increase the labile pool [42, 43]. Furthermore, an inhibitory effect was observed on *E. faecalis* population where photodegraded DOM resulted in both significantly lower growth rate (μ) and maximum growth (A). In addition, there was a differential response between *E. coli* and *E. coli* O157:H7 at lower DOM concentrations (1:140; ~2 - 3mg L^{-1} C). *E. coli* O157:H7 showed a 6 h lag phase and lower maximum growth in I-DOMW compared to N-DOMW while *E. coli*, showed no noticeable inhibitory effect in response to the presence of metabolites produced from DOM photodegradation.

Inhibitory response has been reported by others investigating total heterotrophic bacterial growth in photodegraded DOM [40, 41]. We detected $^1O_2$ and HOOH during DOM

irradiation for 12 h; which has been shown to cause oxidative stress in bacteria, bacterial DNA damage, and increased resistance to ROS and antibiotics [18, 19, 44]. However, the inhibitory role of singlet oxygen may be limited by its low concentration and short half-life. In a controlled laboratory study (see supplemental material), we used sunlight irradiated rose bengal to generate $^1O_2$ at the same steady state as produced from DOM in this study (7.38^{-13}M), after which bacteria was immediately inoculated and monitored in the dark for 3 h. We observed no decline in bacterial concentrations for *E. coli*, *E. faecalis*, or *E. coli* O157:H7 (Fig. 3S3). Maraccini, et al. [45] also reported no correlation between bulk-phase steady state concentrations of $^1O_2$ and exogenous indirect photo-inactivation rate constants.

Hydrogen peroxide is an uncharged ROS that can penetrate the bacterial membrane. In addition, the lifetime of HOOH in natural waters have been reported to range from several hours to days [46, 47]. Hydrogen peroxide is mutagenic and can directly oxidize unincorporated intracellular ferrous iron in bacteria, some of which is associated with DNA. This series of reactions with iron (fenton reaction) generates the more damaging $OH^{\cdot}$ and also inactivates a family of dehydratases [18, 48]. Approximately, one micromolar of intracellular HOOH is sufficient to cause crippling levels of DNA damage in *E. coli* [49]. Anesio et al.[38] showed that the suppression of bacterial carbon production was highly correlated with the concentration of photochemically formed HOOH and concluded that extracellular HOOH concentrations of about 2μM to 3μM were inhibitory for bacteria. That said, bacteria have developed systems to help scavenge HOOH and minimize DNA damage [19], mostly by converting HOOH to water. This mechanism of defense differs by bacteria. For example, *E. coli* has developed three important scavenging enzymes for HOOH removal: alkyl hydroperoxide reductase (*ahpCF*), catalase G (*katG)* and catalase E

(*katE*) [18, 26, 50]. These genes belong to the OxyR system, which is the regulon responsible for sensing oxidative stress. *E. faecalis* also possesses HOOH scavenging enzymes with similar functions as *E. coli.* Three *E. faecalis* peroxidases, NADH peroxidase (*npr*), alkyl hydroperoxide reductase (*ahp*), and thiol peroxidase (*tpx*), have specialized roles in oxidative defense [51]. Further, the hydrogen peroxide regulon (HypR), an OxyR type regulon now known to regulate the *ahpCF* genes [52] and the Fur regulon, an oxidative stress transcription regulator have both been shown to have specialized roles in oxidative stress resistance in *E. faecalis* [29]. Upon detection of HOOH, the *oxyR* gene serves as a positive transcription factor for the OxyR regulon members. In our study, there was an immediate increase in expression in 7 of 8 genes studied (0.2 -6.4 -FC) from the OxyR regulon at 0.5 h (post inoculation) in *E. coli* and *E. coli* O157:H7; in contrast, for *E. faecalis* there was only minimal induction in 2 of 6 genes at 0.5 h.

The observed low expression of HOOH scavenging genes for *E. faecalis* was unexpected. *E. faecalis* encodes an NADH peroxidase (*npr*) that uses NADH to directly reduce HOOH to water; and has been shown to be an important defense against both exogenously added and endogenously produced HOOH under a variety of growth conditions [53]. Mutants lacking *npr* were observed to accumulate HOOH in the growth medium at an enhanced rate [51, 54]. One of these studies also showed that Δ*npr* exhibited enhanced resistance to ceftriaxone, a β-lactam antibiotic [54]. We observed no substantial expression of the *npr* gene (< 2- FC), however the *npr* gene was the only gene upregulated at each time point (Fig. 4a). It should be noted that *E. faecalis* growth rate and maximum growth was also significantly lower in I-DOMW compared to N-DOMW control. More importantly, HOOH concentration increased significantly in the I-DOMW treatment,

suggesting *E. faecalis* may be accumulating HOOH from the aerobic metabolism of glycerol [55].

Ambient concentrations of HOOH (nM-μM) as produced from DOM in our study have been reported in surface waters, suggesting that peroxide induced biological responses may be a predominant process in aquatic ecosystems [46]. Our results suggest that the inhibitory effect observed on these bacteria was more likely to be due to the presence of HOOH in the DOM-spiked treatments. In our study, HOOH measured in I-DOMW before bacterial inoculation was > 10 μM; with more than 95% reduction observed after *E. coli* and *E. coli* O157:H7 inoculation. On the other hand, HOOH kept increasing in I-DOMW after inoculation of *E. faecalis*. The sensitivity of *E. faecalis* to ROS compared to *E. coli* has been reported [45, 56-58]. Our result provides supporting evidence that under exogenous ROS exposure from photodegraded DOM, *E. faecalis* potential for regrowth may be limited due to the accumulation of deleterious amounts of HOOH in the growing medium. In contrast, *E. coli* and *E. coli* O157: H7 can remove up to 15μM concentrations of exogenous HOOH.

It should be noted that the growth dynamics shown by pure cultures of bacteria under controlled and sterile conditions could differ in the environment owing to other abiotic factors (e.g. temperature) and biotic factors including predation (“top-down control”) and/or competition (“bottom-up control”) [59, 60]. Several studies have suggested that antagonistic agents and indigenous microbiota play important roles in the survival of FIB [61-63]. Our results suggest that these factors concomitantly with the abiotic factor discussed above help control FIB concentrations in environmental systems.

CONCLUSION

This study provides, for the first time, information on the interaction of agriculturally derived DOM, sunlight and HOOH on the growth and survival dynamics of fecal bacteria. Moreover, from a water quality monitoring perspective there are several important implications. Our findings suggest that the behavior of *E. coli* and Enterococci could differ in surface waters depending on the concentration of DOM present and its potential transformations in the presence of sunlight. *E. coli* demonstrated that it can grow under both high and low DOM inputs, which may suggest a potential for regrowth upon entry into eutrophic or meso-oligotrophic surface waters. On the other hand, *E. faecalis* regrowth potential may be limited to only eutrophic environments. More importantly, the indirect role of sunlight from the production of exogenous HOOH from DOM photodegradation may further confound this dynamic. Our results suggests that while *E. coli* has a mechanism to efficiently scavenge exogenous HOOH, *E. faecalis* seems to struggle under high exposures, which could result in a overall limited regrowth potential in environments with high concentrations of ROS.

ACKNOWLEDGEMENTS

We are grateful to Kayleigh Hall and Blake Snyder for their help with sample analysis as well as Roger Burke for his help with nutrient analysis. We also appreciate S.T Purucker and Jonathan Flaishan's assistance with the RT-qPCR analysis and Dr. Richard Zepp for valuable advice during the solar simulation experiments. We thank the Kennedy family at Covenant Valley Farm and the Nixon family at Cane Creek Farm, Inc., for allowing us access to their cattle. This work was supported by the Environmental Protection Agency (EPA) Star Fellowship [FP-91766701 to A.O] and EPA's Office of

Research and Development. Any opinions expressed in this paper are those of the authors and do not necessarily reflect the official positions and policies of the U.S. EPA and any mention of products or trade names does not constitute recommendation for use. The authors declare no competing commercial interests in relation to the submitted work.

FIGURES AND TABLES

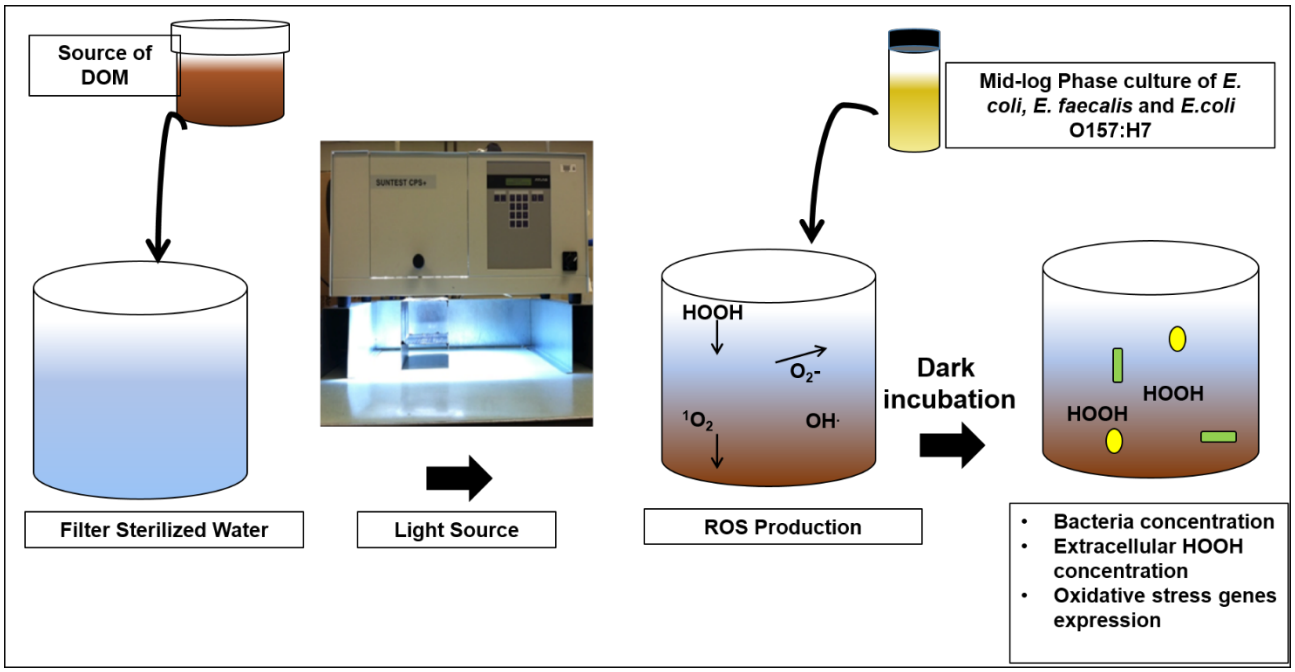

Figure 3.1. Schematic of experimental design. Fresh fecal samples were collected from 5 individual cattle from a commercial farm in Northeast Georgia. Fecal samples were composited, homogenized and made into 1:10 fecal slurry in 0.85% KCl and shook for 1hr in a hand wrist shaker. Fecal slurry was then centrifuged twice at 6000 rpm for 10 min and the resulting supernatant was termed cattle fecal extract (CFE). CFE was sequentially filtered through 1.2µm, 0.45µm and 0.2µm membrane filters. CFE was used as source of DOM throughout the experiment. Solar irradiation was performed in an Atlas SunTest CPS/CPS+ solar simulator (Atlas Materials Testing Technology, Chicago, IL) equipped

with a 1kW xenon arc lamp. Irradiance of the simulator in the UV spectral region was very similar to mid-summer, midday natural sunlight at 33.95^{o}N, 83.33^{o}W (Athens, GA). Laboratory strains of *E. coli*, *E. faecalis* and *E. coli* O157:H7 grown to mid-logarithm phase were separately inoculated into DOM after 12 h sunlight irradiation and incubated in the dark at 25^{o}C for 72 h.

A

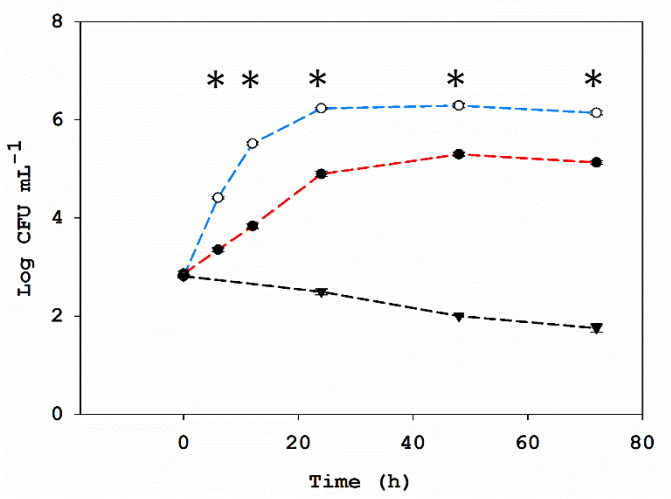
Log CFU mL-1
Time (h)
0
2
4
6
8
0
20
40
60
80
* * * * *

B

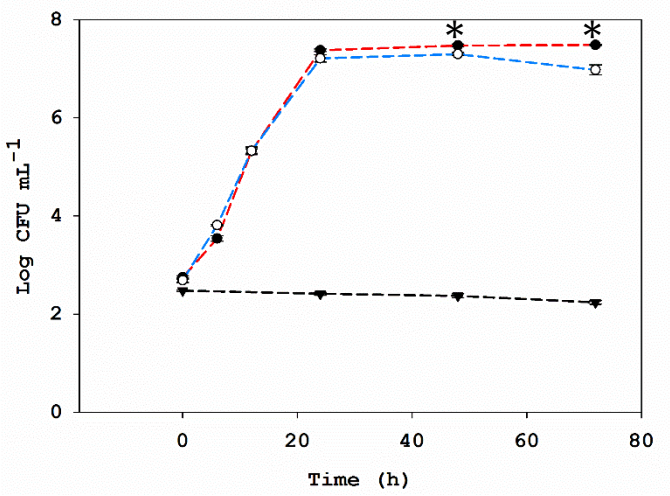
Log CFU mL-1
Time (h)
0
2
4
6
8
0
20
40
60
80
* *

C

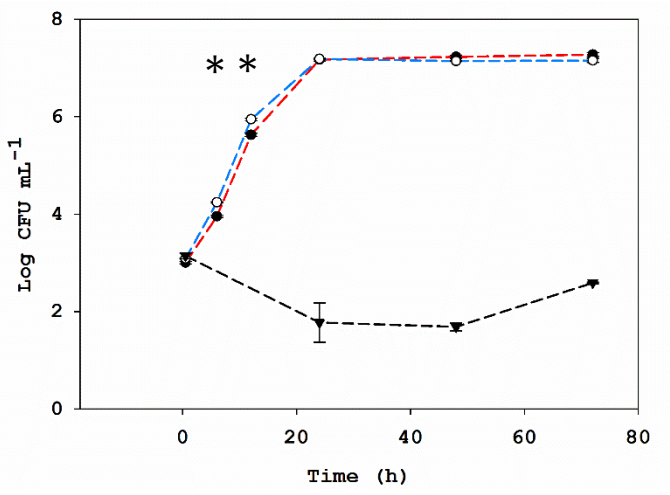
Log CFU mL-1
Time (h)
0
2
4
6
8
0
20
40
60
80
* *

D

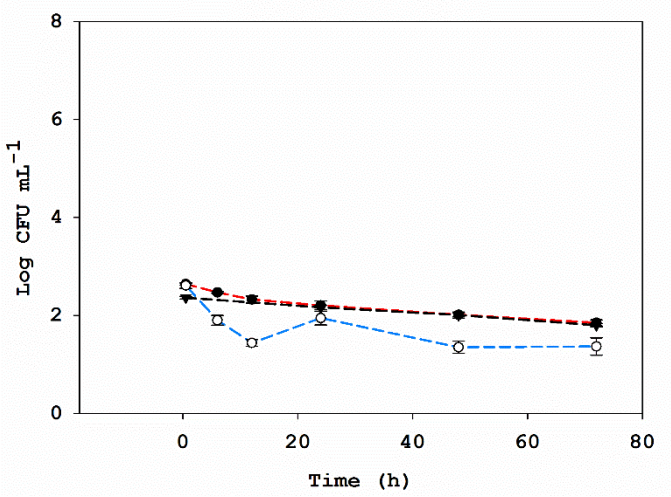
Log CFU mL-1
0
2
4
6
8
0
20
40
60
80
Time (h)

E

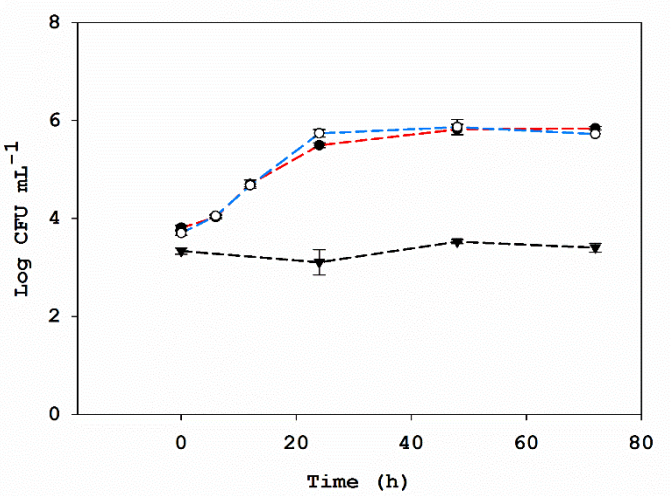
Log CFU mL-1
0
2
4
6
8
0
20
40
60
80
Time (h)

F

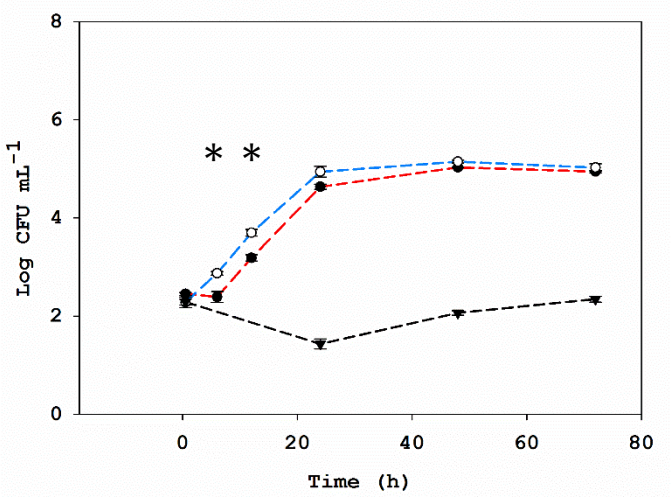
* *
Log CFU mL-1
0
2
4
6
8
0
20
40
60
80
Time (h)

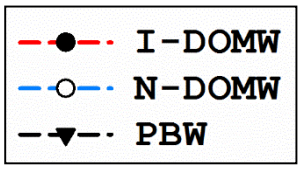

Figure 3.2: Irradiation of DOM had significant effect on bacteria growth. Triplicate samples per bacterium (18 tubes per treatment) were selected for analysis after 0.5, 6, 12, 24, 48 and 72 h of dark incubation. Bacteria was cultured on a selective medium. Concentrations are reported in colony forming units (CFU) per ml. Growth curve of (A) *E. faecalis* (B) *E. coli* (C) *E. coli* O157:H7 in 1:10 DOMW and (D) *E. faecalis* (E) *E. coli* (F) *E. coli* O157:H7 in 1:140 DOMW. Error bars represent standard errors. *denotes significance at P <0.05 level.

A

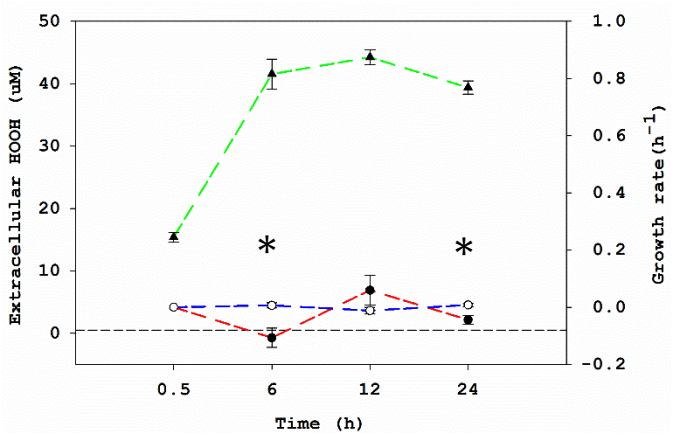
Extracellular HOOH (uM)
Growth rate(h-1)
Time (h)
0.5
6
12
24
*
*

B

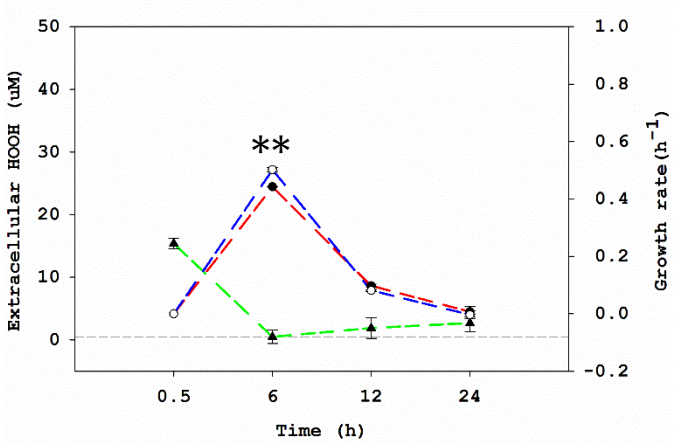
Extracellular HOOH (uM)
Growth rate(h-1)
Time (h)
0.5
6
12
24
**

C

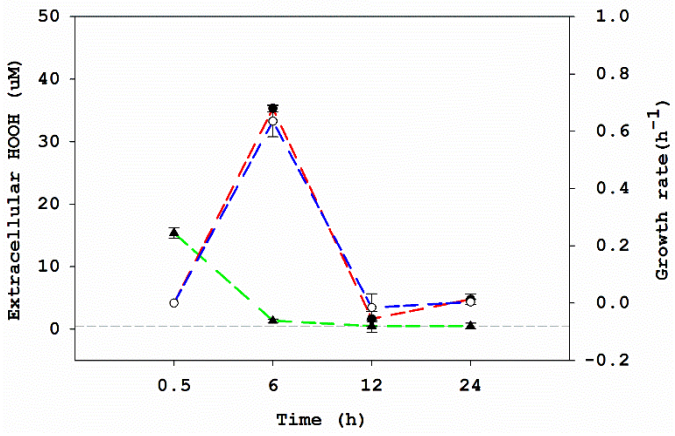
Extracellular HOOH (uM)
Growth rate(h-1)
Time (h)
0.5
6
12
24

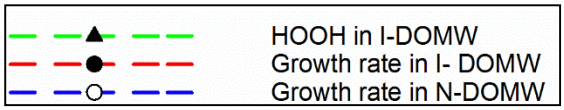

Figure 3.3. Irradiation of DOM (I-DOMW) prior to bacteria inoculation produces exogenous HOOH. Triangles represent extracellular HOOH concentration during dark incubation in I-DOMW and N-DOMW in the presence of (A) *E. faecalis* (B) *E. coli* (C) *E. coli* O157:H7. Bacteria were collected at 0.5, 6, 12, and 24 h during dark incubation and filter sterilized with a 0.22µm syringe filter. Filtrate (n = 3 per group) was quantified for HOOH using the copper-DMP method. Horizontal short dash lines represent method detection limit (0.5µM of pure HOOH). Growth rate per time point are plotted on right y-axis (circles). Growth rate was derived from the following equation: $dN/dt = kN$, where N is the concentration of cells, t is the time and k is the growth rate constant. Error bars represent standard errors. *denotes level of significance for the effect of sunlight irradiation of DOM on bacteria growth rate per time point (*<0.05, **<0.01).

A

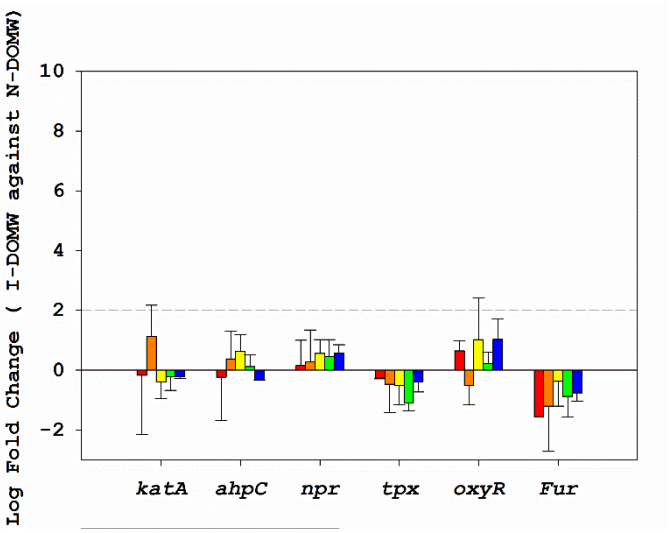
Log Fold Change (I-DOMW against N-DOMW)
10
8
6
4
2
0
-2
katA
ahpC
npr
tpx
oxyR
Fur

B

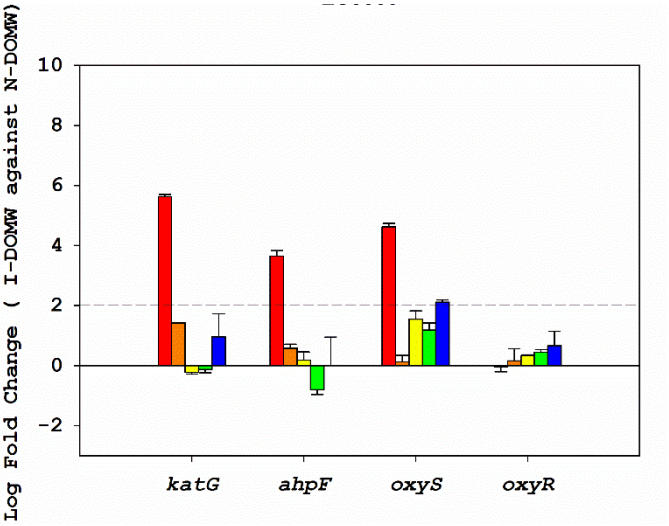
Log Fold Change (I-DOMW against N-DOMW)
10
8
6
4
2
0
-2
katG
ahpF
oxyS
oxyR

C

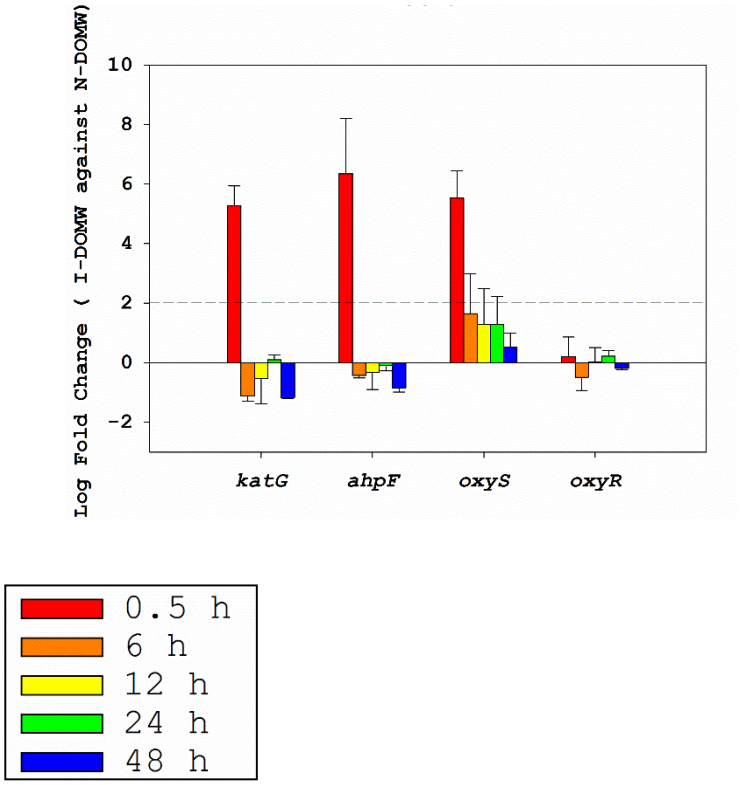

Figure 3.4: Irradiation of DOM alters oxidative stress genes expression profile in FIB and *E. coli* O157:H7. Fold changes (2^{-ddct}) in oxidative stress genes in (A) *E. faecalis* (B) *E. coli* and (C) *E. coli* O157:H7 grown in 1:10 I-DOMW compared to N-DOMW. Total RNA was extracted from bacterial cultures collected at time 0.5, 6, 12, 24 and 48 h. RT-qPCR was performed on duplicate samples per treatment per bacteria. Samples were normalized by the geometric mean of constitutive genes. Short dash lines represent level of significance of ≥ 2- fold change. Error bars represent standard deviation.

Table 3.1: Overall growth rate of FIB and *E. coli* O157:H7 in DOMW was determined using the Gompertz growth model (Zwietering et al., 1990).

Bacteria	CFE concentration	Treatment	Growth rate (h^{-1})	Maximum growth ($LogCFU\ mL^{-1}$)
E. coli	1:10	I-DOMW	0.293	7.49
		N-DOMW	0.235	7.3
	1:140	I-DOMW	0.107	5.84
		N-DOMW	0.0993	5.88
E. coli O157:H7	1:10	I-DOMW	0.257	7.27
		N-DOMW	0.255	7.18
	1:140	I-DOMW	0.115	5.03
		N-DOMW	0.126	5.16
E. faecalis	1:10	I-DOMW	**0.089**	**5.31**
		N-DOMW	0.279	6.29
	1:140	I-DOMW	ND	ND
		N-DOMW	ND	ND

Boldness denotes significant differences between irradiated and non-irradiated CFE ($P<0.05$). ND, not determined.

REFERENCES

1. Oladeinde, A.; Bohrmann, T.; Wong, K.; Purucker, S.; Bradshaw, K.; Brown, R.; Snyder, B.; Molina, M., Decay of Fecal Indicator Bacterial Populations and Bovine-Associated Source-Tracking Markers in Freshly Deposited Cow Pats. *Applied and environmental microbiology* **2014,** *80*, (1), 110-118.

2. USEPA, National water quality inventory: report to congress, 2004 reporting cycle. EPA/841/R-08/001 In Washington DC, 2009.

3. Whelan, G.; Kim, K.; Pelton, M. A.; Soller, J. A.; Castleton, K. J.; Molina, M.; Pachepsky, Y.; Zepp, R., An integrated environmental modeling framework for performing Quantitative Microbial Risk Assessments. *Environmental Modelling & Software* **2014,** *55*, 77-91.

4. John, P.; Haller, L.; Kottelat, R.; Sastre, V.; Arpagaus, P.; Wildi, W., Persistence and growth of faecal culturable bacterial indicators in water column and sediments of Vidy Bay, Lake Geneva, Switzerland. *Journal of Environmental Sciences* **2009,** *21*, (1), 62-69.

5. Vital, M.; Hammes, F.; Egli, T., Escherichia coli O157 can grow in natural freshwater at low carbon concentrations. *Environmental Microbiology* **2008,** *10*, (9), 2387-2396.

6. McCrary, K. J.; Case, C. L. H.; Gentry, T. J.; Aitkenhead-Peterson, J. A., Escherichia coli regrowth in disinfected sewage effluent: Effect of DOC and nutrients on regrowth in laboratory incubations and urban streams. *Water, Air, & Soil Pollution* **2013,** *224*, (2), 1-11.

7. Bradford, S. A.; Morales, V. L.; Zhang, W.; W., H. R.; Packman, A. I.; Mohanram, A.; Welty, C., Transport and Fate of Microbial Pathogens in Agricultural Settings. *Critical Reviews in Environmental Science & Technology* **2013,** *43*, (8), 775-893.

8. van Elsas, J. D.; Semenov, A. V.; Costa, R.; Trevors, J. T., Survival of Escherichia coli in the environment: fundamental and public health aspects. *The ISME journal* **2011,** *5*, (2), 173-183.

9. Fierer, N.; Nemergut, D.; Knight, R.; Craine, J. M., Changes through time: integrating microorganisms into the study of succession. *Research in microbiology* **2010,** *161*, (8), 635-642.

10. Graeber, D.; Boëchat, I. G.; Encina-Montoya, F.; Esse, C.; Gelbrecht, J.; Goyenola, G.; Gücker, B.; Heinz, M.; Kronvang, B.; Meerhoff, M., Global effects of agriculture on fluvial dissolved organic matter. *Scientific reports* **2015,** *5*.

11. Heinz, M.; Graeber, D.; Zak, D.; Zwirnmann, E.; Gelbrecht, J.; Pusch, M. T., Comparison of organic matter composition in agricultural versus forest affected headwaters with special emphasis on organic nitrogen. *Environ Sci Technol* **2015,** *49*, (4), 2081-2090.

12. Bida, M. R.; Tyler, A. C.; Pagano, T., Quantity and composition of stream dissolved organic matter in the watershed of Conesus Lake, New York. *Journal of Great Lakes Research* **2015,** *41*, (3), 730-742.

13. Bushaw, K. L.; Zepp, R. G., Photochemical release of biologically available nitrogen from aquatic dissolved organic matter. *Nature* **1996,** *381*, (6581), 404.

14. Moran, M. A.; Zepp, R. G., Role of photoreactions in the formation of biologically labile compounds from dissolved organic matter. *Limnology and Oceanography* **1997,** *42*, (6), 1307-1316.

15. Häder, D.-P.; Williamson, C. E.; Wängberg, S.-Å.; Rautio, M.; Rose, K. C.; Gao, K.; Helbling, E. W.; Sinha, R. P.; Worrest, R., Effects of UV radiation on aquatic ecosystems

and interactions with other environmental factors. *Photochemical & Photobiological Sciences* **2015,** *14*, (1), 108-126.

16. Scully, N. M.; Cooper, W. J.; Tranvik, L. J., Photochemical effects on microbial activity in natural waters: the interaction of reactive oxygen species and dissolved organic matter. *FEMS microbiology ecology* **2003,** *46*, (3), 353-357.

17. Pullin, M. J.; Bertilsson, S.; Goldstone, J. V.; Voelker, B. M., Effects of sunlight and hydroxyl radical on dissolved organic matter: Bacterial growth efficiency and production of carboxylic acids and other substrates. *Limnology and Oceanography* **2004,** *49*, (6), 2011-2022.

18. Imlay, J. A., The molecular mechanisms and physiological consequences of oxidative stress: lessons from a model bacterium. *Nature Reviews Microbiology* **2013,** *11*, (7), 443-454.

19. Imlay, J. A., Transcription Factors That Defend Bacteria Against Reactive Oxygen Species. *Annual Review of Microbiology* **2015,** *69*, (1).

20. Fratamico, P. M.; Deng, M. Y.; Strobaugh, T. P.; Palumbo, S. A., Construction and characterization of Escherichia coli O157: H7 strains expressing firefly luciferase and green fluorescent protein and their use in survival studies. *Journal of Food Protection*® **1997,** *60*, (10), 1167-1173.

21. Adams, M. H., *Bacteriophages*. Interscience: London, United Kingdom, 1959.

22. Chen, C.-Y.; Zepp, R. G., Probing photosensitization by functionalized carbon nanotubes. *Environ Sci Technol* **2015,** *49*, (23), 13835-13843.

23. Chen, C.-Y.; Jafvert, C. T., Photoreactivity of carboxylated single-walled carbon nanotubes in sunlight: reactive oxygen species production in water. *Environ Sci Technol* **2010,** *44*, (17), 6674-6679.

24. Zhou, K.; Zhou, L.; Lim, Q. E.; Zou, R.; Stephanopoulos, G.; Too, H.-P., Novel reference genes for quantifying transcriptional responses of Escherichia coli to protein overexpression by quantitative PCR. *BMC molecular biology* **2011,** *12*, (1), 18.

25. Kyle, J. L.; Parker, C. T.; Goudeau, D.; Brandl, M. T., Transcriptome analysis of Escherichia coli O157: H7 exposed to lysates of lettuce leaves. *Applied and environmental microbiology* **2010,** *76*, (5), 1375-1387.

26. Michán, C.; Manchado, M.; Dorado, G.; Pueyo, C., In vivo transcription of the Escherichia coli oxyRregulon as a function of growth phase and in response to oxidative stress. *Journal of bacteriology* **1999,** *181*, (9), 2759-2764.

27. Vandesompele, J.; De Preter, K.; Pattyn, F.; Poppe, B.; Van Roy, N.; De Paepe, A.; Speleman, F., Accurate normalization of real-time quantitative RT-PCR data by geometric averaging of multiple internal control genes. *Genome biology* **2002,** *3*, (7), research0034.

28. Livak, K. J.; Schmittgen, T. D., Analysis of relative gene expression data using real-time quantitative PCR and the 2− ΔΔCT method. *methods* **2001,** *25*, (4), 402-408.

29. Riboldi, G. P.; Bierhals, C. G.; Mattos, E. P. d.; Frazzon, A. P. G.; Frazzon, J., Oxidative stress enhances the expression of sulfur assimilation genes: preliminary insights on the Enterococcus faecalis iron-sulfur cluster machinery regulation. *Memórias do Instituto Oswaldo Cruz* **2014,** *109*, (4), 408-413.

30. Crumpton, W. G.; Thomas, I. M.; Mitchell Paul, D., Nitrate and organic N analyses with second-derivative spectroscopy. *Limnol. Oceanogr* **1992,** *37*, (4), 907-9.

31. Zwietering, M.; Jongenburger, I.; Rombouts, F.; Van't Riet, K., Modeling of the bacterial growth curve. *Applied and environmental microbiology* **1990,** *56*, (6), 1875-1881.

32. Team, R. D. C. *R: A language and environment for statistical computing. R Foundation for Statistical Computing*, Vienna, Austria, 2012.

33. Macedo, M.; Waterson, T. Profile Analysis. http://userwww.sfsu.edu/efc/classes/biol710/manova/profileanalysis.htm (December, 2016),

34. Meyer, J., The microbial loop in flowing waters. *Microbial Ecology* **1994,** *28*, (2), 195-199.

35. Paul, A.; Dziallas, C.; Zwirnmann, E.; Gjessing, E. T.; Grossart, H.-P., UV irradiation of natural organic matter (NOM): impact on organic carbon and bacteria. *Aquatic sciences* **2012,** *74*, (3), 443-454.

36. Shelton, D.; Pachepsky, Y.; Kiefer, L.; Blaustein, R.; McCarty, G.; Dao, T., Response of coliform populations in streambed sediment and water column to changes in nutrient concentrations in water. *Water research* **2014,** *59*, 316-324.

37. del Mar Lleò, M.; Bonato, B.; Benedetti, D.; Canepari, P., Survival of enterococcal species in aquatic environments. *FEMS Microbiology Ecology* **2005,** *54*, (2), 189-196.

38. Anesio, A. M.; Granéli, W.; Aiken, G. R.; Kieber, D. J.; Mopper, K., Effect of humic substance photodegradation on bacterial growth and respiration in lake water. *Applied and environmental microbiology* **2005,** *71*, (10), 6267-6275.

39. Lindell, M. J.; Granéli, W.; Tranvik, L. J., Enhanced bacterial growth in response to photochemical transformation of dissolved organic matter. *Limnology and Oceanography* **1995,** *40*, (1), 195-199.

40. Tranvik, L. J.; Bertilsson, S., Contrasting effects of solar UV radiation on dissolved organic sources for bacterial growth. *Ecology Letters* **2001,** *4*, (5), 458-463.

41. Fasching, C.; Battin, T., Exposure of dissolved organic matter to UV-radiation increases bacterial growth efficiency in a clear-water Alpine stream and its adjacent groundwater. *Aquatic Sciences* **2012,** *74*, (1), 143-153.

42. Hansen, A. M.; Kraus, T. E.; Pellerin, B. A.; Fleck, J. A.; Downing, B. D.; Bergamaschi, B. A., Optical properties of dissolved organic matter (DOM): Effects of biological and photolytic degradation. *Limnology and Oceanography* **2016,** *61*, (3), 1015-1032.

43. Bronk, D. A.; Roberts, Q. N.; Sanderson, M. P.; Canuel, E. A.; Hatcher, P. G.; Mesfioui, R.; Filippino, K. C.; Mulholland, M. R.; Loves, N. G., Effluent Organic Nitrogen (EON): Bioavailability and Photochemical and Salinity-Mediated Release. *Environ Sci Technol* **2010,** *44*, (15), 5830-5835.

44. Mosel, M.; Li, L.; Drlica, K.; Zhao, X., Superoxide-mediated protection of Escherichia coli from antimicrobials. *Antimicrobial agents and chemotherapy* **2013,** *57*, (11), 5755-5759.

45. Maraccini, P. A.; Wenk, J.; Boehm, A. B., Photoinactivation of eight health-relevant bacterial species: determining the importance of the exogenous indirect mechanism. *Environ Sci Technol* **2016,** *50*, (10), 5050-5059.

46. Mostofa, K. M.; Liu, C.-q.; Sakugawa, H.; Vione, D.; Minakata, D.; Wu, F., Photoinduced and microbial generation of hydrogen peroxide and organic peroxides in natural waters. In *Photobiogeochemistry of Organic Matter*, Springer: 2013; pp 139-207.

47. Mostofa, K. M.; Sakugawa, H., Spatial and temporal variations and factors controlling the concentrations of hydrogen peroxide and organic peroxides in rivers. *Environmental Chemistry* **2009,** *6*, (6), 524-534.

48. Imlay, J. A., Diagnosing oxidative stress in bacteria: not as easy as you might think. *Current opinion in microbiology* **2015,** *24*, 124-131.

49. Imlay, J. A., Cellular defenses against superoxide and hydrogen peroxide. *Annu Rev Biochem* **2008,** *77*, 755-76.

50. Uhlich, G. A., KatP contributes to OxyR-regulated hydrogen peroxide resistance in Escherichia coli serotype O157: H7. *Microbiology* **2009,** *155*, (11), 3589-3598.

51. La Carbona, S.; Sauvageot, N.; Giard, J. C.; Benachour, A.; Posteraro, B.; Auffray, Y.; Sanguinetti, M.; Hartke, A., Comparative study of the physiological roles of three peroxidases (NADH peroxidase, Alkyl hydroperoxide reductase and Thiol peroxidase) in oxidative stress response, survival inside macrophages and virulence of Enterococcus faecalis. *Molecular microbiology* **2007,** *66*, (5), 1148-1163.

52. Verneuil, N.; Sanguinetti, M.; Le Breton, Y.; Posteraro, B.; Fadda, G.; Auffray, Y.; Hartke, A.; Giard, J.-C., Effects of the Enterococcus faecalis hypR gene encoding a new transcriptional regulator on oxidative stress response and intracellular survival within macrophages. *Infection and immunity* **2004,** *72*, (8), 4424-4431.

53. Vesić, D.; Kristich, C. J., A Rex family transcriptional repressor influences H2O2 accumulation by Enterococcus faecalis. *Journal of bacteriology* **2013,** *195*, (8), 1815-1824.

54. Djorić, D.; Kristich, C. J., Oxidative stress enhances cephalosporin resistance of Enterococcus faecalis through activation of a two-component signaling system. *Antimicrobial agents and chemotherapy* **2015,** *59*, (1), 159-169.

55. Bizzini, A.; Zhao, C.; Budin-Verneuil, A.; Sauvageot, N.; Giard, J.-C.; Auffray, Y.; Hartke, A., Glycerol is metabolized in a complex and strain-dependent manner in Enterococcus faecalis. *Journal of bacteriology* **2010,** *192*, (3), 779-785.

56. Kadir, K.; Nelson, K. L., Sunlight mediated inactivation mechanisms of Enterococcus faecalis and Escherichia coli in clear water versus waste stabilization pond water. *Water research* **2014,** *50*, 307-317.

57. Maraccini, P. A.; Mattioli, M. C. M.; Sassoubre, L. M.; Cao, Y.; Griffith, J. F.; Ervin, J. S.; Van De Werfhorst, L. C.; Boehm, A. B., Solar Inactivation of Enterococci and

Escherichia coli in Natural Waters: Effects of Water Absorbance and Depth. *Environ Sci Technol* **2016,** *50*, (10), 5068-5076.

58. Nguyen, M. T.; Jasper, J. T.; Boehm, A. B.; Nelson, K. L., Sunlight inactivation of fecal indicator bacteria in open-water unit process treatment wetlands: Modeling endogenous and exogenous inactivation rates. *Water research* **2015,** *83*, 282-292.

59. de Brauwere, A.; Ouattara, N. K.; Servais, P., Modeling fecal indicator bacteria concentrations in natural surface waters: a review. *Critical Reviews in Environmental Science and Technology* **2014,** *44*, (21), 2380-2453.

60. Rochelle-Newall, E.; Nguyen, T. M. H.; Le, T. P. Q.; Sengtaheuanghoung, O.; Ribolzi, O., A short review of fecal indicator bacteria in tropical aquatic ecosystems: knowledge gaps and future directions. *Frontiers in microbiology* **2015,** *6*.

61. Korajkic, A.; McMinn, B. R.; Shanks, O. C.; Sivaganesan, M.; Fout, G. S.; Ashbolt, N. J., Biotic interactions and sunlight affect persistence of fecal indicator bacteria and microbial source tracking genetic markers in the upper Mississippi river. *Applied and environmental microbiology* **2014,** *80*, (13), 3952-3961.

62. Feng, F.; Goto, D.; Yan, T., Effects of autochthonous microbial community on the die-off of fecal indicators in tropical beach sand. *FEMS microbiology ecology* **2010,** *74*, (1), 214-225.

63. Wanjugi, P.; Harwood, V. J., The influence of predation and competition on the survival of commensal and pathogenic fecal bacteria in aquatic habitats. *Environmental microbiology* **2013,** *15*, (2), 517-526.

Supplemental Information for Chapter 3

Photo-produced hydrogen peroxide controls fecal indicator bacteria and *E. coli* O157:H7 growth dynamics

Contains:

Supplemental Experimental Procedures

Supplemental Results

Supplemental References

Supplemental Figures 3. S1-S7

Supplemental Tables 3. S1-S3

Supplemental Material and Methods

Reactive oxygen species measurement

Singlet oxygen Measurement

The production of $^1O_2$ during irradiation of DOMW in the solar simulator was monitored by measuring loss of furfuryl alcohol (FFA). The reaction stoichiometry and steady state concentration calculation has been described in Haag and Hoigne [1] and Chen and Jafvert [2]. During irradiation, DOMW samples were periodically removed for up to 12 h from light source and analyzed for FFA using high performance liquid chromatography (HPLC).

Hydroxyl radical Measurement

p-chlorobenzoic acid (*p*CBA) was used as a hydroxyl radical scavenger. The reaction stoichiometry and steady state concentration calculation are described in Haag and Hoigné [3] and Chen and Jafvert [2]. To measure *p*CBA, filter sterilized DOMW was treated with very low initial *p*CBA concentration (2μM) prior to irradiation. Residual *pCBA* was measured periodically for up to 12 h by HPLC with UV/Vis detector set at 230nm.

Extracellular HOOH measurement during dark incubation

Extracellular HOOH concentration during dark incubation in I-DOMW was quantified using the copper-DMP spectrophotometric method [4]. HOOH reduces copper (II) ions to copper (I) ions in the presence of excess 2, 9- diemethyl-1, 10-phenanthroline (DMP). The copper (I) forms a bright yellow cationic complex with DMP at a maximum absorbance of 454nm. Samples were filter sterilized using 0.22μm syringe filter to get rid of all bacteria prior to measuring HOOH. Absorbance reading in I-DOMW were normalized against N-DOMW samples with no bacteria inoculation. A calibration curve was constructed by plotting concentration of known ACS grade HOOH (Sigma Aldrich) solution versus the

absorbance at 454nm of the product formed by the reaction of the solutions with copper sulphate and DMP. Two separate calibration curves were used throughout the experiment.

RNA extraction and purification

Similar experimental design (Figure 3.1) was adopted with an increase in bacteria starting concentration (10^6 CFU mL^{-1}) and volume (50mL) to aid in recovery of adequate RNA for RT-qPCR. Further, irradiation of DOM was performed using a 1L jacketed Pyrex beaker (Ace glass, Vineland, NJ). Following irradiation, bacteria in mid-logarithmic phase of growth were inoculated into I-DOMW and N-DOMW for a final concentration of ~10^6 CFU mL^{-1}. Fifty milliliters of each treatment was dispensed into sterile 250ml Erlenmeyer flasks and incubated in the dark at 25^{o}C in an incubator shaker at 150 rpm (Innova 4230, New Brunswick Scientific, Edison, NJ). Triplicate samples (3 biological replicates) were selected randomly at 0.5, 6, 12, 24 and 48h and filtered through 0.45µm pore size isopore filter (EMD Millipore, Billerica, MA). Filters were folded inwards and saved in lysing matrix B tube (MP Biomedical, Solon, OH) containing 600µL RNAlater (Life Technologies, Grand Island, NY). Tubes were kept at -80^{o}C for 2 weeks prior to total RNA extraction.

Duplicate filters per time point were removed with sterile forceps and carefully opened to expose filter surface. Filter was rinsed twice in cold 1X PBS to remove RNAlater, after which 170µL of 8mg/mL lysozyme was dispensed onto filter surface. Filter containing lysozyme was incubated at 37^{o}C for 5min prior to extraction. RNA extraction was performed with the FastRNA spin kit for microbes (MP Biomedical, Solon, OH) according to the manufacturer's instructions, except that the bead-beating step was repeated twice at 6.5m/s for 60s. Total RNA was eluted twice in 25µL nuclease free water for a final volume of 50µl. Total RNA was quantified with a Nanodrop ND 1000 spectrophotometer (Thermo Scientific, Waltham, MA), examined for quality on an Agilent

Bioanalyzer, and stored at -80^{o}C until used for RT-qPCR. Before RT-qPCR, total bacterial RNA was treated with 8U Turbo DNA-free kit (Life Technologies, Grand Island, NY) to remove genomic DNA contamination.

Rose bengal photo-sensitization experiment

Rose bengal (RB) was added to sterilized phosphate buffered water (PBW) to a final concentration of 0.05μM and irradiated under a solar simulator. The production of $^{1}O_2$ during irradiation was monitored by measuring the loss of furfuryl alcohol (FFA) - see $^{1}O_2$ measurement. During irradiation, irradiated RB were periodically removed for 1 h from light source and analyzed for FFA using high performance liquid chromatography (HPLC) (Fig. 3S1).

Following irradiation, irradiated RB, non-irradiated RB and PBW controls were separately inoculated with mid-logarithmic phase of each bacterium to a final concentration of 10^{2}-10^{3} cells ml^{-1}. Twenty milliliters of each treatment was dispensed into sterile 50ml centrifuge tubes and incubated at 25^{o}C in a refrigerated incubator shaker (150 rpm) (Innova 4230, New Brunswick Scientific, Edison, NJ). Duplicate samples per bacterium and treatment were randomly selected for analysis at 0, 0.3, 0.6, 1, 1.3, 1.6, 2, and 3 h.

Supplemental Results

Starting inocula concentration effect on growth potential

Increase in bacteria starting concentration (10^{6} CFU mL-^{1}) resulted in a decrease in growth rate but no change in *E. coli* final population when compared to the lower inoculum population (10^{3} CFU mL^{-1}) (Table 3S2). There was no noticeable growth in *E. faecalis*, which suggests that it's maximum achievable growth in 1:10 DOMW was ~10^{6} CFU mL^{-1}.

Moreover, *E. faecalis* seem to show a periodic steady state at this concentration (Table 3S3).

Constitutive gene candidates for RT- qPCR measurements

We determined the expression profile of *idnT*, *cysG*, *hcaT*, *gyrB* and *gapA* in *E. coli* under the growth conditions studied here. In silico analysis of these candidate constitutive genes using the algorithms geNorm predicted *gapA* and *gyrB* to be the most stably expressed genes for data normalization (Supp. Table 3S2). These two housekeeping genes were further used in this study for the normalization of *oxyR*-regulated genes in both *E. coli* and *E. coli* O157:H7.

Nutrient loss in 1:10 DOM dilution

There was no noticeable decline in [NH_4^+] during 24 h incubation for *E. coli*, followed by a 50% loss observed after 48 h of incubation (Fig. 3S4). A similar trend was observed for [NO_3^-] but final loss at 72 h was not more than 45% (Fig. 3S5). Also, during growth, there was a gradual decline in DOC concentration in N-DOMW, with up to 70% loss after 72 h incubation. In contrast, there was an overall increase in DOC concentration in I-DOMW (Fig. 3S6). *E. coli* O157:H7 showed a gradual decline in [NH_4^+] for up to 12 h and sharply declined afterwards resulting in a total loss of ~ 92% after 72 h incubation. Nitrate showed an overall decline in concentration but total loss was not more than 33%. There was a 33% loss in DOC after 24 h but there was 25% and 100% gain in DOC at 48 h for I-DOMW and N-DOMW respectively. For *E. faecalis*, [NH_4^+] increased steadily for up to 24 h before a steep decline after 48 h of incubation. Overall gain in [NH_4^+] was 33% and loss differed by treatment, with 60% for I-DOMW and 30% for N-DOMW. Nitrate showed a steady decline in concentration, with a 28% loss for I-DOMW and 18% in N-DOMW observed. There was a 60% gain in DOC after 6 h of incubation before decreasing to

levels below the starting concentration. There was no noticeable decline in orthophosphate concentration for any of the bacteria (Figure 3S7).

Supplemental Figures

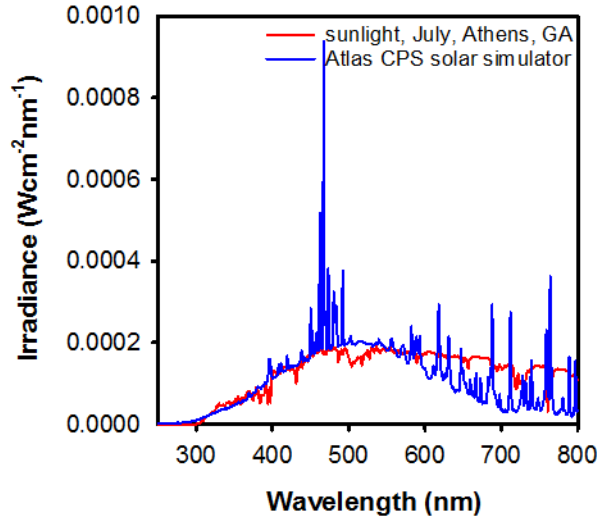

Figure 3.S1: Spectra of natural sunlight and light emitted by the Xenon lamp in solar simulator in this study.

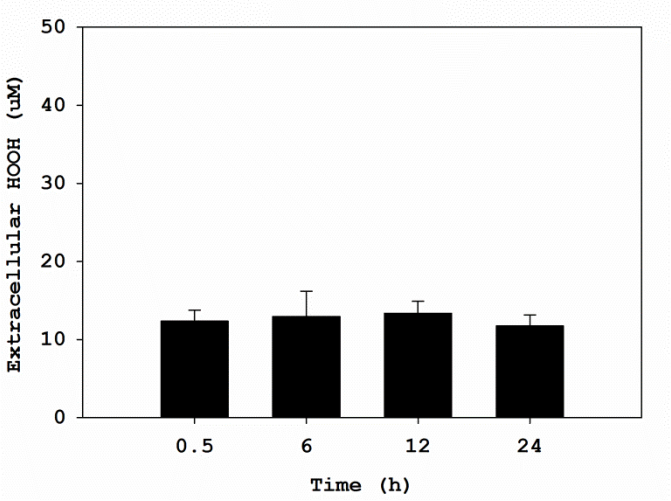

Figure 3.S2: Extracellular HOOH concentration in I-DOMW controls (n =3, 1 per bacterium) with no bacteria inoculation.

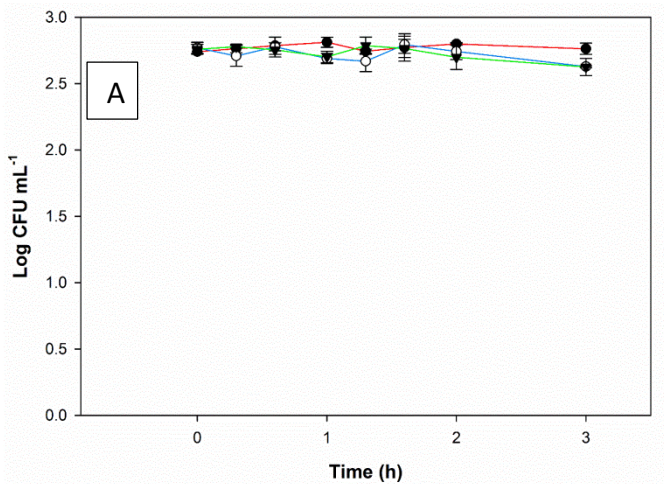
A
Log CFU mL-1
Time (h)
3.0
2.5
2.0
1.5
1.0
0.5
0.0
0
1
2
3

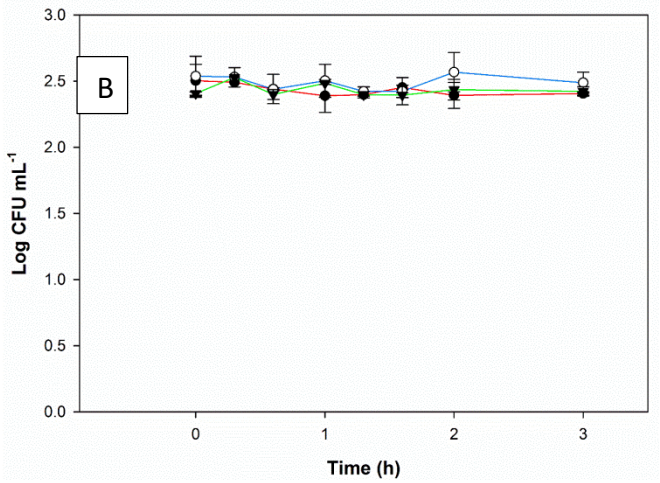
B
Log CFU mL-1
Time (h)
3.0
2.5
2.0
1.5
1.0
0.5
0.0
0
1
2
3

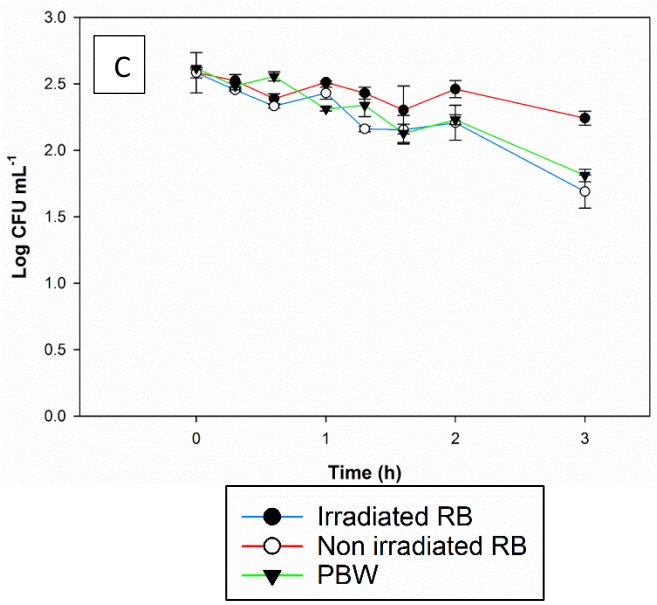
C
Log CFU mL-1
Time (h)
3.0
2.5
2.0
1.5
1.0
0.5
0.0
0
1
2
3
Irradiated RB
Non irradiated RB
PBW

Figure 3.S3: **Photo-production of singlet oxygen from rose bengal (RB) had no inactivation effect on FIB and *E. coli* O157:H7**. Singlet oxygen was produced at a steady state of 7.38^{-13}M after 1 h of sunlight irradiation. Bacteria was cultured on a selective medium. Concentrations are reported in colony forming units (CFU) per ml. Inactivation of (**A**) *E. faecalis* (**B**) *E. coli* (**C**) *E. coli* O157:H7 in photo-sensitized RB. Error bars represent standard deviation.

A

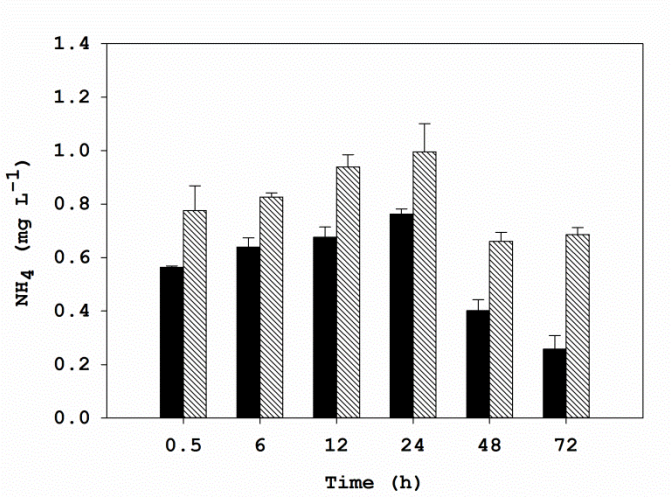
1.4
1.2
1.0
0.8
0.6
0.4
0.2
0.0
NH4 (mg L-1)
0.5
6
12
24
48
72
Time (h)

B

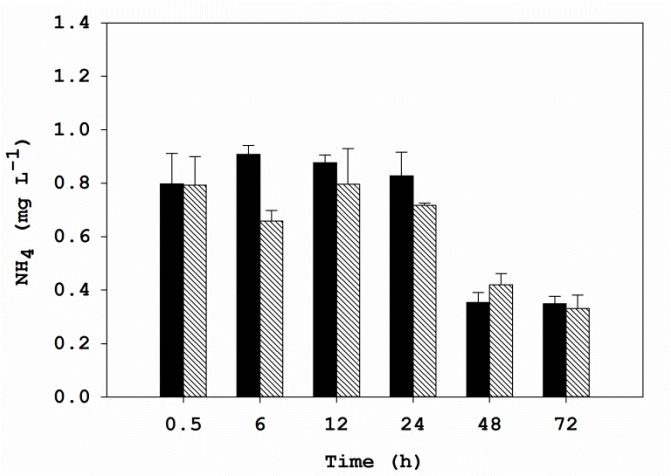
1.4
1.2
1.0
0.8
0.6
0.4
0.2
0.0
NH4 (mg L-1)
0.5
6
12
24
48
72
Time (h)

C

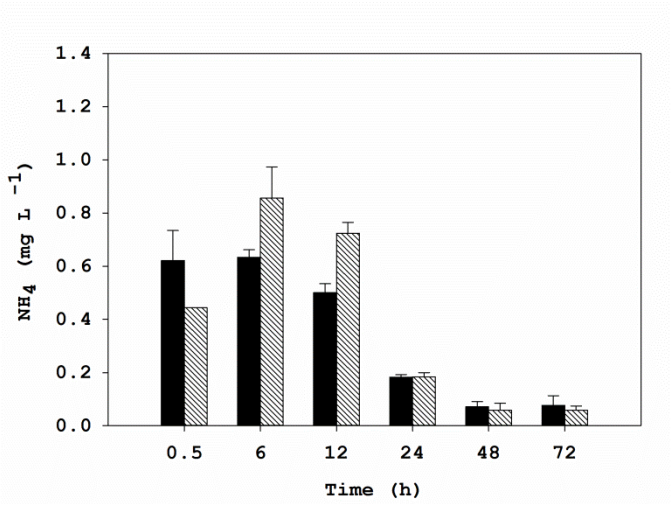
1.4
1.2
1.0
0.8
0.6
0.4
0.2
0.0
NH4 (mg L-1)
0.5
6
12
24
48
72
Time (h)

D

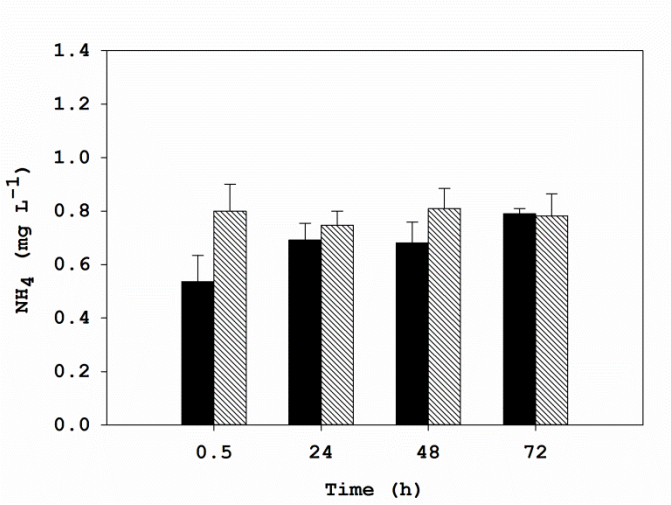
1.4
1.2
1.0
0.8
0.6
0.4
0.2
0.0
NH4 (mg L-1)
0.5
24
48
72
Time (h)

E

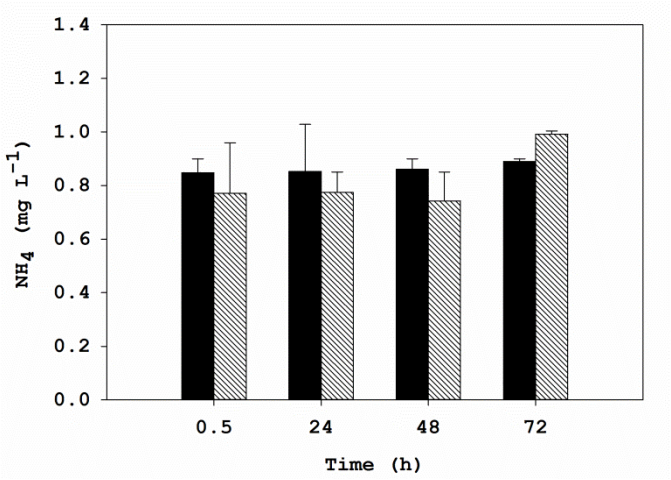
1.4
1.2
1.0
0.8
0.6
0.4
0.2
0.0
NH4 (mg L-1)
0.5
24
48
72
Time (h)

F

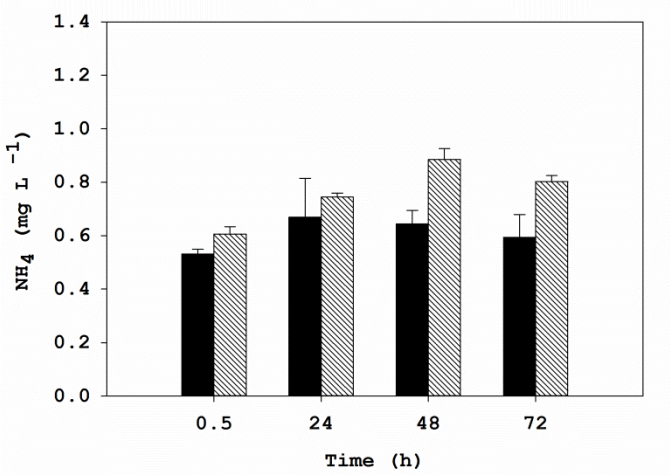
1.4
1.2
1.0
0.8
0.6
0.4
0.2
0.0
NH4 (mg L-1)
0.5
24
48
72
Time (h)

Figure 3.S4: Extracellular ammonium concentration in (A) *E. faecalis* (B) *E. coli* and (C) *E. coli* O157:H7 during growth 1:10 DOMW and their corresponding controls (D, E, F) with no bacteria inoculated. Error bars represent standard errors (N=3) for treatment and standard deviation (N=2) for controls.

A

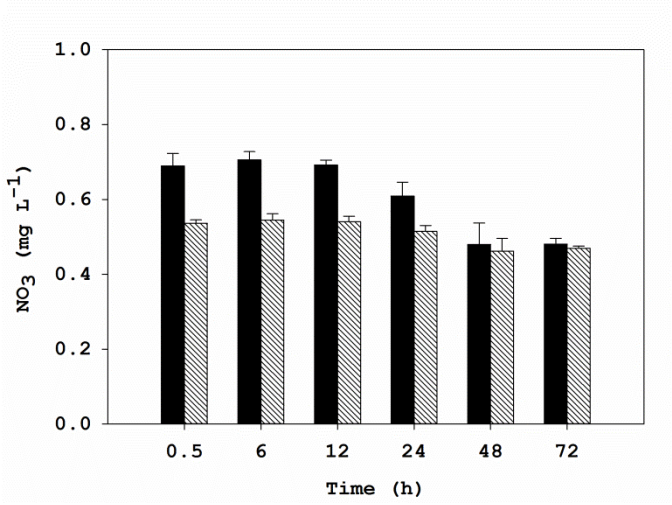
1.0
0.8
0.6
0.4
0.2
0.0
NO3 (mg L-1)
0.5
6
12
24
48
72
Time (h)

B

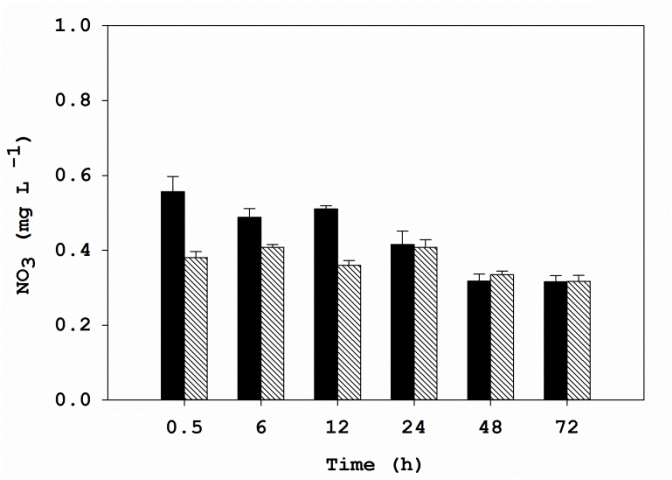
1.0
0.8
0.6
0.4
0.2
0.0
NO3 (mg L-1)
0.5
6
12
24
48
72
Time (h)

C

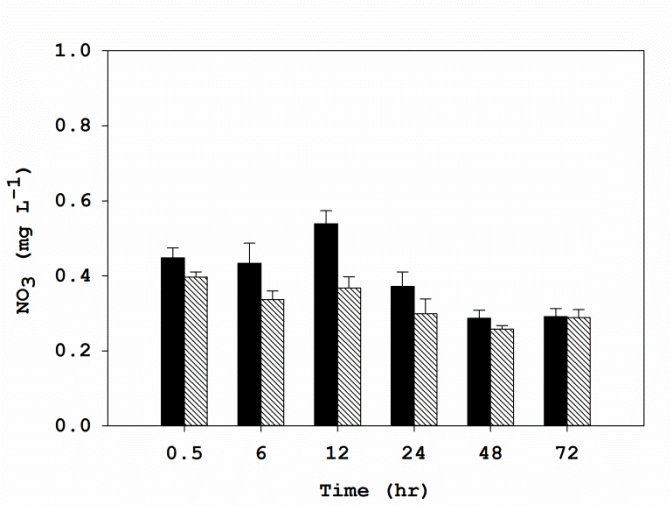
1.0
0.8
0.6
0.4
0.2
0.0
NO3 (mg L-1)
0.5
6
12
24
48
72
Time (hr)

D

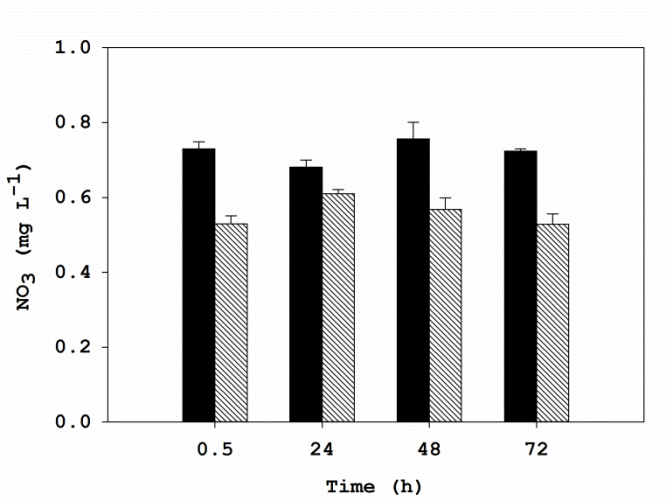
1.0
0.8
0.6
0.4
0.2
0.0
NO3 (mg L-1)
0.5
24
48
72
Time (h)

E

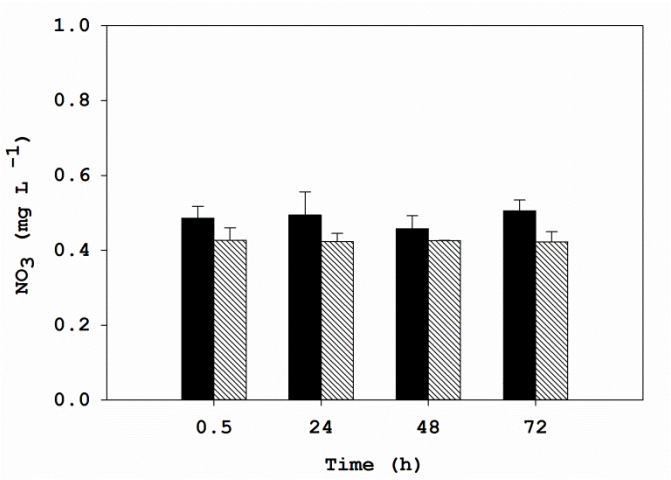
1.0
0.8
0.6
0.4
0.2
0.0
NO3 (mg L-1)
0.5
24
48
72
Time (h)

F

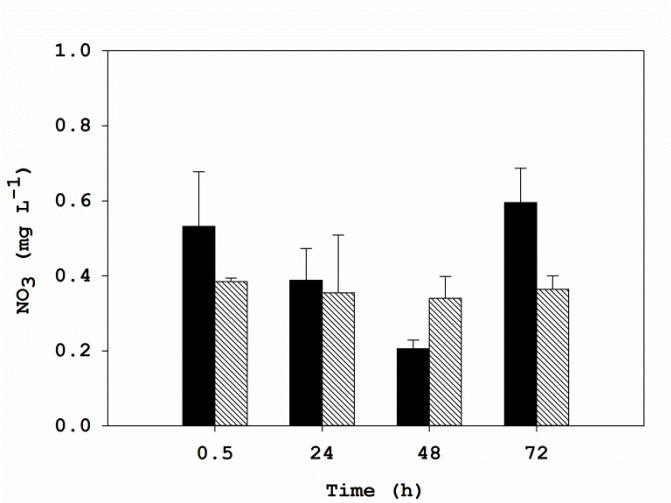
1.0
0.8
0.6
0.4
0.2
0.0
NO3 (mg L-1)
0.5
24
48
72
Time (h)

Figure 3S5: Extracellular nitrate concentration in (A) *E. faecalis* (B) *E. coli* and (C) *E. coli* O157:H7 during growth 1:10 DOMW and their corresponding controls (D, E, F) with no bacteria inoculated. Error bars represent standard errors (N=3) for treatment and standard deviation (N=2) for controls.

A

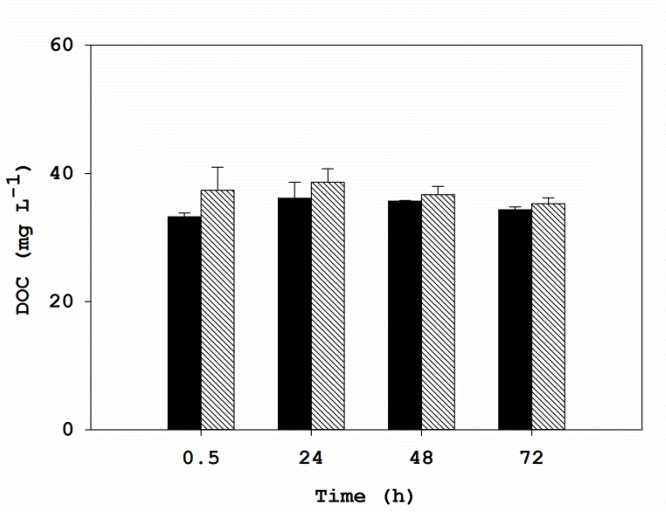
60
40
20
0
DOC (mg L-1)
0.5
24
48
72
Time (h)

B

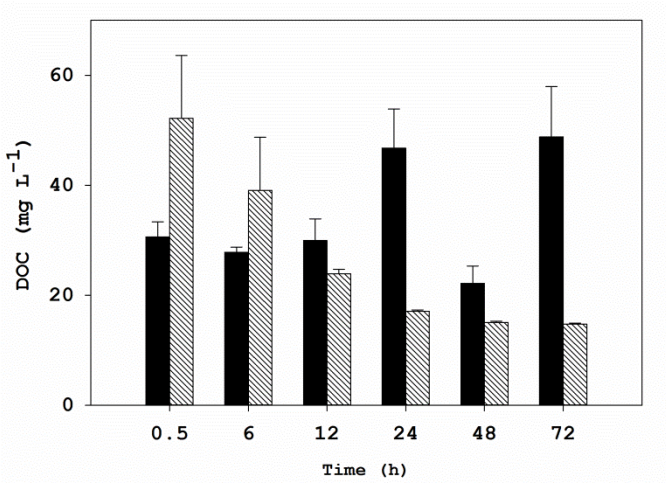
60
40
20
0
DOC (mg L-1)
0.5
6
12
24
48
72
Time (h)

C

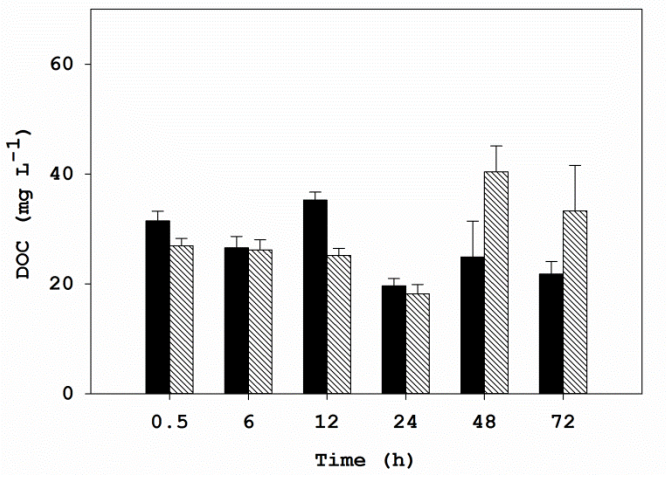
60
40
20
0
DOC (mg L-1)
0.5
6
12
24
48
72
Time (h)

D

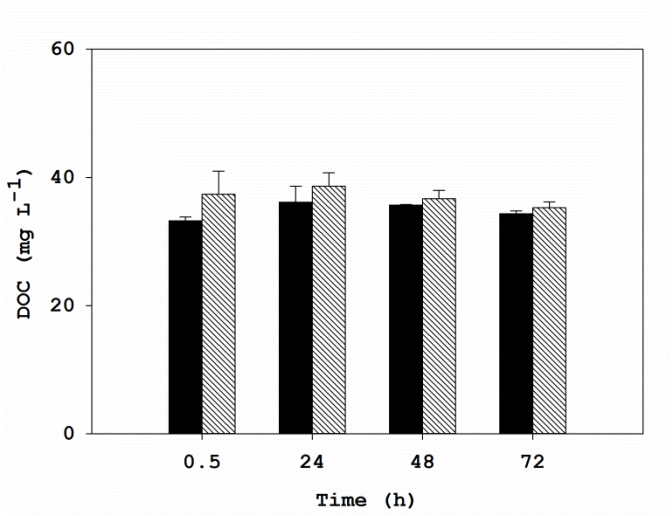
60
40
20
0
DOC (mg L-1)
0.5
24
48
72
Time (h)

E

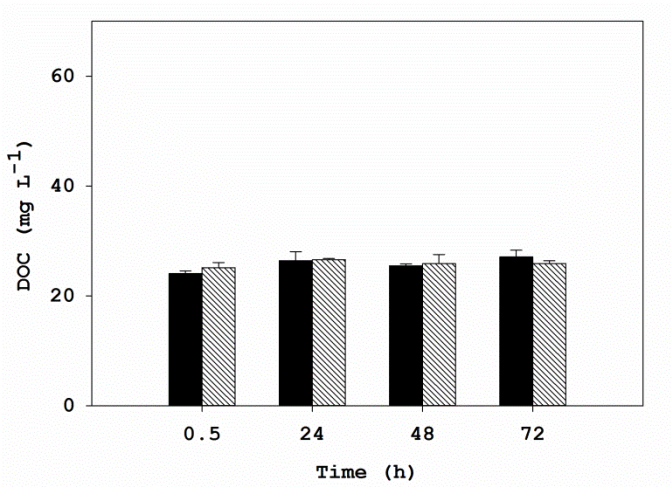
60
40
20
0
DOC (mg L-1)
0.5
24
48
72
Time (h)

F

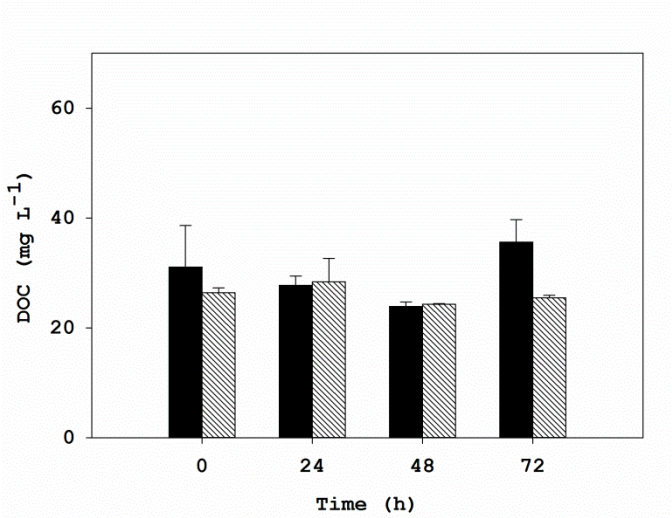
60
40
20
0
DOC (mg L-1)
0
24
48
72
Time (h)

Figure 3S6: Extracellular dissolved organic carbon (DOC) concentration in (A) *E. faecalis* (B) *E. coli* and (C) *E. coli* O157:H7 during growth 1:10 DOMW and their corresponding controls (D, E, F) with no bacteria inoculated. Error bars represent standard errors (N=3) for treatment and standard deviation (N=2) for controls.

A

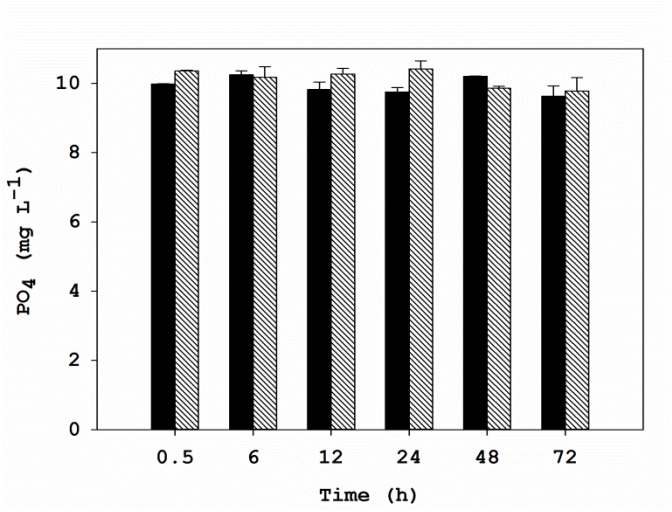
PO4 (mg L-1)
0
2
4
6
8
10
0.5
6
12
24
48
72
Time (h)

B

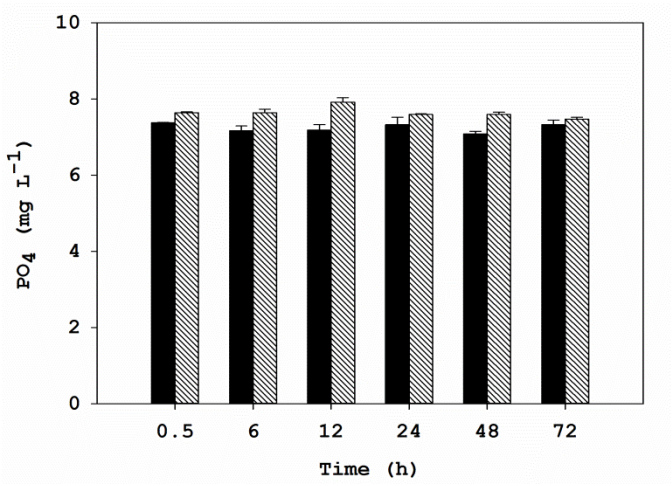
PO4 (mg L-1)
0
2
4
6
8
10
0.5
6
12
24
48
72
Time (h)

C

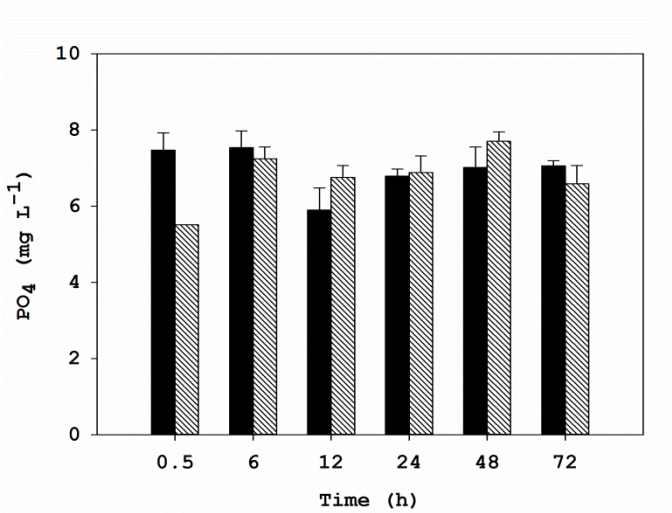
PO4 (mg L-1)
0
2
4
6
8
10
0.5
6
12
24
48
72
Time (h)

D

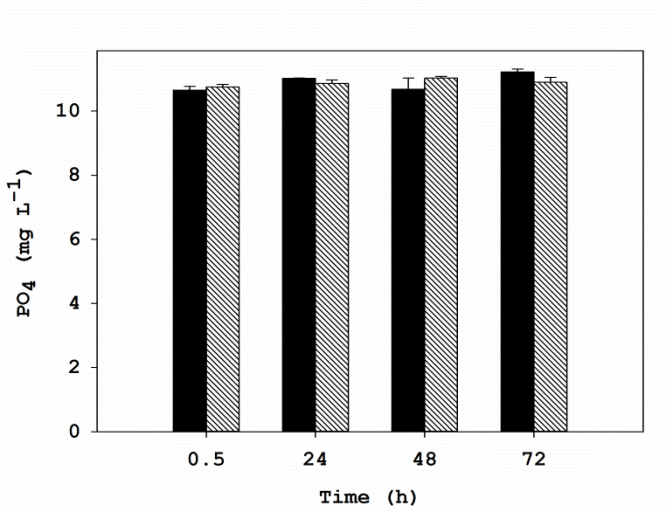
PO4 (mg L-1)
0
2
4
6
8
10
0.5
24
48
72
Time (h)

E

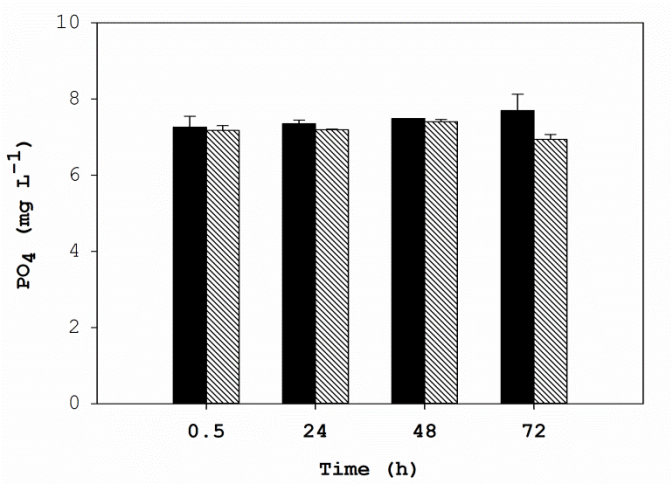
PO4 (mg L-1)
0
2
4
6
8
10
0.5
24
48
72
Time (h)

F

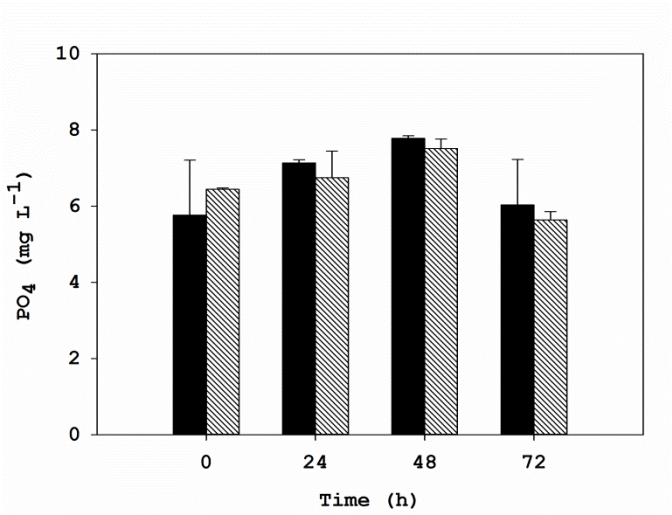
PO4 (mg L-1)
0
2
4
6
8
10
0
24
48
72
Time (h)

Figure 3S7: Extracellular orthophosphate concentration in (A) *E. faecalis* (B) *E. coli* and (C) *E. coli* O157:H7 during growth 1:10 DOMW and their corresponding controls (D, E, F) with no bacteria inoculated. Error bars represent standard errors (N=3) for treatment and standard deviation (N=2) for controls.

Table 3.S1: Primers used for RT-qpCR

Gene	Primers (5'-3')	Gene product name	Base pair (bp)	Reference
cysG	F: ATGCGGTGAACTGTGGAATAAACG R: TTGTCGGCGGTGGTGATGTC	Siroheme synthase	105	[5]
idnT	F: CTGTTTAGCGAAGAGGAGATGC R: ACAAACGGCGGCGATAGC	Gluconate permease	90	[5]
hcaT	F: GGGCATTATGGGAGCAACTA R: GGCAGAGTAAACCGCCTGTA	3-phenyl propionic acid transporter	154	This study
gapA	F: GTCGCTGAAGCAACTGGTCT R: AAGTTAGCGCCTTTAACGAACAT	Glyceraldehyde-3-phosphate dehydrogenase	131	[6]
gyrB	F: GCAAGCCACGCAGTTTCTC R: GGAAGCCGACCTCTCTGATG	DNA gyrase subunit B	254	[7]
katG	F: CTGCGTTTTGATCCTGAGTTC R: GGCCCGATGTAGCGAGATT	Catalase peroxidase	137	[6]
ahpF	F: GCCCTGACCAAACTCTTTCC R: GCAGATTCGCCATATTGACG	Alkyl hydroperoxide reductase subunit F	204	[7]
oxyS	F: GAGCGGCACCTCTTTTAACCCTTG R: CCTGGAGATCCGCAAAAGTTCACG	Oxidative stress regulator	97	[7]
oxyR	F: CGCGATCAGGCAATGG R: CAGCGCTGGCAGTAAAGTGAT	Hydrogen peroxide transcription regulator	129	[6]
gyrB[a]	F: ACACGGGTTCGTGAATTAGC R: TTGGCTCTGGGAAAATAACG	DNA gyrase subunit B	163	This study
rpoB[a]	F: CCTGTACCTACCCACGGAGA R: TGGACGTTTCACCAAAACAA	RNA polymerase subunit B	150	This study
katA[a]	F: TCTCATTCACCGGAAAGTCTTC R: CAGCAGCATTGACCCATTTG	Catalase/Peroxidase	121	This study
ahpC[a]	F: CCAATTGGCTGGACAAACTT R: ACGGTCAACTTGCTCGTTTC	Peroxiredoxin	209	This study

Npr[a]	F: GGCCTAATCAAGACGGATGA R: TCCTTGAACACCAGGGAAAG	NADH peroxidase	195	This study
Tpx[a]	F: GGTTCCGACGAAACTTCTGA R: GGTGTCGAAATGGAAATGCT	Thiol peroxidase	161	This study
Fur[a]	F: CCAAACACTTTCACCACCAT R: TTTGCTCTACTTCACCAAGCA	Ferric uptake regulation protein	87	[8]
hypR[a]	F: TCTCGACAAGCACAAGTTCC R: ACCTAGCCCAGCTTCTACCA	Hydrogen peroxide regulator-arsR family protein	126	[8]

[a] Primers for *E. faecalis*

Table 3S2: Stability analysis of five commonly used reference genes in *E. coli* by geNorm [9]

Target	M value
gapA	0.900
gyrB	0.900
cysG	1.542
hcaT	1.904
idnT	4.843

A lower 'M-value' correlates to higher gene expression stability.

Table 3S3: Growth rate comparison at low and high starting inocula of FIB and *E. coli* O157:H7

Bacteria	Inocula concentration	Treatment	Growth rate (hr-1)	Maximum growth (LogCFU mL^{-1})
E. coli	High	I-DOMW	0.135	7.56
		N-DOMW	0.167	7.49
	Low	I-DOMW	0.293	7.49
		N-DOMW	0.235	7.3
E. coli O157:H7	High	I-DOMW	0.266	7.62
		N-DOMW	0.242	7.72
	Low	I-DOMW	0.257	7.27
		N-DOMW	0.255	7.18
E. faecalis	High	I-DOMW	SS	ND
		N-DOMW	SS	ND
	Low	I-DOMW	0.089	5.31
		N-DOMW	0.279	6.29

High and low inocula concentration represents ~10^6 and ~10^3 CFU mL^{-1} of starting bacteria concentration respectively. SS, Periodic steady state; ND, not determined.

Chapter 3 Supplemental References

1. Haag, W. R.; Hoigne, J., Singlet oxygen in surface waters. 3. Photochemical formation and steady-state concentrations in various types of waters. *Environmental science & technology* **1986,** *20*, (4), 341-348.

2. Chen, C.-Y.; Jafvert, C. T., Photoreactivity of carboxylated single-walled carbon nanotubes in sunlight: reactive oxygen species production in water. *Environmental science & technology* **2010,** *44*, (17), 6674-6679.

3. Haag, W. R.; Hoigné, J., Photo-sensitized oxidation in natural water via. OH radicals. *Chemosphere* **1985,** *14*, (11-12), 1659-1671.

4. Kosaka, K.; Yamada, H.; Matsui, S.; Echigo, S.; Shishida, K., Comparison among the methods for hydrogen peroxide measurements to evaluate advanced oxidation processes: application of a spectrophotometric method using copper (II) ion and 2, 9-dimethyl-1, 10-phenanthroline. *Environmental science & technology* **1998,** *32*, (23), 3821-3824.

5. Zhou, K.; Zhou, L.; Lim, Q. E.; Zou, R.; Stephanopoulos, G.; Too, H.-P., Novel reference genes for quantifying transcriptional responses of Escherichia coli to protein overexpression by quantitative PCR. *BMC molecular biology* **2011,** *12*, (1), 18.

6. Michán, C.; Manchado, M.; Dorado, G.; Pueyo, C., In vivo transcription of the Escherichia coli oxyRregulon as a function of growth phase and in response to oxidative stress. *Journal of bacteriology* **1999,** *181*, (9), 2759-2764.

7. Kyle, J. L.; Parker, C. T.; Goudeau, D.; Brandl, M. T., Transcriptome analysis of Escherichia coli O157: H7 exposed to lysates of lettuce leaves. *Applied and environmental microbiology* **2010,** *76*, (5), 1375-1387.

8. Riboldi, G. P.; Bierhals, C. G.; Mattos, E. P. d.; Frazzon, A. P. G.; Frazzon, J., Oxidative stress enhances the expression of sulfur assimilation genes: preliminary insights on the Enterococcus faecalis iron-sulfur cluster machinery regulation. *Memórias do Instituto Oswaldo Cruz* **2014,** *109*, (4), 408-413.

9. Vandesompele, J.; De Preter, K.; Pattyn, F.; Poppe, B.; Van Roy, N.; De Paepe, A.; Speleman, F., Accurate normalization of real-time quantitative RT-PCR data by geometric averaging of multiple internal control genes. *Genome biology* **2002,** *3*, (7), research0034.

CHAPTER 4

TRANSCRIPTOMIC ANALYSIS REVEAL DIFFERENCES IN THE HYDROGEN PEROXIDE RESPONSE MECHANISM OF *ESCHERICHIA COLI*, *ENTEROCOCCUS FAECALIS* AND *E. COLI* O157:H7

Oladeinde, A., Erin Lipp, Chia-Ying Chen, Richard Muirhead, Travis Glenn and Marirosa Molina. Submitted to Environmental Science and Technology

ABSTRACT

Hydrogen peroxide (HOOH) is the most environmentally stable reactive oxygen species. In nature, HOOH originates from photo-chemical reactions involving dissolved organic matter (DOM) and as a by-product of microbial metabolism. In this study, we produced ~15μM of HOOH from sunlight irradiation of water spiked with filter sterilized cow fecal extract. We employed whole transcriptome sequencing (WTS) to identify differentially expressed temporal transcripts between fecal bacteria (*E. coli*, *E. coli* O157:H7, and *Enterococcus faecalis*) incubated in irradiated spiked water microcosms and non-irradiated spiked microcosm for up to 24 h. The number of differentially expressed genes (DEG) differed between bacteria and duration of dark incubation. For *E. coli* and *E. coli* O157:H7, the majority of DEG were observed immediately following inoculation (< 30 min), while for *E. faecalis*, expression took at least 6 h. Incubation of *E. faecalis* in irradiated spiked water resulted in an increase in expression of genes encoding oligopeptide transport, beta-lactam resistance and ABC transporters. In non-irradiated spiked microcosms, there was an increase in transcripts associated with phosphoenolpyruvate: phophotransferase system and glycerol metabolism. *E. coli* and *E. coli* O157:H7 showed an increase in the expression of Oxy-R regulated genes, including transcripts for catalase-peroxidase, iron-sulfur cluster, siderophore transport, iron uptake, quorum sensing, and biofilm formation. These results indicate that *E. coli* and *E. faecalis* have different mechanisms for removal and production of HOOH and differ in their overall survival dynamics. Furthermore, our results also indicate that photo-degradation and microbial metabolism of manure derived DOM can produce micromolar concentrations of HOOH that may be detrimental to the presence of specific types of fecal indicator bacteria.

INTRODUCTION

The survival of bacteria in the environment is dictated by their ability to grow or persist under diverse abiotic and biotic stressors. In aquatic ecosystems, resource availability, sunlight, temperature, pH and competition have been shown to be important drivers of bacterial population dynamics [1-3]. Of these factors, substrate availability in the form of dissolved organic matter (DOM) is key for bacteria to proliferate in surface waters [4, 5]. Further, DOM transformations mediated by sunlight and microbes can have an interacting effect on bacterial survival [6, 7].

The colored fraction of DOM (CDOM) is primarily responsible for the absorbance of UV light and for the production of labile nutrients from refractive fractions of DOM, which can be subsequently used for growth or survival [8-10]. Another important transient product of absorption of UV/visible light by CDOM is the formation of reactive oxygen species (ROS) from photochemical reactions involving oxygen [11]. ROS including hydrogen peroxide (HOOH), hydroxyl radical (.OH) and super oxide radicals (O_2^-) are intermediates formed during photo-oxidation of CDOM. Hydrogen peroxide is uncharged, and unlike other ROS, it can easily permeate the bacterial cell surface. It can also persist in natural waters for long periods of time, from several hours to days [12, 13]. More importantly, its concentration has been shown to have a diel cycle, with peak concentrations typically noted at noontime during summer months [14].

At steady state concentrations, hydrogen peroxide concentrations are reported to range from 6nM in marine waters to as high as 3.2μM in rivers and streams [15]. The concentration of photo-produced HOOH in surface water is dependent on the source/type of DOM, DOM concentration, and sunlight irradiance. At high extracellular HOOH concentrations, microbes can experience toxicity from significant changes in their cell

redox homeostasis. Nevertheless, bacteria have developed elegant systems to help alleviate themselves of HOOH induced oxidative stress [16].

To understand the role of photo-produced HOOH on survival of specific fecal bacteria, we attempted to isolate the effect of HOOH using controlled microcosms of natural water spiked with cattle fecal extract that were irradiated prior to inoculation with bacteria. Following bacterial inoculation, microcosms were incubated in the dark for 24 h. We employed high throughput RNA-Seq to investigate the expression of transcripts that are required for HOOH detoxification and oxidative stress. We provide valuable insights into the differential survival mechanism used by two important FIB for water quality monitoring and a zoonotic pathogen of public health interest.

MATERIALS AND METHODS

Cattle Fecal Extract Preparation. Fresh fecal samples were collected from 5 individual cows from a commercial farm in northeast Georgia on July 13, 2013. Fecal samples were composited, homogenized and made into 1:10 fecal slurry in 0.85% KCl and mixed for 1 h in a hand wrist shaker. The fecal slurry was then centrifuged twice at 4000 x g for 10 min and the resulting supernatant was saved and referred to as cattle fecal extract (CFE). CFE was sequentially filtered through 1.2µm, 0.45µm and 0.2µm pore –sized polycarbonate membrane filters. Dissolved organic carbon (DOC) concentration in CFE was determined using a total organic carbon analyzer (TOC-V_{CPH}, Shimadzu, Kyoto, Japan) equipped with auto samplers. CFE was spiked into autoclaved phosphate buffered water (PBW) microcosms to concentrations mimicking nutrient inputs from direct fecal deposition into streams (i.e., final DOC concentration of 32.48±1.52 mg L^{-1}). The absence of bacteria and relevant lytic phages in CFE was confirmed by culturing 100µl of CFE in Brain Heart Infusion (BHI) broth and by performing phage double agar overlay assay [17], respectively.

For the overlay assay, bacterial strains used in the present study were used as phage hosts. Thereafter, CFE/DOM spiked water was divided into two volumes with one exposed to solar radiation (Irradiated DOM-Spiked Water (I-DOMW)) and the other as a dark control (Non-irradiated DOM Spiked Water (N-DOMW)).

Inoculum Preparation. Overnight cultures of *E. coli* C3000 (ATCC 15597), hereafter referred to as *E. coli*, *Enterococcus faecalis* (ATCC 29212) and *Escherichia coli* O157:H7 B6914, hereafter referred to as *E. coli* O157:H7, were grown for 1.5 h to mid-logarithm phase (OD_{600} of 0.1) in BHI broth. Each culture was centrifuged at 4000 x g for 5 min and washed twice in phosphate buffered water (PBW) before preparing serial dilutions to the desired concentrations.

Irradiation of DOM spiked water. Solar irradiation was performed in an Atlas SunTest CPS/CPS+ solar simulator (Atlas Materials Testing Technology, Chicago, IL) equipped with a 1kW xenon arc lamp. Samples were irradiated for 12 h using a 1L jacketed Pyrex beaker (Ace glass, Vineland, NJ). Following irradiation, bacteria in mid-logarithmic phase of growth were separately inoculated into I-DOMW, N-DOMW and PBW for a final concentration of ~10^6 CFU mL^{-1}. Fifty milliliter aliquots of each treatment were dispensed into sterile 250ml Erlenmeyer flasks (12 per treatment) and incubated in the dark at 25^oC in an incubator shaker at 150 rpm (Innova 4230, New Brunswick Scientific, Edison, NJ). Individual flasks were randomly selected at ~ 0.5, 6, 12 and 24 h for microbiological analysis, measurement of exogenous HOOH and for RNA-Seq (Fig. 4.1).

Microbiological Analysis. One ml of each duplicate sample was serially diluted in PBW and quantified on selective agar media. *E. coli, E. faecalis* and *E. coli* O157:H7 were quantified using modified mTEC agar (EPA method 1603), mEI agar (EPA method 1600)

and MUG *E. coli* O157:H7 agar supplemented with 100µg ml^{-1} ampicillin (Sigma Aldrich), respectively.

Extracellular HOOH measurement. Extracellular HOOH concentration before and after bacterial inoculation were quantified using the copper-DMP spectrophotometric method [18]. HOOH reduces copper (II) ions to copper (I) ions in the presence of excess 2, 9-diemethyl-1, 10-phenanthroline (DMP). The copper (I) forms a bright yellow cationic complex with DMP at a maximum absorbance of 454nm. Samples were filter sterilized using 0.22µm syringe filter to remove bacteria prior to measuring HOOH. Absorbance readings in I-DOMW and N-DOMW were normalized against N-DOMW controls (no bacteria inoculation). A calibration curve was constructed by plotting concentration of known ACS grade HOOH (Sigma Aldrich) solution versus the absorbance at 454nm of the product formed by the reaction of the solutions with copper sulphate and DMP. Two separate calibration curves were used throughout the experiment for quality control purposes and ensure reproducibility of results.

RNA isolation. Samples were selected randomly at 0.5, 6, 12, and 24 h and ~ 45ml was filtered through 0.45µm pore size isopore membrane (EMD Millipore, Billerica, MA). Filters were folded inwards and saved in a lysing matrix B tube (MP Biomedical, Solon, OH) containing 600µL RNAlater (Life Technologies, Grand Island, NY). Tubes were kept at -80^{o}C for 2 weeks prior to total RNA extraction. Duplicate filters per time point were removed with sterile forceps and carefully opened to expose the filter surface. Filters were rinsed twice in cold 1X phosphate buffer saline to remove RNAlater, after which 170µL of 8mg mL^{-1} lysozyme were dispensed onto the filter surface. Filters containing lysozyme were incubated at 37^{o}C for 5 min prior to extraction. RNA extraction was performed with the FastRNA spin kit for microbes (MP Biomedical, Solon, OH) according to the

manufacturer's instructions, except that the bead-beating step was repeated twice at 6.5m s^{-1} for 60s. Total RNA was eluted twice in 25µL DEPC treated water for a final volume of 50µl. Total RNA was concentrated using a vacufuge (Eppendorf, NY, USA) with no heat treatment for 2.5 h. RNA pellets were rehydrated with 20µl DEPC treated water and treated with 8U Turbo DNA-free kit (Life Technologies, Grand Island, NY) to remove genomic DNA contamination. Recovered RNA was quantified with a Nanodrop ND 1000 spectrophotometer (Thermo Fisher Scientific, MA, USA), examined for quality on an Agilent Bioanalyzer, and stored at -80^{o}C until used for RNA-seq (between 2 – 3 months).

mRNA enrichment. Twenty microliters of DNASE treated RNA was pelleted as described earlier and reconstituted in 15µl (75ng to 2.5µg) 1X TE buffer. Bacterial 16S and 23S ribosomal RNA removal was completed using MICROBExpress Bacterial mRNA Enrichment Kit (Life Technologies, Grand Island, NY) according to manufacturer's instruction but with half of the suggested reaction volumes. The recovered mRNA was quantified using Nanodrop ND 1000 spectrophotometer (Thermo Scientific, Waltham, MA).

cDNA library preparation. cDNA synthesis was performed on enriched mRNA (~2 - 160ng) using the KAPA stranded RNA-seq library preparation kit (Kapa Biosystems, Inc. MA, USA) with a few modifications. Half the suggested reaction volumes were used throughout. RNA fragmentation was completed in a thermocycler at 87.5^{o}C for 6 min. Adapterama I adapters and primers [19] were used for ligation and PCR amplification reactions at a final reaction concentration of 357nM and 250nM, respectively. For PCR amplification, iTru5 forward and iTru7 reverse primers with unique indexes for sample multiplexing were employed [19]. The concentrations of amplicons from different samples were quantified using a Qubit dsDNA HS Assay Kit (Thermo Fisher Scientific, MA, USA). The libraries were pooled in equimolar concentrations and sequenced at the Georgia

Genomics Facility using an Illumina NextSeq (150 cycles) Mid Output Flow Cell. A 75 bp paired-end sequencing reaction was performed on a NextSeq platform (Illumina, San Diego, CA, USA). cDNA fragments (~339bp) were obtained for all 24 biosamples. Reads were submitted to NCBI SRA under submission ID SUB1913975 and bioproject PRJNA341849.

Bioinformatics analysis. Forward and reverse barcode combinations were used to identify each sample for de-multiplexing. Unfiltered fastq sequences of each bacterium were aligned to available bacteria reference genomes using BWA [20] with default parameters. SAM alignment was converted to BAM (samtools view –bS), sorted by coordinates (samtools sort) and PCR duplicates removed (samtools rmdup) using SAMtools [21]. Mapped reads were counted using BEDTools (multiBamCov –bams) [22]. Read counts were exported in a tab delimited file for normalization and differential gene expression (DGE) (see Supp. Mat.) in R [23]. DGE analysis was completed with DESeq2 package [24]. Reads with 0 or 1 count were removed before DGE was performed (see supporting information). For each RNAseq data set, genes with an absolute fold change ≥ 2 and adjusted p-value of <0.01 were used for further analysis. The proteins corresponding to the obtained gene sets were searched against the version 10 of the STRING database [25] to display functional protein-association networks. Interactions were considered with a STRING confidence ≥0.4 (medium and high confidence). A markov cluster algorithim (MCL) [26] of 2 was used for clustering.

Statistical analysis. Bacteria growth rate was derived from the equation below, where N is the concentration of cells, t is the time and k is the growth rate constant.

$$(1)\ dN/dt = kN$$

A profile analysis was performed to compare bacterial growth rates (μ_6 vs. $\mu_{0.5}$, μ_{12} vs. μ_6, μ_{24} vs. μ_{12}) between treatments, after which a multivariate analysis of variance (MANOVA) was used to test for significant differences in growth rate between bacteria incubated in I-DOMW and N-DOMW microcosms. Although small sample size can affect the power and the homogeneity of the variance test, profile analysis still provides more power than univariate tests [27]. Graphs were plotted in SigmaPlot (Systat Software, San Jose, CA). A linear regression analysis was used to model the relationship between bacterial concentration (Log CFUmL^{-1}) and extracellular HOOH concentration (μM).

RESULTS AND DISCUSSION

RNA sequencing. The quality and number of reads were documented and all reads were mapped to their corresponding genome (>90%) using BWA (see Supp. Mat.). The average number of reads mapped per sample for *E. coli*, *E. feacalis* and *E. coli* O157:H7 were 1,806,326 ± 144,075 (SE), 1,529,044 ± 124,201(SE) and 1,962,671 ± 446,418 (SE), respectively. The number of genes differentially expressed differed as a function of the type of bacteria and the dark incubation time (P. adjusted < 0.05) (Table 4.1).

Bacteria growth potential differed in water spiked with DOM. All three bacteria differed in their growth dynamics following inoculation into I-DOMW and N-DOMW. *E. coli* and *E. coli* O157:H7 grew by 1-log after 6 h of dark incubation in I-DOMW and N-DOMW, (data not shown) but growth rate was significantly higher for *E. coli* in N-DOMW than I-DOMW (*P*.value < 0.01). (Fig. 4.1). *E. faecalis* showed no significant increase in concentration after 24 h of dark incubation, but decreased in concentration after 6 and 24 h of incubation in I-DOMW. These results suggest that *E. coli* may have a greater potential than *E. faecalis* to grow in the environment under highly bioavailable DOC (concentrations >30mg L^{-1} C). In contrast, *E. faecalis* exhibited a steady state with no significant growth,

suggesting very different growth requirements when compared to *E. coli*. It is noteworthy to mention that *E. faecalis* was able to grow when inoculum concentration was reduced to 10^3 CFU ml^{-1}; however, the final concentration did not surpass 10^6 CFU ml^{-1} (submitted). Further, multivariate analysis of variance (MANOVA) showed that sunlight irradiation of DOM had a small but significant negative effect (*P*. value < 0.05) on *E. coli* and *E. faecalis* growth during dark incubation, suggesting that photo-degradation of DOM might play an inhibitory role (Table 4S1).

Re-growth of *E. coli* in diverse environmental matrices has been reported previously [28-33]. Overnight growth has been implicated in high counts of *E. coli* in surface waters reported in early morning [34, 35]. Few studies have reported re-growth in *E. faecalis* [36-38], implying that these bacteria might have different nutrient requirements in the environment. More importantly, the potential for re-growth may be further limited by the inhibitory role of direct sunlight and production of ROS from DOM [11].

Extracellular HOOH influences bacteria growth dynamics. The concentration of photo-produced HOOH was negatively correlated with *E. coli* (Adj. R^2 = 0.74; *P*-value = 0.004) and *E. coli* O157:H7 concentrations (Adj. R^2= 0.93; *P*-value < 0.001) (Fig. 4S1), with extracellular HOOH decreasing, and bacterial populations increasing in I-DOMW during the first 6 h of dark incubation (Fig 4.1). On the other hand, extracellular HOOH increased significantly in the presence of *E. faecalis*. Further, extracellular HOOH was measured in µM concentrations with all three types of bacteria during dark incubation in N-DOMW microcosms, suggesting that HOOH was produced by bacteria (Fig 4.1). However, bacterial produced HOOH showed no significant correlation with bacterial concentration (P-value > 0.05) (Fig. 4S1). There was no significant decline in HOOH concentration for I-DOMW controls with no bacteria inoculated (Fig. 4S2).

Light and dark production of peroxides from DOM photo-degradation and microbial processes play a significant role in controlling bacterial survival dynamics in environmental waters [15, 39, 40]. Peroxides have the potential to cross bacterial cell membranes and can persist in surface waters for several hours [15, 41]. More importantly, upon entering the cell, HOOH reacts with ferrous iron to form reactive $OH^{\cdot}$ which causes DNA lesions via fenton reactions [42]. Facultative anaerobes including *E. coli* and *E. faecalis*, have developed robust systems, that are capable of detoxifying HOOH and can also alleviate damage caused by $OH^{\cdot}$.

In the present study, *E. coli* efficiently scavenged 95% of photo-produced HOOH within 6 h of dark incubation, while there was an accumulation of HOOH in the *E. faecalis* treatment. The observed buildup of HOOH in *E. faecalis* suggests that bacteria likely differ in their production and detoxification of HOOH [43]. Moreover, *E. faecalis* produces HOOH as a by-product of aerobic glycerol metabolism, which could have contributed to the observed increase in I-DOMW treatment. [44].

HOOH photo-production induces OxyR responsive genes in *E. coli* and *E. coli* O157:H7. The OxyR regulon in *E. coli* is responsible for sensing oxidative stress and positively regulates the induction of several genes [45]. Unsupervised analysis of RNA-Seq on bacterial mRNA recovered at ~0.5, 6, 12 and 24 h showed consistent transcriptional changes in bacteria incubated in I-DOMW compared to N-DOMW controls (Fig. 4.2a and c). The genetic and protein interactions inferred from differentially expressed transcripts (Szklarczyk et al. 2014) included up-regulated gene networks for oxidative stress, HOOH detoxification and an iron-sulfur cluster.

Following inoculation in I-DOMW, a significant increase in expression of *oxyR* regulated genes in both *E. coli* and *E. coli* O157:H7 was observed (Fig. 4.2a and c). Many

of these genes play a central role in the detoxification of HOOH and its conversion to water. Catalase (*katG*) and peroxidase (*ahpCF*) genes were among the most highly expressed (>2- Fold change) after 0.5 h (Fig. 4.2 and 4.3). Further, genes involved in iron sequestration (*dps* and Fe-S cluster) and fenton reactions during oxidative stress were also highly expressed immediately after inoculation. In addition, there was increased expression in transcripts involved in iron uptake and siderophore transport in *E. coli* O157: H7 (Fig. 4.2 and 4.3).

On the other hand, peroxidase (*npr, ahpC, tpx*), heme-dependent catalase (*katA*) and thioredoxin (*trx*) genes in *E. faecalis* did not show significant differential expression following inoculation (Fig. 4.3b) despite the relevant role of these genes in peroxide metabolism as demonstrated by prior work showing that mutations in these genes can limit the survival of *E. faecalis* exposed to exogenously added HOOH [46]. A possible explanation could be a requirement for an endogenous peroxide concentration threshold before these genes are activated or turned on. In the study by La Carbona et al. (2007), the authors used >5mM concentration of HOOH while µM concentrations were produced in our study. Yan, et al. [47] also reported less than two-fold change in these genes when exposed to low levels of HOOH (1.5-2mM). Therefore, it is plausible that in our study, HOOH generated inside *E. faecalis* cells (endogenous) is more deleterious than the low concentrations produced exogenously following DOM irradiation. Although a small decrease in growth rate was observed in I-DOMW treatments, *E. faecalis* was able to rebound quickly to achieve the same growth rate observed in N-DOMW.

The ability for *E. coli* and *E. coli* O157:H7 to efficiently induce oxidative stress genes in response to ambient levels of HOOH may offer them an advantage in the environment. Upon exposure to photo-produced HOOH, these bacteria have the ability to remove

significant concentrations of HOOH and repair DNA lesions within hours, with a potential to grow overnight if required substrates are available. Morris, et al. [48], using diel metatranscriptomic data from five published marine studies spanning a variety of open ocean sites showed that the abundance of transcripts with catalase and peroxidase activity peaked in the late afternoon, coinciding with the highest concentration of HOOH. This might not be the case for *E. faecalis*, as its inability to scavenge exogenously produced HOOH and its accumulation during growth may further limit its proliferation in the environment. Consequently, *E. faecalis's* role in HOOH fluctuation in surface waters may be restricted to production.

Glycerol metabolism is important for *E. faecalis* survival. The major structural barrier in *E. faecalis* is its peptidoglycan wall which is anchored by teichoic acids (TA) and lipotechoic acids (LTA). TA and LTA are polymers of poly- glycerol phosphate which are joined together by phosphodiester linkages [49]. They provide several functions including scavenging of cations, phosphate reservoir, cell envelope adhesiveness, and immunogenicity. Glycerol metabolism is important for the synthesis of glycerol phosphate in a reaction involving glycerol facilitator protein (*glpF*) and phosphorylated glycerol kinase (*glpK*). The phosphoenolpyruvate (PEP): carbohydrate phosphotransferase system (PTS) is responsible for the phosphorylation of *glpK* [44, 50]. Immediately after inoculation, these genes were significantly upregulated in N-DOMW for up to 12 h (*P*. value < 0.05) (Fig. 4.2b and 4.3b). The majority of the proteins in the PEP: PTS are involved with the transport of sugars including lactose, sorbose, mannose, sucrose, cellobiose and fructose across the cell membrane. The PTS in *E. faecalis* is also involved in inducer expulsion, inducer exclusion, and catabolite repression [51]. Phosphorylation of *glpK* by PTS is ATP-dependent and it is important for catabolism of glycerol, suggesting *E. faecalis* may have limited the

expression of these genes to conserve ATP by limiting the active transport of carbohydrates into the cell. As a consequence, *E. faecalis* appears to be unable to achieve maximum growth and its survival dynamics maybe compromised.

Extracellular HOOH signaling contributes to adaptive response. Environmental cues including non-lethal doses of ROS, antimicrobials, nutrient limitation, and temperature can make bacteria alter their transcriptome rapidly [52-54]. Such responses can prolong their survival and, more importantly, enhance resistance to higher doses of the same stressor or other stressors [55, 56]. This form of adaptive resistance is believed to be transient and usually reverts upon removal of the inducing agent [54].

In our study, multiple genetic networks associated with virulence, quorum sensing, and antibiotic resistance were up-regulated in I-DOMW. These differentially expressed genes included significant increases in genes for outer membrane receptors that facilitate the import of iron-chelating siderophores and iron from host organisms (Fig. 4.2c) which are important for *E. coli* O157:H7 pathogenicity [57]. The tryptophan operon is a repressor operon that is turned-on or turned-off based on the levels of tryptophan in the environment. In addition, tryptophan is the primary source of indole production in *E. coli*, an organic compound that plays a role in quorum sensing, biofilm formation and antibiotic resistance [58, 59]. [59] Kuczynska-Wisnik et al. showed that the addition of dimethyl sulfoxide (HOOH scavenger) partly restored *E. coli* biofilm formation in the presence of antibiotics and decreased indole production. Transcripts for tryptophan biosynthesis (*trpEDCBA*) increased significantly following inoculation (0.5 h) into I-DOMW and after 6 h in N-DOMW (Fig. 4.2c and 4S2). In addition, extracellular HOOH concentration in I-DOMW and N-DOMW at 0.5 h and 6 h was 15.4 ± 0.81 and 2.59 ± 1.26 (SE) μM respectively (Fig. 4.1). Results from this study indicate that indole production may be required for *E. coli* O157: H7

survival under increased extracellular peroxide concentration and consequently, may be enhancing this pathogen's biofilm formation and antibiotic resistance capability.

Curli is a proteinaceous extracellular matrix associated with attachment and biofilm formation, and it plays a major role in bacterial pathogenesis [60]. Moreover, biofilm formation has been associated with oxidative stress including HOOH exposure [61-63]. Extracellular HOOH measured at 6 h was higher in N-DOMW than I-DOMW (4.58 ± 0.71μM vs < LOQ) (Fig. 4.1a). Further, the expression of *csgAB* genes encoding curli/amyloid fibers increased significantly in N-DOMW after 6 h of dark incubation (Fig. 4S4). This provides supporting evidence that *E. coli* may increase biofilm formation in response to endogenously produced HOOH [64].

The expression of genes coding for porins and efflux pumps play important roles in adaptive resistant development [54, 65]. They are efficiently regulated in order to respond to specific cues, thereby changing the resistance of a bacterium based on growth conditions. For example, Suzuki, Horinouchi and Furusawa [53] demonstrated that antibiotic resistance development in *E. coli* could be quantitatively predicted by the expression changes of a small number of genes. Oligopeptide (*opp*) genes encoding sex pheromones (EF0063, EF1513) and peptide transport (EF0909) significantly increased in *E. faecalis* after 6 h of dark incubation in I-DOMW (Fig. 4.2b). These genes play important roles in beta-lactamase resistance and quorum sensing in *E. faecalis*, and their induction in response to HOOH and growth in urine has been reported [47, 66]. In the present study, time point 6 h corresponded with 170% increase in extracellular HOOH (Fig. 4.1b), suggesting oligopeptide genes may be responsive to oxidative stress.

The potential for sublethal levels of ROS to increase bacterial minimum inhibitory concentration (MIC) to antibiotics requires more research. Dwyer, et al. [67] reported that

pretreatment of *E. coli* cells with 1 or 5mM HOOH for 15 min did not induce any lethality or growth inhibition; however, it resulted in a transient 1-log protection of cells from antibiotic killing.

Genes associated with quorum sensing were significantly upregulated in *E. coli* (Fig. 4.2a and 4S3). Quorum sensing (QS) is a form of regulation of gene expression used by the majority of bacteria in response to fluctuations in cell population density. Quorum sensing bacteria produce and release chemical signal molecules called autoinducers that increase in concentration as a function of cell density. Gram-positive and Gram-negative bacteria use QS communication signals to regulate a diverse array of physiological activities [68]. The level of auto-inducer -2 (AI-2) produced extracellularly varies depending upon the growth conditions, and its transport is mediated by *lsrACDBFGE* operon. In *E. coli*, expression of *lsrBFG* transcripts significantly increased in I-DOMW after 6 h (Fig. 4S3), which corresponds to the time point with the highest growth rate (Fig. 4.1a). Further, the upregulation of QS genes may be influenced by HOOH exposure. For instance, Yu, et al. [69] showed that ΔLuxS *Yersinia pestis* mutants (LuxS regulates *lsr*) were more sensitive to killing by HOOH than their wildtype.

CONCLUSION

Hydrogen peroxide is omnipresent in surface waters. Its prevalence in water bodies is determined by several factors including sunlight, DOM, temperature and the microbial communities present. These interconnected processes all play a vital role in the survival and growth of bacteria in the environment. We provide for the first time valuable insights on the dynamics of survival in two widely used indicator bacteria and a zoonotic pathogen of public health importance, under environmentally relevant concentrations of peroxides. Upon exposure to photo-produced HOOH, *E. coli* and *E. coli* O157:H7 immediately

increased the expression of catalase, peroxidase, and iron sequestering proteins. These proteins protect and alleviate bacteria from DNA damaging hydroxyl radicals and provides them with an advantage to survive and potentially proliferate in the presence of ambient concentration of exogenous peroxides. The sensitivity of *E. faecalis* to light-produced ROS has been reported [70-72], but its mechanism of survival warrants further study. In our study, *E. faecalis* did not demonstrate an increased expression of peroxidase or catalase genes, suggesting its survival mechanism differs from that of *E. coli*. In contrast, following exposure to micromolar exogenous HOOH concentrations, *E. faecalis* decreased the expression of several proteins involved in glycerol metabolism and transport of carbohydrates, for up to 6 h. A consequence of such response was limited growth and accumulation of HOOH in the growth medium. Although, *E. faecalis* represents only a species of the genus *Enterococcus,* our results provide evidence supporting the notion that enterococci have a low re-growth potential in environmental waters.

Dark production of HOOH, presumably through the accidental autoxidation of redox enzymes, was observed among all three bacteria investigated. Studies have shown that *E. coli* generates about 10 to 15μM s^{-1} of endogenous HOOH during growth in air-saturated glucose medium [73]. Intracellular HOOH will accumulate in a closed system by flowing out of the cell rather than into the cytoplasm [45]. For *E. faecalis*, HOOH dark production is controlled by glycerol-3-P oxidase (*glpO*) via oxidation to dihydroxyacetone phosphate, an intermediate of glycolytic pathway [50]. This enzyme uses molecular oxygen as the electron sink, which leads to the formation of HOOH. In natural oxic ecosystems (e.g., streams, rivers and ponds), the excreted HOOH would not build up but would be lost to the environment.

Our results showed that *E. coli* and *E. faecalis* respond to ambient levels of exogenous HOOH via different mechanisms. Consequently, their survival dynamics in surface waters containing peroxides are expected to differ. Moreover, *E. faecalis* may depend on efficient peroxidase and catalase producers like *E. coli* for survival. Overall, HOOH signaling seems to play a significant role in altering the bacterial transcriptome, including transcripts associated with virulence, biofilm formation, quorum sensing and antibiotic resistance.

ACKNOWLEDGEMENTS

We are grateful to Kyler Herrington and Troy Kieran for their help with sample analysis. We also appreciate Dr. Richard Zepp for valuable advice during the solar simulation experiments and Mary Katherine Crews for manuscript review. We thank the Kennedy family at Covenant Valley Farm and the Nixon family at Cane Creek Farm, Inc., for allowing us access to their cattle. This work was supported by the Environmental Protection Agency (EPA) Star Fellowship [FP-91766701 to A.O] and EPA's Office of Research and Development. Any opinions expressed in this paper are

those of the authors and do not necessarily reflect the official positions and policies of the U.S. EPA and any mention of products or trade names does not constitute recommendation for use. The authors declare no competing commercial interests in relation to the submitted work.

FIGURES AND TABLES

A

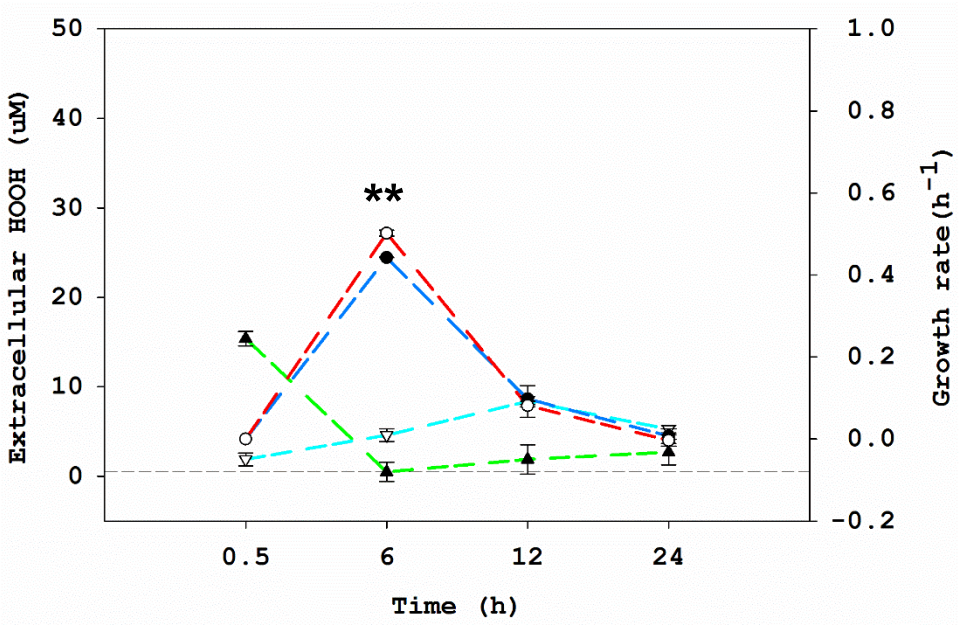

B

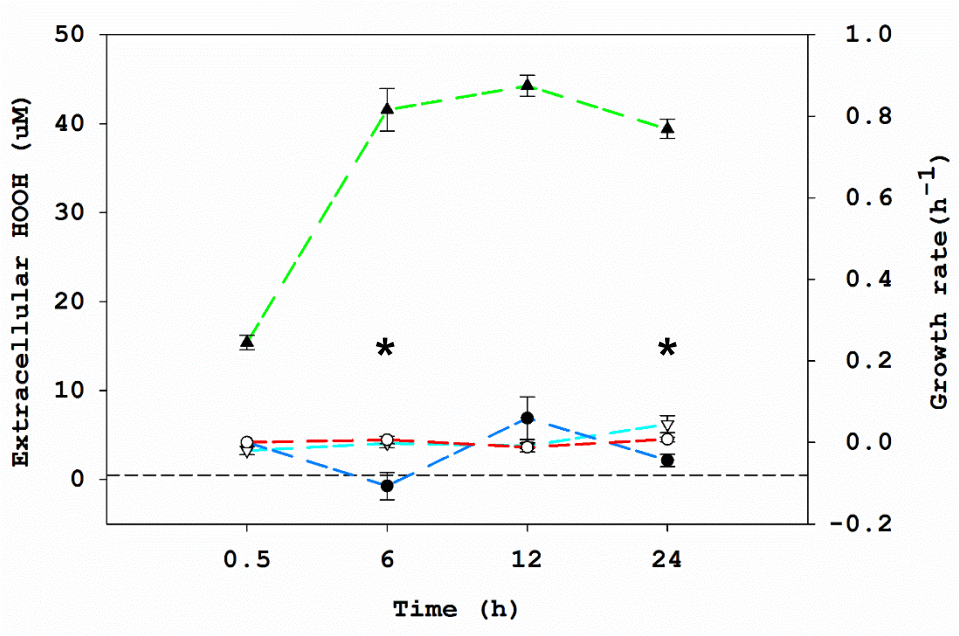

C

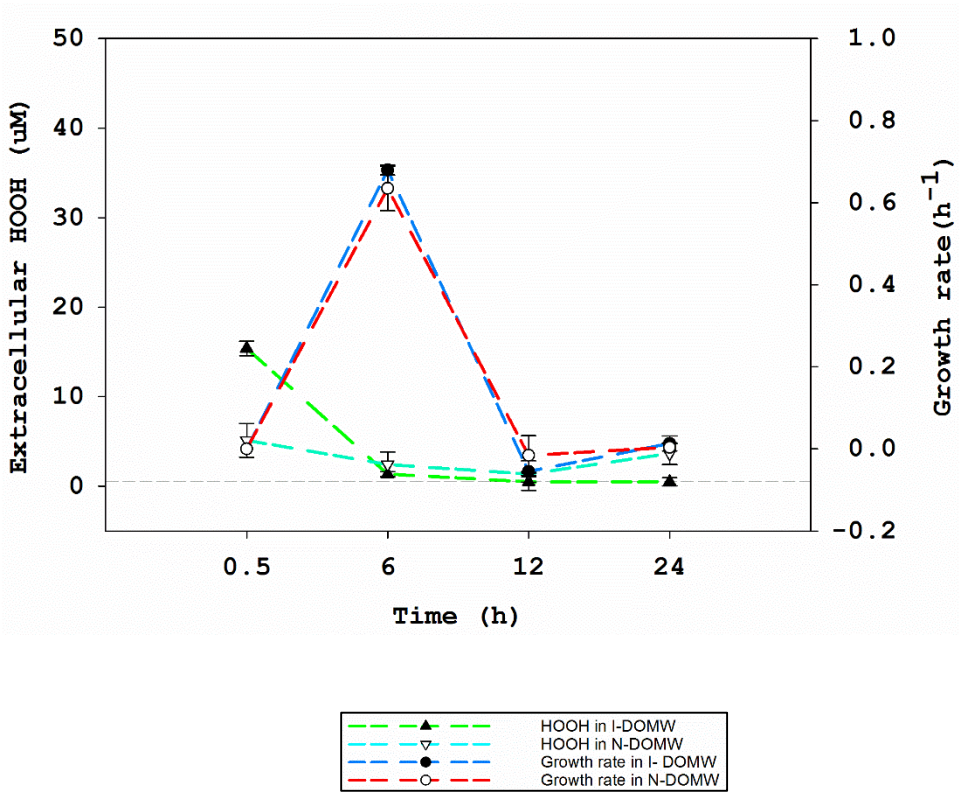

Figure 4.1. Irradiation of water spiked (I-DOMW) with CFE prior to bacteria inoculation produces exogenous HOOH and inhibits growth of FIB. Triangles represent extracellular HOOH concentration during dark incubation in I-DOMW and N-DOMW in the presence of (A) *E. coli* (B) *E. faecalis* (C) *E. coli* O157:H7. Bacteria were collected 0.5, 6, 12, and 24 h during dark incubation and filter sterilized with a 0.22µm syringe filter. Filtrate (n = 3 per group) was quantified for HOOH using the copper-DMP method. Horizontal short dash lines represent method detection limit (0.5µM of pure HOOH). Growth rates per time point per group were plotted on the right y-axis (circles). Error bars represent standard errors. *denotes level of significance for the effect of sunlight irradiation on bacteria growth rate per time point (*P<0.05, **P<0.01). Figure modified from Oladeinde et al. 2017[74].

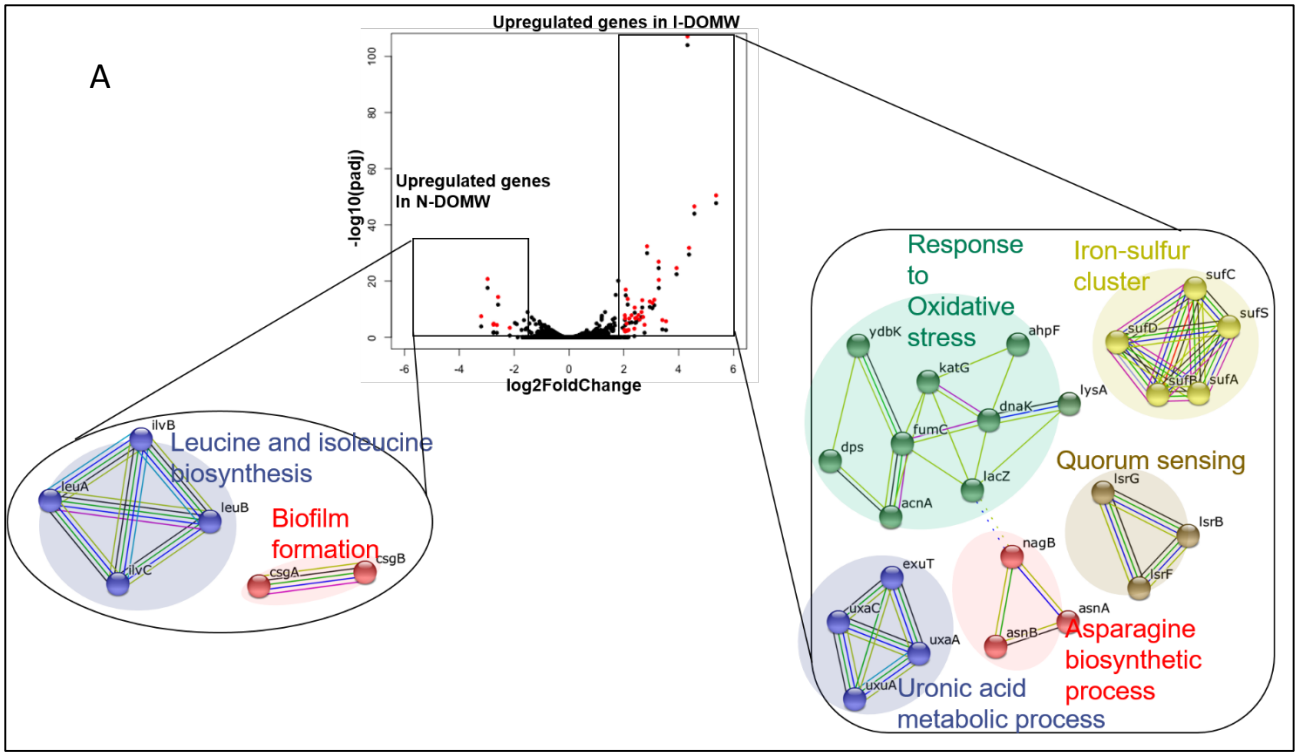
A
Upregulated genes in I-DOMW
Upregulated genes
In N-DOMW
-log10(padj)
log2FoldChange
Leucine and isoleucine
biosynthesis
ilvB
leuA
leuB
ilvC
Biofilm
formation
csgA
csgB
Response
to
Oxidative
stress
ydbK
ahpF
katG
dnaK
lysA
fumC
dps
lacZ
acnA
Iron-sulfur
cluster
sufC
sufS
sufD
sufB
sufA
Quorum sensing
lsrG
lsrB
lsrF
nagB
exuT
uxaC
uxaA
uxuA
asnA
asnB
Asparagine
biosynthetic
process
Uronic acid
metabolic process

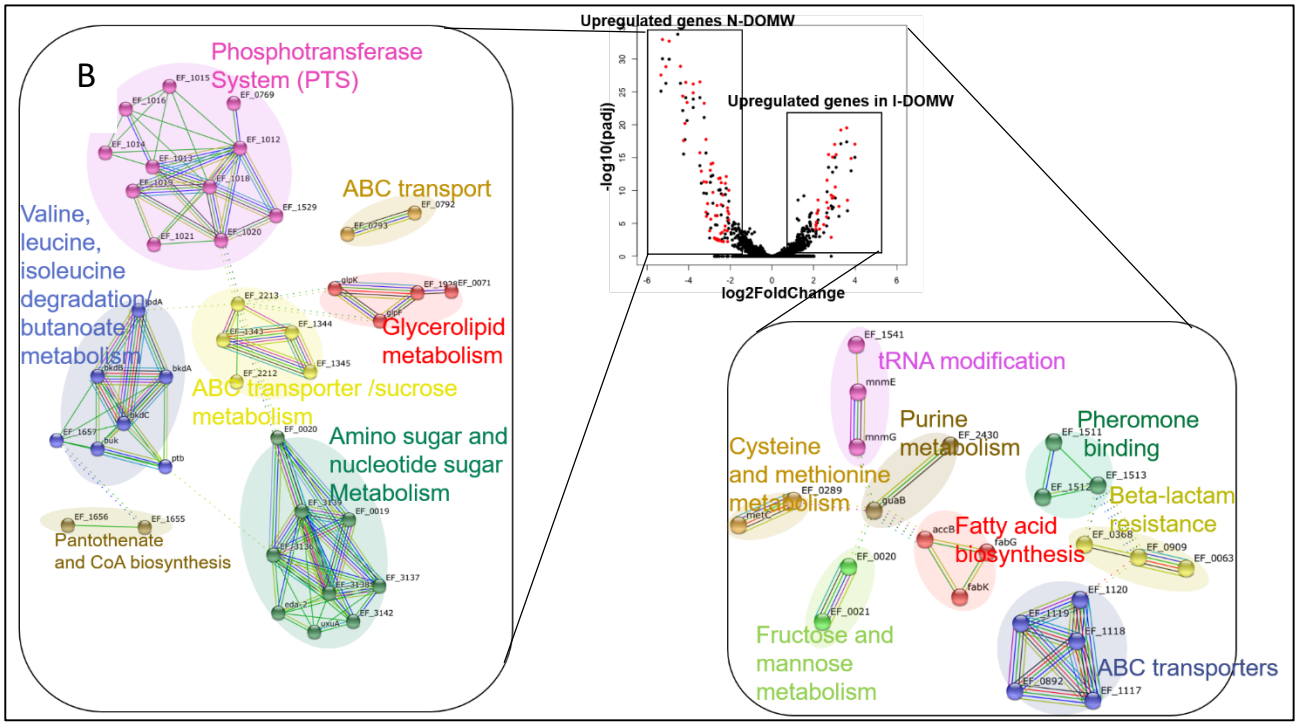
B
Upregulated genes N-DOMW
Upregulated genes in I-DOMW
-log10(padj)
log2FoldChange
Phosphotransferase
System (PTS)
ABC transport
Valine,
leucine,
isoleucine
degradation/
butanoate
metabolism
Glycerolipid
metabolism
ABC transporter /sucrose
metabolism
Amino sugar and
nucleotide sugar
Metabolism
Pantothenate
and CoA biosynthesis
tRNA modification
Cysteine
and methionine
metabolism
Purine
metabolism
Pheromone
binding
Beta-lactam
resistance
Fatty acid
biosynthesis
Fructose and
mannose
metabolism
ABC transporters

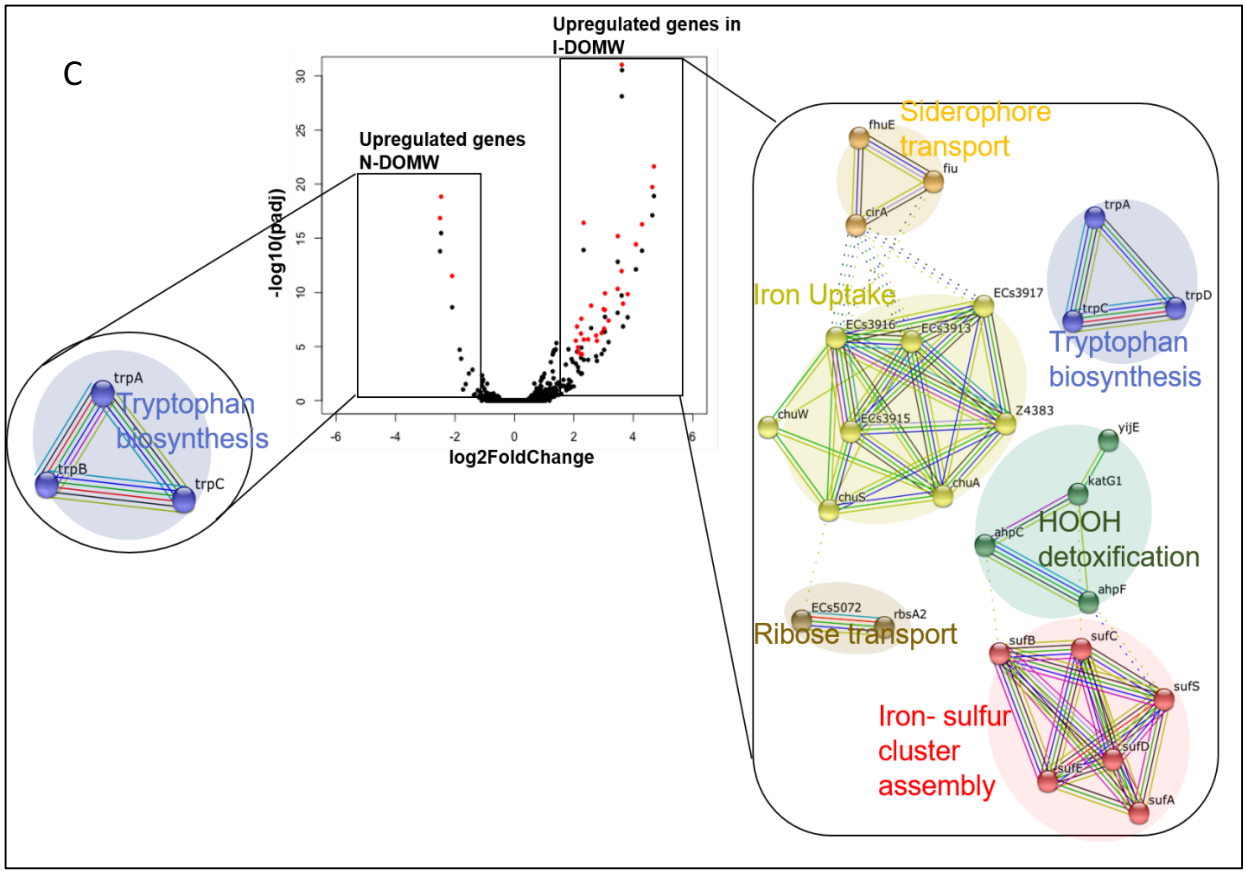

Figure 4.2. Exposure to photo-produced hydrogen peroxide causes extensive changes in bacterial gene expression profile during dark incubation. Center: Volcano plot showing fold-change of gene expression in I-DOMW compared to N-DOMW. Transcripts with significantly increase in expression between the groups (*P*.adj < 0.01; fold- change ≥ 2) are highlighted in red; lower: STRING analysis for significantly altered genes in each case for (A) *E. coli* (B) *E. faecalis* and (C) *E. coli* O157:H7. Total RNA was extracted from bacterial cultures collected at 0.5, 6, 12 and 24 h and used for WTS (n=2 per group).

A

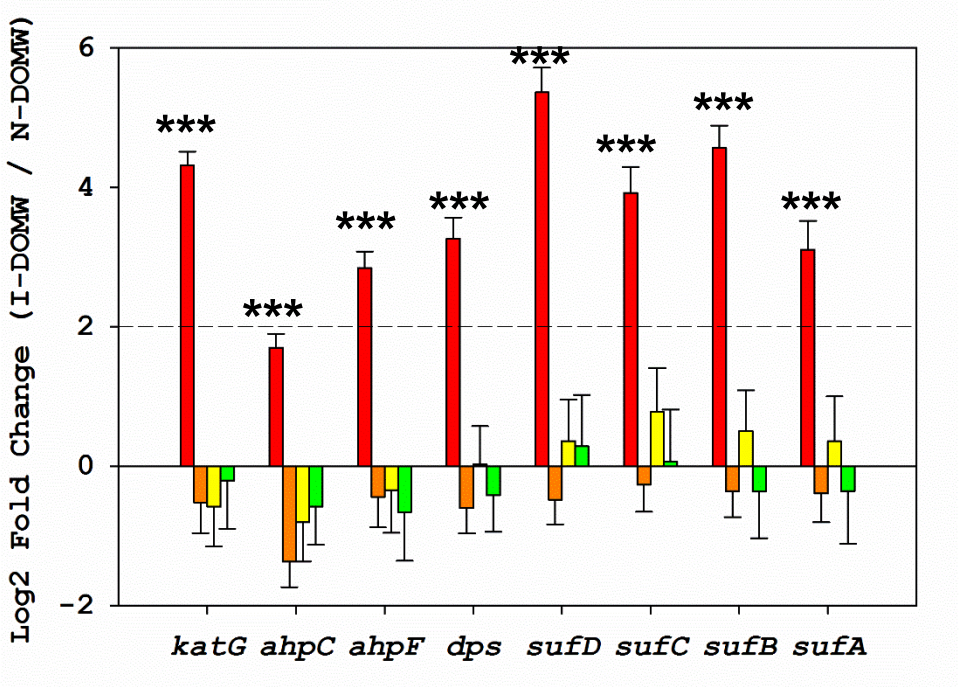
Log2 Fold Change (I-DOMW / N-DOMW)
6
4
2
0
-2
***
***
***
***
***
***
***
katG ahpC ahpF dps sufD sufC sufB sufA

B

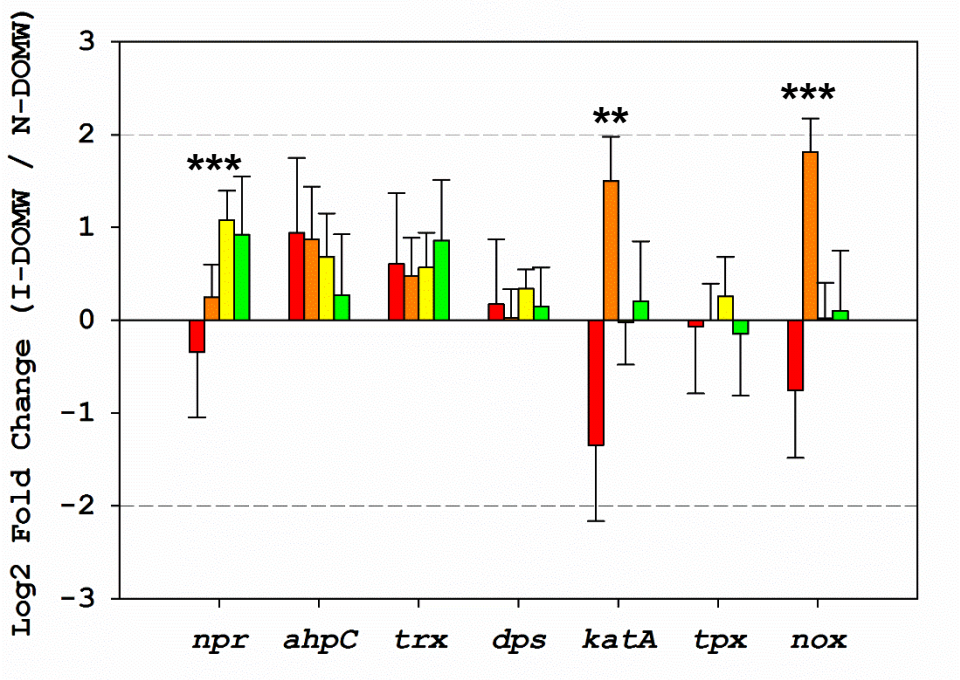
Log2 Fold Change (I-DOMW / N-DOMW)
3
2
1
0
-1
-2
-3
***
**
***
npr ahpC trx dps katA tpx nox

C

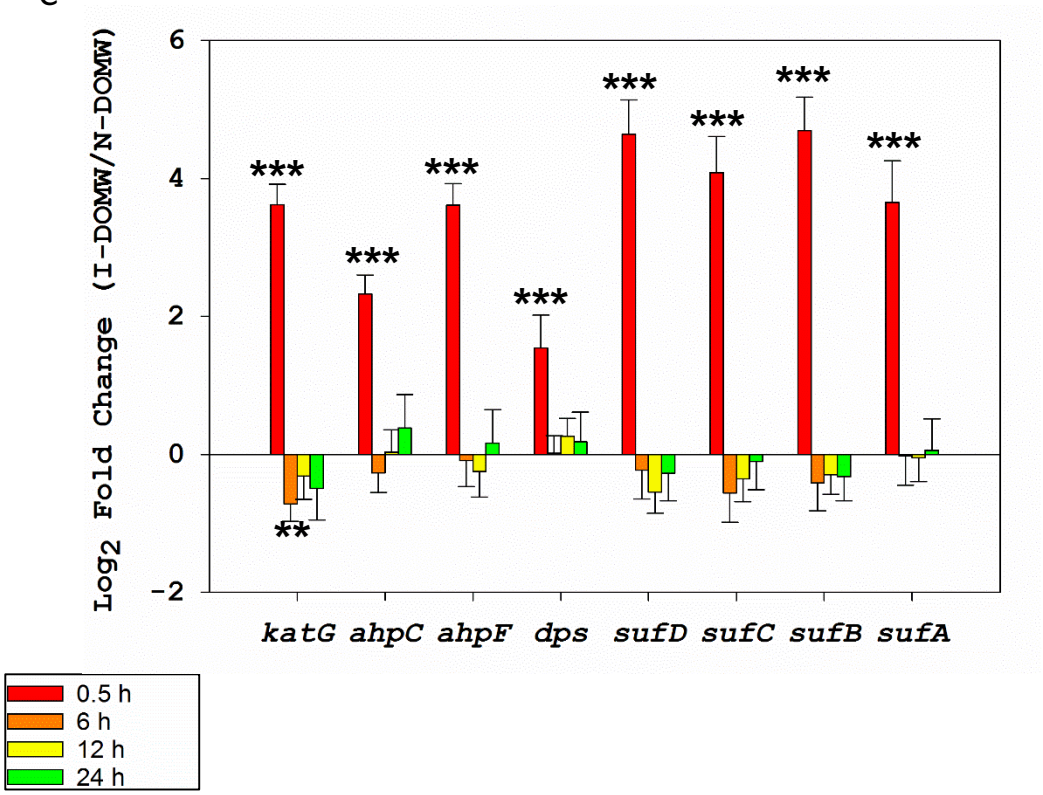

Figure 4.3. Peroxidase and catalase producing enzymes are significantly upregulated in *E. coli* upon exposure to photo-produced HOOH. Fold-change of selected transcripts for oxidative stress between I-DOMW and N-DOMW for (A) *E. coli* (B) *E. faecalis* and (C) *E. coli* O157:H7. (**P* value <0.05, **<0.01, **<0.001)

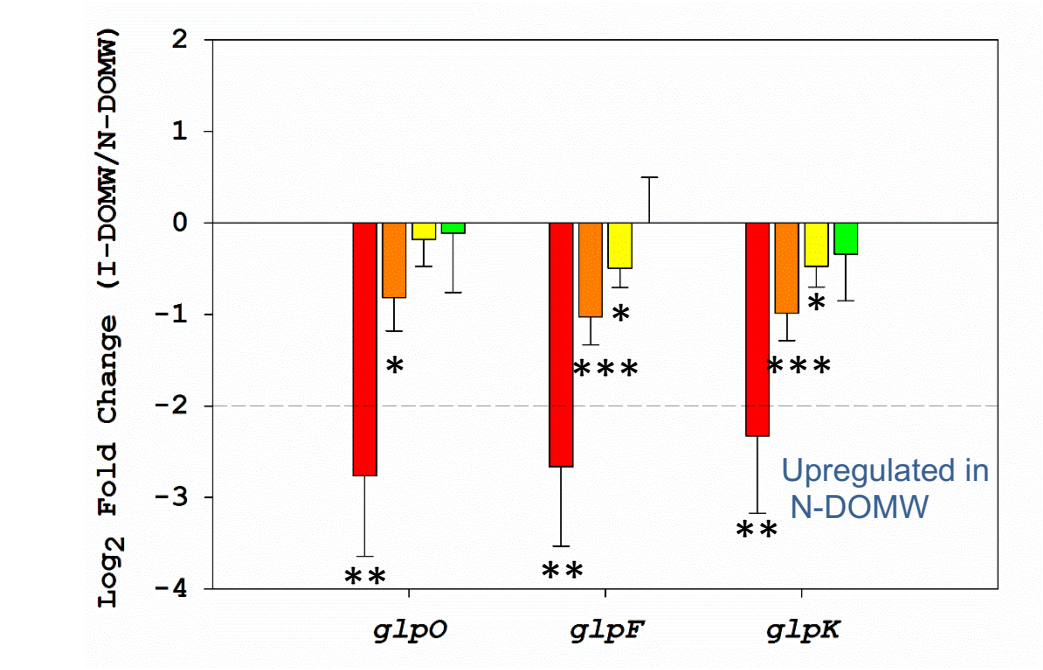

Figure 4.4. Glycerol metabolism contributes to dark production of HOOH. Fold-change of genes involved in the aerobic metabolism of glycerol via the *glpK* pathway between I-DOMW and N-DOMW for *E. faecalis* (**P* value <0.05, **<0.01, **<0.001

Table 4.1: Number of differentially expressed genes (DEG) (*P*.adj <0.05) between bacteria incubated in I-DOMW and N-DOMW

Bacteria	Time (h)	Upregulated genes in I-DOMW	Upregulated genes in N-DOMW
E. coli	0.5	76	88
	6	10	5
	12	3	4
	24	0	0
E. faecalis	[#] 0.5	22	36
	6	130	143
	12	25	23
	24	2	19
E. coli O157:H7	0.5	47	6
	6	21	7
	12	0	0
	24	1	0

[#] *p. value reported instead of p. adjusted due to low sample size (n=1) at 0.5 h for E. faecalis*.

REFERENCES

1. Bradford, S. A.; Morales, V. L.; Zhang, W.; W., H. R.; Packman, A. I.; Mohanram, A.; Welty, C., Transport and Fate of Microbial Pathogens in Agricultural Settings. *Critical Reviews in Environmental Science & Technology* **2013,** *43*, (8), 775-893.

2. Bradford, S. A.; Schijven, J.; Harter, T., Microbial Transport and Fate in the Subsurface Environment: Introduction to the Special Section. *Journal of environmental quality* **2015,** *44*, (5), 1333-1337.

3. Pachepsky, Y. A. In *Fate and transport of manure-borne indicators and pathogen microorganisms*, Office of Research and Development U.S Environmental Protection Agency, Athens, GA, November 15, 2011; Athens, GA, 2011.

4. Azam, F.; Fenchel, T.; Field, J. G.; Gray, J.; Meyer-Reil, L.; Thingstad, F., The ecological role of water-column microbes in the sea. *Estuaries* **1983,** *50*, (2).

5. Meyer, J., The microbial loop in flowing waters. *Microbial Ecology* **1994,** *28*, (2), 195-199.

6. Mostofa, K. M.; Yoshioka, T.; Mottaleb, A.; Vione, D., *Photobiogeochemistry of organic matter: principles and practices in water environments*. Springer Science & Business Media: 2012.

7. Häder, D.-P.; Williamson, C. E.; Wängberg, S.-Å.; Rautio, M.; Rose, K. C.; Gao, K.; Helbling, E. W.; Sinha, R. P.; Worrest, R., Effects of UV radiation on aquatic ecosystems and interactions with other environmental factors. *Photochemical & Photobiological Sciences* **2015,** *14*, (1), 108-126.

8. Bushaw, K. L.; Zepp, R. G., Photochemical release of biologically available nitrogen from aquatic dissolved organic matter. *Nature* **1996,** *381*, (6581), 404.

9. Moran, M. A.; Zepp, R. G., Role of photoreactions in the formation of biologically labile compounds from dissolved organic matter. *Limnology and Oceanography* **1997,** *42*, (6), 1307-1316.

10. Häder, D.-P.; Helbling, E.; Williamson, C.; Worrest, R., Effects of UV radiation on aquatic ecosystems and interactions with climate change. *Photochemical & Photobiological Sciences* **2011,** *10*, (2), 242-260.

11. Anesio, A. M.; Granéli, W.; Aiken, G. R.; Kieber, D. J.; Mopper, K., Effect of humic substance photodegradation on bacterial growth and respiration in lake water. *Applied and environmental microbiology* **2005,** *71*, (10), 6267-6275.

12. Mostofa, K. M.; Sakugawa, H., Spatial and temporal variations and factors controlling the concentrations of hydrogen peroxide and organic peroxides in rivers. *Environmental Chemistry* **2009,** *6*, (6), 524-534.

13. Kieber, D. J.; Peake, B. M.; Scully, N. M., Reactive oxygen species in aquatic ecosystems. *UV effects in aquatic organisms and ecosystems. Royal Society of Chemistry* **2003**, 251-288.

14. Clark, C. D.; De Bruyn, W. J.; Jakubowski, S. D.; Grant, S. B., Hydrogen peroxide production in marine bathing waters: implications for fecal indicator bacteria mortality. *Marine pollution bulletin* **2008,** *56*, (3), 397-401.

15. Mostofa, K. M.; Liu, C.-q.; Sakugawa, H.; Vione, D.; Minakata, D.; Wu, F., Photoinduced and microbial generation of hydrogen peroxide and organic peroxides in natural waters. In *Photobiogeochemistry of Organic Matter*, Springer: 2013; pp 139-207.

16. Imlay, J. A., Transcription Factors That Defend Bacteria Against Reactive Oxygen Species. *Annual Review of Microbiology* **2015,** *69*, (1).

17. Adams, M. H., *Bacteriophages*. Interscience: London, United Kingdom, 1959.

18. Kosaka, K.; Yamada, H.; Matsui, S.; Echigo, S.; Shishida, K., Comparison among the methods for hydrogen peroxide measurements to evaluate advanced oxidation processes: application of a spectrophotometric method using copper (II) ion and 2, 9-dimethyl-1, 10-phenanthroline. *Environ Sci Technol* **1998,** *32*, (23), 3821-3824.

19. Glenn, T.; Nilsen, R.; Kieran, T., Adapterama I: Universal stubs and primers for thousands of dual-indexed Illumina libraries (iTru & iNext). bioRxiv, 049114. **2016**.

20. Li, H.; Durbin, R., Fast and accurate short read alignment with Burrows–Wheeler transform. *Bioinformatics* **2009,** *25*, (14), 1754-1760.

21. Li, H.; Handsaker, B.; Wysoker, A.; Fennell, T.; Ruan, J.; Homer, N.; Marth, G.; Abecasis, G.; Durbin, R., The sequence alignment/map format and SAMtools. *Bioinformatics* **2009,** *25*, (16), 2078-2079.

22. Quinlan, A. R.; Hall, I. M., BEDTools: a flexible suite of utilities for comparing genomic features. *Bioinformatics* **2010,** *26*, (6), 841-842.

23. Team, R. D. C. *R: A language and environment for statistical computing. R Foundation for Statistical Computing*, Vienna, Austria, 2012.

24. Love, M. I.; Huber, W.; Anders, S., Moderated estimation of fold change and dispersion for RNA-seq data with DESeq2. *Genome biology* **2014,** *15*, (12), 1.

25. Szklarczyk, D.; Franceschini, A.; Wyder, S.; Forslund, K.; Heller, D.; Huerta-Cepas, J.; Simonovic, M.; Roth, A.; Santos, A.; Tsafou, K. P., STRING v10: protein–protein interaction networks, integrated over the tree of life. *Nucleic acids research* **2014**, gku1003.

26. Van Dongen, S., Graph clustering via a discrete uncoupling process. *SIAM Journal on Matrix Analysis and Applications* **2008,** *30*, (1), 121-141.

27. Macedo, M.; Waterson, T. Profile Analysis. http://userwww.sfsu.edu/efc/classes/biol710/manova/profileanalysis.htm (December, 2016),

28. Giannakis, S.; Darakas, E.; Escalas-Canellas, A.; Pulgarin, C., Elucidating bacterial regrowth: Effect of disinfection conditions in dark storage of solar treated secondary effluent. *J Photoch Photobio A* **2014,** *290*, 43-53.

29. Giannakis, S.; Darakas, E.; Escalas-Cañellas, A.; Pulgarin, C., Solar disinfection modeling and post-irradiation response of Escherichia coli in wastewater. *Chemical Engineering Journal* **2015,** *281*, 588-598.

30. Sanders, E. C.; Yuan, Y. P.; Pitchford, A., Fecal Coliform and E. coli Concentrations in Effluent-Dominated Streams of the Upper Santa Cruz Watershed. *Water-Sui* **2013,** *5*, (1), 243-261.

31. Oladeinde, A.; Bohrmann, T.; Wong, K.; Purucker, S.; Bradshaw, K.; Brown, R.; Snyder, B.; Molina, M., Decay of Fecal Indicator Bacterial Populations and Bovine-Associated Source-Tracking Markers in Freshly Deposited Cow Pats. *Applied and environmental microbiology* **2014,** *80*, (1), 110-118.

32. Oliver, D. M.; Bird, C.; Burd, E.; Wyman, M., Quantitative PCR profiling of E. coli in livestock faeces reveals increased population resilience relative to culturable counts under temperature extremes. *Environ Sci Technol* **2016**.

33. Harvey, W. H.; Underwood, J. I.; Lisle, J.; Metge, D. W.; Aiken, G. In *Role of Surface Water Dissolved Organic Carbon in the Survival, Growth, and Transport of Escherichia coli in a Deep Limestone Aquifer in South Florida*, U.S. Geological Survey Karst Interest Group Proceedings, Carlsbard, New Mexico, April 29–May 2

, 2014; Kuniansky, E. L.; Spanler, L. E., Eds. U.S. Geological Survey Scientific Investigations Report Carlsbard, New Mexico, 2014; pp 129-132.

34. Whitman, R. L.; Nevers, M. B.; Korinek, G. C.; Byappanahalli, M. N., Solar and temporal effects on Escherichia coli concentration at a Lake Michigan swimming beach. *Applied and Environmental Microbiology* **2004,** *70*, (7), 4276-4285.

35. Desai, A. M.; Rifai, H. S., Escherichia coli Concentrations in Urban Watersheds Exhibit Diurnal Sag: Implications for Water-Quality Monitoring and Assessment. *JAWRA Journal of the American Water Resources Association* **2013,** *49*, (4), 766-779.

36. Litton, R. M.; Ahn, J. H.; Sercu, B.; Holden, P. A.; Sedlak, D. L.; Grant, S. B., Evaluation of Chemical, Molecular, and Traditional Markers of Fecal Contamination in an Effluent Dominated Urban Stream. *Environ Sci Technol* **2010,** *44*, (19), 7369-7375.

37. Kim, M.; Wuertz, S., Survival and persistence of host-associated Bacteroidales cells and DNA in comparison with Escherichia coli and Enterococcus in freshwater sediments as quantified by PMA-qPCR and qPCR. *Water Research* **2015,** *87*, 182-192.

38. Dubinsky, E. A.; Butkus, S. R.; Andersen, G. L., Microbial source tracking in impaired watersheds using PhyloChip and machine-learning classification. *Water Research* **2016**.

39. Zhang, T.; Hansel, C. M.; Voelker, B. M.; Lamborg, C. H., Extensive dark biological production of reactive oxygen species in brackish and freshwater ponds. *Environ Sci Technol* **2016,** *50*, (6), 2983-2993.

40. Cory, R.; Davis, T.; Dick, G.; Johengen, T.; Denef, V.; Berry, M.; Page, S.; Watson, S.; Yuhas, K.; Kling, G., Seasonal Dynamics in Dissolved Organic Matter, Hydrogen Peroxide, and Cyanobacterial Blooms in Lake Erie. Front. *Mar. Sci* **2016,** *3*, 54.

41. Imlay, J. A., Cellular defenses against superoxide and hydrogen peroxide. *Annu Rev Biochem* **2008,** *77*, 755-76.

42. Imlay, J. A., Diagnosing oxidative stress in bacteria: not as easy as you might think. *Current opinion in microbiology* **2015,** *24*, 124-131.

43. Marsico, R. M.; Schneider, R. J.; Voelker, B. M.; Zhang, T.; Diaz, J. M.; Hansel, C. M.; Ushijima, S., Spatial and temporal variability of widespread dark production and decay of hydrogen peroxide in freshwater. *Aquatic Sciences* **2015,** *77*, (4), 523-533.

44. Bizzini, A.; Zhao, C.; Budin-Verneuil, A.; Sauvageot, N.; Giard, J.-C.; Auffray, Y.; Hartke, A., Glycerol is metabolized in a complex and strain-dependent manner in Enterococcus faecalis. *Journal of bacteriology* **2010,** *192*, (3), 779-785.

45. Kumar, S. R.; Imlay, J. A., How Escherichia coli tolerates profuse hydrogen peroxide formation by a catabolic pathway. *Journal of bacteriology* **2013,** *195*, (20), 4569-4579.

46. La Carbona, S.; Sauvageot, N.; Giard, J. C.; Benachour, A.; Posteraro, B.; Auffray, Y.; Sanguinetti, M.; Hartke, A., Comparative study of the physiological roles of three peroxidases (NADH peroxidase, Alkyl hydroperoxide reductase and Thiol peroxidase) in oxidative stress response, survival inside macrophages and virulence of Enterococcus faecalis. *Molecular microbiology* **2007,** *66*, (5), 1148-1163.

47. Yan, X.; Budin-Verneuil, A.; Verneuil, N.; Gilmore, M. S.; Artigaud, S.; Auffray, Y.; Pichereau, V., Transcriptomic Response of Enterococcus faecalis V583 to Low Hydrogen Peroxide Levels. *Current microbiology* **2015,** *70*, (2), 156-168.

48. Morris, J. J.; Johnson, Z. I.; Wilhelm, S. W.; Zinser, E. R., Diel regulation of hydrogen peroxide defenses by open ocean microbial communities. *Journal of Plankton Research* **2016**, fbw016.

49. Brown, S.; Santa Maria Jr, J. P.; Walker, S., Wall teichoic acids of gram-positive bacteria. *Annual review of microbiology* **2013,** *67*.

50. Ramsey, M.; Hartke, A.; Huycke, M., The physiology and metabolism of enterococci. **2014**.

51. Saier, M. H.; Chauvaux Jr, S.; Cook, G. M.; Deutscher, J.; Paulsen, I. T.; Reizer, J.; Ye, J.-J., Catabolite repression and inducer control in Gram-positive bacteria. *Microbiology* **1996,** *142*, (2), 217-230.

52. Kyle, J. L.; Parker, C. T.; Goudeau, D.; Brandl, M. T., Transcriptome analysis of Escherichia coli O157: H7 exposed to lysates of lettuce leaves. *Applied and environmental microbiology* **2010,** *76*, (5), 1375-1387.

53. Suzuki, S.; Horinouchi, T.; Furusawa, C., Prediction of antibiotic resistance by gene expression profiles. *Nature communications* **2014,** *5*.

54. Fernández, L.; Hancock, R. E., Adaptive and mutational resistance: role of porins and efflux pumps in drug resistance. *Clinical microbiology reviews* **2012,** *25*, (4), 661-681.

55. Liu, Y.; Imlay, J. A., Cell death from antibiotics without the involvement of reactive oxygen species. *Science* **2013,** *339*, (6124), 1210-3.

56. Djorić, D.; Kristich, C. J., Oxidative stress enhances cephalosporin resistance of Enterococcus faecalis through activation of a two-component signaling system. *Antimicrobial agents and chemotherapy* **2015,** *59*, (1), 159-169.

57. Hagan, E. C. Iron acquisition by uropathogenic Escherichia coli: ChuA and Hma heme receptors as virulence determinants and vaccine targets. University of Michigan, 2009.

58. Hu, M.; Zhang, C.; Mu, Y.; Shen, Q.; Feng, Y., Indole affects biofilm formation in bacteria. *Indian J Microbiol* **2010,** *50*, (4), 362-8.

59. Kuczynska-Wisnik, D.; Matuszewska, E.; Furmanek-Blaszk, B.; Leszczynska, D.; Grudowska, A.; Szczepaniak, P.; Laskowska, E., Antibiotics promoting oxidative stress inhibit formation of Escherichia coli biofilm via indole signalling. *Research in Microbiology* **2010,** *161*, (10), 847-853.

60. Normark, S.; Ericson, C.; Jonsson, A.; Olsen, A., Global Regulatory Control of Curli Expression and Fibronectin Binding in Enterobacteria. In *Microbial Adhesion and Invasion*, Springer: 1992; pp 95-99.

61. Boles, B. R.; Singh, P. K., Endogenous oxidative stress produces diversity and adaptability in biofilm communities. *Proc Natl Acad Sci U S A* **2008,** *105*, (34), 12503-8.

62. Fink, R. C.; Black, E. P.; Hou, Z.; Sugawara, M.; Sadowsky, M. J.; Diez-Gonzalez, F., Transcriptional responses of Escherichia coli K-12 and O157: H7 associated with lettuce leaves. *Applied and environmental microbiology* **2012,** *78*, (6), 1752-1764.

63. Geier, H.; Mostowy, S.; Cangelosi, G. A.; Behr, M. A.; Ford, T. E., Autoinducer-2 triggers the oxidative stress response in Mycobacterium avium, leading to biofilm formation. *Applied and Environmental Microbiology* **2008,** *74*, (6), 1798-1804.

64. Jang, I.-A.; Kim, J.; Park, W., Endogenous hydrogen peroxide increases biofilm formation by inducing exopolysaccharide production in Acinetobacter oleivorans DR1. *Scientific reports* **2016,** *6*.

65. Motta, S. S.; Cluzel, P.; Aldana, M., Adaptive resistance in bacteria requires epigenetic inheritance, genetic noise, and cost of efflux pumps. *PLoS One* **2015,** *10*, (3), e0118464.

66. Vebø, H. C.; Solheim, M.; Snipen, L.; Nes, I. F.; Brede, D. A., Comparative genomic analysis of pathogenic and probiotic Enterococcus faecalis isolates, and their transcriptional responses to growth in human urine. *PloS one* **2010,** *5*, (8), e12489.

67. Dwyer, D. J.; Belenky, P. A.; Yang, J. H.; MacDonald, I. C.; Martell, J. D.; Takahashi, N.; Chan, C. T.; Lobritz, M. A.; Braff, D.; Schwarz, E. G., Antibiotics induce redox-related physiological alterations as part of their lethality. *Proceedings of the National Academy of Sciences* **2014,** *111*, (20), E2100-E2109.

68. Rutherford, S. T.; Bassler, B. L., Bacterial quorum sensing: its role in virulence and possibilities for its control. *Cold Spring Harb Perspect Med* **2012,** *2*, (11).

69. Yu, J.; Madsen, M. L.; Carruthers, M. D.; Phillips, G. J.; Kavanaugh, J. S.; Boyd, J. M.; Horswill, A. R.; Minion, F. C., Analysis of autoinducer-2 quorum sensing in Yersinia pestis. *Infection and immunity* **2013,** *81*, (11), 4053-4062.

70. Kadir, K.; Nelson, K. L., Sunlight mediated inactivation mechanisms of Enterococcus faecalis and Escherichia coli in clear water versus waste stabilization pond water. *Water research* **2014,** *50*, 307-317.

71. Nguyen, M. T.; Jasper, J. T.; Boehm, A. B.; Nelson, K. L., Sunlight inactivation of fecal indicator bacteria in open-water unit process treatment wetlands: Modeling endogenous and exogenous inactivation rates. *Water research* **2015,** *83*, 282-292.

72. Maraccini, P. A.; Wenk, J.; Boehm, A. B., Photoinactivation of eight health-relevant bacterial species: determining the importance of the exogenous indirect mechanism. *Environ Sci Technol* **2016,** *50*, (10), 5050-5059.

73. Seaver, L. C.; Imlay, J. A., Are respiratory enzymes the primary sources of intracellular hydrogen peroxide? *Journal of Biological Chemistry* **2004,** *279*, (47), 48742-48750.

74. Oladeinde, A.; Lipp, E.; Chen, Y. C.; Molina, M., Photo-produced hydrogen peroxide controls fecal indicator bacteria and E. coli O157:H7 growth dynamics. In Manuscript submitted for publication, 2017.

Supplemental Information for Chapter 4

Transcriptomic analysis reveal differences in the hydrogen peroxide response mechanism of *Escherichia coli*, *Enterococcus faecalis* and *E. coli* O157:H7

Contains:

Supplemental Figures 4. S1-5

A

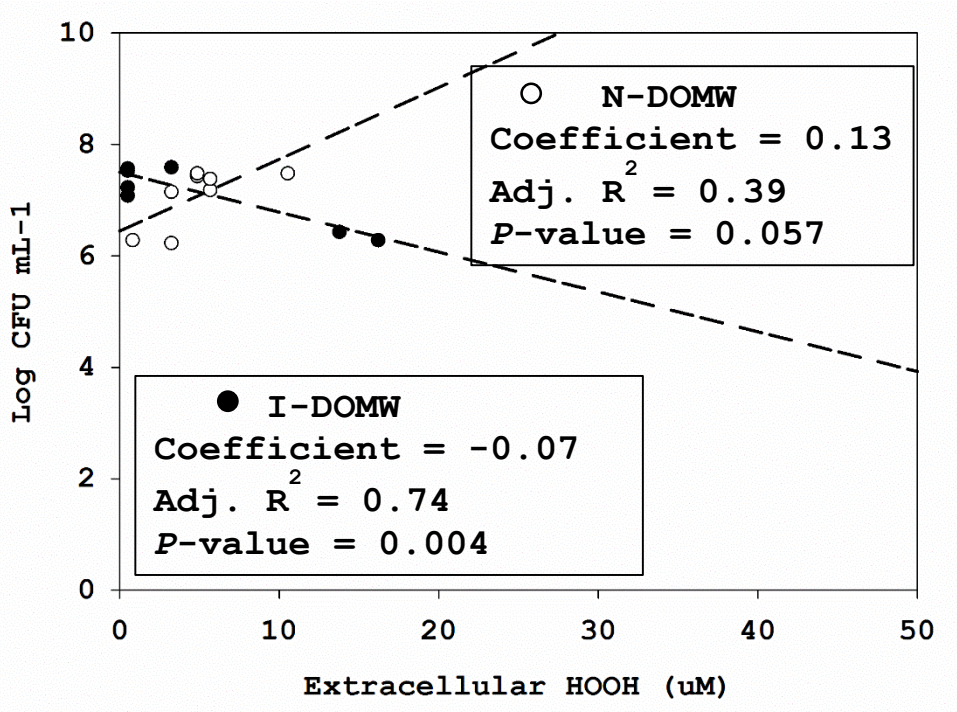
N-DOMW
Coefficient = 0.13
Adj. R2 = 0.39
P-value = 0.057
I-DOMW
Coefficient = -0.07
Adj. R2 = 0.74
P-value = 0.004
Log CFU mL-1
Extracellular HOOH (uM)
0
2
4
6
8
10
0
10
20
30
40
50

B

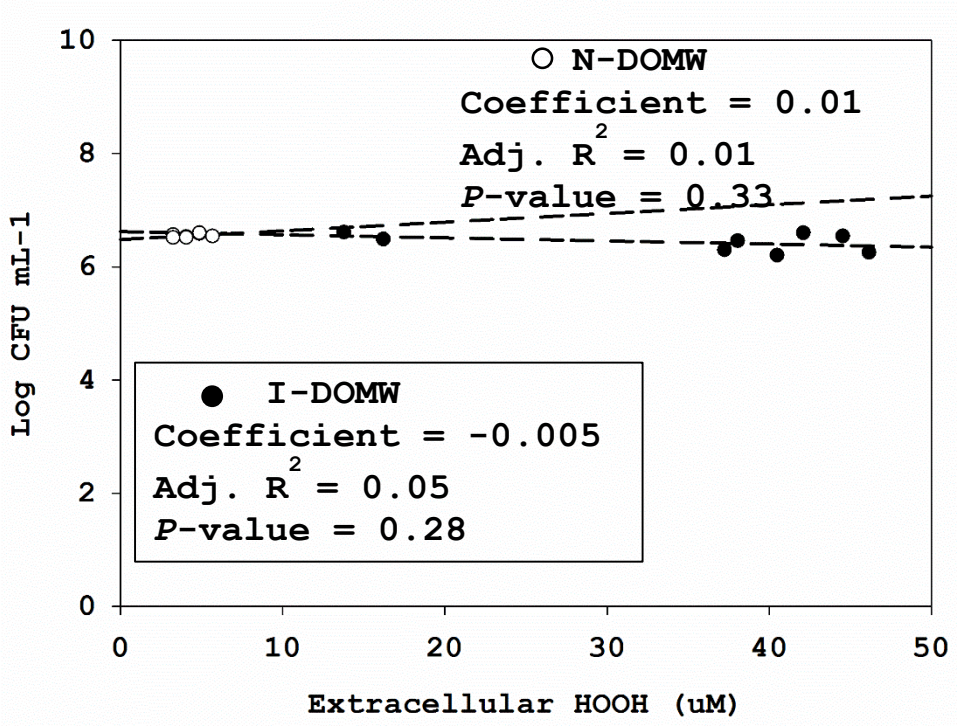
N-DOMW
Coefficient = 0.01
Adj. R2 = 0.01
P-value = 0.33
I-DOMW
Coefficient = -0.005
Adj. R2 = 0.05
P-value = 0.28
Log CFU mL-1
Extracellular HOOH (uM)
0
2
4
6
8
10
0
10
20
30
40
50

C

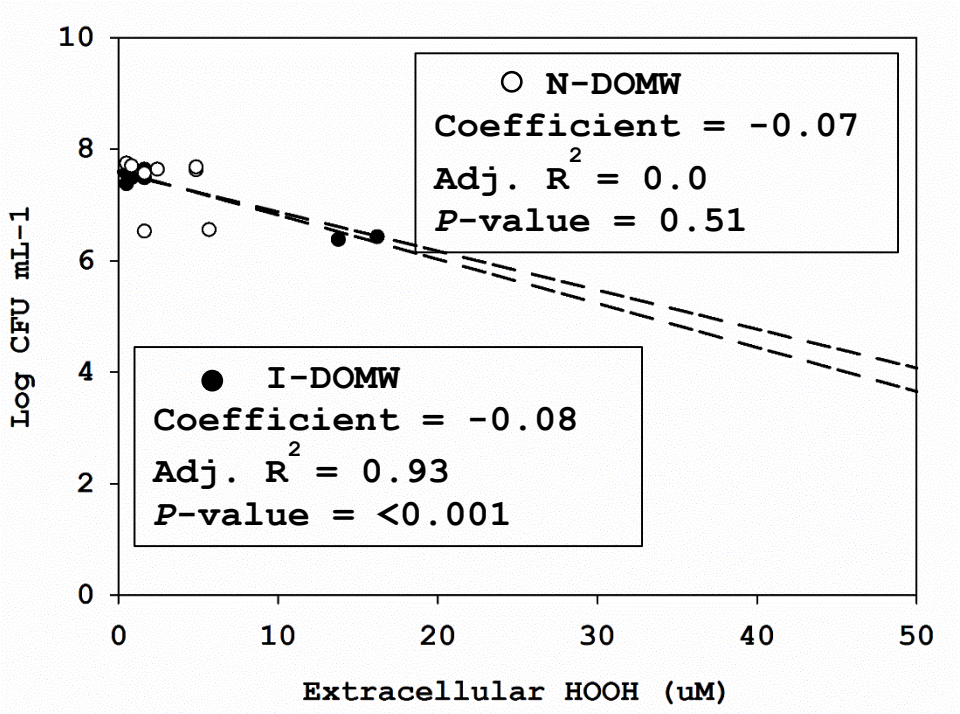

Figure 4S1. Linear regression of HOOH concentration on fecal bacteria concentration for (A) *E. coli* (B) *E. faecalis* and (C) *E. coli* O157: H7 (n=2 per group).

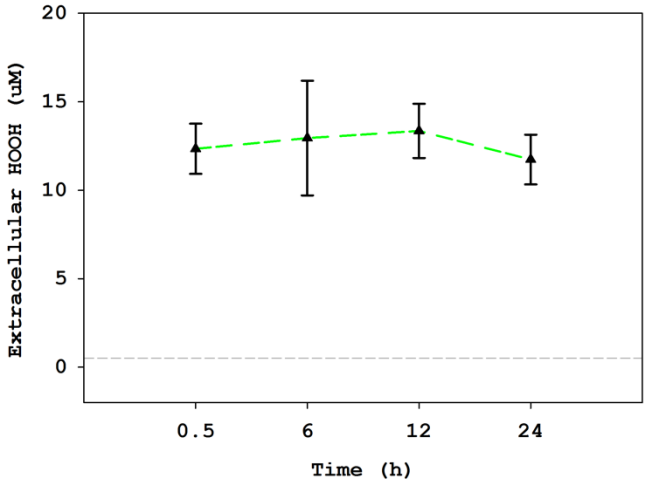

Figure 4S2: Extracellular HOOH concentration in irradiated spiked CFE (I-DOMW) controls (n =3, 1 per experiment) with no bacteria inoculation.

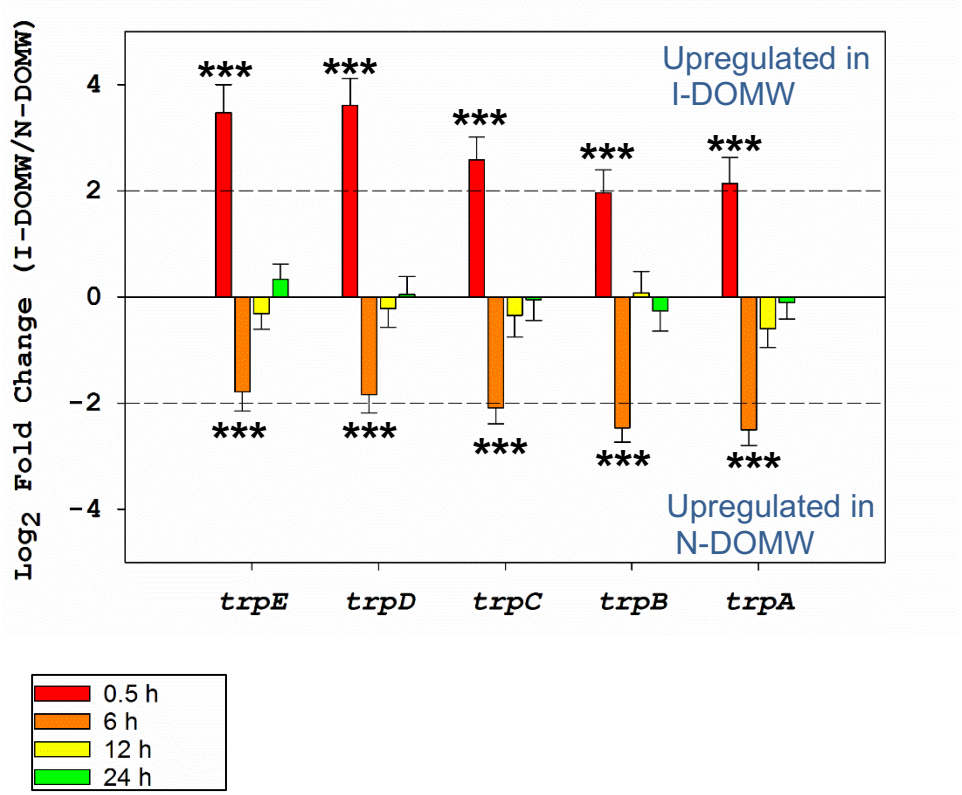

Figure 4S3. Exposure to HOOH contributes to indole production. Fold change in expression of tryptophan operon genes for *E. coli* O157:H7 in I-DOMW relative to N-DOMW. Horizontal dash lines represent 2- fold change (***p.adj < 0.001).

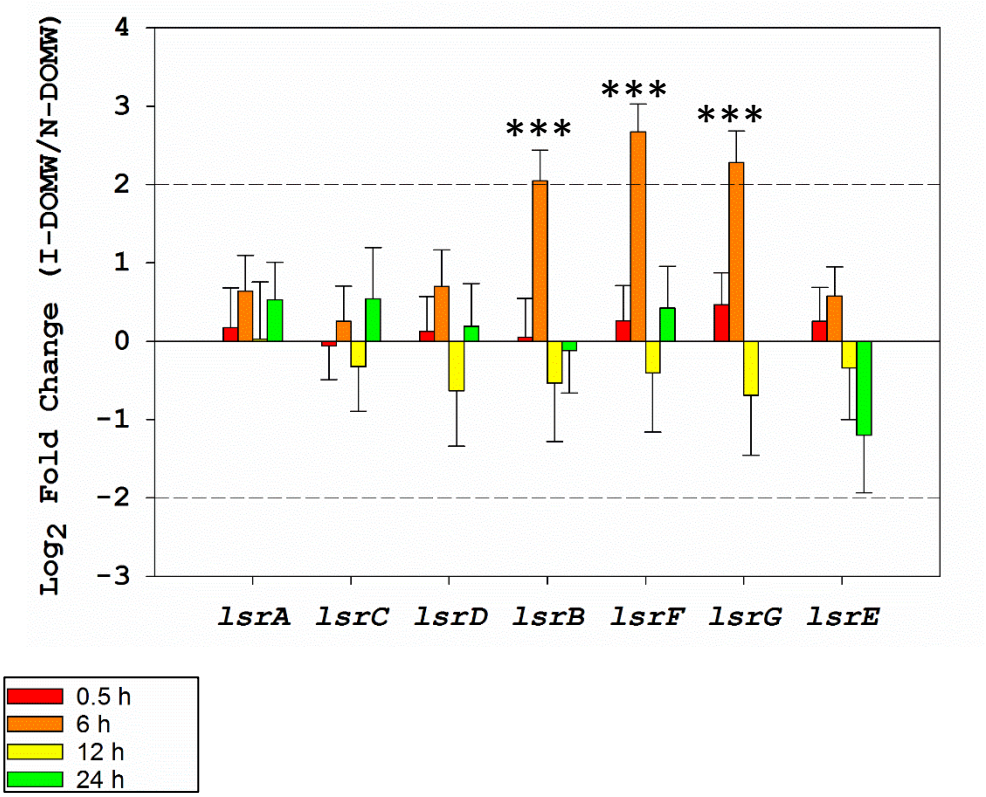

Figure 4S4. Quorum sensing genes expression during dark incubation. Fold change in expression of LuxS regulated *lsr* operon for *E. coli* in I-DOMW relative to N-DOM. Horizontal dash lines represent 2- fold change (***p.adj < 0.001).

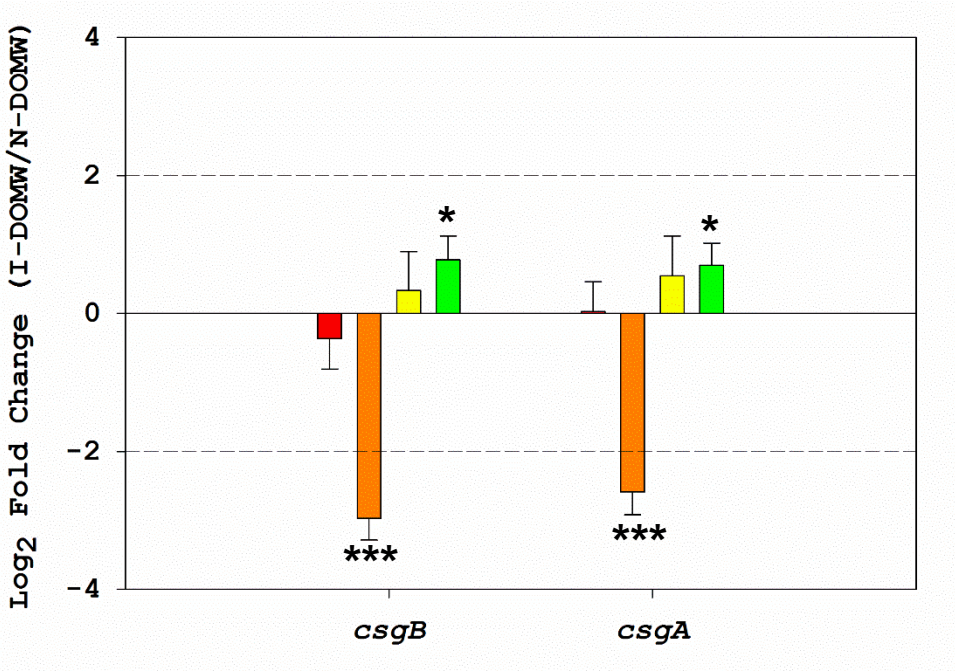

Figure 4S5. Expression of biofilm forming genes. Fold change in expression of *csgBA* operon (encoding curli) for *E. coli* in I-DOMW relative to N-DOMW. Horizontal dash lines represent 2- fold change (***p.adj < 0.001).

Table 4S1: Multivariate analysis of variance between bacteria incubated in I-DOMW and N-DOMW

Bacteria	Treatment effect	F - value	Degrees of freedom (treatment, error)	*P.* value
E. coli	$\mu_6 - \mu_{0.5}$	121	1, 2	0.0081
	$\mu_{12} - \mu_6$	13	1, 2	0.069
	$\mu_{24} - \mu_{12}$	0.4	1, 2	0.58
E. faecalis	$\mu_6 - \mu_{0.5}$	21.3	1, 2	0.043
	$\mu_{12} - \mu_6$	3.6	1, 2	0.19
	$\mu_{24} - \mu_{12}$	20.6	1, 2	0.045
E. coli O157:H7	$\mu_6 - \mu_{0.5}$	1.1	1, 2	0.40
	$\mu_{12} - \mu_6$	1.0	1, 2	0.42
	$\mu_{24} - \mu_{12}$	0.4	1, 2	0.57

CHAPTER 5

HYDROGEN PEROXIDE TRIGGERS COMPETITION DYNAMICS BETWEEN *ESCHERICHIA COLI* AND *ENTEROCOCCUS FAECALIS* BACTERIAL POPULATIONS

Oladeinde, A., Erin K. Lipp, Chia-Ying Chen, Richard Muirhead, Travis Glenn, Brad Acrey, Quincy Teng, Matthew Henderson, Ha Nguyen, Kyler Herrington and Marirosa Molina

To be submitted to Science

ABSTRACT

Bacterial survival in aquatic ecosystems is dependent on the availability of resources such as dissolved organic matter (DOM) and the transformations that DOM undergoes by both by biotic and abiotic processes. Recent studies have shown that photo-degradation and microbial metabolism of DOM are the major sources of hydrogen peroxide (HOOH) in surface waters. Here we show that the removal and production of HOOH is critical for the survival or growth of laboratory strains of *E. coli* and *Ent. faecalis*. Most importantly, we observed a form of "exploitative competition" between these strains in co-culture microcosm experiments, where chorismate and arginine/ornithine served as shared public goods for the biosynthesis of enterobactin and polyamines. For this cooperative competition to be efficient, both bacteria increased the expression of genetic networks associated with oxidative stress, bacteriophage activation, non-ribosomal peptide production, plasmid virulence, toxin-antitoxin systems, quorum sensing, biofilm formation and antimicrobial resistance. We provide first time evidence of such cooperation between two distantly related species of bacteria.

INTRODUCTION

Fecal indicator bacteria (FIB) such as *E. coli* and enterococci are employed as indicators of water quality worldwide [1]. Their use as surrogates for fecal contamination is based on several assumptions including their inability to proliferate in environments outside their primary hosts [2]. However, several studies have reported FIB's ability to grow and survive over a long period in secondary habitats [3-5]. This poses a great challenge from a water quality monitoring stand-point, as observed increases in FIB concentration may stem from bacterial regrowth and not from a recent fecal contamination event [6].

The potential for FIB to grow or survive in extra-intestinal environments is dependent on several factors including resource availability in the form of dissolved organic matter (DOM) and DOM transformations mediated by sunlight. DOM represents a major source of nutrients in aquatic ecosystems and plays a major role in bacterial survival [7, 8]. Further, exposure of DOM to solar radiation can lead to the formation of reactive oxygen species (ROS), which can alter bacterial cell redox homeostasis via oxidative stress [9, 10]. We have previously shown that photo-produced hydrogen peroxide (HOOH) can limit the growth potential of *Enterococcus faecalis*, while *E. coli* has a robust mechanism to detoxify photo-produced HOOH in microcosms[11, 12].

HOOH is also produced via various pathways not involving sunlight [13]. For example, Gram positive bacteria like *Ent. faecalis* metabolize glycerol aerobically through the oxidation of dihydroxyacetone phosphate by glycerol-3-P oxidase (*glpO*) [14]. This enzyme uses molecular oxygen as the electron sink, which leads to the formation of HOOH. This form of dark production can be used by *Ent. faecalis* to gain a competitive advantage over other bacterial populations in aquatic habitats [15]. The difference in survival strategy mechanisms suggests that the removal of high concentrations of exogenous HOOH may

be critical for survival and growth in the environment. More importantly, Enterococci may be reliant on efficient HOOH scavengers like *E. coli*[12] to survive in the presence of photo-produced HOOH. Therefore, we sought to determine whether *E. coli* HOOH scavenging ability enhances the growth potential of *E. faecalis* in the presence of exogenous HOOH, and to identify ways in which such an interaction may drive competition.

To understand the role of photo-produced HOOH and competition on the survival of *E. coli* and *Ent. faecalis*, we attempted to isolate the effect of HOOH using controlled microcosms of phosphate buffered water and natural stream water water spiked with extracts derived from cattle feces that were irradiated prior to inoculation with bacteria. Following bacterial inoculation, microcosms were incubated in the dark for 24 h. We employed high throughput RNA-Seq to investigate bacteria transcriptional changes after 0.5, 3, 6 and 12 h of dark incubation, and NMR and GC/MS for untargeted analysis of intracellular and extracellular metabolites. We show that *E. coli* can indeed increase the tolerance of *Ent. faecalis* in the presence of photo-produced HOOH and overall survival was dependent on exploitative and cooperative competition between the two of them. Our data suggest that *E. coli* has a greater capability to remove photo-produced HOOH and overall higher regrowth potential than *Ent*. *faecalis*.

RESULTS AND DISCUSSION

Extracellular HOOH is removed by different mechanisms in *E. coli* and *Ent. faecalis*. HOOH produced from (I-DOMW) decreased gradually for up to 12 h in the dark while measured FIB concentrations increased (Fig. 5.1A-C). Whole transcriptome analysis of RNA extracted from co-culture at 0.5, 3, 6 and 12 h indicated consistent transcriptional changes in both bacteria incubated in I-DOMW and N-DOMW compared to PBW (Table

5S1 and 5S2). Following inoculation into I-DOMW, there was a significant increase in expression of multiple transcripts associated with bacterial SOS response in *E. coli* and general stress response in *Ent. faecalis* (Fig. 5.1D). Bacterial SOS response is induced as a global response to DNA damage in which the bacterial growth cycle is halted and DNA repair and mutagenesis is activated. Among the genetic networks upregulated in I-DOMW compared to N-DOMW were genes important for oxidative stress in *E. coli* (Fig. 5.1E). These transcripts are under the control of an OxyR transcriptional regulator. Upon detection of deleterious concentrations of endogenous or exogenous HOOH, the *oxyR* gene induces the expression of multiple genes capable of removing HOOH (*katG*, *ahpCF*, *trxC*), sequestering free iron (*dps*) and replenishing iron-sulfur (Fe-S) clusters (*sufABCD*)[10, 15, 31]. These genes were significantly upregulated for 12 h (>2-fold change [FC], *P*. adj < 0.01) in I-DOMW compared to N-DOMW for *E. coli* (Fig. 5.1E). However, in *Ent. faecalis* transcripts associated with HOOH response were not significantly expressed in I-DOMW compared to N-DOMW (Fig. 5.1F), except the NADH oxidase (*nox*) gene, which suggested that *E. coli* was mostly responsible for the removal of exogenous HOOH.

To address this, we compared the growth of *Ent. faecalis* in a separate mono-culture experiment to the co-culture experiments reported here. The growth rate of *Ent. faecalis* in co-culture doubled compared to that in mono-culture (Fig. 5S2, Table 5S3), suggesting *E. coli* may have played a beneficial role. Furthermore, in the absence of *E. coli*, HOOH accumulated in the growth medium of *Ent. faecalis*[12]. There was no difference in growth rate between *E. coli* incubated in mono-culture or co-culture. More importantly, photo-produced HOOH was below the limit of detection after 6 h of dark incubation in mono-culture[12]. In addition, there was also a significant increase in expression of *oxyR* regulated transcripts in I-DOMW compared to N-DOMW at 0.5 h in mono-culture of *E. coli*

(Fig. 5S4)[11, 12]. These results imply that *E. coli* has a greater ability to remove exogenous HOOH concentrations from their surrounding environment than *Ent. faecalis*.

In dark controls (no prior sunlight irradiation) we also measured micromolar levels of extracellular HOOH immediately upon inoculation of co-culture into N-DOMW or PBW, with a gradual decrease for 12 h (Fig. 5.1B and 5.1C). Dark production of HOOH could be related to glycerol metabolism by *Ent. faecalis* which is important for the synthesis of glycerol phosphate, an essential precursor for peptidoglycan formation[32]. This reaction involves glycerol facilitator protein (*glpF*), phosphorylated glycerol kinase (*glpK*), and phosphoenolpyruvate (PEP): a carbohydrate phosphotransferase system (PTS) for the phosphorylation of *glpK* [14, 33]. This pathway uses molecular oxygen as the electron sink, which leads to the formation of HOOH as a by-product. We observed a significant increase in all 3 transcripts (*glpF*, *glpO* and *glpK*) involved in *Ent. faecalis* glycerol metabolism following bacterial inoculation (Fig. 5.1G; Fig. 5S6). Further, there was a significant increase in expression of thioredoxin reductase (*trx*) and peroxidase encoding transcripts (*npr* and a*hpC*) in N-DOMW and PBW compared to I-DOMW after 3, 6, and 12 h of dark incubation (Fig. 5.1F, Fig. 5S5). In comparison, an increase in expression of catalase (*katG*) and peroxidase (*ahpCF*) genes were only observed in PBW for *E. coli* (Fig. 5S5A_2).). In addition, transcripts belonging to the cytochrome (*cydAB* and *appBAC)* and hydrogenase family were significantly upregulated in N-DOM and PBW compared to I-DOM for *E. coli* (Fig, 5.1H). Cytochrome systems play significant roles in oxidative stress and have been shown to exhibit strong catalase activity in *E. coli* [34, 35].

Given that there was no increase in expression of transcripts with peroxidase activity or concomitant decrease in extracellular HOOH for *Ent. faecalis* in mono-culture

experiments, we concluded that the observed upregulation of oxidative stress genes in N-DOMW and PBW was driven by the presence of *E. coli*.

No study to our knowledge has reported on the mechanism of survival used by *E. coli* or enterococci under exposure to environmentally relevant HOOH concentrations. Nevertheless, studies that have investigated the transcriptomic response of *E. coli* or *Ent. faecalis* to exogenously added HOOH, have used millimolar concentrations in experiments done using single cultures[36, 37]. Our data implies that fecal bacteria growth is dependent on the efficient removal of exogenous HOOH from the surrounding environment via the induction of *oxyR* regulated genes.

Competition controls *E. coli* and *Ent. faecalis* population dynamics. A competitive interaction between *E. coli* and *Ent. faecalis* was observed during dark incubation in DOMW. The concentration of *Ent. faecalis* decreased by ~3-log while *E. coli* decreased by < 1-log in N-DOMW (Fig. 5.1B). In I-DOMW, there was a ~3 h lag phase of no growth in *Ent. faecalis*, while *E. coli* showed ~0.5-log decrease in concentration (Fig. 5.1A). Our results were unexpected since such declines in growth was not observed in mono-culture experiments or PBW treatments with either *E. coli* or *Ent. faecalis* (Fig. 5S2). Further, in co-culture both bacteria could regrow after this short phase of decline or steady state. Consequently, we hypothesized that allelopathy was in play, via production of secondary metabolites such as bacteriocins, antimicrobial peptides, siderophores and toxins.

Polyamines and Methylamines are essential for fecal bacteria survival. We employed Nuclear Magnetic Resonance Spectroscopy (NMR) and Gas Chromatography/Mass Spectrometry (GC/MS) for untargeted analysis of bacterial intracellular and extracellular metabolites during dark incubation in DOMW. There were significant differences in metabolites produced in I-DOMW compared to N-DOMW. Following co-culture inoculation,

there was a significant increase in intracellular putrescine production at 0.5, 3 and 6 h in N-DOMW compared to I-DOMW (Fig. 5.2A). In contrast, spermidine production was significantly higher in I-DOMW compared to N-DOMW at 0.5, 3 and 6 h. Further, extracellular cadaverine was higher at 3 and 6 h in I-DOMW compared to N-DOMW (Fig. 5.2B).

Polyamines are small polycationic molecules with a hydrocarbon backbone and multiple amino functional groups [38-40]. They play diverse and important physiological roles including translation, gene regulation, stress resistance, cell proliferation and differentiation, quorum sensing, biofilm formation, production of secondary metabolites and virulence [38, 41, 42]. In bacteria, putrescine, spermidine, spermine, and cadaverine are the most predominant polyamines; however, their intracellular concentrations may differ by bacterial strains [40]. For example, the concentration of putrescine is higher in *E. coli* compared to almost all other types of bacteria where spermidine typically predominates [40]. Putrescine biosynthesis in *E. coli* occurs via two pathways involving the decarboxylation of ornithine to putrescine by ornithine decarboxylase (*speC*) and arginine decarboxylation to agmatine by arginine decarboxylase (*speA)*. Followed by conversion to putrescine by agmatine ureohydrolase (*speB*). In *Ent. faecalis*, putrescine production occurs via deamination of agmatine to carbomoyl putrescine by agmatine deaminase (*aguA*) [40, 43, 44] (Fig. 5.2C$_1$). In our study, we observed these transcripts to be differentially expressed for *E. coli* in I-DOMW and N-DOMW compared to PBW (Fig. 5.2C, Fig. 5S7 and 5S8). On the other hand, only genes required for arginine biosynthesis were significantly expressed in *Ent. faecalis*, suggesting that *E. coli* may be the major producer of putrescine in our study (Fig. 5.2B, Fig. 5S7). Further, when we compared the expression of these genes in mono-culture experiments (Fig. 5S7A & B), we did not observe any significant differential

expression in putrescine genes implying that putrescine production may be prompted by competition from *Ent. faecalis*. Moreover, the *puuR* transcriptional regulator required for repressing putrescine degradation was significantly upregulated at 12 h in mono-culture experiments for *E. coli*. Given that putrescine offers many survival advantages to bacteria [39, 41], their transport in and out of the cell may be regulated in both bacteria in a sophisticated manner. There was a significant increase in putrescine transport systems in *E. coli* especially the *potFGHI* and *PuuP* transporters in N-DOM (Fig. 5.2D$_2$). For *Ent. faecalis*, spermidine transport is aided by four transporters (DR75_1350 – 1353), which share homology with the *potABCD* transport system of *E. coli* [40]. These transcripts were significantly expressed in I-DOM compared to N-DOM at 6 and 12 h (Fig. 5.2E; Fig. 5S8), which suggests that *Ent. faecalis* was using spermidine produced by *E. coli* for survival under oxidative stress. In addition, *E. coli* can catabolize putrescine to succinate which can be used in the TCA cycle for adenosine triphosphate (ATP) synthesis [38, 45](Fig. 5.2D$_1$). We observed a significant increase in genes required for putrescine catabolism at 0.5 and 3 h in PBW and 6 and 12 h in I-DOM and N-DOM, implying that succinate production from putrescine was more important in PBW than in DOMW during the first 3 h of dark incubation (Fig. 5.2D; Fig. 5S8).

Putrescine conversion to spermidine by spermidine synthase (SpeE) occurs in the presence of decarboxylated S-adenosyl methionine (SAM) [40]. The *speE* gene was significantly upregulated at 0.5 h in I-DOMW and N-DOMW compared to PBW for *E. coli*, further corroborating NMR results (Fig. 5.2D, Fig. 5S8). Higher spermidine levels have been shown to correlate with increased survival in response to oxidative stress, including exposure to HOOH[38, 46]. In *Shigella*, it was demonstrated that high levels of spermidine stimulated the expression of OxyR, thus promoting the expression HOOH scavenging

genes. This process may also be at play in our study given that higher intracellular concentrations of spermidine was measured in I-DOMW samples (Fig. 5.2A). It is important to note that exogenous spermidine could become toxic to bacteria at a certain concentration[38]. To alleviate the stress from such exposures, some bacteria strains can convert spermidine to its inert form (acetylspermidine) by spermidine acetytransferase (*speG* or *bltD*) [38, 47]. The *bltD* (DR75_161) gene in *E. faecalis* was significantly upregulated in PBW compared to I-DOMW at 12 h (Fig. 5.2E), suggesting that SpeG-mediated polyamine detoxification may be required for survival in PBW.

Cadaverine biosynthesis occurs in *E. coli* in the presence of lysine as a precursor amino acid, and at low pH or in the absence of putrescine[44]. Genes for lysine decarboxylase (*cadA*) and cadaverine antiporter (*cadB*) were significantly upregulated in PBW compared to I-DOMW or N-DOMW at 3, 6 and 12 h (Fig. 5S8C). This implies that cadaverine biosynthesis may be critical for survival in PBW. Cadaverine has been shown to facilitate *E. coli* survival in inorganic phosphorus limited medium and under acid stress by increasing the pH of the growth media [48].

Methylamines including trimethylamine oxide (TMAO), glycine betaine and glycerophosphoryl choline are important counteracting osmolytes produced by bacteria under diverse environmental stressors [49-53]. Further, TMAO can be metabolized to small methylated amines like dimethylamine (DMA) [52, 53]. In our study, intracellular bacterial concentrations of TMAO, glycine betaine, choline and DMA was higher in I-DOMW compared to N-DOMW at 0.5, 3 and 6 h, suggesting they offer some protective advantage under oxidative stress (Fig. 5.2A). Choline uptake in *E. coli* is facilitated by *betT* gene and choline can be converted to betaine by two genes encoding betaine aldehyde (*betAB*) [49, 54, 55](Fig. 5.2F$_1$). These genes were significantly upregulated in I-DOMW and N-DOMW

compared to PBW for the 12 h duration, implying that betaine was actively being produced from choline (Fig. 5.2F, Fig. 5S9B). To determine whether transcripts for betaine transport were significantly expressed in either *E. coli* or *Ent. faecalis*, we looked at the expression of betaine transport genes. *ProVW* transcripts in *E. coli* were significantly upregulated in PBW and N-DOMW, whereas in *Ent. faecalis* betaine transport proteins were upregulated in I-DOMW compared to PBW for 12 h (Fig. 5.2F$_3$, Fig. 5S9C). TMAO respiration is controlled by a two-component regulatory system (*torRS*) and its transport is mediated by the *torD* in *E. coli* [52]. The *torD* gene was significantly expressed in I-DOMW and N-DOMW compared to PBW suggesting that *E. coli* might preferentially use TMAO over betaine as an osmoprotectant (Fig. 5S9A).

Our results show that methylamines are important metabolites produced by fecal bacteria and/or obtained from the environment under exposure to HOOH induced oxidative stress. More importantly, we provide evidence supporting *Ent. faecalis* as the major user of betaine in I-DOMW. This was also observed in mono-culture experiments were the *proV* gene (DR75_1341) was significantly upregulated >2-FC in I-DOMW compared to N-DOMW at 0.5 h.

Phages contributed to *E. coli* survival. The *E. coli* $_{C3000}$ strain used in our study (>99 % homology with *E. coli* K-12) harbored 9 cryptic phages. Additionally, we found transcripts belonging to 6 prophages to be differentially expressed between the three treatments (I-DOMW, N-DOMW and PBW) (Fig. 5.3A$_{1\text{-}6}$). These included CP4-6, Qin, rac, CPS-53, DLP12 and CP4-44 prophages, which have been shown to help bacteria cope with diverse environments by improving stress tolerance, antibiotic resistance, biofilm formation or virulence [56-59]. The CP4-6 and Qin prophage had the most differentially expressed genes for 12 h and the expression of these transcripts were significantly higher in N-DOMW

compared to PBW or I-DOMW (Fig. 5S10). Upregulated transcripts in N-DOMW for CP4-6 and Qin prophages included several genes associated with biofilm formation, toxin-antitoxin (TA) system, arginine biosynthesis, peroxide resistance, iron transport, cold shock proteins, S-methionine biosynthesis, and DNA recombination (Table 5S1A, Fig. 5S10). Further, CP4-6 possesses 4 insertion elements (IS) that are not prophage genes, but inserted into non-regulatory intergenic genes or pseudogenes. We observed these transcripts to be significantly upregulated in N-DOMW compared to PBW suggesting a form of active lysogeny or horizontal gene transfer (HGT) may be occurring (Fig, 5.3A_1, Fig. 5S10A). This increased expression in IS elements with transposase activity and integrases (for prophage excision and insertion), was observed in other prophages including CPS-53 and DLP12 (Fig. 5.3A_4 and $_6$). In active lysogeny, temperate phages integrated within bacterial functional genes, cooperate with their hosts to regulate the proper and timely expression of disrupted genes[57]. This seems to be the case for some cryptic phage genes in our study. For example, the *ykfI* gene in CP4-6 is a pseudogene (functionless toxin of a *ykfI-yafW* TA system), but was significantly expressed in N-DOMW for 12 h, providing further evidence for pseudogene activation (Fig. 5S10A; Fig. 5.5A_2). Further, by activating this gene, it opens the possibility for transposable elements to be transferred between bacteria strains [60].

The integration of selfish replicators such as transposable elements, phages and conjugative plasmids can lead to high transcriptional and translational costs or even cell death [58, 61]. Hence, bacteria have developed elegant systems that help confer resistance to foreign genetic elements e. g. CRISPR (clustered regularly interspaced short palindromic repeat), Cas (CRISP-associated) protein and ssRNA endonuclease [58, 62-64]. CRISPR clusters contain sequences complementary to antecedent mobile elements and target

invading nucleic acids. These transcripts were significantly upregulated in N-DOM compared to PBW at 0.5 h, providing more evidence for HGT between *E. coli* populations (Fig. 5.3A_7). Further, for bacteria to exploit the adaptive potential of foreign DNA and enable its integration into the host regulatory circuit, they have evolved a mechanism called xenogeneic silencing (XS)[65]. This mechanism relies on global regulatory proteins or nucleoid associated proteins to target and inhibit the expression of foreign DNA, when they are not required for survival. The H-NS type proteins are important XS proteins and are responsible for modulating the expression of over 700 genes in *Salmonella* [66]*.* In our study, the *hns* gene was upregulated in PBW compared to I-DOMW or N-DOMW, whereas H-NS binding transcriptional regulators (*hha* and *bglJ*) were upregulated in N-DOMW and I-DOMW compared to PBW (Fig. 5.3C). Consequently, the number of mobile genetic elements induced in DOMW treatments were higher than PBW treatments for *E. coli* (Table 5S1A).

Finally, we performed gene enrichment on all transcripts upregulated in N-DOMW compared to I-DOMW at 0.5 h for *E. coli*. We found the pathway for homologous recombination to be significantly enriched in KEGG pathways (P. adj.< 0.05) (Table 5.1) and transcripts for type IV pilus synthesis which are required for transformative transfer of genetic elements to be upregulated in N-DOMW (Fig. 5S13)

Plasmid as a fitness cost to *Ent. faecalis.* Plasmids are extra-chromosomal genetic elements coding for a wide range of traits that allow bacteria to adapt to different environmental stressors and can spread horizontally among bacteria by conjugation. Plasmids can pose multi-level fitness costs on their bacterial host. The origin of this cost comes from plasmid metabolism including cytotoxic effects derived from the presence of the plasmid [61]. Further, plasmid loss during segregation remains a major survival cost

even though bacteria have developed several mechanisms to limit this loss[61, 67]. The *Ent. faecalis* strain used here, carries two highly conjugative plasmids, hereafter referred to as plasmid 1 and 2. They both shared homology with the pAD1 plasmid of *Ent. faecalis*[68, 69]. Plasmid 1 was ~66kb in length and plasmid 2 was ~41kb and both encoded proteins for class II bacteriocins production (CylL) and plasmid maintenance system (ParA) [70] (Fig. 5S11). The cytolysin encoding transcripts in plasmid 1 were upregulated in I-DOMW at 0.5 and 3 h and at 6 and 12 in PBW (Fig. 5.4A). Bacteriocins are secreted to kill off closely related streptococcal species [71, 72], implying that *Ent. faecalis* cells carrying plasmid 1 may have some competitive advantage during those time points. Moreover, plasmid 1 also encodes a gene for cytolysin immunity (DR75_2991), this gene was significantly upregulated at 6 and 12 h for I-DOMW; providing more support for their role in *Ent. faecalis* virulence (Fig. 5.4A). The ParA protein is required for plasmid stability/maintenance [67-69] and their expression was significantly upregulated in I-DOM compared to PBW for both plasmids. By contrast, the *parA* gene of plasmid 1 was only significantly upregulated at 0.5 h for N-DOMW suggesting that segregational loss might be occurring in N-DOMW and PBW (Fig. 5.4A_2). This was corroborated by culture results where we observed ~3-log decrease in *Ent. faecalis* population after 3 h dark incubation in N-DOMW (Fig. 5.1B).

Ent. faecalis strains carrying pAD1 plasmids possess a sex pheromone encoding protein (cAD1) that are expressed by cells that have lost their plasmids (recipient)[68, 69]. Donor cells upon detecting this quorum sensing signal, secrete aggregation substance (AS) that form clumps on their cell surface. Donor to plasmid-free recipient aggregates can efficiently exhibit plasmid transfer[69]. We found the cAD1 pheromone to be significantly upregulated in N-DOMW and PBW compared to I-DOMW for the 12 h duration, providing

more evidence for segregational loss of plasmid in these treatments (Fig. 5.4C). In addition, LPxTG cell anchor proteins which have been shown to participate in AS formation and are important for conjugative transfer of plasmids [73] were upregulated in I-DOMW and PBW compared to N-DOMW (Fig. 5.4A). Collectively, our results show that the presence of plasmids in *E. faecalis* played an important role in its survival dynamics.

Toxin-antitoxin systems contribute to *E. coli* and *Ent. faecalis* population fluctuations. Bacteria toxin-antitoxin (TA) modules are genetic elements composed of a toxin protein component that disrupts bacterial growth by interfering with vital cell processes and an antitoxin that impairs the functionality of the toxin until this inhibition is abolished in response to cellular signaling [74-77]. TA systems are classified based on the nature of the antitoxin or its mode of action, but so far, only type I and type II TA systems have been widely studied[74, 78]. Type II TA systems are sequence-specific endoribonucleases that inhibit DNA gyrase and translation and induce bacterial stasis or programmed cell death [74, 77, 79]. These TA systems can give rise to two stable populations of bacteria, a small dormant population and a rapidly growing population [78]. On the other hand, type I toxins are small proteins that form pores in bacterial membranes to collapse the proton-motive force and stop ATP synthesis[74]. We observed a significant differential expression of multiple type II TA modules in both *E. coli* and *Ent. faecalis* (Fig. 5.5A and B; Table 5S1). For *E. coli*, RelE and MazF TA families were significantly upregulated in I-DOMW and N-DOMW compared to PBW. For example, the *relBE* TA system of *E. coli* which is carried on the Qin prophage was differentially expressed between N-DOMW and PBW. At 0.5 h, the toxin component (*relE*) of the *relBE* TA module was significantly upregulated in N-DOMW, while it's antitoxic component *relB* was upregulated in PBW. As expected, at 3 h, we observed the exact opposite; *relB* was upregulated in N-DOMW and

relE was upregulated in PBW (Fig. 5.5A$_2$). This time point (3h) corresponds with the start of growth in N-DOM, while in PBW *E. coli* experienced a slow die-off, suggesting the antitoxin was required for growth resumption in N-DOM. In addition, we identified type I TA system (symE/symR and tisB/istR) to be upregulated in I-DOMW compared to PBW at 0.5, 3, and 6 h for *E. coli* (Fig. 5.5E).

For *Ent. faecalis*, MazF and Doc TA families were the type II TA modules found to be differentially expressed. The death on curing (doc) toxin and phd antitoxin were significantly upregulated at 0.5, 6 and 12 h in N-DOMW relative to PBW while in I-DOMW they were only upregulated at 0.5 h (Fig. 5.5B). Further, plasmid 2 encodes a *yafQ*/*dinJ* TA (RelE family) which were upregulated at 6 and 12 h for I-DOMW and N-DOMW. Overall, for *Ent. faecalis* no TA system was obersved to be significantly expressed at 3 h, the time point which growth resumed suggesting TA modules play an essential role in controlling *Ent. faecalis* population.

TA modules are controlled by transcriptional and post-transcriptional regulation, as well as antitoxin degradation[74]. In *E. coli*, type I TA modules are activated by SOS and stringent stress response (ppGpp), while type II antitoxins are degraded by proteases (Lon and Clp) in response to ppGpp or oxidative stress[74, 77, 78]. These TA regulators (spoT and RelA - ppGpp synthetases, ObgE encoding GTPase, and Crp - cAMP-activated global transcriptional regulator) to be significantly upregulated in I-DOMW and N-DOMW compared to PBW (Fig. 5.5F). The *clpS* and *clpA* proteases were upregulated in I-DOMW compared to PBW, while Lon was only upregulated at 3 h in N-DOMW (Fig. 5.5C). There was also significant differential expression in proteases for *E. faecalis*. For instance, the *clpC*, *clpE* and *clpP* were all significantly upregulated in N-DOM at 0.5 h, while *clpX* was significantly upregulated in I-DOM at 6 and 12 h compared to PBW (Fig. 5.5D). The

general stress proteins (*gspA*- 1 and *gspA*-2) and ppGpp were upregulated in I-DOMW compared to PBW (Fig. 5.5G). Our results provide supporting evidence on the significant role played by TA modules in bacteria survival and persistence [74, 78].

Adaptive resistance as a major means of survival in *E. coli* and *Ent. faecalis*. Bacteria respond to environmental cues such as non-lethal doses of ROS, antimicrobials, nutrient limitation, and temperature by quantitatively and qualitatively modulating their transcriptome. Such responses can prolong their survival and, more importantly, enhance resistance to higher doses of the same stressor or other stressors [37, 80]. This form of adaptive resistance has been implicated in the phenotypic conversion of bacteria to persister cells, a concept known as responsive diversification[74]. Numerous factors beyond TA modules, phages and plasmids have been proposed to participate in the adaptive response in bacteria[81-83].

Unsupervised analysis of whole transcriptomic expression [24] showed a significant increase in the network of transcripts involved in the production of secondary metabolites in DOMW treatments for *E. coli* and *Ent. faecalis* (Fig. 5.6A; Fig. 5S12). Bacteria secondary metabolites (e.g. nonribosomal antimicrobial peptides (NRP), siderophores, polyamines, toxins, pigments, etc.) are low molecular mass products that are not essential for growth but mostly produced during the stationary phase of growth of the producing cell[84, 85]. Supporting this hypothesis, we found genetic networks for NRPs and siderophore production to be significantly upregulated in N-DOMW and I-DOMW compared to PBW (Fig. 5.1D, Fig. 5.6A, Fig. 5S12, Table 5.1, Table 5S1). NRPs are structurally diverse and are short (2 to about 50 amino acids). They contain amino acids different than the classical 20 (non-proteinogenic) and are synthesized by large enzymatic complexes called non-ribosomal peptide synthetases (NRPSs)[85]. These NRPSs are modularly organized and

genes coding for them are in operons or clusters[86]. Three main modules are required for NRP synthesis; they include initiation module (adenylation and thiolation domain), elongation module (condensation domain) and the release module (thio-esterase domain)[85-87]. This was the case in our study, as several genetic networks required for their biosynthesis were differentially expressed. These included transcripts for pyrimidine nucleoside synthesis, cellular nitrogen compound synthesis, pyruvate metabolism, quinone oxidoreductase, alcohol metabolism, chorismate biosynthesis, arginine biosynthesis and oligopeptide transport for *Ent. faecalis* at 0.5 h and *E. coli* at 3 h in N-DOMW (Fig. 5.6A, Fig. 5S12). In addition, metabolomics results revealed a significantly higher intracellular concentration of isoleucine in N-DOMW compared to I-DOMW at 0.5 and 3h suggesting they may be important non-ribosomal amino acids (Fig. 5.2A). This was corroborated by gene enrichment analysis on DEG for *E. coli.* Among the genes enriched for secondary metabolite production were transcripts for leucine, valine and isoleucine biosynthesis, further supporting their role in NRP synthesis (Table 5.1).

Increased expression in transcripts for chorismate, pyruvate, and arginine metabolism was likely a modification step where the peptide can be glycosylated, acylated, halogenated, or hydroxylated[88]. In addition, arginine and chorismate seem to be important "public goods" that were used to produce other metabolites, which could be incorporated into NRPs during this modification stage. For example, the *arcB* and argF gene in the arginine synthesis pathway converts carbomoyl phosphate to citrulline (Fig. 5.2B), an important component of the polypeptide antibiotic called Enramycin[88]. This antibiotic acts as an inhibitor of peptidoglycan biosynthesis in Gram-positive bacteria[89].

The production of chorismate via the shikimate pathway can be used to produce enterobactin [90](Fig. 5.6$C_{1)}$ the strongest siderophore known to bind ferric ion[91]. Both *E. coli*

and *Ent. faecalis* have the shikimate pathway (Fig. 5.6B$_1$). Transcripts for this pathway were significantly expressed in both bacteria (Fig. 5.6B$_{2-3}$). However, the production of enterobactin has been more commonly reported to be present in Gram-negative bacteria[91]. We found all the genes required for the synthesis and transport of enterobactin to be significantly upregulated in I-DOMW and N-DOMW for 12 h (Fig. 5.6C; Fig. 5S14B). It is important to note that public goods such as siderophores can be available to non-producers in a community for use[92, 93], which suggest that cooperative competition[94-96] may be in play between *Ent. faecalis* and *E. coli* in our study. [92]Scholz and Greenberg demonstrated that enterobactin mutant *E. coli* could grow well in low-iron medium supplemented with enterobactin and these mutants could compete equally with wild type cells at high cell densities. Furthermore, the authors showed that the growth rate of the wild type was unaffected by cell density. In our study, the growth rate of *Ent. faecalis* increased in the presence of *E. coli* compared to its absence, whereas *E. coli* growth rate did not statistically change between mono-culture and co-culture (Fig. 5S2; Table 5S3). This suggests that *Ent. faecalis* may have made use of this public good. Iron –sulfur dependent serine dehydratase proteins (sdaAA and sdaAB) and seryl tRNA synthetases gene (*serS*) were significantly upregulated in N-DOM compared to I-DOMW at 0.5, 3 and 6 h (> 2-Fold Change) but were not differentially expressed in mono-culture (Fig. 5.6D; Oladeinde et al., 2016b). These transcripts are involved in many processes including the catabolism of L-serine to pyruvate and ammonia and biosynthesis of antibiotics and secondary metabolites[55]. Serine/proline was also a significant extracellular metabolite detected at 3 and 6 h in I-DOMW and N-DOMW (Fig. 5.2B). L-serine is regarded as the most effective amino acid inhibitor against bacterial growth and can sensitize *E. coli* cells to gentamicin and fluoroquinolones[97, 98]. [98]Duan et al. showed that L-serine can disrupt Fe-

S clusters and increase the production of endogenous ROS in *E. coli*. Further, an Δ*sdaA* mutant of *Campylobcter jejuni* was not able to support growth on or utilize L-serine in a defined medium[99]. Collectively, these results support the hypothesis that lactic acid bacteria, while not requiring iron to stimulate growth, can use it to produce heme and Fe-S cluster dependent proteins[100]. More importantly, the transcription of these genes in our study seemed to be a competitive mechanism promulgated by the presence of *E. coli*.

Genes responsive to the production of NRPs were significantly upregulated in I-DOMW and N-DOMW compared to PBW. These genetic networks are associated with antimicrobial resistance including beta-lactam resistance, peptidoglycan synthesis, multidrug efflux pumps, tryptophan biosynthesis, bleomycin/glyoxalases resistance, quorum sensing, biofilm formation and DNA recombination/replication (Fig. 5.7, Table 5.1, Fig. 5S15 and 5S16, Table 5S1).

***E. coli* and *Ent. faecalis* differ in regrowth potential under sunlight exposure.** Interactions between co-cultures were also tested in outdoor mesocosm experiments. We hypothesized that exposure of mesocosms to direct sunlight would inactivate *E. coli* and *Ent. faecalis* while increasing production of HOOH. Further, the removal of photo-produced HOOH would be critical for *E. coli* and *Ent. faecalis* to re-grow. To address this, filter sterilized (0.2 μm pore size) stream water (with ~4 – 5 mg L^{-1} DOC) was spiked with CFE and exposed to natural sunlight for 4 h to initiate HOOH production prior to co-culture inoculation (~10^6 CFU mL^{-1} of each bacterium) in the dark. Following inoculation, mesocosms were incubated in the dark for 20 h before the next cycle of sunlight exposure and dark incubation (experimental design - Fig. 5S18). For the 72-h cycle, we observed a diel pattern of daylight die off and overnight regrowth in *E. coli* populations, while *Ent. faecalis* populations remained at steady state conditions overnight and died off during

daylight (Fig. 5.9A and B). Following inoculation, photo-produced HOOH concentrations declined in the dark for the first 20 h, and remained below our MDL for the 72-h cycle. However, in exposed controls (sunlight + stream water only + bacteria) HOOH was detected at micro-molar levels throughout the experiment and *Ent. faecalis* was never detected after the first cycle of direct sunlight exposure (Fig. 5.9A and B). In unexposed DOMW mesocosms (no sunlight + DOMW+ bacteria), *E. coli* re-grew after 28 h of dark incubation while *Ent. faecalis* exhibited a steady state or decline in population (Fig. 5S19A and B). In addition, extracellular HOOH was below our MDL after 24 h of dark incubation. In contrast, HOOH was detected after 52 h period in unexposed controls (no sunlight + stream water only + bacteria) and *Ent. faecalis* experienced a gradual decline in population, whereas *E. coli* re-grew after 24 h. Collectively, our results suggest that DOM addition to stream water facilitated a longer survival time and regrowth of *E. coli* and *Ent. faecalis* in co-culture.

Our results clearly show that DOM addition to stream water aided in a longer survival and regrowth of fecal bacteria. We investigated, if this effect was associated with the degradability of DOM present by sunlight or by bacterial interactions. Biodegradation and photodegradation of DOM can lead to the conversion of DOM to inorganic compounds and its subsequent loss from the water column, and to the alteration of DOM chemical composition [115]. We measured the specific UV absorbance at 254nm ($SUVA_{254}$), a proxy for DOM aromaticity and molecular weight. The initial $SUVA_{254}$ values for exposed and unexposed DOMW mesocosms were below 1 L Mg-C^{-1} m^{-1}, which suggests that a large fraction of available DOM is composed of low molecular weight, aliphatic compounds that may not absorb at 254 nm. In the dark, $SUVA_{254}$ values decreased in exposed and unexposed DOMW treatments, consistent with biodegradation preferentially removing low

molecular weights compounds – via conversion to CO_2. In controls, however, $SUVA_{254}$ decreased and increased with no clear trends throughout the experiment (Fig. 5.9C and D; Fig. 5S18C and D). The observed increases possibly reflect transient DOM pools made up of degradation byproducts that were subsequently consumed and/or transformed [115].

CONCLUSION

We show here that the removal of HOOH is critical for *E. coli* and *Ent. faecalis* survival and its removal is dictated by the source of HOOH and the strain of bacteria. When exogenous HOOH was produced from sunlight irradiation of DOM, we found transcripts responsible for HOOH removal to be significantly up-regulated in *E. coli*, whereas such genes showed no significant changes in *Ent. faecalis*. Conversely, when the source of extracellular HOOH was microbial in origin (e.g., dark production) the expression of these transcripts increased significantly in *Ent. faecalis*. In addition, *Ent. faecalis* increased the expression of transcripts involved with the aerobic metabolism of glycerol, a process that produces HOOH as a by-product[12]. Our results provide supporting evidence that these genes may be restricted to the removal of endogenously produced HOOH in *Ent. faecalis* [116].

Competition plays a significant role in controlling bacterial populations[95]. Here, we showed that in the absence of an exogenous stressor like HOOH, *E. coli* and *Ent. faecalis* increased the number of genes expressed for survival. Further, we demonstrated that this increase was attributable to competition from either bacterium in co-culture. Most importantly, we observed an increase in growth rate for *Ent. feacalis* in co-culture with *E. coli* compared to mono-culture, suggesting a type of cooperative competition. This form of competition is suggested to enable bacterial strains to coexist in the same niche in an "exploitative relationship"[95]. For this type of competition to exist, the Black Queen

Hypothesis proposes that, in a group of species in which a public good is required, if all but one species loses the ability to produce it, the producing species must ramp up production to avoid its own extinction, even if it benefit its competitors[95, 117, 118]. Similar equilibria were observed between *Ent. faecalis* and *E. coli* in our study. Chorismate and arginine/ornithine were important public goods provided by *Ent. faecalis*, while *E. coli* produced enterobactin and putrescine, among others. This was supported with mono-culture results, where transcripts for chorismate and arginine biosynthesis were only differentially expressed at 0.5 h in N-DOMW for *Ent. faecalis*. By contrast, these transcripts were significantly upregulated for the 12 h period in N-DOMW compared to I-DOMW in co-culture. The overall benefit of such cooperation is accessibility to more nutrients and cost saving in terms of public good production[95].

More broadly, our results suggest that *E. coli* and *Ent. faecalis* do differ in their mechanisms for survival under photo-produced HOOH stress and in competition with eachother. We believe this afforded them the ability to coexist in our co-culture microcosms and mesocosms and achieve stable population. Moreover, *E. coli* and *Ent. faecalis* are distantly related species, suggesting that their metabolic niches may not overlap[95]. We recognize that the dynamics shown here may not directly mimic the natural environment where several other factors might be in play including temperature, protozoan predation, and other competitors. Nevertheless, our study provides for the first time invaluable insights on the role of HOOH as direct regulator of bacterial growth and the competition dynamic between on two important laboratory strains of indicator bacteria.

FIGURES AND TABLES

A

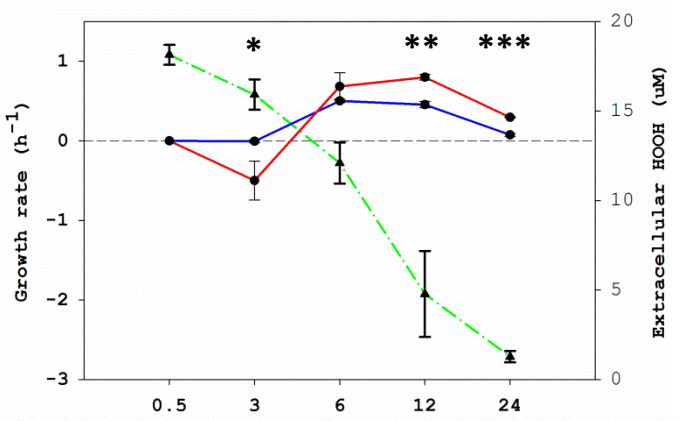

B

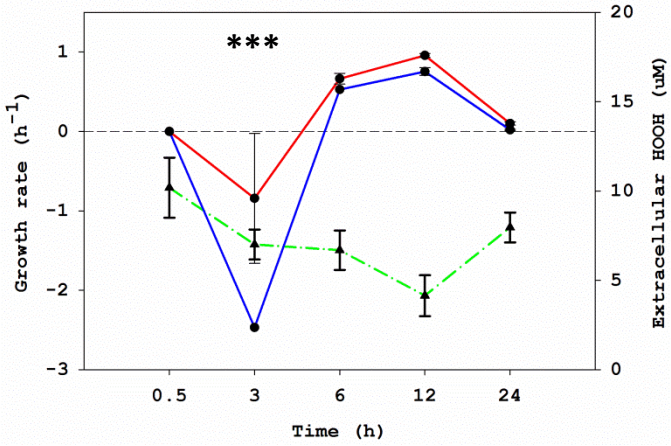

C

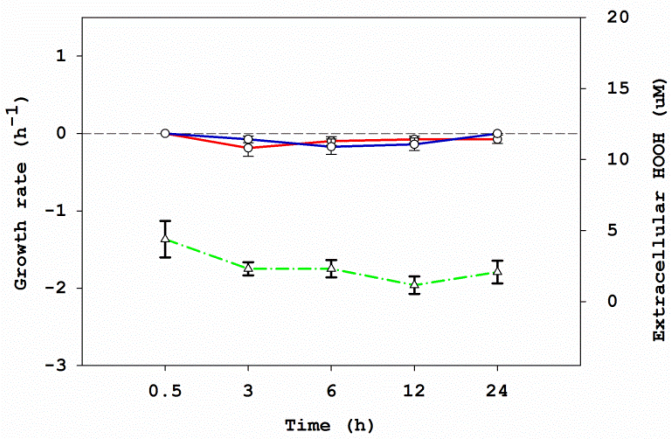

D1

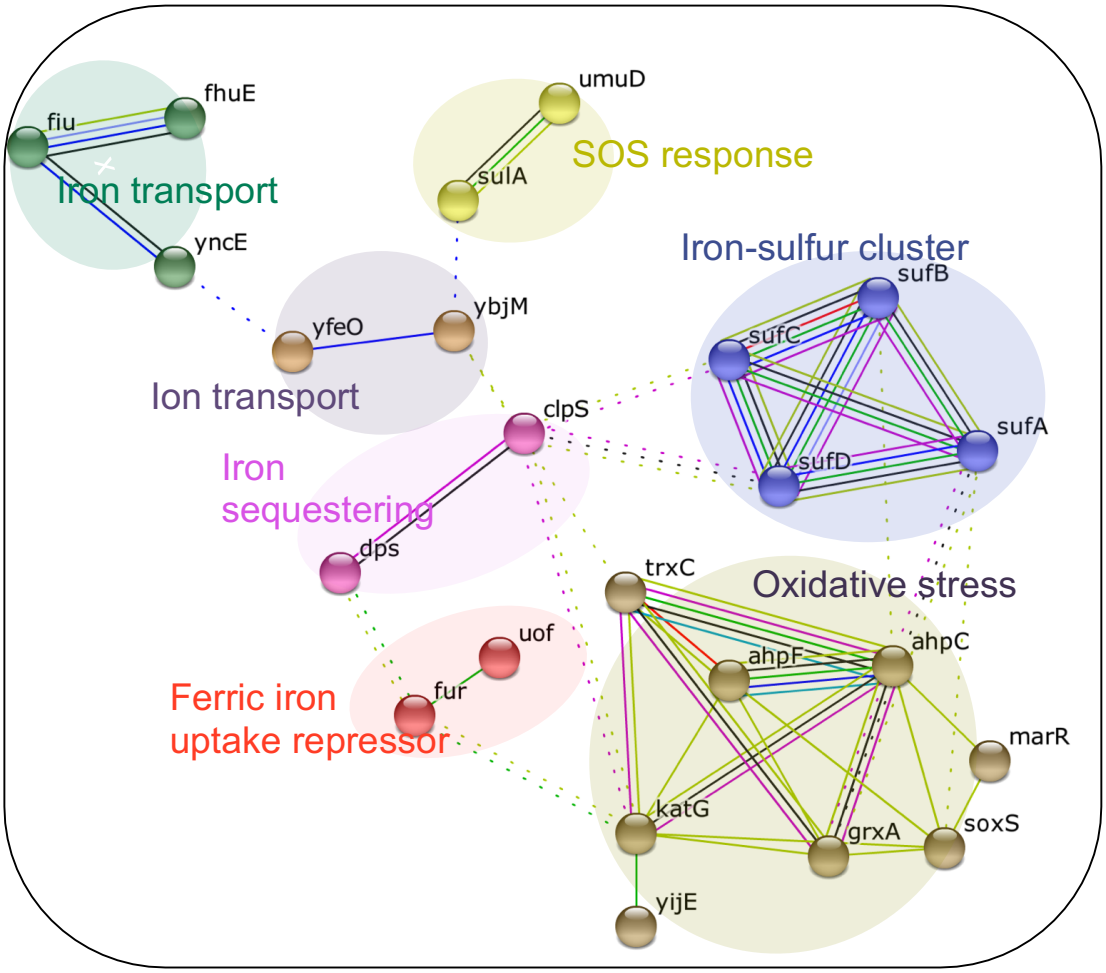
fhuE
fiu
Iron transport
yncE
umuD
sulA
SOS response
Iron-sulfur cluster
sufB
sufC
sufA
sufD
yfeO
ybjM
Ion transport
clpS
Iron
sequestering
dps
trxC
Oxidative stress
ahpC
ahpF
marR
uof
fur
Ferric iron
uptake repressor
katG
grxA
soxS
yijE

D2

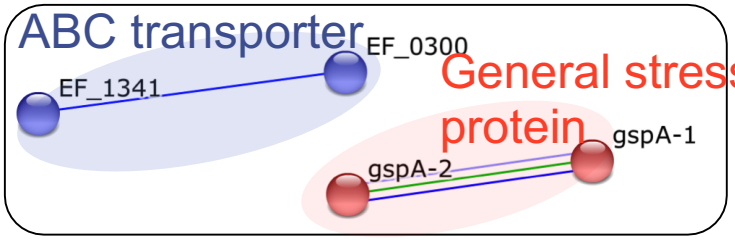
ABC transporter
EF_0300
EF_1341
General stress
protein
gspA-1
gspA-2

E

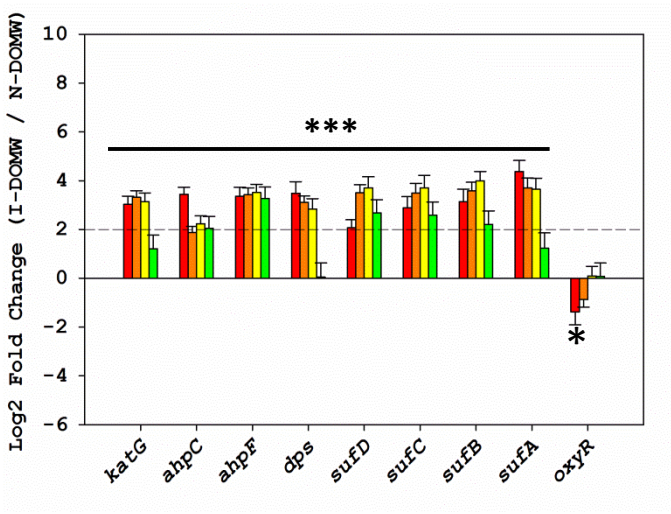
Log2 Fold Change (I-DOMW / N-DOMW)
10
8
6
4
2
0
-2
-4
-6
***
*
katG
ahpC
ahpF
dps
sufD
sufC
sufB
sufA
oxyR

F

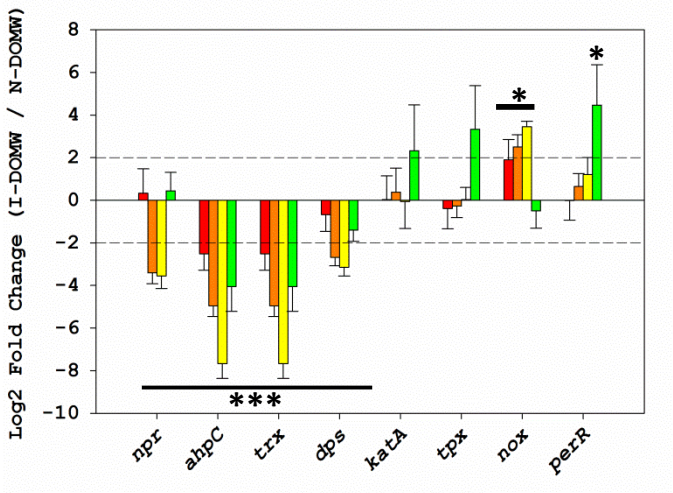
Log2 Fold Change (I-DOMW / N-DOMW)
8
6
4
2
0
-2
-4
-6
-8
-10
*
*
***
npr
ahpC
trx
dps
katA
tpx
nox
perR

G

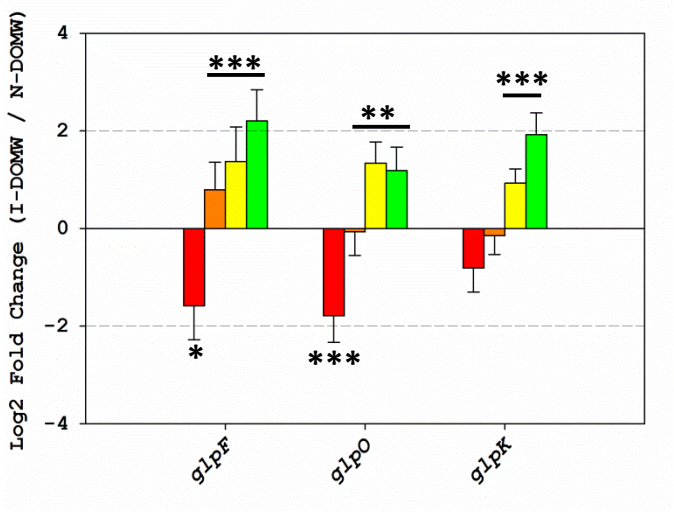
Log2 Fold Change (I-DOMW / N-DOMW)
4
2
0
-2
-4
***
**
***
*
***
glpF
glpO
glpK

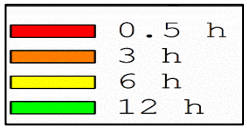
0.5 h
3 h
6 h
12 h

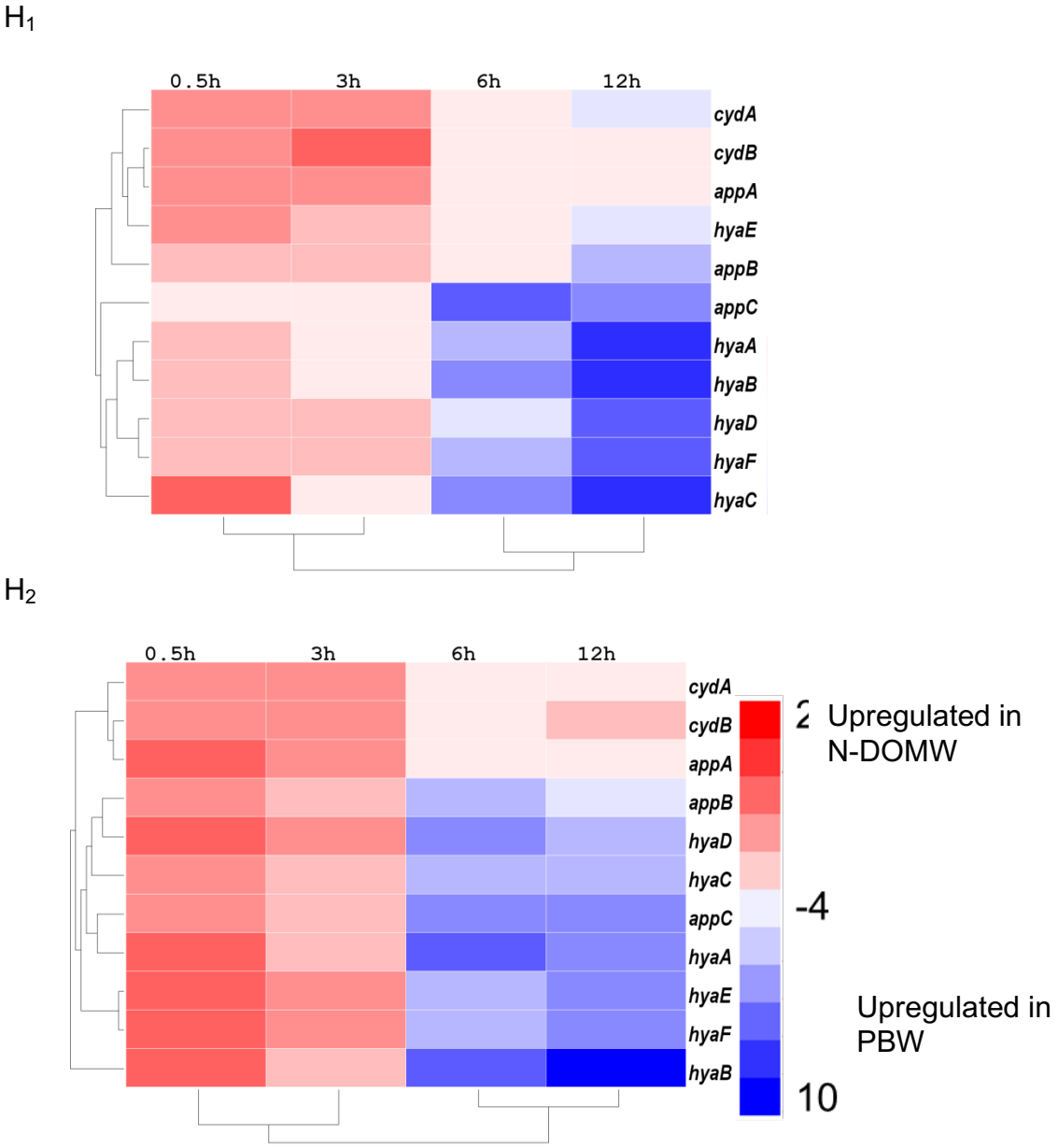

Figure 5.1. Hydrogen peroxide controls fecal bacteria survival dynamics and causes extensive changes in gene expression profile of *E. coli*. (**A**, **B**, and **C**) *E. coli* and *Ent. faecalis* concentration were determined at 0.5, 3, 6, 12 and 24 h during dark incubation and filter sterilized with a 0.22µm syringe filter for extracellular HOOH determination (n = 3 per group). Green dashed lines represent extracellular HOOH concentration during dark incubation in (A) I-DOMW (B) N-DOMW and (C) PBW in the presence of both *E. coli* (red solid line) and *Ent. faecalis* (blue solid line). Growth rates per time point per group are plotted on the y-axis (dark circles). Error bars represent standard errors. *denotes significant difference in growth rate between *E. coli* and *Ent. faecalis*per time point (**P* value <0.05, **<0.01, ***<0.001). (**D** to **H**) Total RNA was extracted from co-cultures collected at 0.5, 3, 6 and 12 h and used for whole transcriptome sequencing (WTS) (n=2

per group). (D) STRING analysis for significantly altered transcripts in IDOM-W compared to N-DOMW for *E. coli* (1) and (2) *Ent. faecalis*at 0.5 h (fold-change ≥ 2; *P*. padj < 0.01). Fold-change of selected OxyR regulated genes in I-DOMW compared to N-DOMW for (E) *E. coli* and (F) *Ent. faecalis* for the 12 h duration. (**P* value <0.05, **<0.01, ***<0.001) (F) Fold-change of genes involved in the aerobic metabolism of glycerol via the *glpK* pathway between I-DOMW and N-DOMW for *Ent. faecalis*(H) Heatmap for cytochrome and hydrogenase genes differentially expressed between (1) I-DOMW and (2) N-DOMW for *E. coli*. The color scale shows fold-change compared to PBW

A

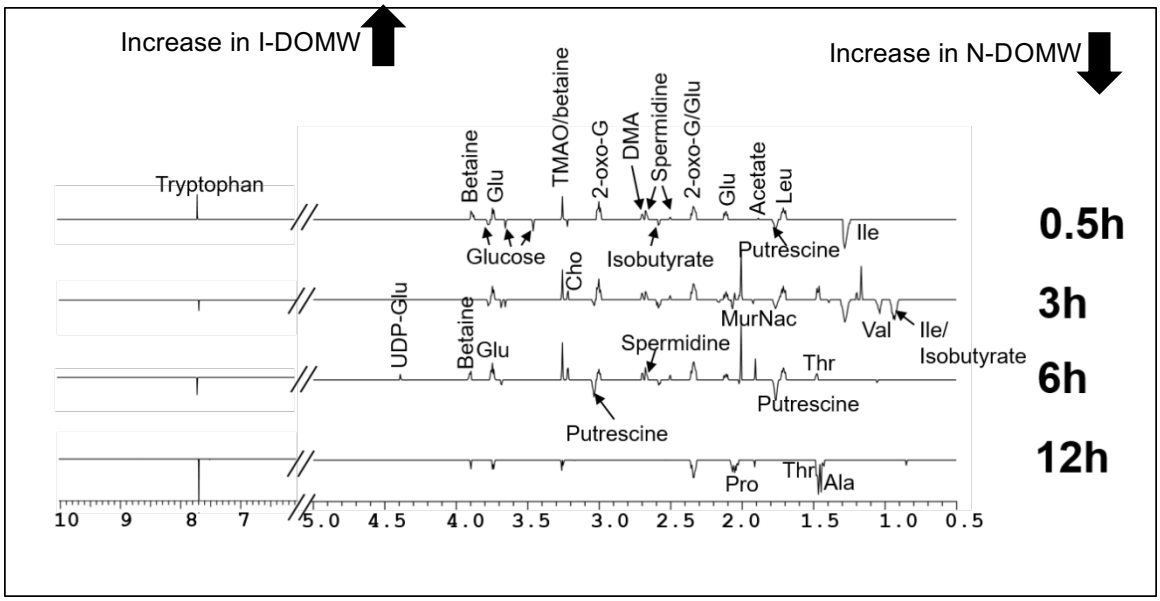

B . GC/MS Metabolites Identified in Media
I-DOMW vs. N-DOMW

	Time			
Metabolite	**0 h**	**3 h**	**6 h**	**12 h**
Alanine	+	-	+	-
C16 fatty acid		+	+	+
C18 fatty acid	+		+	+
Cadaverine		+	+	
Citrate	+	+	+	
FAMES (long chain)		-	+	+
Fumarate		+	+	
Glucose	+	-	+	+
Glutamate		+	+	+
Glutamic acid		+	-	
Glycine	+	+	+	-
Homocysteine	-	-	-	
Phenylalanine			+	
Phosphate	-		-	-
Purine(s)		+	+	-
Pyruvate	+		+	
Serine/proline		+	+	
Succinate		+	+	
Sugar phosphates		+	+	

Tryptophan		-	+	+

+ = higher in I-DOMW compared to N-DOMW

C_1

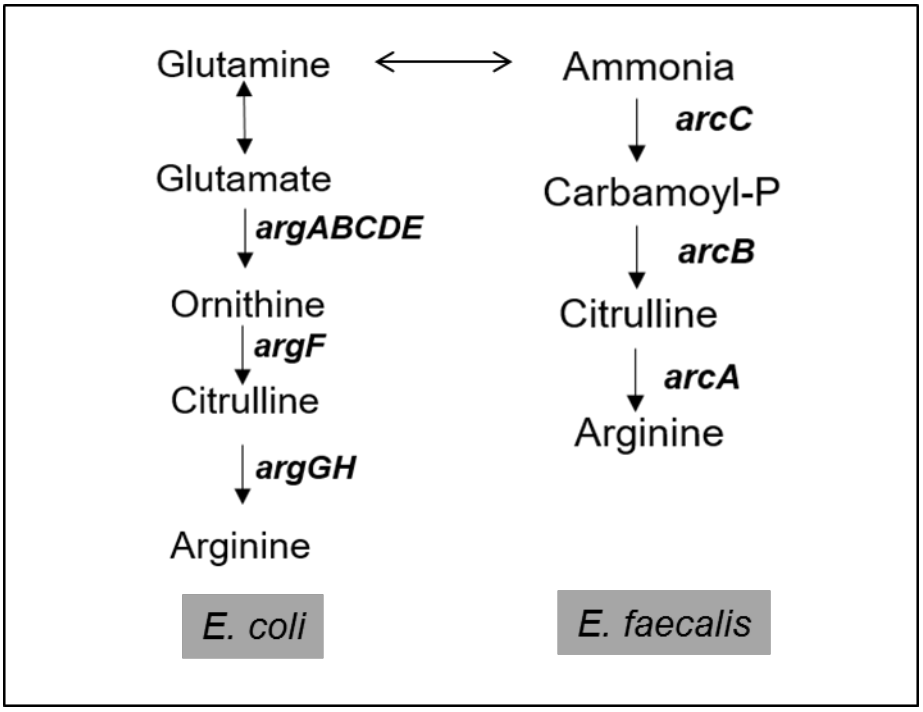

C_2

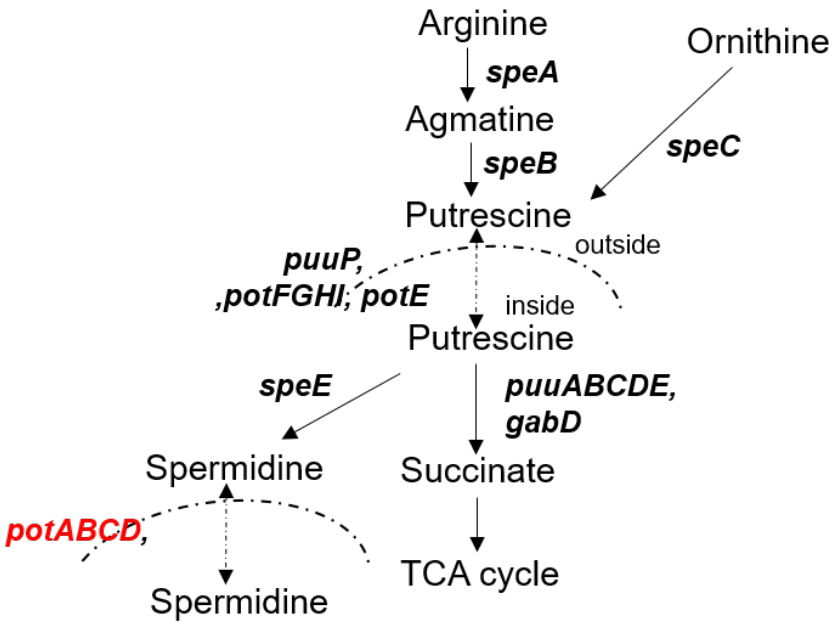

D1

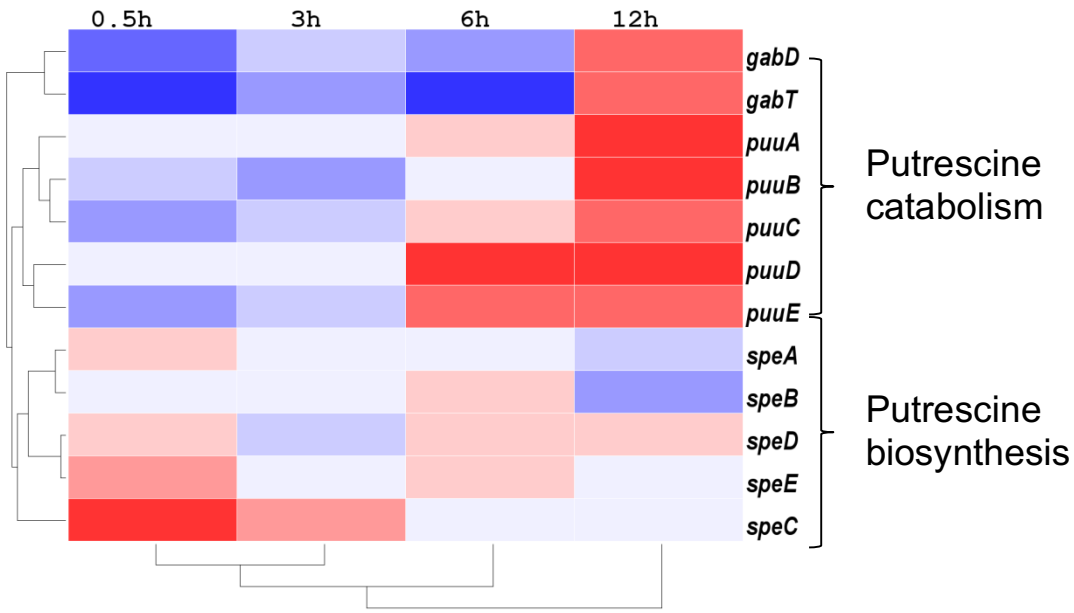
0.5h
3h
6h
12h
gabD
gabT
puuA
puuB
puuC
puuD
puuE
speA
speB
speD
speE
speC
Putrescine catabolism
Putrescine biosynthesis

D2

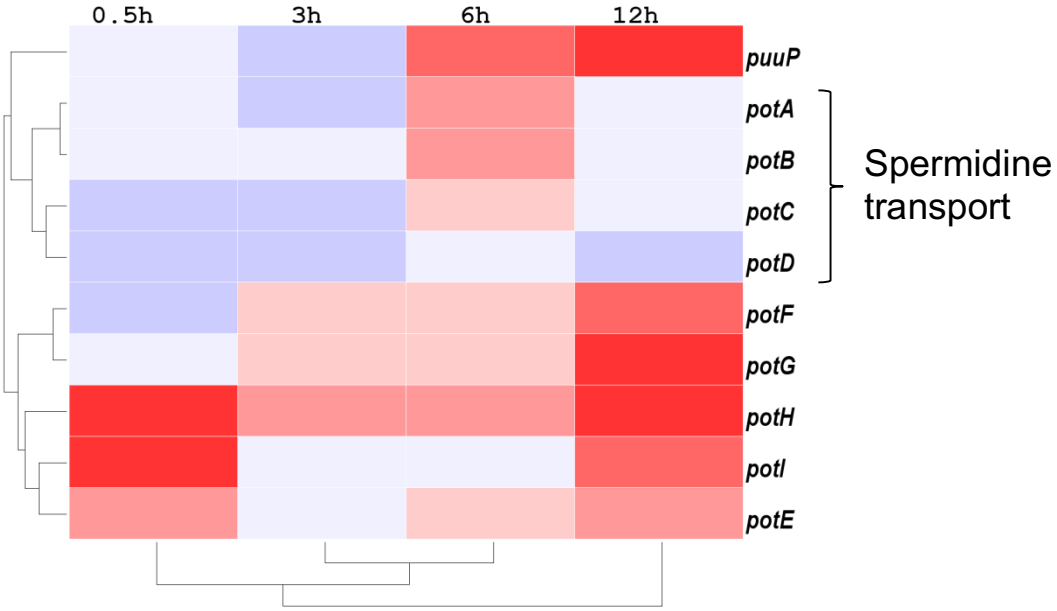
0.5h
3h
6h
12h
puuP
potA
potB
potC
potD
potF
potG
potH
potI
potE
Spermidine transport

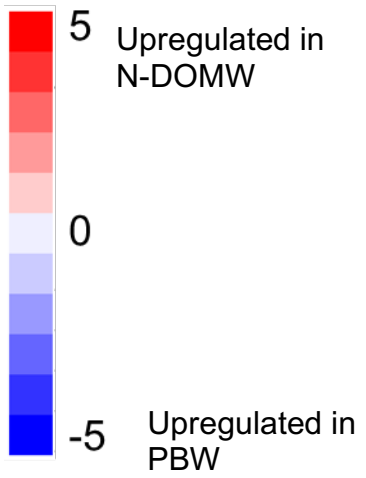
5
Upregulated in N-DOMW
0
-5
Upregulated in PBW

E

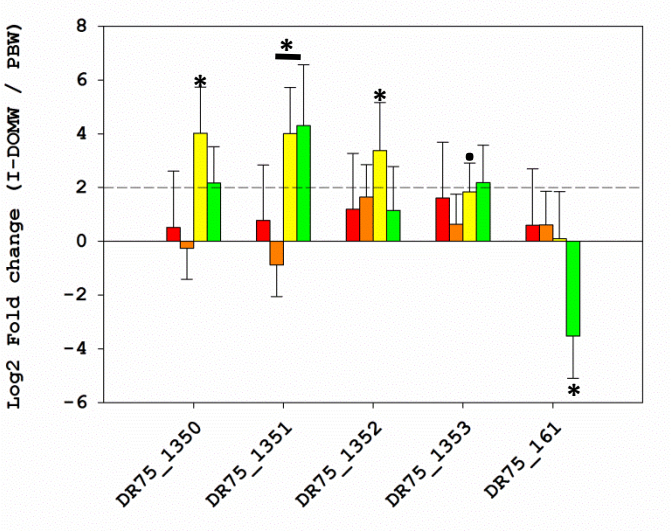
Log2 Fold change (I-DOMW / PBW)
8
6
4
2
0
-2
-4
-6
DR75_1350
DR75_1351
DR75_1352
DR75_1353
DR75_161

F_1

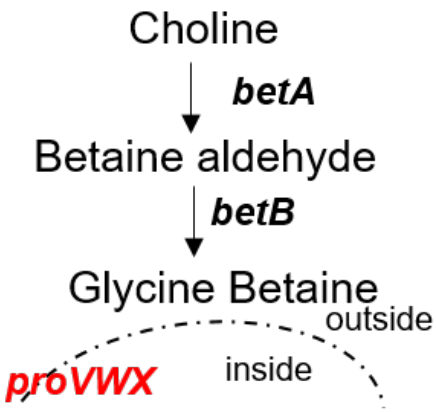
Choline
betA
Betaine aldehyde
betB
Glycine Betaine
outside
inside
proVWX

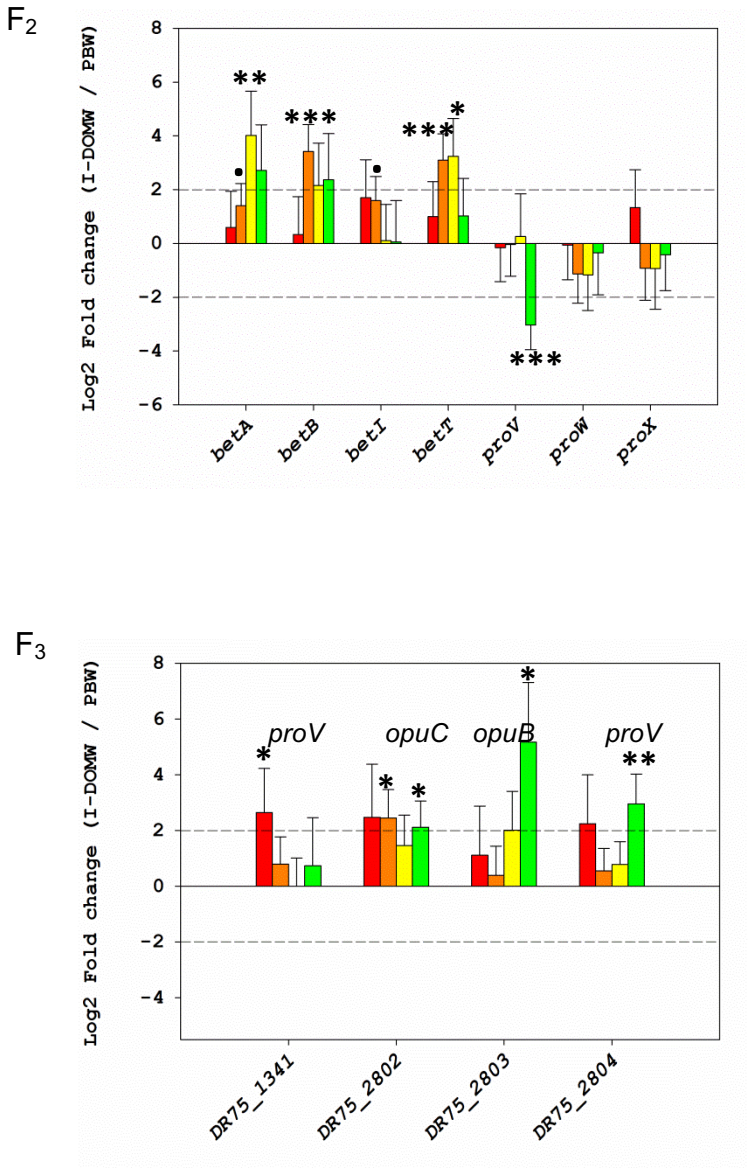

Figure 5.2. Production of secondary metabolites aids in *E. coli* and *Ent. faecalis* survival. Intracellular and extracellular metabolites were extracted from co-culture of *E. coli* and *Ent. faecalis*at 0.5, 3, 6, and 12 h during dark incubation (n= 6 per treatment) and analyzed by NMR and GC/MS. (**A and B**) Representative 1H NMR spectra (A) and top 20 peaks identified on GC/MS (B) in I-DOMW compared to N-DOMW. (Abbreviations: Glu- Glucose, TMAO-Trimethylamine-oxide, DMA- Dimethylamine, val- Valine, Ile- Isoleucine,

leu- Leucine, Pro-Proline, Thr-Threonine, Ala- Alanine, oxoG- oxoglutarate, MurNac- N-Acetylmuramic acid). **(C)** Pathway for polyamine production and transport via (1) Arginine and (2) Ornithine biosynthesis (bold gene name denotes gene was differentially expressed between treatments and red font in gene names denotes the presence of similar pathway genes in *E. coli* and *Ent. feacalis*). **(D**) Heatmap for putrescine/spermidine biosynthesis (1) and transport (2) transcripts in N-DOMW compared to PBW for *E. coli*. Color scale shows fold-change compared to PBW. **(E**) Fold-change in putrescine/spermidine transport transcripts in I-DOMW compared to PBW for *Ent. faecalis*(**F**) Pathway for Glycine betaine biosynthesis and transport (1) and fold-changes in pathway genes expressed between I-DOMW and PBW (2) for *E. coli* (3) and *Ent. faecalis*.
(**P* value .<0.1. *<0.05, **<0.01, ***<0.001)

A1

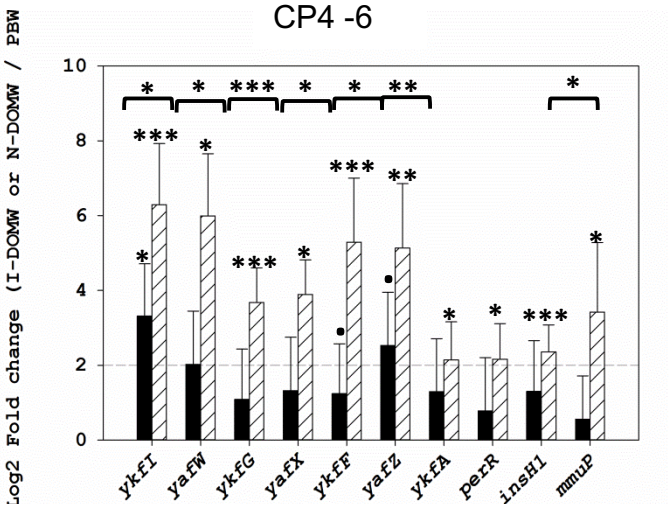
CP4 -6
Log2 Fold change (I-DOMW or N-DOMW / PBW
10
8
6
4
2
0
ykfI
yafW
ykfG
yafX
ykfF
yafZ
ykfA
perR
insH1
mmuP

A2

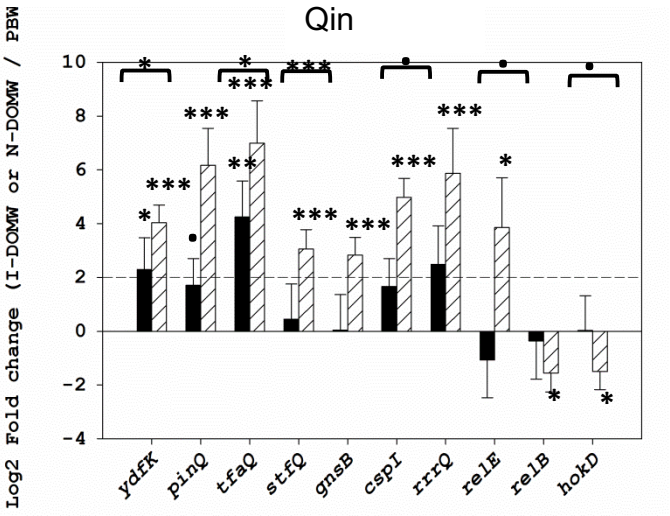
Qin
Log2 Fold change (I-DOMW or N-DOMW / PBW
10
8
6
4
2
0
-2
-4
ydfK
pinQ
tfaQ
stfQ
gnsB
cspI
rrrQ
relE
relB
hokD

A3

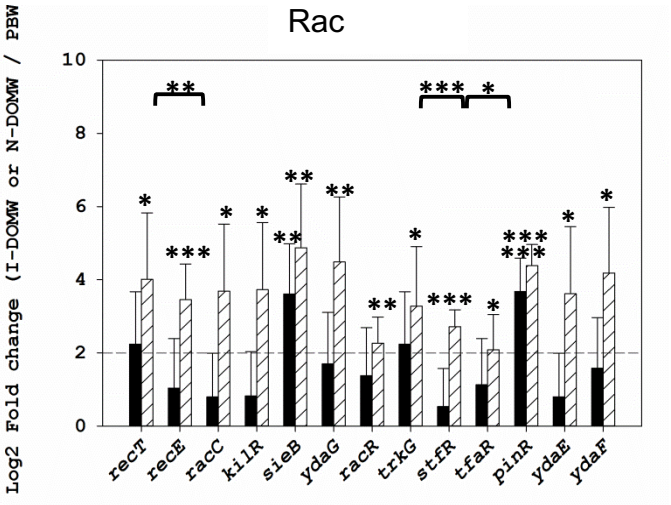
Rac
Log2 Fold change (I-DOMW or N-DOMW / PBW
10
8
6
4
2
0
recT
recE
racC
kilR
sieB
ydaG
racR
trkG
stfR
tfaR
pinR
ydaE
ydaF

A4

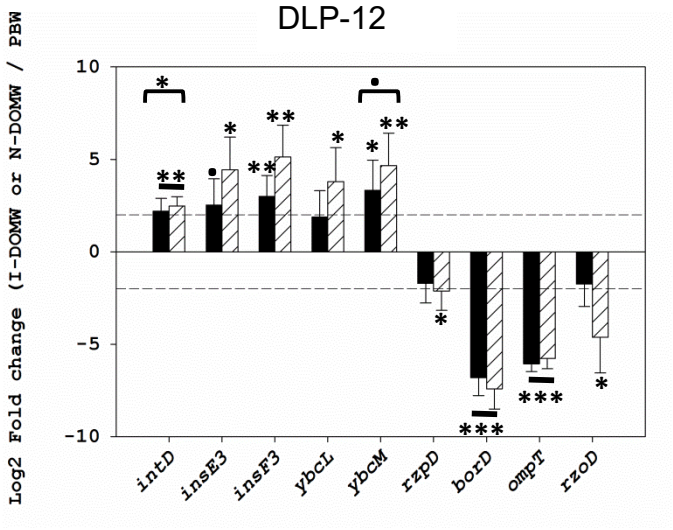
DLP-12
Log2 Fold change (I-DOMW or N-DOMW / PBW
10
5
0
-5
-10
intD
insE3
insF3
ybcL
ybcM
rzpD
borD
ompT
rzoD

A5

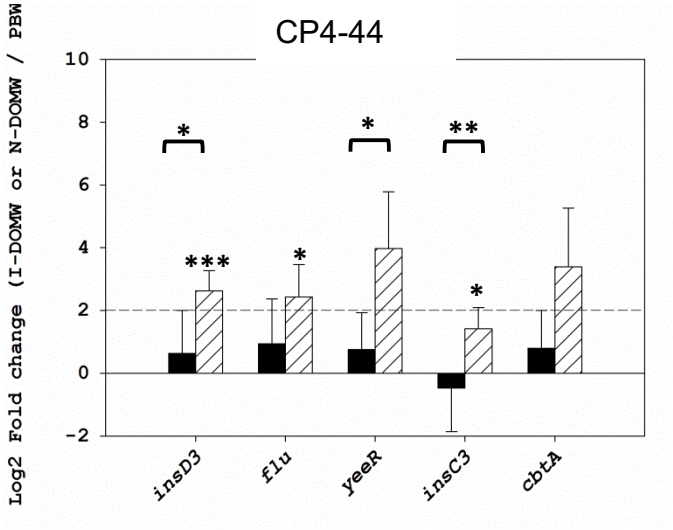
CP4-44
Log2 Fold change (I-DOMW or N-DOMW / PBW
10
8
6
4
2
0
-2
insD3
flu
yeeR
insC3
cbtA

A6

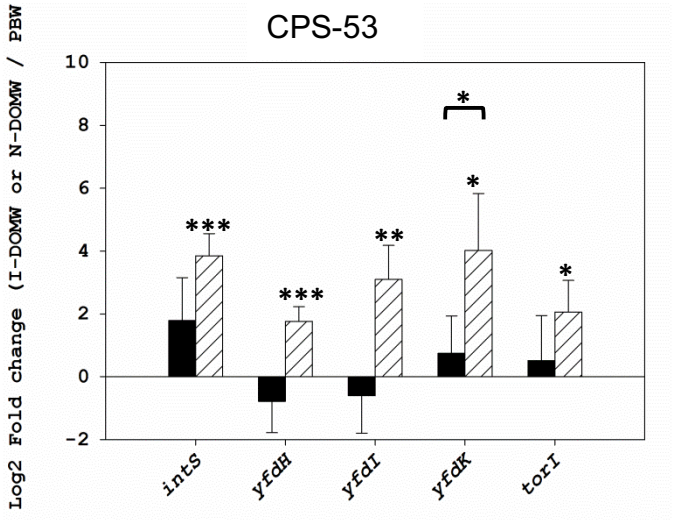
CPS-53
Log2 Fold change (I-DOMW or N-DOMW / PBW
10
8
6
4
2
0
-2
intS
yfdH
yfdI
yfdK
torI

A7

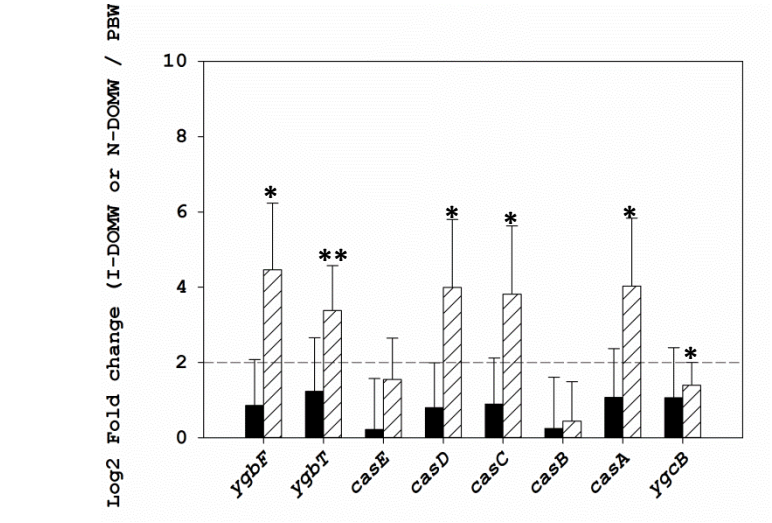
Log2 Fold change (I-DOMW or N-DOMW / PBW)
10
8
6
4
2
0
ygbF
ygbI
casE
casD
casC
casB
casA
ygcB

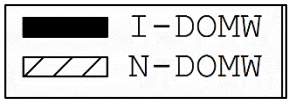
I-DOMW
N-DOMW

B1

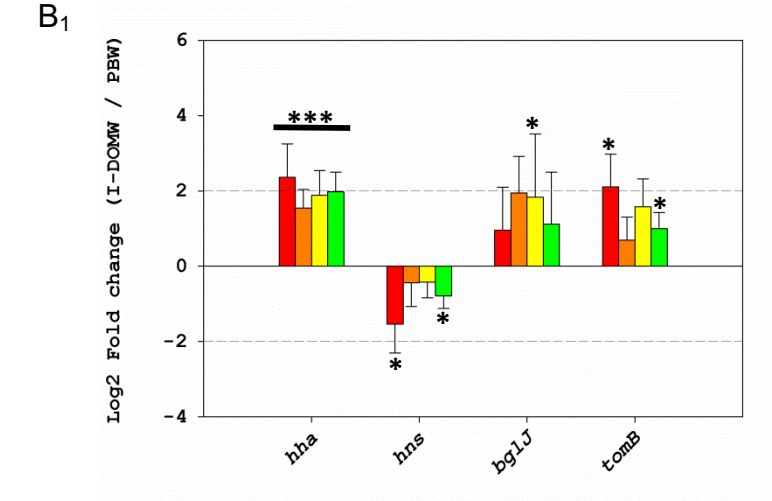
Log2 Fold change (I-DOMW / PBW)
6
4
2
0
-2
-4
hha
hns
bglJ
tomB

B2

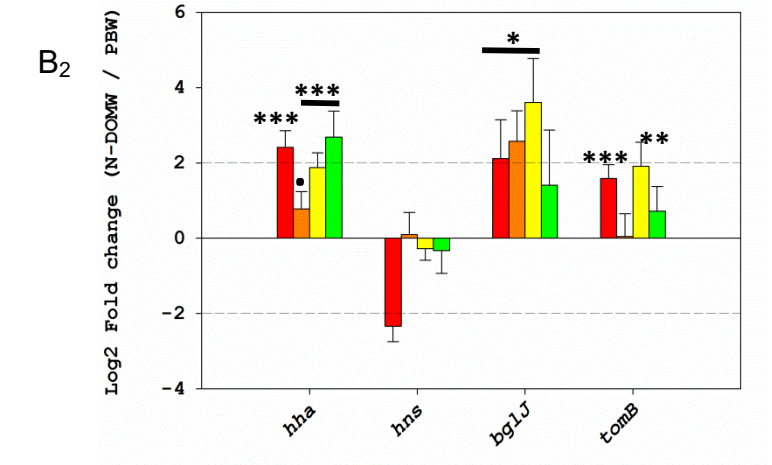
Log2 Fold change (N-DOMW / PBW)
6
4
2
0
-2
-4
hha
hns
bglJ
tomB

Figure 5.3. Bacteriophages are important survival elements for *E. coli*. (A_{1-7}) Fold-change in cryptic phage (1-6) and (7) CRISP-R genes significantly upregulated in N-DOMW compared to PBW at 0.5 h for *E. coli*. (**B**) Fold-change in DNA recombination regulatory proteins in (1) I-DOMW and (2) N-DOMW compared to PBW for *E. coli*.
(**P* value ·<0.1· *<0.05, **<0.01, ***<0.001; Brackets represent significant difference between I-DOMW and N-DOMW)

A1

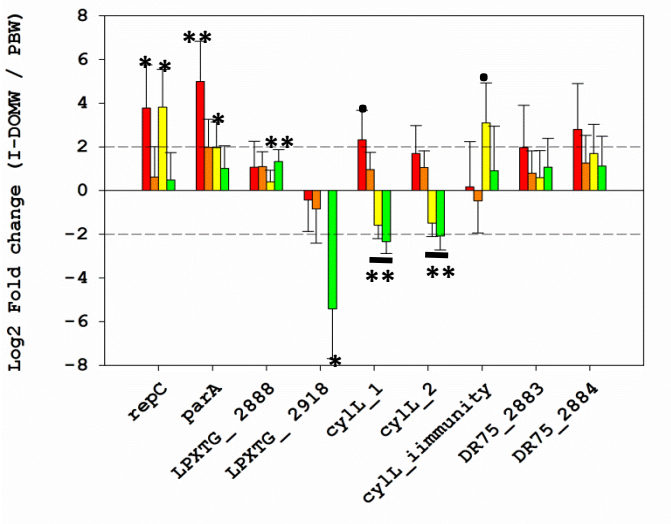
Log2 Fold change (I-DOMW / PBW)
8
6
4
2
0
-2
-4
-6
-8
repC
parA
LPXTG_2888
LPXTG_2918
cylL_1
cylL_2
cylL_iimmunity
DR75_2883
DR75_2884

A2

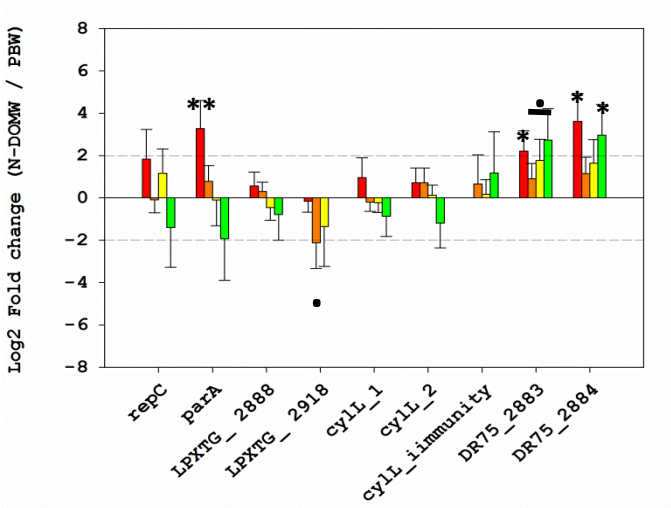
Log2 Fold change (N-DOMW / PBW)
8
6
4
2
0
-2
-4
-6
-8
repC
parA
LPXTG_2888
LPXTG_2918
cylL_1
cylL_2
cylL_iimmunity
DR75_2883
DR75_2884

B1

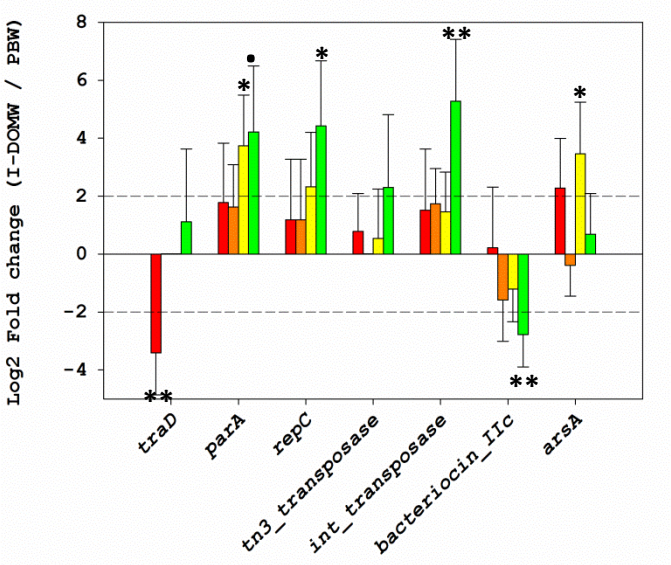
Log2 Fold change (I-DOMW / PBW)
8
6
4
2
0
-2
-4
traD
parA
repC
tn3_transposase
int_transposase
bacteriocin_IIc
arsA

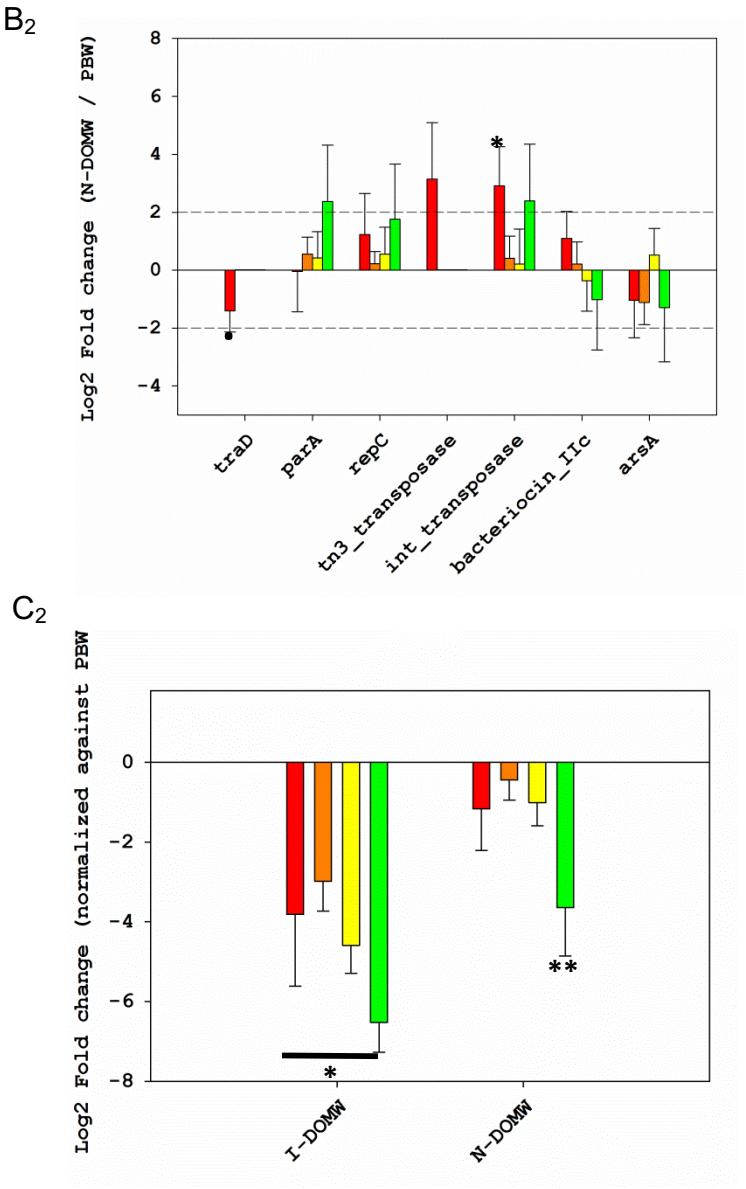

Figure 5.4. Conjugative plasmids contributed to *Ent. Faecalis* fitness. **(A and B)** Fold-change in differentially expressed genes carried on (A) plasmid 1 and (B) plasmid 2 of *Ent. faecalis* in (1) I-DOMW and (2) N-DOMW compared to PBW. Gene names represents protein class or family, and number in gene names denotes associated NCBI locus_id. (**C**) Fold-change in sex pheromone (cAD1) protein in I-DOMW and N-DOMW compared to PBW.
(**P* value ·<0.1· *<0.05, **<0.01, ***<0.001)

A1

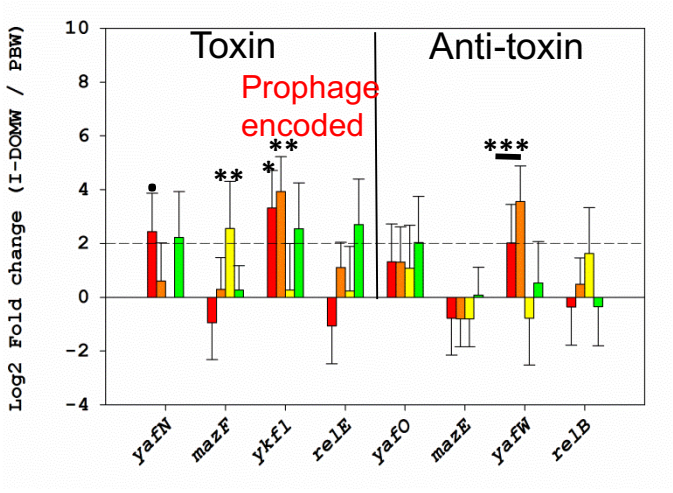
Toxin
Anti-toxin
Prophage encoded
Log2 Fold change (I-DOMW / PBW)
yafN
mazF
ykfI
relE
yafO
mazE
yafW
relB

A2

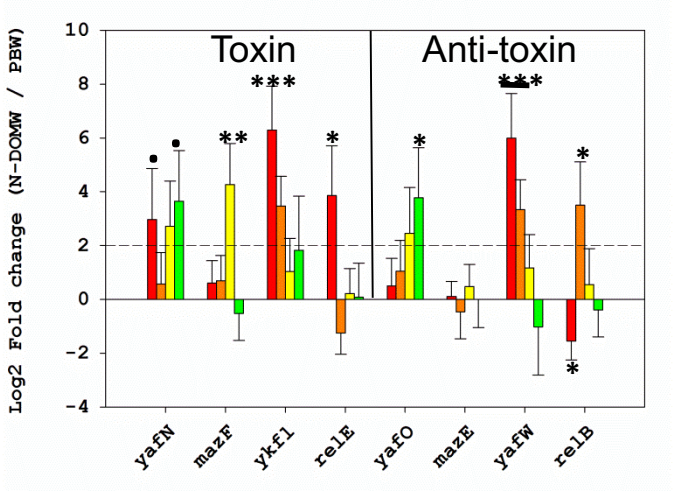
Toxin
Anti-toxin
Log2 Fold change (N-DOMW / PBW)
yafN
mazF
ykfI
relE
yafO
mazE
yafW
relB

B1

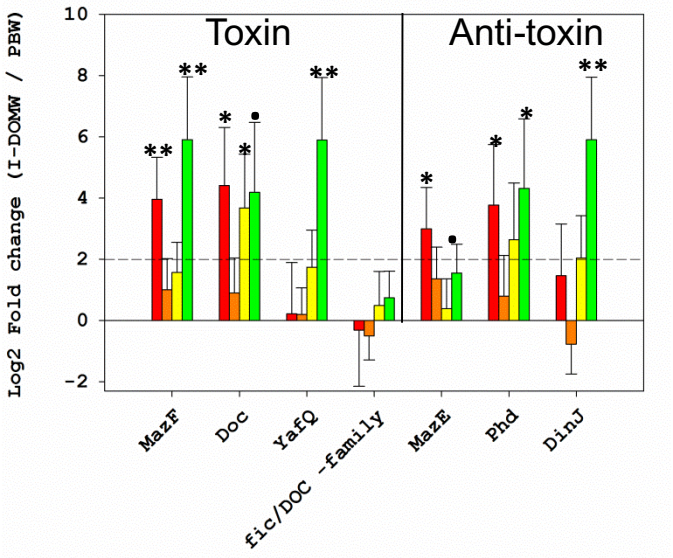
Toxin
Anti-toxin
Log2 Fold change (I-DOMW / PBW)
MazF
Doc
YafQ
fic/DOC -family
MazE
Phd
DinJ

B_2

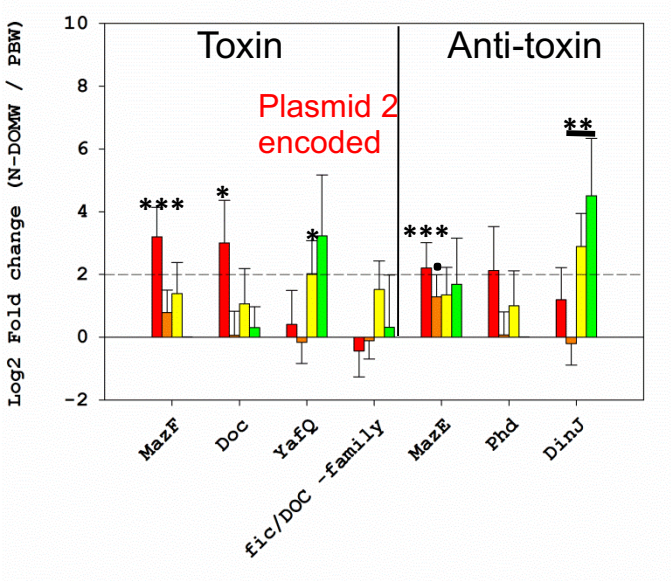
Toxin
Anti-toxin
Plasmid 2 encoded
Log2 Fold change (N-DOMW / PBW)
10
8
6
4
2
0
-2
***
*
*
***
**
MazF
Doc
YafQ
fic/DOC -family
MazE
Phd
DinJ

C_1

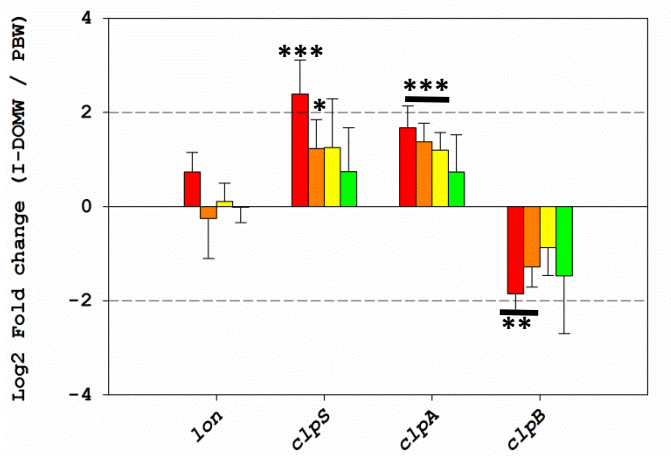
Log2 Fold change (I-DOMW / PBW)
4
2
0
-2
-4
***
*
***
**
lon
clpS
clpA
clpB

C_2

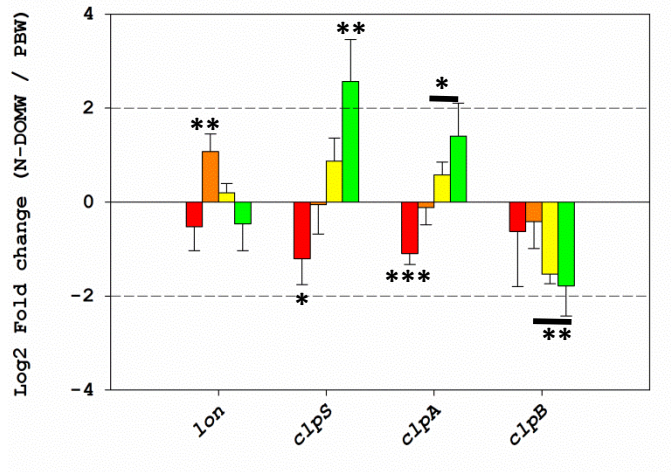
Log2 Fold change (N-DOMW / PBW)
4
2
0
-2
-4
**
**
*
*
***
**
lon
clpS
clpA
clpB

D_1

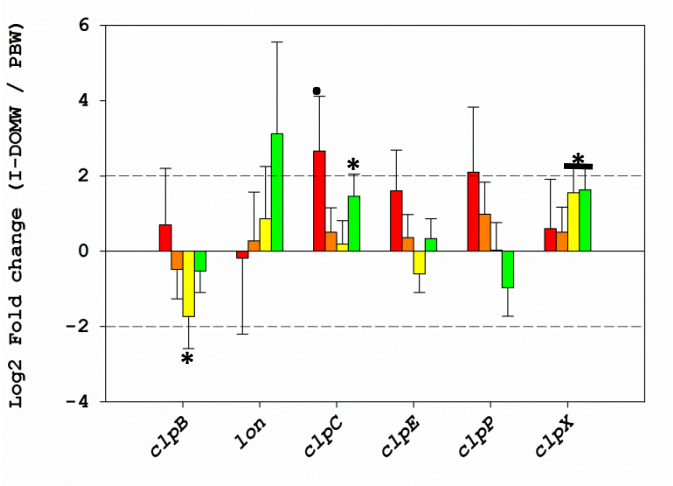
Log2 Fold change (I-DOMW / PBW)
6
4
2
0
-2
-4
*
*
*
clpB
lon
clpC
clpE
clpP
clpX

D_2

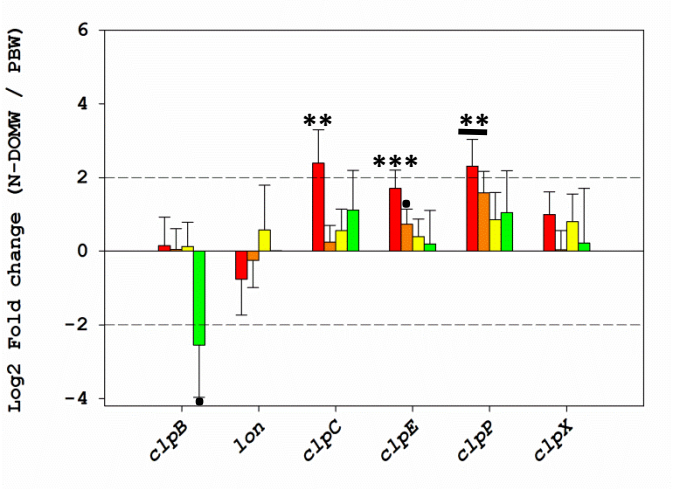
Log2 Fold change (N-DOMW / PBW)
6
4
2
0
-2
-4
**
***
**
clpB
lon
clpC
clpE
clpP
clpX

E_1

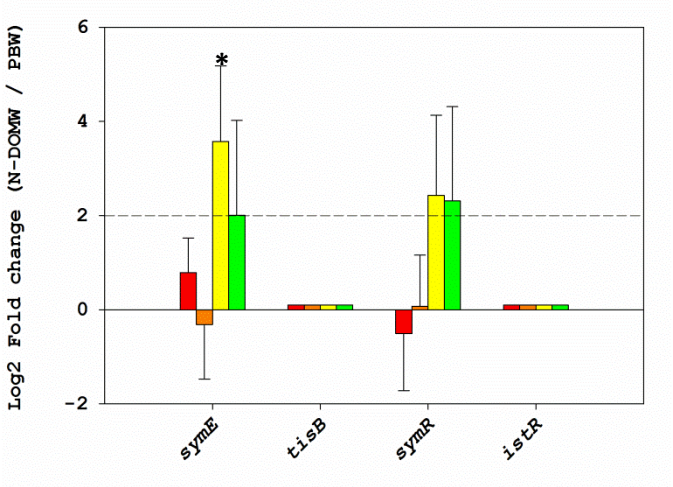
Log2 Fold change (N-DOMW / PBW)
6
4
2
0
-2
*
symE
tisB
symR
istR

E_2

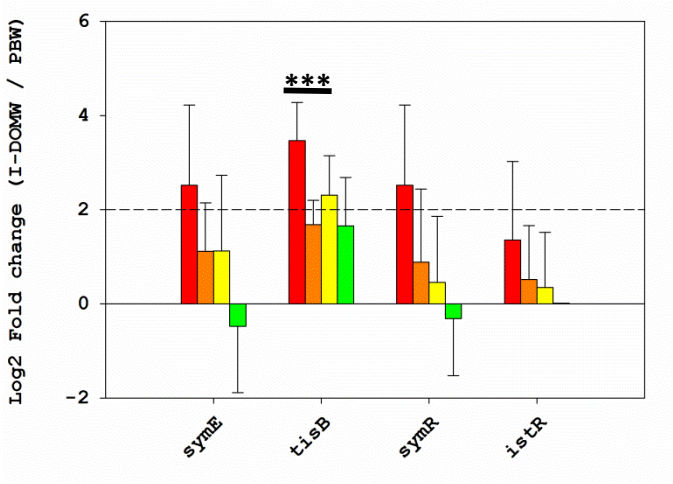
Log2 Fold change (I-DOMW / PBW)
6
4
2
0
-2
***
symE
tisB
symR
istR

F_1

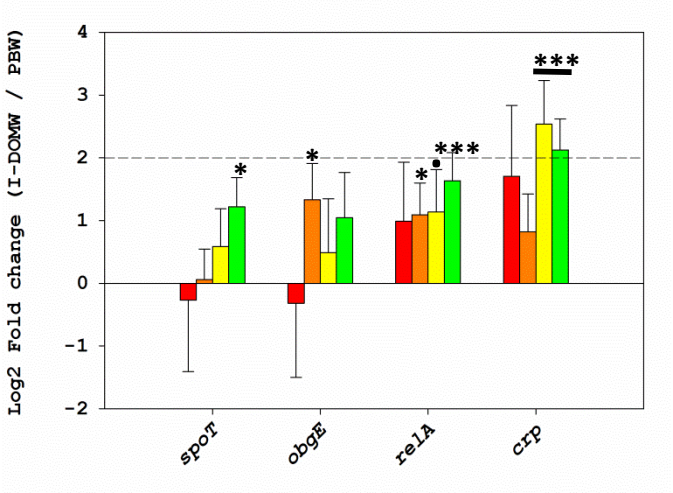
Log2 Fold change (I-DOMW / PBW)
4
3
2
1
0
-1
-2
*
*
*
***
***
spoT
obgE
relA
crp

F_2

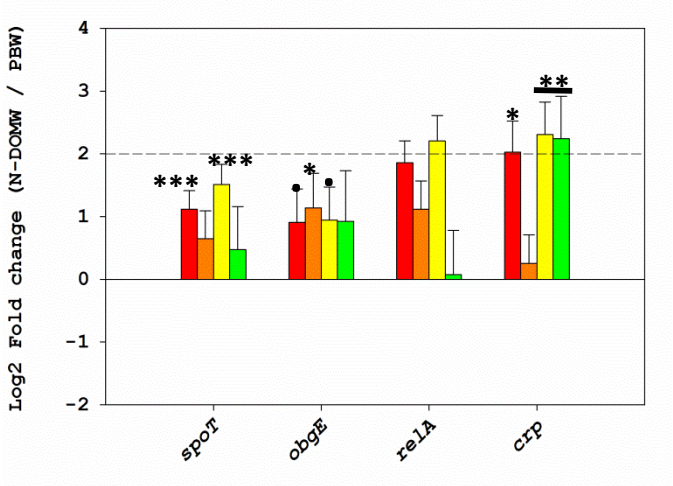
Log2 Fold change (N-DOMW / PBW)
4
3
2
1
0
-1
-2
***
***
*
*
**
spoT
obgE
relA
crp

G1

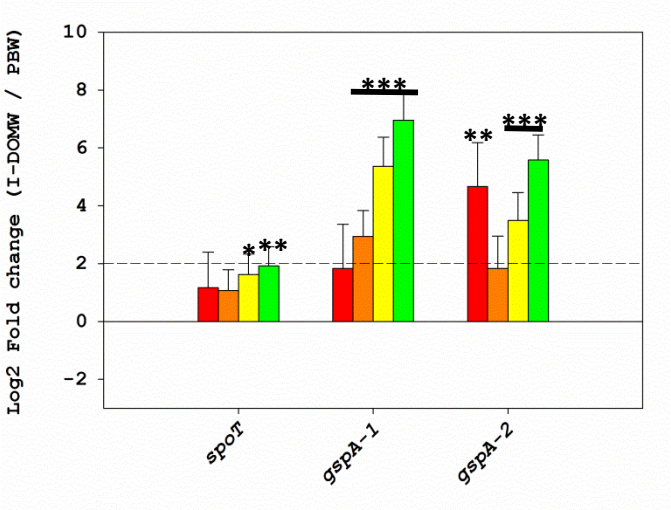

G2

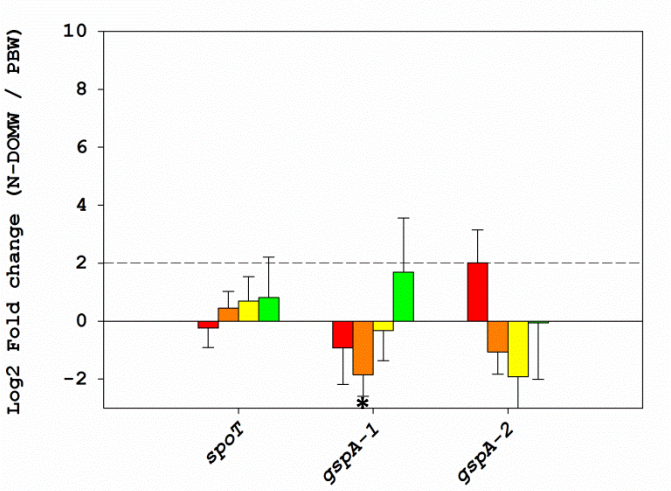

Figure 5.5: Toxin- antitoxin (TA) systems played an important role in regulating *E. coli* and *Ent. faecalis* populations. (A and B) Fold-change in selected type 2 TA genes for (A) *E. coli* and (B) *Ent. faecalis*in (1) I-DOMW and (2) N-DOMW compared to PBW. **(C and D)** Fold-change in known type 2 antitoxin proteases for (C) *E. coli* and (D) *Ent. faecalis*in (1) I-DOMW and (2) N-DOMW compared to PBW. (**E**) Fold-change in selected type 1 genes for *E. coli* in (1) I-DOMW and (2) N-DOMW compared to PBW **(F and G)** Fold-change in known TA regulatory proteins for (F) *E. coli* and (G) *Ent. faecalis*in (1) I-DOMW and (2) N-DOMW compared to PBW.
(**P* value ·<0.1· *<0.05, **<0.01, ***<0.001)

A

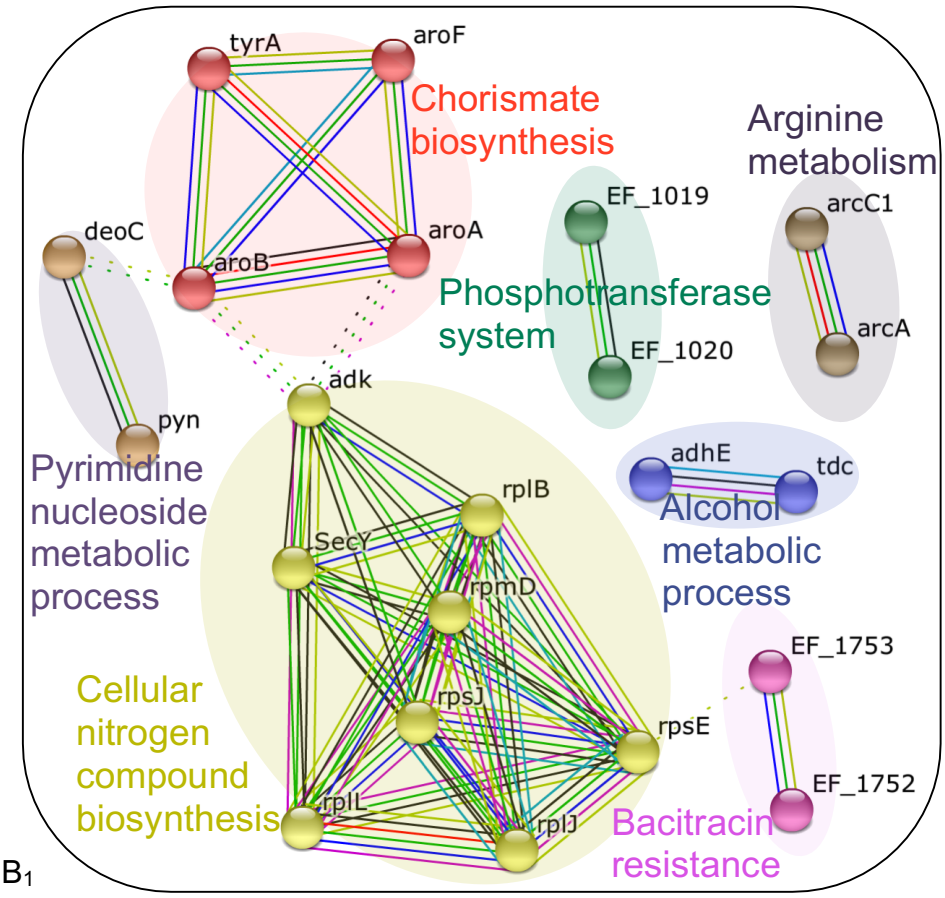
tyrA
aroF
Chorismate biosynthesis
Arginine metabolism
EF_1019
arcC1
deoC
aroA
aroB
Phosphotransferase system
arcA
EF_1020
adk
pyn
adhE
tdc
rplB
Pyrimidine nucleoside metabolic process
Alcohol metabolic process
SecY
rpmD
EF_1753
Cellular nitrogen compound biosynthesis
rpsJ
rpsE
EF_1752
rplL
rplJ
Bacitracin resistance

B1

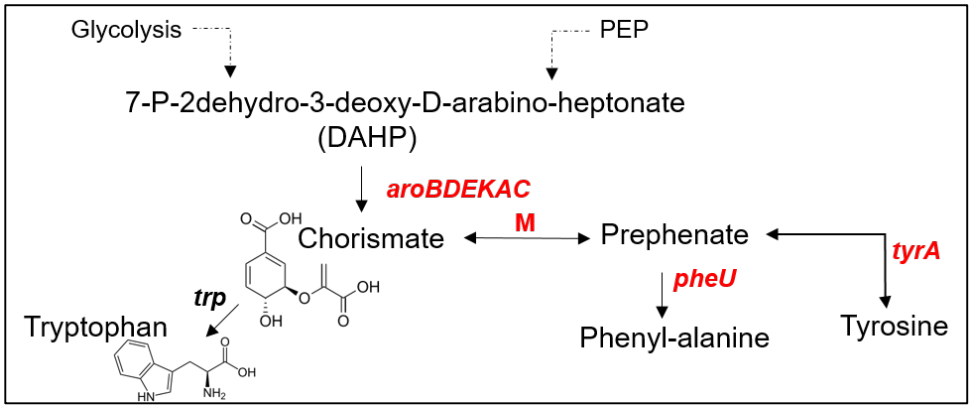
Glycolysis
PEP
7-P-2dehydro-3-deoxy-D-arabino-heptonate
(DAHP)
aroBDEKAC
Chorismate
M
Prephenate
tyrA
pheU
trp
Tryptophan
Phenyl-alanine
Tyrosine

B_2

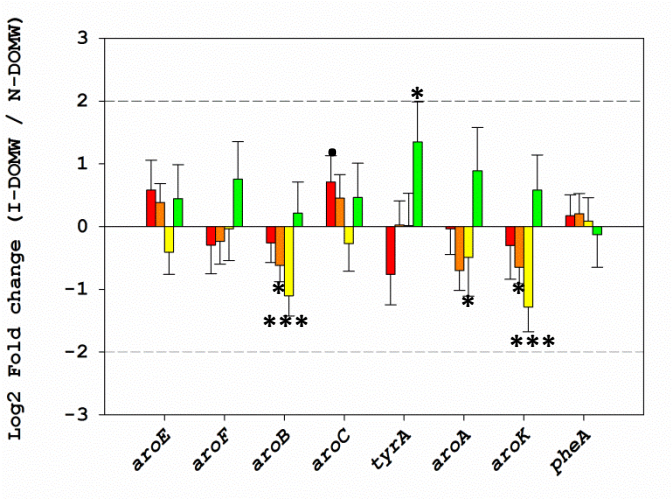
Log2 Fold change (I-DOMW / N-DOMW)
3
2
1
0
-1
-2
-3
*
*
***
*
*
*
***
aroE
aroF
aroB
aroC
tyrA
aroA
aroK
pheA

B_3

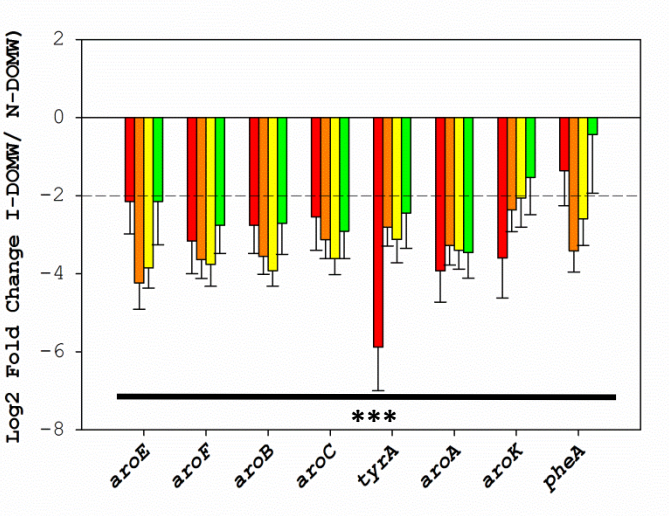
Log2 Fold Change I-DOMW/ N-DOMW)
2
0
-2
-4
-6
-8
***
aroE
aroF
aroB
aroC
tyrA
aroA
aroK
pheA

C_1

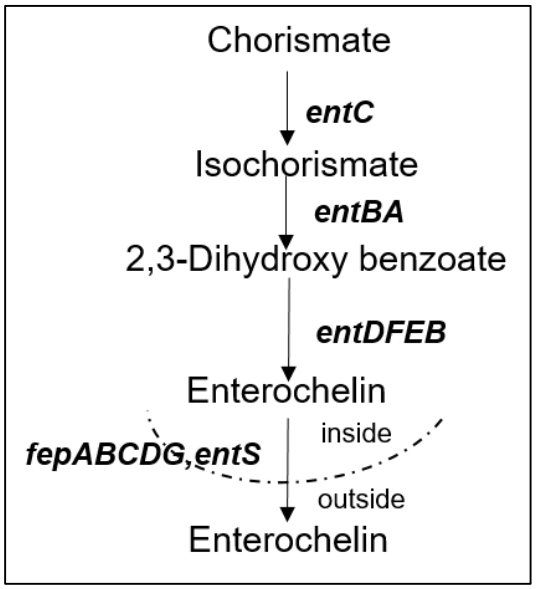
Chorismate
entC
Isochorismate
entBA
2,3-Dihydroxy benzoate
entDFEB
Enterochelin
fepABCDG,entS
inside
outside
Enterochelin

C_2

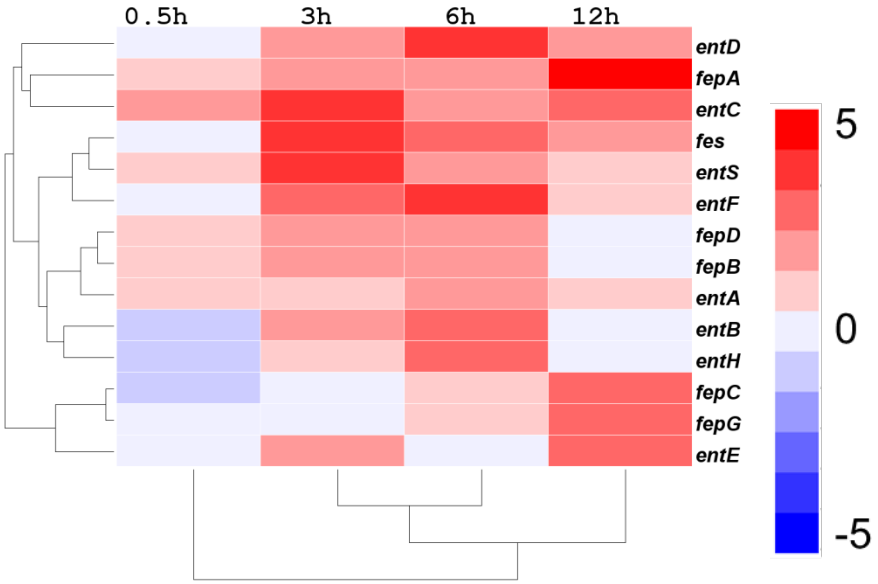
0.5h
3h
6h
12h
entD
fepA
entC
fes
entS
entF
fepD
fepB
entA
entB
entH
fepC
fepG
entE
5
0
-5

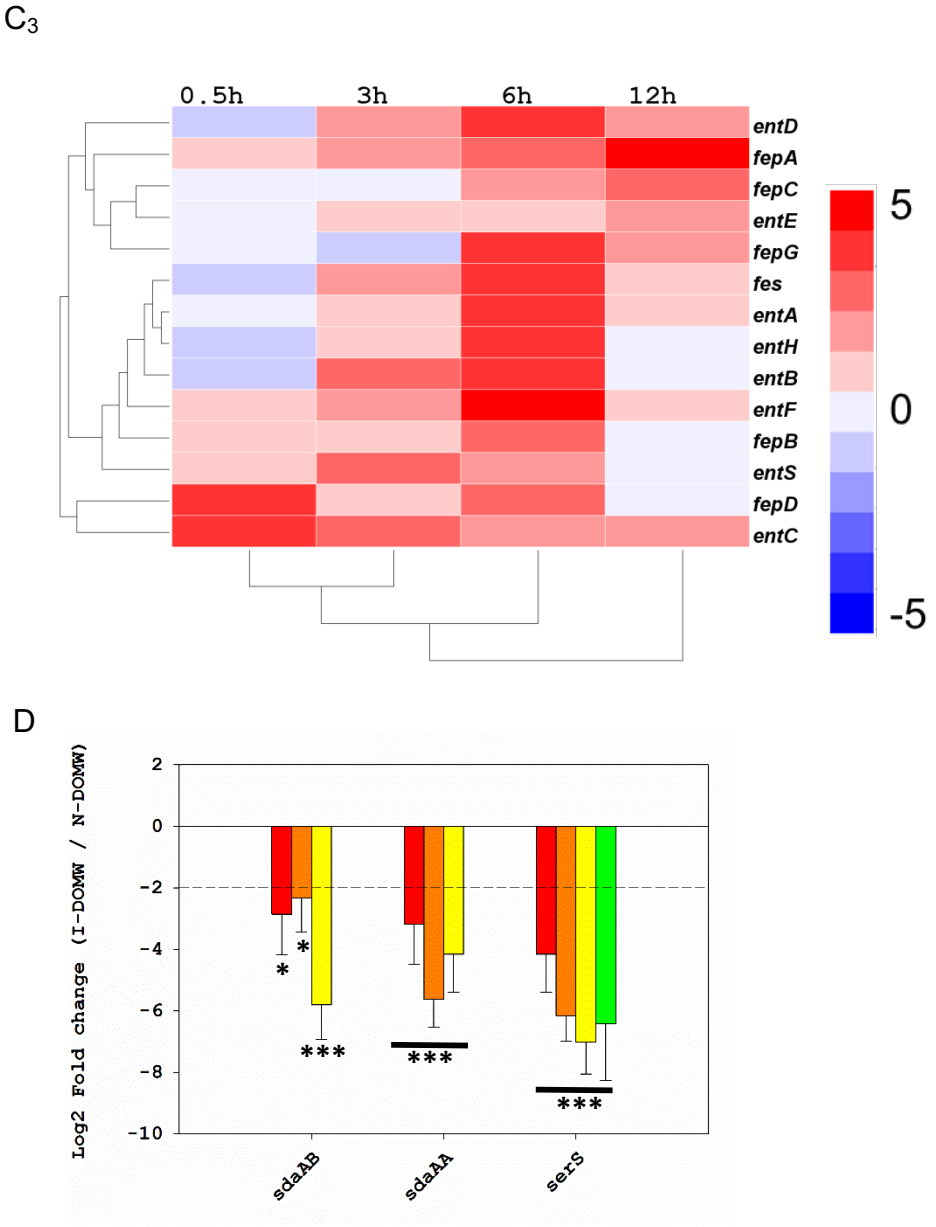

Figure 5.6: Chorismate is a public good used for the synthesis of secondary metabolites. (**A**) STRING analysis for significantly altered transcripts in NDOM-W compared to I-DOMW for *Ent. faecalis*at 0.5 h (Fold-change ≥ 2; *P*. padj < 0.01). (**B_{1-3}**) (1) Shikimate pathway (red font in gene names denotes the presence of similar pathway genes in both bacteria). Fold-change in pathway genes for (2) *E. coli* and (3) *Ent. faecalis*in I-DOMW compared to N-DOMW. (**C_{1-3}**) (1) Pathway for enterobactin biosynthesis via chorismate (2) Heatmap for enterobactin biosynthesis and transport genes in (1) I-DOMW and (2) N-DOMW compared to PBW. Color scale shows fold-change compared to PBW. **(D)** Fold-change in selected iron-sulfur dependent serine proteins for *Ent. faecalis*in I-DOMW compared to N-DOMW.
(**P* value ·<0.1· *<0.05, **<0.01, ***<0.001)

A

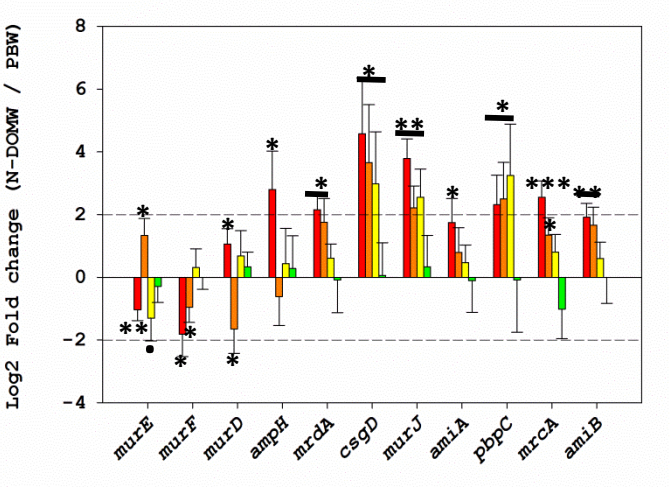
Log2 Fold change (N-DOMW / PBW)
8
6
4
2
0
-2
-4
murE
murF
murD
ampH
mrdA
csgD
murJ
amiA
pbpC
mrcA
amiB

B

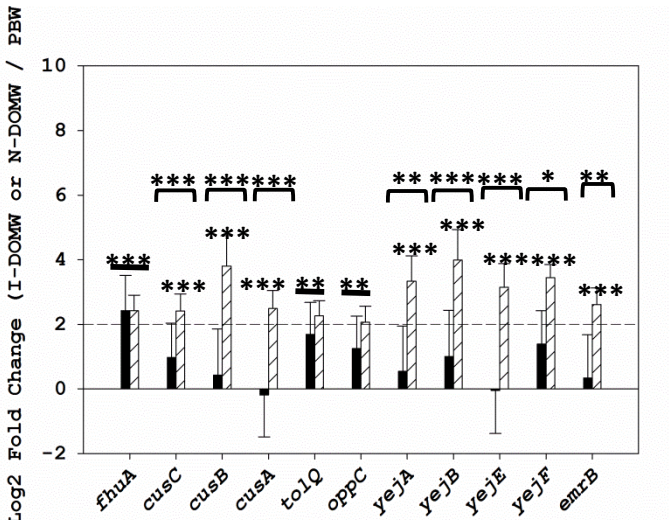
Log2 Fold Change (I-DOMW or N-DOMW / PBW
10
8
6
4
2
0
-2
fhuA
cusC
cusB
cusA
tolQ
oppC
yejA
yejB
yejE
yejF
emrB

C

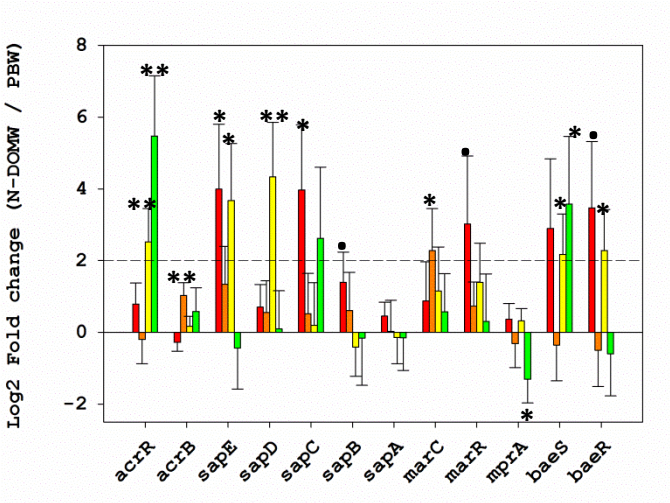
Log2 Fold change (N-DOMW / PBW)
8
6
4
2
0
-2
acrR
acrB
sapE
sapD
sapC
sapB
sapA
marC
marR
mprA
baeS
baeR

D

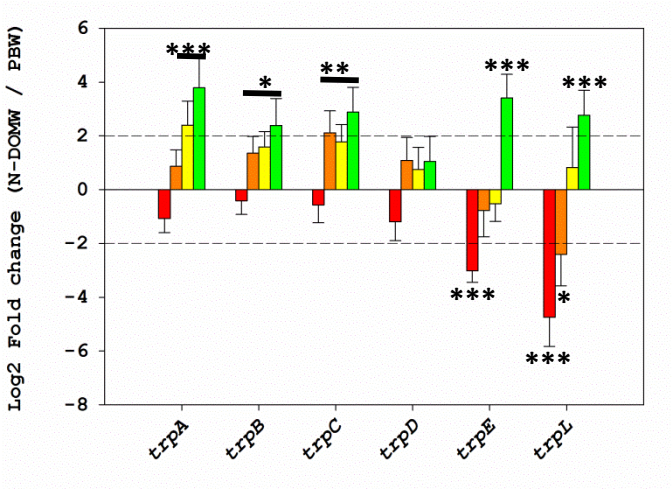
Log2 Fold change (N-DOMW / PBW)
6
4
2
0
-2
-4
-6
-8
***
*
**
***
***
***
*
***
trpA
trpB
trpC
trpD
trpE
trpL

E

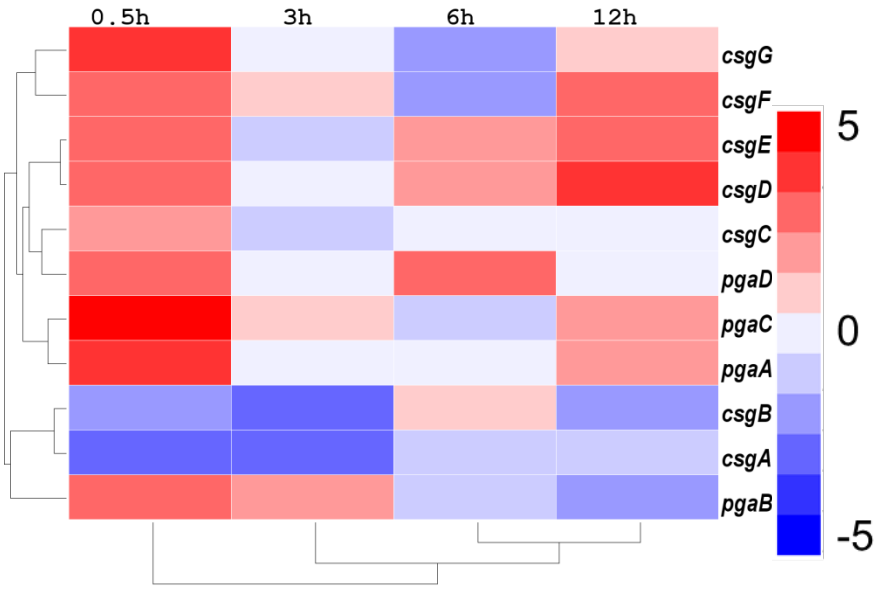
0.5h
3h
6h
12h
csgG
csgF
csgE
csgD
csgC
pgaD
pgaC
pgaA
csgB
csgA
pgaB
5
0
-5

F

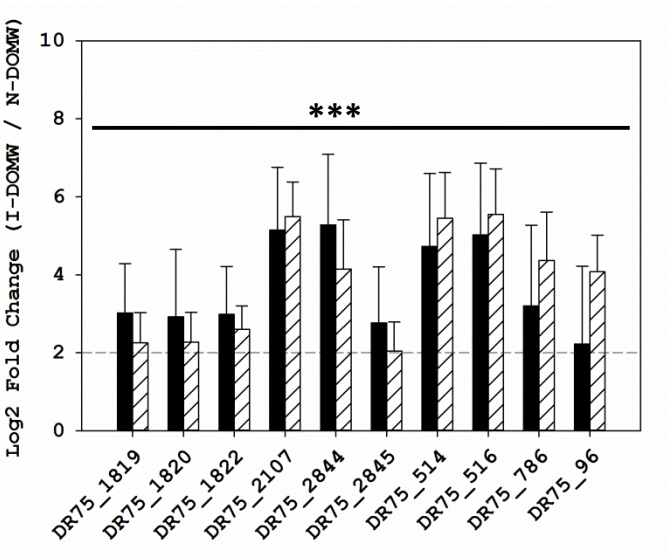

G

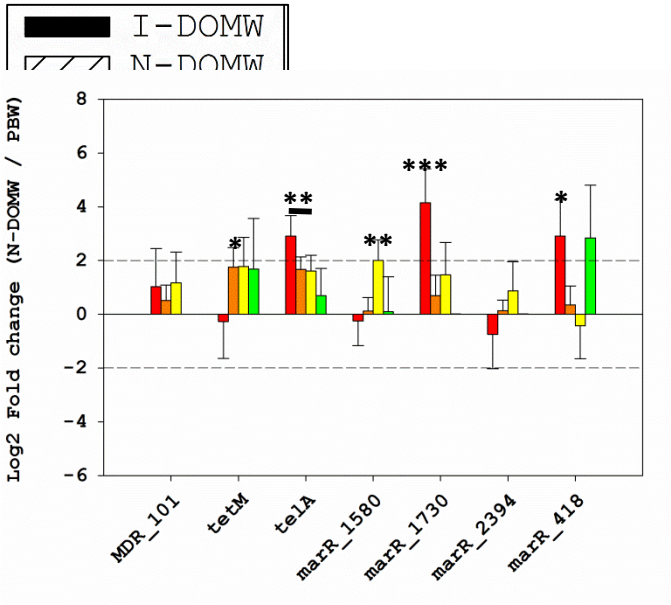

Figure 5.7: Adaptive response was a major survival mechanism employed by *E. coli* and *Ent. faecalis*. (A – C) Fold-change in selected transcripts for (A) Peptidoglycan/penicillin biosynthesis (B) Multidrug efflux pumps at 0.5 h and (C) Antimicrobial resistance/regulation for *E. coli* in I-DOMW and N-DOMW compared to PBW. (**D**) Fold-change in transcripts for tryptophan biosynthesis in I-DOMW compared to N-DOMW for *E. coli*. **(E)** Heatmap of selected genes required for biofilm formation in N-DOM compared to PBW for *E. coli*. Color scale shows fold-change compared to PBW. (**F and G)** Fold-change in selected transcripts for (F) Beta-lactam resistance/quorum sensing at 0.5 h

and (G) Antimicrobial resistance/regulation in I-DOMW and N-DOMW compared to PBW for *Ent. feacalis.*
(*P value .<0.1. *<0.05, **<0.01, ***<0.001; Brackets represent significant difference between I-DOMW and N-DOM)

A

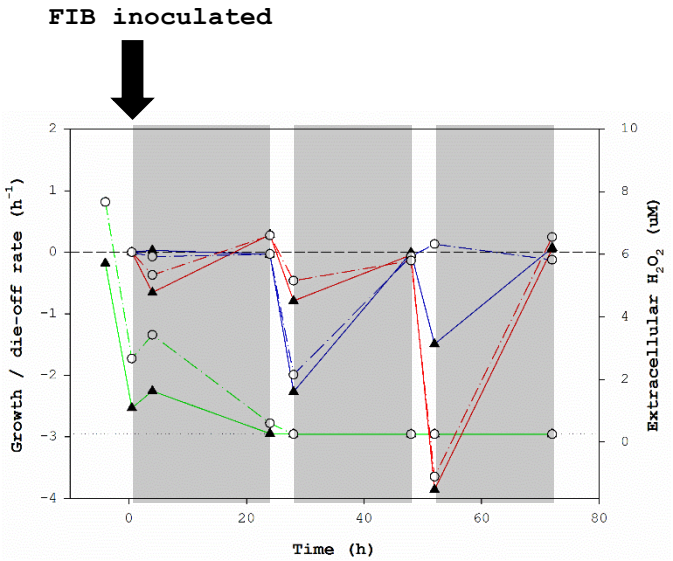
FIB inoculated
Growth / die-off rate (h^{-1})
Extracellular H_2O_2 (uM)
Time (h)

B

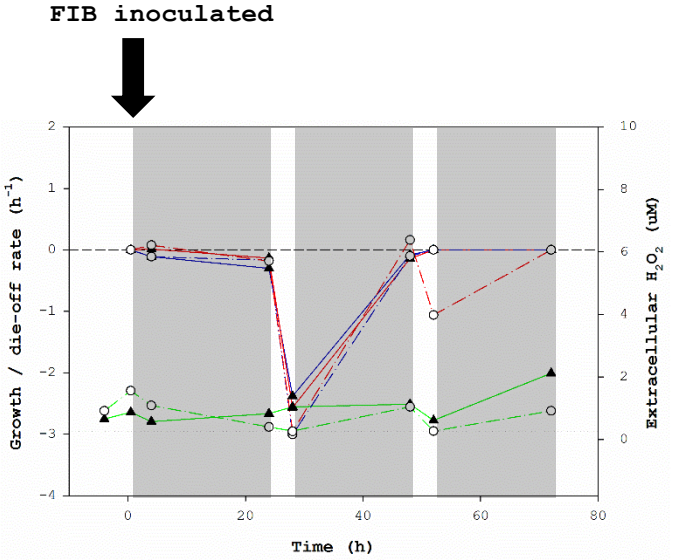
FIB inoculated
Growth / die-off rate (h^{-1})
Extracellular H_2O_2 (uM)
Time (h)

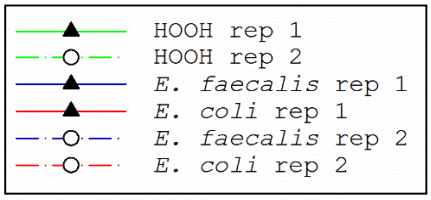
HOOH rep 1
HOOH rep 2
E. faecalis rep 1
E. coli rep 1
E. faecalis rep 2
E. coli rep 2

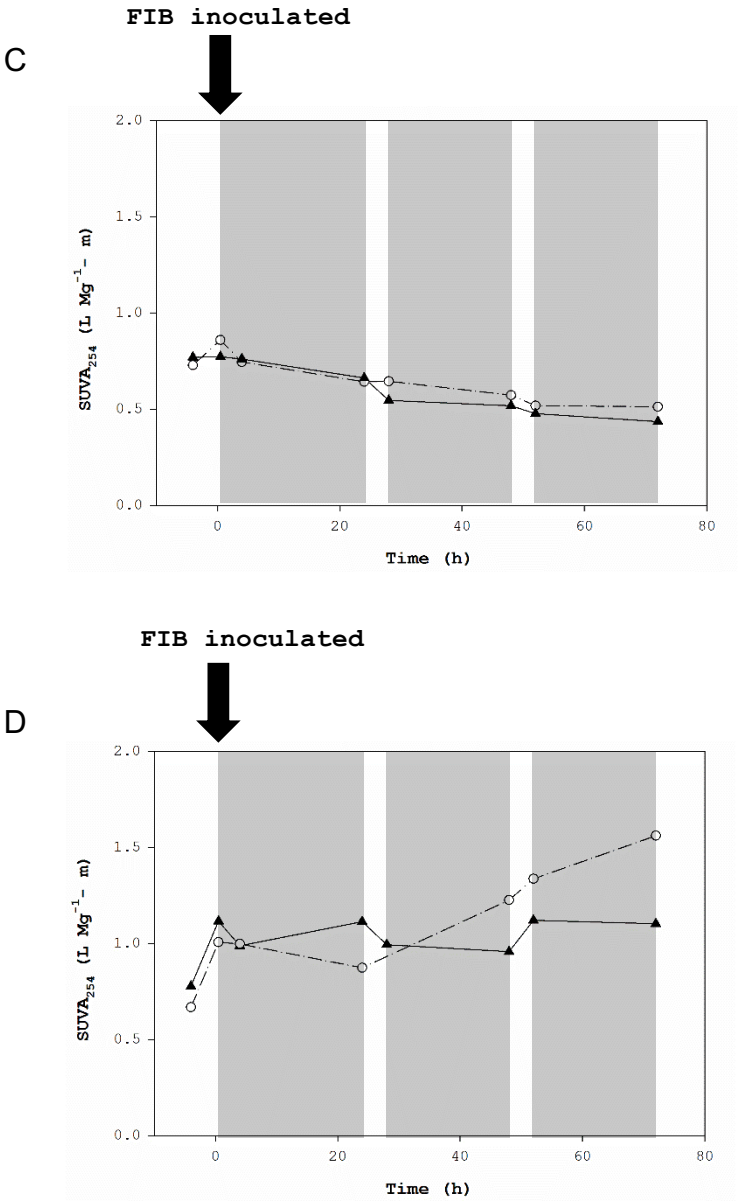

Figure 5.8. Removal of extracellular HOOH is critical for fecal bacteria to survive or re-grow. Outdoor mesocosm study was conducted to investigate the interacting effects of direct sunlight and DOM. Filter sterilized stream water was spiked with CFE and exposed to natural sunlight for 4 h to initiate HOOH production prior to *E. coli* and *Ent. faecalis*co-

culture inoculation in the dark Following inoculation, mesocosms were incubated in the dark for 20 h before the next cycle of sunlight exposure and dark incubation. (**A** and **B**) Water samples were collected 0.5, 4, 24, 28, 48, 52 and 72 h for bacteria concentration, extracellular HOOH, DOC, and UV-Vis measurement. Grey shaded rectangles represents when mesocosm was in the dark whereas white rectangles represents exposure to direct sunlight. Green solid or dashed lines represent extracellular HOOH concentration in (A) DOM spiked mesocosm (treatment) (B) Unspiked mesocosm (control) in the presence of both *E. coli* (red solid or dashed line) and *Ent. faecalis* (blue solid or dashed line). Dotted black line represents HOOH method detection limit of 250nM. Growth or die-off rates per time point per group are plotted on the y-axis (dark circles). (**C** and **D**) Specific Ultraviolet absorbance (SUVA) of DOM present post-irradiation, 0.5, 4, 24, 28, 48, 52 and 72 h was determined by dividing their absorption coefficient at 254nm by DOC concentration. (C) $SUVA_{254}$ (L Mg-C^{-1} m^{-1}) over time in treatment and (D) control.

Table 5.1: Gene set enrichment analysis on differentially expressed transcripts (*P*. value < 0.05) in N-DOMW compared to I-DOMW for *E. coli.*

0.5 h	3 h	6 h	12 h
Oxidative phosphorylation	Ribosome	Oxidative phosphorylation	Degradation of aromatic compounds
Flagellar assembly	Oxidative phosphorylation	Flagellar assembly	Phenylalanine metabolism
Homologous recombination	Metabolic pathways	Ribosome	Microbial metabolism in diverse environments
Nitrotoluene degradation	Biosynthesis of secondary metabolites	Bacterial chemotaxis	Fatty acid degradation
Alanine, aspartate and glutamate metabolism	Beta-Lactam resistance		Pyruvate metabolism
Nitrogen metabolism	Carbon metabolism		Starch and sucrose metabolism
Metabolic pathways	Citrate cycle (TCA cycle)		Beta-Alanine metabolism
	Pyrimidine metabolism		Geraniol degradation
	RNA polymerase		Butanoate metabolism
	Biosynthesis of amino acids		Metabolic pathways

Note: Only top 10 enriched KEGG pathways are reported (P. adj < 0.05)

REFERENCES

1. de Brauwere, A.; Ouattara, N. K.; Servais, P., Modeling fecal indicator bacteria concentrations in natural surface waters: a review. *Critical Reviews in Environmental Science and Technology* **2014,** *44*, (21), 2380-2453.

2. Harwood, V. J.; Staley, C.; Badgley, B. D.; Borges, K.; Korajkic, A., Microbial source tracking markers for detection of fecal contamination in environmental waters: relationships between pathogens and human health outcomes. *FEMS microbiology reviews* **2014,** *38*, (1), 1-40.

3. Oliver, D. M.; Bird, C.; Burd, E.; Wyman, M., Quantitative PCR profiling of E. coli in livestock faeces reveals increased population resilience relative to culturable counts under temperature extremes. *Environ Sci Technol* **2016**.

4. Sanders, E. C.; Yuan, Y. P.; Pitchford, A., Fecal Coliform and E. coli Concentrations in Effluent-Dominated Streams of the Upper Santa Cruz Watershed. *Water-Sui* **2013,** *5*, (1), 243-261.

5. Oladeinde, A.; Bohrmann, T.; Wong, K.; Purucker, S.; Bradshaw, K.; Brown, R.; Snyder, B.; Molina, M., Decay of Fecal Indicator Bacterial Populations and Bovine-Associated Source-Tracking Markers in Freshly Deposited Cow Pats. *Applied and environmental microbiology* **2014,** *80*, (1), 110-118.

6. Boehm, A. B.; Ashbolt, N. J.; Colford, J. M., Jr.; Dunbar, L. E.; Fleming, L. E.; Gold, M. A.; Hansel, J. A.; Hunter, P. R.; Ichida, A. M.; McGee, C. D.; Soller, J. A.; Weisberg, S. B., A sea change ahead for recreational water quality criteria. *J Water Health* **2009,** *7*, (1), 9-20.

7. Anesio, A. M.; Granéli, W.; Aiken, G. R.; Kieber, D. J.; Mopper, K., Effect of humic substance photodegradation on bacterial growth and respiration in lake water. *Applied and environmental microbiology* **2005,** *71*, (10), 6267-6275.

8. Meyer, J., The microbial loop in flowing waters. *Microbial Ecology* **1994,** *28*, (2), 195-199.

9. Mostofa, K. M.; Yoshioka, T.; Mottaleb, A.; Vione, D., *Photobiogeochemistry of organic matter: principles and practices in water environments*. Springer Science & Business Media: 2012.

10. Imlay, J. A., Transcription Factors That Defend Bacteria Against Reactive Oxygen Species. *Annual Review of Microbiology* **2015,** *69*, (1).

11. Oladeinde, A.; Lipp, E.; Chen, Y. C.; Molina, M., Photo-produced hydrogen peroxide controls fecal indicator bacteria and E. coli O157:H7 growth dynamics. In Manuscript submitted for publication, 2017.

12. Oladeinde, A.; Lipp, E.; Chen, Y. C.; Muirhead, R.; Glenn, T.; Molina, M., Regulation of hydrogen peroxide response in fecal indicator bacteria and E. coli O157:H7. In Manuscript submitted for publication, 2017.

13. Mostofa, K. M.; Liu, C.-q.; Sakugawa, H.; Vione, D.; Minakata, D.; Wu, F., Photoinduced and microbial generation of hydrogen peroxide and organic peroxides in natural waters. In *Photobiogeochemistry of Organic Matter*, Springer: 2013; pp 139-207.

14. Bizzini, A.; Zhao, C.; Budin-Verneuil, A.; Sauvageot, N.; Giard, J.-C.; Auffray, Y.; Hartke, A., Glycerol is metabolized in a complex and strain-dependent manner in Enterococcus faecalis. *Journal of bacteriology* **2010,** *192*, (3), 779-785.

15. Imlay, J. A., Cellular defenses against superoxide and hydrogen peroxide. *Annu Rev Biochem* **2008,** *77*, 755-76.

16. Adams, M. H., *Bacteriophages*. Interscience: London, United Kingdom, 1959.

17. Kosaka, K.; Yamada, H.; Matsui, S.; Echigo, S.; Shishida, K., Comparison among the methods for hydrogen peroxide measurements to evaluate advanced oxidation processes: application of a spectrophotometric method using copper (II) ion and 2, 9-dimethyl-1, 10-phenanthroline. *Environ Sci Technol* **1998,** *32*, (23), 3821-3824.

18. Glenn, T.; Nilsen, R.; Kieran, T., Adapterama I: Universal stubs and primers for thousands of dual-indexed Illumina libraries (iTru & iNext). bioRxiv, 049114. **2016**.

19. Li, H.; Durbin, R., Fast and accurate short read alignment with Burrows–Wheeler transform. *Bioinformatics* **2009,** *25*, (14), 1754-1760.

20. Li, H.; Handsaker, B.; Wysoker, A.; Fennell, T.; Ruan, J.; Homer, N.; Marth, G.; Abecasis, G.; Durbin, R., The sequence alignment/map format and SAMtools. *Bioinformatics* **2009,** *25*, (16), 2078-2079.

21. Quinlan, A. R.; Hall, I. M., BEDTools: a flexible suite of utilities for comparing genomic features. *Bioinformatics* **2010,** *26*, (6), 841-842.

22. Team, R. D. C. *R: A language and environment for statistical computing. R Foundation for Statistical Computing*, Vienna, Austria, 2012.

23. Love, M. I.; Huber, W.; Anders, S., Moderated estimation of fold change and dispersion for RNA-seq data with DESeq2. *Genome biology* **2014,** *15*, (12), 1.

24. Szklarczyk, D.; Franceschini, A.; Wyder, S.; Forslund, K.; Heller, D.; Huerta-Cepas, J.; Simonovic, M.; Roth, A.; Santos, A.; Tsafou, K. P., STRING v10: protein–protein interaction networks, integrated over the tree of life. *Nucleic acids research* **2014**, gku1003.

25. Van Dongen, S., Graph clustering via a discrete uncoupling process. *SIAM Journal on Matrix Analysis and Applications* **2008,** *30*, (1), 121-141.

26. Teng, Q.; Huang, W.; Collette, T. W.; Ekman, D. R.; Tan, C., A direct cell quenching method for cell-culture based metabolomics. *Metabolomics* **2009,** *5*, (2), 199-208.

27. Henderson, W. M.; Bouchard, D.; Chang, X.; Al-Abed, S. R.; Teng, Q., Biomarker analysis of liver cells exposed to surfactant-wrapped and oxidized multi-walled carbon nanotubes (MWCNTs). *Sci Total Environ* **2016,** *565*, 777-86.

28. Niu, W.; Knight, E.; Xia, Q.; McGarvey, B. D., Comparative evaluation of eight software programs for alignment of gas chromatography-mass spectrometry chromatograms in metabolomics experiments. *J Chromatogr A* **2014,** *1374*, 199-206.

29. Macedo, M.; Waterson, T. Profile Analysis. http://userwww.sfsu.edu/efc/classes/biol710/manova/profileanalysis.htm (December, 2016),

30. Deng, W.; Wang, Y.; Liu, Z.; Cheng, H.; Xue, Y., HemI: a toolkit for illustrating heatmaps. *PLoS One* **2014,** *9*, (11), e111988.

31. Kumar, S. R.; Imlay, J. A., How Escherichia coli tolerates profuse hydrogen peroxide formation by a catabolic pathway. *Journal of bacteriology* **2013,** *195*, (20), 4569-4579.

32. Brown, S.; Santa Maria Jr, J. P.; Walker, S., Wall teichoic acids of gram-positive bacteria. *Annual review of microbiology* **2013,** *67*.

33. Ramsey, M.; Hartke, A.; Huycke, M., The physiology and metabolism of enterococci. **2014**.

34. Borisov, V. B.; Forte, E.; Davletshin, A.; Mastronicola, D.; Sarti, P.; Giuffre, A., Cytochrome bd oxidase from Escherichia coli displays high catalase activity: an additional defense against oxidative stress. *FEBS Lett* **2013,** *587*, (14), 2214-8.

35. Korshunov, S.; Imlay, K. R.; Imlay, J. A., The cytochrome bd oxidase of Escherichia coli prevents respiratory inhibition by endogenous and exogenous hydrogen sulfide. *Mol Microbiol* **2016,** *101*, (1), 62-77.

36. Yan, X.; Budin-Verneuil, A.; Verneuil, N.; Gilmore, M. S.; Artigaud, S.; Auffray, Y.; Pichereau, V., Transcriptomic Response of Enterococcus faecalis V583 to Low Hydrogen Peroxide Levels. *Current microbiology* **2015,** *70*, (2), 156-168.

37. Liu, Y.; Imlay, J. A., Cell death from antibiotics without the involvement of reactive oxygen species. *Science* **2013,** *339*, (6124), 1210-3.

38. Di Martino, M. L.; Campilongo, R.; Casalino, M.; Micheli, G.; Colonna, B.; Prosseda, G., Polyamines: emerging players in bacteria-host interactions. *Int J Med Microbiol* **2013,** *303*, (8), 484-91.

39. Michael, A. J., Polyamines in Eukaryotes, Bacteria, and Archaea. *J Biol Chem* **2016,** *291*, (29), 14896-903.

40. Shah, P.; Swiatlo, E., A multifaceted role for polyamines in bacterial pathogens. *Mol Microbiol* **2008,** *68*, (1), 4-16.

41. Tkachenko, A. G.; Kashevarova, N. M.; Karavaeva, E. A.; Shumkov, M. S., Putrescine controls the formation of Escherichia coli persister cells tolerant to aminoglycoside netilmicin. *FEMS Microbiol Lett* **2014,** *361*, (1), 25-33.

42. Nesse, L. L.; Berg, K.; Vestby, L. K., Effects of norspermidine and spermidine on biofilm formation by potentially pathogenic Escherichia coli and Salmonella enterica wild-type strains. *Appl Environ Microbiol* **2015,** *81*, (6), 2226-32.

43. Llacer, J. L.; Polo, L. M.; Tavarez, S.; Alarcon, B.; Hilario, R.; Rubio, V., The gene cluster for agmatine catabolism of Enterococcus faecalis: study of recombinant putrescine

transcarbamylase and agmatine deiminase and a snapshot of agmatine deiminase catalyzing its reaction. *J Bacteriol* **2007,** *189*, (4), 1254-65.

44. Shah, P.; Nanduri, B.; Swiatlo, E.; Ma, Y.; Pendarvis, K., Polyamine biosynthesis and transport mechanisms are crucial for fitness and pathogenesis of Streptococcus pneumoniae. *Microbiology* **2011,** *157*, (Pt 2), 504-15.

45. Schneider, B. L.; Hernandez, V. J.; Reitzer, L., Putrescine catabolism is a metabolic response to several stresses in Escherichia coli. *Mol Microbiol* **2013,** *88*, (3), 537-50.

46. Barbagallo, M.; Di Martino, M. L.; Marcocci, L.; Pietrangeli, P.; De Carolis, E.; Casalino, M.; Colonna, B.; Prosseda, G., A new piece of the Shigella Pathogenicity puzzle: spermidine accumulation by silencing of the speG gene [corrected]. *PLoS One* **2011,** *6*, (11), e27226.

47. Joshi, G. S.; Spontak, J. S.; Klapper, D. G.; Richardson, A. R., Arginine catabolic mobile element encoded speG abrogates the unique hypersensitivity of Staphylococcus aureus to exogenous polyamines. *Mol Microbiol* **2011,** *82*, (1), 9-20.

48. Moreau, P. L., The lysine decarboxylase CadA protects Escherichia coli starved of phosphate against fermentation acids. *J Bacteriol* **2007,** *189*, (6), 2249-61.

49. Wargo, M. J., Homeostasis and catabolism of choline and glycine betaine: lessons from Pseudomonas aeruginosa. *Appl Environ Microbiol* **2013,** *79*, (7), 2112-20.

50. Metris, A.; George, S. M.; Mulholland, F.; Carter, A. T.; Baranyi, J., Metabolic shift of Escherichia coli under salt stress in the presence of glycine betaine. *Appl Environ Microbiol* **2014,** *80*, (15), 4745-56.

51. Pichereau, V.; Bourot, S.; Flahaut, S.; Blanco, C.; Auffray, Y.; Bernard, T., The osmoprotectant glycine betaine inhibits salt-induced cross-tolerance towards lethal treatment in Enterococcus faecalis. *Microbiology* **1999,** *145 (Pt 2)*, 427-35.

52. Samuelsson, L. M.; Bedford, J. J.; Smith, R. A.; Leader, J. P., A comparison of the counteracting effects of glycine betaine and TMAO on the activity of RNase A in aqueous urea solution. *Comp Biochem Physiol A Mol Integr Physiol* **2005,** *141*, (1), 22-8.

53. Lidbury, I.; Murrell, J. C.; Chen, Y., Trimethylamine N-oxide metabolism by abundant marine heterotrophic bacteria. *Proc Natl Acad Sci U S A* **2014,** *111*, (7), 2710-5.

54. Kiene, R. P., Uptake of choline and its conversion to glycine betaine by bacteria in estuarine waters. *Appl Environ Microbiol* **1998,** *64*, (3), 1045-51.

55. Kanehisa, M.; Furumichi, M.; Tanabe, M.; Sato, Y.; Morishima, K., KEGG: new perspectives on genomes, pathways, diseases and drugs. *Nucleic Acids Res* **2016**.

56. Wang, X.; Kim, Y.; Ma, Q.; Hong, S. H.; Pokusaeva, K.; Sturino, J. M.; Wood, T. K., Cryptic prophages help bacteria cope with adverse environments. *Nat Commun* **2010,** *1*, 147.

57. Feiner, R.; Argov, T.; Rabinovich, L.; Sigal, N.; Borovok, I.; Herskovits, A. A., A new perspective on lysogeny: prophages as active regulatory switches of bacteria. *Nat Rev Microbiol* **2015,** *13*, (10), 641-50.

58. Pfeifer, E.; Hunnefeld, M.; Popa, O.; Polen, T.; Kohlheyer, D.; Baumgart, M.; Frunzke, J., Silencing of cryptic prophages in Corynebacterium glutamicum. *Nucleic Acids Res* **2016,** *44*, (21), 10117-10131.

59. Zeng, Z.; Liu, X.; Yao, J.; Guo, Y.; Li, B.; Li, Y.; Jiao, N.; Wang, X., Cold adaptation regulated by cryptic prophage excision in Shewanella oneidensis. *ISME J* **2016,** *10*, (12), 2787-2800.

60. Casacuberta, E.; Gonzalez, J., The impact of transposable elements in environmental adaptation. *Mol Ecol* **2013,** *22*, (6), 1503-17.

61. San Millan, A.; Pena-Miller, R.; Toll-Riera, M.; Halbert, Z. V.; McLean, A. R.; Cooper, B. S.; MacLean, R. C., Positive selection and compensatory adaptation interact to stabilize non-transmissible plasmids. *Nat Commun* **2014,** *5*, 5208.

62. Swarts, D. C.; Mosterd, C.; van Passel, M. W.; Brouns, S. J., CRISPR interference directs strand specific spacer acquisition. *PLoS One* **2012,** *7*, (4), e35888.

63. Barrangou, R.; Fremaux, C.; Deveau, H.; Richards, M.; Boyaval, P.; Moineau, S.; Romero, D. A.; Horvath, P., CRISPR provides acquired resistance against viruses in prokaryotes. *Science* **2007,** *315*, (5819), 1709-12.

64. Severinov, K., CRISPR-Cas: outstanding questions remain: comment on "Diversity, evolution, and therapeutic applications of small RNAs in prokaryotic and eukaryotic immune systems" by Edwin L. Cooper and Nicola Overstreet. *Phys Life Rev* **2014,** *11*, (1), 146-8; discussion 149-51.

65. Navarre, W. W.; McClelland, M.; Libby, S. J.; Fang, F. C., Silencing of xenogeneic DNA by H-NS-facilitation of lateral gene transfer in bacteria by a defense system that recognizes foreign DNA. *Genes Dev* **2007,** *21*, (12), 1456-71.

66. Ali, S. S.; Whitney, J. C.; Stevenson, J.; Robinson, H.; Howell, P. L.; Navarre, W. W., Structural insights into the regulation of foreign genes in Salmonella by the Hha/H-NS complex. *Journal of Biological Chemistry* **2013,** *288*, (19), 13356-13369.

67. Dmowski, M.; Jagura-Burdzy, G., Active stable maintenance functions in low copy-number plasmids of Gram-positive bacteria II. Post-segregational killing systems. *Pol J Microbiol* **2013,** *62*, (1), 17-22.

68. Gilmore, M. S.; Segarra, R. A.; Booth, M. C.; Bogie, C. P.; Hall, L. R.; Clewell, D. B., Genetic structure of the Enterococcus faecalis plasmid pAD1-encoded cytolytic toxin system and its relationship to lantibiotic determinants. *J Bacteriol* **1994,** *176*, (23), 7335-44.

69. Clewell, D. B., Properties of Enterococcus faecalis plasmid pAD1, a member of a widely disseminated family of pheromone-responding, conjugative, virulence elements encoding cytolysin. *Plasmid* **2007,** *58*, (3), 205-27.

70. Minogue, T. D.; Daligault, H. E.; Davenport, K. W.; Broomall, S. M.; Bruce, D. C.; Chain, P. S.; Coyne, S. R.; Chertkov, O.; Freitas, T.; Gibbons, H. S.; Jaissle, J.; Koroleva, G. I.; Ladner, J. T.; Palacios, G. F.; Rosenzweig, C. N.; Xu, Y.; Johnson, S. L., Complete Genome Assembly of Enterococcus faecalis 29212, a Laboratory Reference Strain. *Genome Announc* **2014,** *2*, (5).

71. Perez, R. H.; Zendo, T.; Sonomoto, K., Novel bacteriocins from lactic acid bacteria (LAB): various structures and applications. *Microb Cell Fact* **2014,** *13 Suppl 1*, S3.

72. Bali, V.; Panesar, P. S.; Bera, M. B.; Kennedy, J. F., Bacteriocins: Recent Trends and Potential Applications. *Crit Rev Food Sci Nutr* **2016,** *56*, (5), 817-34.

73. Hendrickx, A. P.; Willems, R. J.; Bonten, M. J.; van Schaik, W., LPxTG surface proteins of enterococci. *Trends Microbiol* **2009,** *17*, (9), 423-30.

74. Peng, C.; Tao, X.; Wenhong, Z.; Ying, Z., Molecular mechanisms of bacterial persistence and phenotypic antibiotic resistance. *Yi Chuan* **2016,** *38*, (10), 859-871.

75. Daimon, Y.; Narita, S.; Akiyama, Y., Activation of Toxin-Antitoxin System Toxins Suppresses Lethality Caused by the Loss of sigmaE in Escherichia coli. *J Bacteriol* **2015,** *197*, (14), 2316-24.

76. Gerdes, K., Hypothesis: type I toxin-antitoxin genes enter the persistence field-a feedback mechanism explaining membrane homoeostasis. *Philos Trans R Soc Lond B Biol Sci* **2016,** *371*, (1707).

77. Lobato-Marquez, D.; Diaz-Orejas, R.; Garcia-Del Portillo, F., Toxin-antitoxins and bacterial virulence. *FEMS Microbiol Rev* **2016,** *40*, (5), 592-609.

78. Page, R.; Peti, W., Toxin-antitoxin systems in bacterial growth arrest and persistence. *Nat Chem Biol* **2016,** *12*, (4), 208-14.

79. Yamaguchi, Y.; Park, J. H.; Inouye, M., Toxin-antitoxin systems in bacteria and archaea. *Annu Rev Genet* **2011,** *45*, 61-79.

80. Djorić, D.; Kristich, C. J., Oxidative stress enhances cephalosporin resistance of Enterococcus faecalis through activation of a two-component signaling system. *Antimicrobial agents and chemotherapy* **2015,** *59*, (1), 159-169.

81. Fernández, L.; Hancock, R. E., Adaptive and mutational resistance: role of porins and efflux pumps in drug resistance. *Clinical microbiology reviews* **2012,** *25*, (4), 661-681.

82. Motta, S. S.; Cluzel, P.; Aldana, M., Adaptive resistance in bacteria requires epigenetic inheritance, genetic noise, and cost of efflux pumps. *PLoS One* **2015,** *10*, (3), e0118464.

83. Blair, J. M.; Webber, M. A.; Baylay, A. J.; Ogbolu, D. O.; Piddock, L. J., Molecular mechanisms of antibiotic resistance. *Nat Rev Microbiol* **2015,** *13*, (1), 42-51.

84. Kleinkauf, H.; van Liempt, H.; Palissa, H.; von Dohren, H., [Biosynthesis of peptides: a non-ribosomal system]. *Naturwissenschaften* **1992,** *79*, (4), 153-62.

85. Wang, H.; Fewer, D. P.; Holm, L.; Rouhiainen, L.; Sivonen, K., Atlas of nonribosomal peptide and polyketide biosynthetic pathways reveals common occurrence of nonmodular enzymes. *Proc Natl Acad Sci U S A* **2014,** *111*, (25), 9259-64.

86. Strieker, M.; Tanovic, A.; Marahiel, M. A., Nonribosomal peptide synthetases: structures and dynamics. *Curr Opin Struct Biol* **2010,** *20*, (2), 234-40.

87. Reimer, J. M.; Aloise, M. N.; Harrison, P. M.; Schmeing, T. M., Synthetic cycle of the initiation module of a formylating nonribosomal peptide synthetase. *Nature* **2016,** *529*, (7585), 239-42.

88. Caboche, S.; Pupin, M.; Leclere, V.; Fontaine, A.; Jacques, P.; Kucherov, G., NORINE: a database of nonribosomal peptides. *Nucleic Acids Res* **2008,** *36*, (Database issue), D326-31.

89. Kawakami, M.; Nagai, Y.; Fujii, T.; Mitsuhashi, S., Anti-microbial activities of enduracidin (enramycin) in vitro and in vivo. *J Antibiot (Tokyo)* **1971,** *24*, (9), 583-6.

90. Walsh, C. T.; Liu, J.; Rusnak, F.; Sakaitani, M., Molecular studies on enzymes in chorismate metabolism and the enterobactin biosynthetic pathway. *Chemical Reviews* **1990,** *90*, (7), 1105-1129.

91. Raymond, K. N.; Dertz, E. A.; Kim, S. S., Enterobactin: an archetype for microbial iron transport. *Proc Natl Acad Sci U S A* **2003,** *100*, (7), 3584-8.

92. Scholz, R. L.; Greenberg, E. P., Sociality in Escherichia coli: Enterochelin Is a Private Good at Low Cell Density and Can Be Shared at High Cell Density. *J Bacteriol* **2015,** *197*, (13), 2122-8.

93. Vasse, M.; Noble, R. J.; Akhmetzhanov, A. R.; Torres-Barcelo, C.; Gurney, J.; Benateau, S.; Gougat-Barbera, C.; Kaltz, O.; Hochberg, M. E., Antibiotic stress selects against cooperation in the pathogenic bacterium Pseudomonas aeruginosa. *Proc Natl Acad Sci U S A* **2017,** *114*, (3), 546-551.

94. Molina, C. A.; Vilchez, S., Cooperation and bacterial pathogenicity: an approach to social evolution. *Revista chilena de historia natural* **2014,** *87*, (1), 1.

95. Ghoul, M.; Mitri, S., The Ecology and Evolution of Microbial Competition. *Trends in microbiology* **2016,** *24*, (10), 833-845.

96. Mitri, S.; Richard Foster, K., The genotypic view of social interactions in microbial communities. *Annual Review of Genetics* **2013,** *47*, 247-273.

97. Shan, Y.; Lazinski, D.; Rowe, S.; Camilli, A.; Lewis, K., Genetic basis of persister tolerance to aminoglycosides in Escherichia coli. *MBio* **2015,** *6*, (2).

98. Duan, X.; Huang, X.; Wang, X.; Yan, S.; Guo, S.; Abdalla, A. E.; Huang, C.; Xie, J., l-Serine potentiates fluoroquinolone activity against Escherichia coli by enhancing endogenous reactive oxygen species production. *J Antimicrob Chemother* **2016,** *71*, (8), 2192-9.

99. Velayudhan, J.; Jones, M. A.; Barrow, P. A.; Kelly, D. J., L-serine catabolism via an oxygen-labile L-serine dehydratase is essential for colonization of the avian gut by Campylobacter jejuni. *Infect Immun* **2004,** *72*, (1), 260-8.

100. Neilands, J. B., Siderophores: structure and function of microbial iron transport compounds. *J Biol Chem* **1995,** *270*, (45), 26723-6.

101. Suzuki, S.; Horinouchi, T.; Furusawa, C., Prediction of antibiotic resistance by gene expression profiles. *Nature communications* **2014,** *5*.

102. Wang, Z.; Bie, P.; Cheng, J.; Lu, L.; Cui, B.; Wu, Q., The ABC transporter YejABEF is required for resistance to antimicrobial peptides and the virulence of Brucella melitensis. *Sci Rep* **2016,** *6*, 31876.

103. Sugiyama, Y.; Nakamura, A.; Matsumoto, M.; Kanbe, A.; Sakanaka, M.; Higashi, K.; Igarashi, K.; Katayama, T.; Suzuki, H.; Kurihara, S., A Novel Putrescine Exporter SapBCDF of Escherichia coli. *J Biol Chem* **2016,** *291*, (51), 26343-26351.

104. Normark, S.; Ericson, C.; Jonsson, A.; Olsen, A., Global Regulatory Control of Curli Expression and Fibronectin Binding in Enterobacteria. In *Microbial Adhesion and Invasion*, Springer: 1992; pp 95-99.

105. Boles, B. R.; Singh, P. K., Endogenous oxidative stress produces diversity and adaptability in biofilm communities. *Proc Natl Acad Sci U S A* **2008,** *105*, (34), 12503-8.

106. Fink, R. C.; Black, E. P.; Hou, Z.; Sugawara, M.; Sadowsky, M. J.; Diez-Gonzalez, F., Transcriptional responses of Escherichia coli K-12 and O157: H7 associated with lettuce leaves. *Applied and environmental microbiology* **2012,** *78*, (6), 1752-1764.

107. Geier, H.; Mostowy, S.; Cangelosi, G. A.; Behr, M. A.; Ford, T. E., Autoinducer-2 triggers the oxidative stress response in Mycobacterium avium, leading to biofilm formation. *Applied and Environmental Microbiology* **2008,** *74*, (6), 1798-1804.

108. Lister, J. L.; Horswill, A. R., Staphylococcus aureus biofilms: recent developments in biofilm dispersal. *Front Cell Infect Microbiol* **2014,** *4*, 178.

109. Sharma-Kuinkel, B. K.; Mann, E. E.; Ahn, J. S.; Kuechenmeister, L. J.; Dunman, P. M.; Bayles, K. W., The Staphylococcus aureus LytSR two-component regulatory system affects biofilm formation. *J Bacteriol* **2009,** *191*, (15), 4767-75.

110. Hu, M.; Zhang, C.; Mu, Y.; Shen, Q.; Feng, Y., Indole affects biofilm formation in bacteria. *Indian J Microbiol* **2010,** *50*, (4), 362-8.

111. Kuczynska-Wisnik, D.; Matuszewska, E.; Furmanek-Blaszk, B.; Leszczynska, D.; Grudowska, A.; Szczepaniak, P.; Laskowska, E., Antibiotics promoting oxidative stress inhibit formation of Escherichia coli biofilm via indole signalling. *Research in Microbiology* **2010,** *161*, (10), 847-853.

112. Overballe-Petersen, S.; Harms, K.; Orlando, L. A.; Mayar, J. V.; Rasmussen, S.; Dahl, T. W.; Rosing, M. T.; Poole, A. M.; Sicheritz-Ponten, T.; Brunak, S.; Inselmann, S.; de Vries, J.; Wackernagel, W.; Pybus, O. G.; Nielsen, R.; Johnsen, P. J.; Nielsen, K. M.; Willerslev, E., Bacterial natural transformation by highly fragmented and damaged DNA. *Proc Natl Acad Sci U S A* **2013,** *110*, (49), 19860-5.

113. Putnam, C. D., Evolution of the methyl directed mismatch repair system in Escherichia coli. *DNA Repair (Amst)* **2016,** *38*, 32-41.

114. Lenhart, J. S.; Pillon, M. C.; Guarne, A.; Biteen, J. S.; Simmons, L. A., Mismatch repair in Gram-positive bacteria. *Res Microbiol* **2016,** *167*, (1), 4-12.

115. Hansen, A. M.; Kraus, T. E.; Pellerin, B. A.; Fleck, J. A.; Downing, B. D.; Bergamaschi, B. A., Optical properties of dissolved organic matter (DOM): Effects of biological and photolytic degradation. *Limnology and Oceanography* **2016,** *61*, (3), 1015-1032.

116. La Carbona, S.; Sauvageot, N.; Giard, J. C.; Benachour, A.; Posteraro, B.; Auffray, Y.; Sanguinetti, M.; Hartke, A., Comparative study of the physiological roles of three peroxidases (NADH peroxidase, Alkyl hydroperoxide reductase and Thiol peroxidase) in oxidative stress response, survival inside macrophages and virulence of Enterococcus faecalis. *Molecular microbiology* **2007,** *66*, (5), 1148-1163.

117. Morris, J. J., Black Queen evolution: the role of leakiness in structuring microbial communities. *Trends Genet* **2015,** *31*, (8), 475-82.

118. Morris, J. J.; Lenski, R. E.; Zinser, E. R., The Black Queen Hypothesis: evolution of dependencies through adaptive gene loss. *MBio* **2012,** *3*, (2).

119. Crabtree, J.; Agrawal, S.; Mahurkar, A.; Myers, G. S.; Rasko, D. A.; White, O., Circleator: flexible circular visualization of genome-associated data with BioPerl and SVG. *Bioinformatics* **2014,** *30*, (21), 3125-7.

Supplementary Materials for Chapter 5

Hydrogen peroxide triggers competition dynamics between *Escherichia coli* and *Enterococcus faecalis* bacterial populations

Contains:

Supplementary Material and Methods

Supplementary Results and Discussion

Supplementary Figures 5. S1-S22

Tables 5. S1-S3

Materials and methods

Indoor Microcosm

Cattle Fecal Extract Preparation. Fresh fecal samples were collected from 5 individual cows from a commercial farm in northeast Georgia on July 13, 2013. Approximately 100g of feces from each cowpat were composited and homogenized by hand. Composited cowpats were saved at -20^{o}C and served as the source of DOM throughout our study. A 1:10 fecal slurry was made in 0.85% KCl, and mixed for 1 h in a multi-wrist shaker model 3589 (Labline Scientific Instruments, Mumbai, India). The resulting fecal slurry was then centrifuged twice at 4000 x g for 10 min and the resulting supernatant was saved and referred to as cattle fecal extract (CFE). CFE was sequentially filtered through polycarbonate membrane filters with pore sizes of 1.2 µm, 0.45 µm and 0.2 µm, and a diameter of 47mm. Filtered CFE was then spiked into autoclaved phosphate buffered water (PBW) to concentrations mimicking nutrient inputs from direct fecal deposition into streams using a value of 32.48±1.52 mg L^{-1} as a proxy. The absence of bacteria and lytic phages in CFE was confirmed by culturing 100 µl of CFE in Brain Heart Infusion (BHI) broth and conducting a double agar overlay assay [14], respectively. For the overlay assay, bacteria strains used in the present study were used as phage hosts. Thereafter, CFE spiked water was divided into two volumes with one receiving solar radiation (Irradiated Spiked Water (I-DOMW)) and the other as a dark control (Non-irradiated Spiked Water (N-DOMW)).

Inoculum Preparation. Overnight cultures of *E. coli* C3000 (American Type Culture Collection (ATCC) 15597; hereafter referred to as *E. coli*) and *Enterococcus faecalis* (ATCC 29212; hereafter referred to as *Ent. faecalis* were grown for 1.5 h to mid-logarithm

phase (OD_{600} of 0.1) in BHI broth. Each culture was centrifuged at 4000 x g for 5 min and washed twice in PBW. Thereafter, serial dilutions were made to the desired concentrations.

Solar irradiation and co-culture inoculation. The experimental design used has been described previously (Oladeinde et al., 2016 a and b). Solar irradiations were performed in an Atlas SunTest CPS/CPS+ solar simulator (Atlas Materials Testing Technology, Chicago, IL) equipped with a 1 kW xenon arc lamp. Samples were irradiated using a 1 L jacketed Pyrex beaker (Ace glass, Vineland, NJ). Following irradiation, bacteria were individually inoculated into I-DOMW, N-DOMW and PBW for a final concentration of ~10^4 CFU mL^{-1} for each bacterium (Fig. 5S1). Fifty milliliters of each treatment were dispensed into sterile 250 ml Erlenmeyer flasks and incubated at 25^oC in an incubator shaker at 150 rpm (Innova 4230, New Brunswick Scientific, Edison, NJ). Samples were randomly selected at 0.5, 3, 6 and 12 h for microbiological analysis, measurement of extracellular HOOH, RNA-Sequencing, and metabolomics (see supplemental information).

Microbiological Analysis. One ml samples were serially diluted in PBW in duplicate and quantified on selective media by membrane filtration. *E. coli* and *Ent. faecalis* were quantified by culture methods using modified mTEC agar (EPA method 1603) and mEI agar (EPA method 1600), respectively.

Extracellular HOOH measurement. HOOH concentration before and after bacterial inoculation was quantified using the copper-DMP spectrophotometric method [15]. HOOH reduces copper (II) ions to copper (I) ions in the presence of excess 2, 9- diemethyl-1, 10-phenanthroline (DMP). The copper (I) forms a bright yellow cationic complex with DMP at a maximum absorbance of 454 nm. Samples were filter sterilized using 0.22 µm PVDF membrane syringe filter to get remove bacteria prior to measuring HOOH. Absorbance

readings in I-DOMW and N-DOMW were normalized against N-DOMW controls (no bacteria inoculation). A calibration curve was constructed by plotting concentration of known ACS grade H_2O_2 (Sigma Aldrich Corp. MO, USA) solution versus the absorbance at 454 nm of the product formed by the reaction of the solutions with copper sulfate and DMP. Absorbance at 454nm was read on a Nanodrop ND 1000 Spectrophotometer (Thermo Fisher Scientific, MA, USA). Two separate calibration curves were used throughout the experiment.

RNA isolation. Forty-five milliliters of co-culture samples were filtered through 0.45 µm pore size isopore membranes (EMD Millipore, Billerica, MA). Filters were folded inwards and saved in a lysing matrix B tube (MP Biomedical, Solon, OH). Tubes were kept at -80^{o}C for 2 weeks prior to total RNA extraction. RNA extraction was performed on two biological replicates with the FastRNA Pro Blue kit for microbes (MP Biomedical, Solon, OH) per the manufacturer's instructions, except that the bead-beating step was repeated twice at 6.5 m s^{-1} for 60 s. Following extraction, ethyl alcohol precipitation of RNA at -80^{o}C was carried out overnight for 18-24 h. Total RNA was resuspended in 50 µL DEPC treated water and concentrated using a vacufuge (Eppendorf, NY, USA) with no heat treatment for 1 h. RNA pellet was rehydrated with 20 µl DEPC treated water and treated with 4U DNA-free DNase (Life Technologies, Grand Island, NY) to remove genomic DNA contamination. Recovered RNA was quantified with a Nanodrop ND 1000 spectrophotometer (Thermo Fisher Scientific, MA, USA), examined for quality on an Agilent Bioanalyzer, and stored at -80^{o}C until used for RNA-seq.

mRNA enrichment. Twenty microliters of DNase treated RNA was pelleted as described earlier and reconstituted in 15 µl 1 X TE buffer. Bacterial 16S and 23S ribosomal RNA removal was completed using MICROBExpress Bacterial mRNA Enrichment Kit (Life

Technologies, Grand Island, NY) per manufacturer's instruction but with half of the suggested reaction volumes. The recovered mRNA was quantified using Nanodrop ND 1000 spectrophotometer (Thermo Scientific, Waltham, MA).

cDNA library preparation. cDNA synthesis was performed on enriched mRNA using the KAPA stranded RNA-seq library preparation kit (Kapa Biosystems, Inc. MA, USA) with a few modifications. Half the suggested reaction volumes were used throughout. RNA fragmentation was completed in a thermocycler at 87.5^{o}C for 6 min. Adapterama I adapters and primers [16] were used for ligation and PCR amplification reactions at a final reaction concentration of 357 nM and 250 nM, respectively. For PCR amplification, iTru5 forward and iTru7 reverse primers with unique indexes for sample multiplexing were employed [16]. The concentrations of amplicons from different samples were quantified using a Qubit dsDNA HS Assay Kit (Thermo Fisher Scientific, MA, USA). The libraries were pooled in equimolar concentrations and sequenced at Oklahoma Medical Research Foundation. A 150 bp paired-end sequencing reaction was performed on a HiSeq 3000 platform (Illumina, San Diego, CA, USA). Sequenced libraries were demultiplexed with bcl2fastq v2.17 (Illumina, San Diego, CA, USA). Reads will be submitted to NCBI SRA database.

Bioinformatics analysis. Forward and reverse barcode combinations were used to identify each sample for de-multiplexing. Unfiltered fastq sequences for each bacterium were aligned to available bacterial reference genomes using BWA (bwa mem -k 24 -T 0 -B 100 -O 100 -E 100 -t 8) [17]. SAM alignment was converted to BAM (samtools view –bS), sorted by coordinates (samtools sort) and PCR duplicates removed (samtools rmdup) using SAMtools [18]. Mapped reads were counted using BEDTools (multiBamCov –bams) [19].

Read counts were exported in a tab delimited file for normalization and differential gene expression (DGE) (see supp. mat.) in R [20]. DGE analysis was completed with DESeq2 package [21]. Reads with 0 or 1 count were removed before DGE was performed (see supp. mat.). For each RNAseq data set, genes with an absolute fold change ≥ 2 and p-value of <0.05 were used for further analysis. The proteins corresponding to the obtained gene sets were searched against the version 10 of the STRING database [22] to display functional protein-association networks . Interactions were considered with a STRING confidence ≥ 0.4 (medium and high confidence). A markov cluster algorithim (MCL) [23] of 2 was used for clustering.

To acquire gene names for uncharacterized proteins of *E. faecalis* strain ATCC 29212, we blasted protein sequences against the reference genome of vancomycin resistant *E. faecalis* V583 (NC_004668) available on the NCBI database (blast.ncbi.nlm.nih.gov/Blast.cgi). When no match was found (e.value > 0.01), we reported the locus tag of current strain. All bioinformatics data set including raw reads (NCBI Bio project - PRJNA341849).

Metabolomics (metabolite extraction and derivatization). A separate experiment was conducted using the same experimental design as described above, with only an increase in starting bacteria inoculum and number of replicates per time point. A starting inoculum of ~10^6 CFU mL^{-1} was used for each bacterium in co-culture and six Erlenmeyer flasks were randomly selected for metabolome analysis at 0.5, 3, 6 and 12 h (72 flasks in total). For intracellular metabolites, 45 mL of co-culture samples were filtered through 0.45µm pore size isopore filter (EMD Millipore, Billerica, MA), and followed by a quick wash step with 10 squirts of autoclaved PBW using a narrow mouth wash bottle before vacuum

source was closed. Filters were immediately folded inwards, transferred into Lysing Matrix B tube (MP Biomedical, Solon, OH) and quenched with ice–cold methanol using a modified protocol from Teng et al (Henderson et al. 2016, Teng et al. 2009). Briefly, 485µL of a 58% methanol solution (final) and 400µL CCl_3 were added to filters and tubes were vortexed vigorously for 30 secs. Time from sampling to quenching was < 2 minutes per sample. Next, we performed two runs of bead-beating on a FastPrep - 24 bead-beater (MP Biomedical, Solon, OH) at 6.5m/s for 60s per run. Samples were kept on cold tube racks for ~5 minutes between bead-beatings; and throughout metabolite extraction. Each metabolite-containing phase was transferred into a 2mL glass vial and evaporated under vacuum in a SpeedVac Concentrator (Thermo Scientific, Waltham, MA). The polar extracts were reconstituted in 0.22 mL 100 mM phosphate buffer (pH = 7.4) in D_2O with 20µM DSS (4,4-dimethyl-4-silapentane-1-sulfonic acid) for ^1H NMR analysis.

For extracellular metabolites, 4.5 mL of co-culture samples was filter sterilized (0.22 µm) and metabolites were extracted as described by Henderson et al. Briefly, the filtrate was evaporated under vacuum in a SpeedVac (Thermo Scientific, Waltham, MA).

Metabolome analysis. All ^1H NMR spectra were acquired at 20 °C on an Agilent Inova 600 MHz spectrometer (14.1 Tesla) using a 3-mm triple-resonance probe (Teng, et al, 2009). Following data acquisition, ^1H NMR spectra were processed with 0.3 Hz apodization. Residual solvent regions were removed, and spectra were aligned and normalized to unit total intensity. Spectra of polar samples with a range of 0.50–10.00 ppm were segmented into 0.005 ppm bins and imported to Excel prior to multivariate or univariate analysis. SIMCA-P + 13.0 (Umetrics, Sweden) was used for multivariate analysis. Principal component analysis (PCA) was performed on binned and normalized

NMR spectra. Pareto scaling was applied to each variable to reduce the influence of intense peaks in the spectra (Ramadan et al., 2006). The altered metabolites were determined by Student's *t*-test ($p \leq 0.05$) comparison of I-DOMW to N-DOMW treatments, and DOMW treatments to PBW controls and identified by metabolome databases (Human Metabolome Database 3.6 and Chenomx 7.6) and/or *in-house* standards.

Extracellular metabolites were analyzed on an Agilent 6890 gas chromatograph (Agilent Technologies, CA, USA) interfaced to a Waters magnetic sector mass spectrometer (Waters, Milford, MS). Metabolite derivatives were separated on a Rxi-5Sil MS (30m, 0.25 µm thickness, and 0.25 mm ID; Restek, PA, USA) and helium was kept at a constant pressure of 65 kpa. The injector, transfer line and source temperatures were 250°C, 280°C, and 200°C, respectively. The trap and detector were set for 350 µA and 300 V and all samples were introduced at 2 uL (splitless mode). Chromatographic separation was achieved by an initial oven temperature held for 2 min (60°C) and then ramped at 6°C/min to 280°C and held for 3 mins. Mass spectra were acquired over a mass range from 50-650 m/z. Chromatograms were then exported as netcdf files and imported into MetAlign for data preprocessing and alignment. Distributor recommended parameters for fast scan analysis was used. Following alignment, Excel was used to filter and truncate the data as described by Niu et al.[28].

Statistical analysis. Bacteria growth rate was derived from the equation below, where N is the concentration of cells, t is the time and k is the growth rate constant.

$$(2)\ dN/dt = kN$$

A profile analysis was performed to compare bacterial growth rates (μ_3 vs. $\mu_{0.5}$, μ_6 vs. μ_3, μ_6 vs. μ_{12}, μ_{24} vs. μ_{12}) between treatments, after which a multivariate analysis of

variance (MANOVA) was used to test for significant differences in growth rate between bacteria-type. Although small sample size can affect the power and the homogeneity of the variance test, profile analysis still provides more power than univariate tests [26]. Graphs were plotted in SigmaPlot (Systat Software, San Jose, CA) and heatmaps were plotted using Heml[30].

Outdoor mesocosm

Mesocosm preparation. Fresh water used to prepare mesocosms for this study were collected from a stream along the Upper Oconee Watershed (33° 57.916´N, -83° 25.503´E) a day prior to mesocosm set up. Approximately 5L of water was filter - sterilized (0.22µm) and confirmed for the absence of bacteria or viruses. Half of the filter - sterilized water was spiked with CFE and this constituted the DOMW treatment group while the rest (unspiked) were used as controls.

Inoculum preparation. Fecal bacteria strains used and method of preparation was the same as described for indoor microcosms studies.

Experimental design. Exposed mesocosms were established in 600mL and 1L jacketed Pyrex beakers and in 1L glass beakers for unexposed mesocosms. Five hundred milliliters of spiked (treatment) and unspiked (control) filtered stream water was dispensed into appropriate beakers. The beakers were covered with clear acetate films (80% UV transmission; Grafix Plastics, Cleveland, OH) to prevent contamination and equipped with an external syringe tubing for bacteria inoculation and sampling. Exposed mesocosms were connected to a recirculating water chiller maintained at 25^{o}C to buffer against temperature changes, while unexposed mesocosms were kept in an incubator shaker (Innova 4230, New Brunswick Scientific, Edison, NJ) in a dark room. Exposed mesocosm

beakers were set up on a Speedsafe magnetic stirrer (Hanna instruments, RI, USA) throughout the experiment. Experiment was conducted at a field site located at the U. S EPA Ecosystems Research Division in Athens, GA in July, 2016 (Fig. 5S18).

HOOH photo-production and bacteria inoculation. Prior to bacteria inoculation, mesocosms were exposed to natural sunlight for 4 h and immediately covered in aluminum foil and transferred to a dark room. Mid-log phase cultures of *E. coli* and *E. faecalis* were separately inoculated into each beaker to give a final concentration of ~ 10^6 CFU/mL for each bacterium.

Sampling and processing. Following inoculation, mesocosms were kept in the dark for 20 h before the next cycle of 4 h sunlight exposure and 20 h dark incubation. Experiments were conducted over a period of 72 h and sampled post-irradiation, 0.5, 4, 24, 28, 48, 52 and 72 h. Approximately fifteen milliliters of water were collected at every sampling and processed to determine the concentration of bacteria, extracellular HOOH, dissolved organic carbon (DOC), and UV-Vis absorbance of DOM present.

Microbiological analysis. *E. coli and E. faecalis* were quantified by culture methods using modified mTEC agar (EPA method 1603) and mEI agar (EPA method 1600).

Extracellular HOOH measurement. HOOH concentration in exposed and unexposed mesocosms was quantified using the copper-DMP spectrophotometric method as described earlier with a few modifications. Samples were filter sterilized using 0.22µm syringe filter to get rid of all bacteria prior to measuring HOOH. Absorbance reading in exposed and unexposed mesocosms were normalized against corresponding unexposed treatments or controls with no bacteria added. Absorbance was read on a 96-well plate

reader (Bio Tek Synergy HT, VT, USA). Two separate calibration curves were used for treatments and controls to account for differences in DOM content and DOM interference.

DOC measurement. Dissolved organic carbon was determined using a total organic carbon analyzer (TOC-V_{CPH}, Shimadzu, Kyoto, Japan) equipped with auto samplers. All samples were filter-sterilized (0.45μm) and diluted if necessary before measurements were taken.

UV-Vis measurement. Absorbance readings (200-800nm) were obtained with a PerkinElmer® Lambda 35 Spectrophotometer following in-house protocol. Briefly, water samples were filter sterilized with 0.22μm syringe filter to remove all bacteria prior to measurement. A cuvette with a 1 cm pathlength was used for samples that had an approximate absorbance value greater than 0.1. Cells with a 5 cm pathlength were used for samples with a more dilute absorbance to allow for better sensitivity. Nanopure water served as the reference for each run. Nanopure water was also scanned as a control for every five samples scanned to control for any baseline drift. Two replicate measurements were made for each sample.

Temperature and sunlight. Sunlight intensity and temperature in exposed mesocosms was monitored throughout the experiment with a HOBO data logger UA-002-08 (Onset Computer Corporation, MA, USA) (Fig. 5S12). HOBO data loggers were placed in two separate 600mL jacketed Pyrex beakers and filled with 500mL of spiked stream water (treatment) and stream water only (control). Beakers were covered as described previously and equipped with a recirculating water chiller. Bacteria was not added at any time during the experiment. Data loggers were configured to record temperature and sunlight intensity every 15 min.

Results and discussion

RNA sequencing. The average number of reads mapped after removal of PCR artifacts per sample in I-DOMW, N-DOMW and PBW were 3,594,656 ± 1,534,738 (SE), 6,449,247 ± 1,550,947 (SE), and 1,628,947 ± 316,525 (SE) for *E. coli*, and 1,586,985 ± 419,871 (SE), 2,145,191± 1,115,458 (SE), 692,796 ± 144,186 (SE) for *E. faecalis* respectively.

Dissolved Organic Carbon (DOC) in outdoor mesocosms. Starting DOC concentration in spiked stream water mesocosms (DOMW-treatment) was 21 ± 0.98 (SE) mg L^{-1} and 4.32 ± 0.72 (SE) mg L^{-1} in stream water only mesocosms (control) (Fig. 5S19). After the 72-h cycle, DOC decreased approximately 56%, 57%, 23% in unexposed DOMW treatment, exposed DOMW treatment and unexposed control respectively. For exposed control, an increase of 13% was observed.

On the other hand, DOC showed no overall decrease in exposed mesocosms that had no bacteria inoculated (Fig. 5S21B). However, we observed bacterial growth in the exposed treatment mesocosm after 20 h of dark cycle. We suspect the source of contamination to be the HOBO data loggers. We had no effective way to decontaminate the data loggers and, moreover, they have been previously used in field sites.

Adaptive responses used by *E. coli* and *Ent. faecalis* for survival

Beta-lactams inhibit cell wall synthesis machinery and induces futile peptidoglycan production, leading to osmotic lysis, especially in growing cells[71]. There was an upregulation of transcripts required for peptidoglycan synthesis in both bacteria. More importantly, the penicillin binding proteins (pbp) were significantly upregulated in I-DOMW and N-DOMW compared to PBW for *E. coli*, while for *E. faecalis* these genes were only upregulated in N-DOMW (Fig. 5.7A_1; Fig. 5S15B). Evidence for peptidoglycan synthesis

was further supported by NMR results, where a significantly higher concentration of N-acetylmuramic acid (MurNac) was observed in I-DOMW compared to N-DOMW at 3 and 6 h (Fig. 5.2A). MurNac is part of the peptidoglycan polymer of Gram-positive bacterial cell walls suggesting *E. faecalis* was responsible for the synthesis. These time points also represent the exponential phase of growth for *E. faecalis* in I-DOMW (Fig. 5.1A), suggesting *E. faecalis* might be actively building its peptidoglycan

The expression of genes coding for porins and efflux pumps play important roles in adaptive resistance development [78, 79]. They are efficiently regulated to respond to specific cues, thereby changing the resistance of a bacterium based on growth conditions. For example, Suzuki, et al. [97] demonstrated that antibiotic resistance development in *E. coli* could be quantitatively predicted by the expression changes of a small number of these genes. Multiple networks coding for these efflux pumps and their transcriptional regulators were differentially expressed in *E. coli* including the *yejABEF* encoding microcin transport and associated with virulence[98], *sapBCDF* encoding antimicrobial peptide transport and putrescine export[99], and *cusABCD* for copper transport (Fig. 5.7A-C). For *E. faecalis*, multiple antibiotic resistance protein families (MarR), beta-lactam resistance, quorum sensing and bleomycin/glyoxalases resistance transcripts were significantly differentially expressed (Fig. 5.7F and G; Fig. 5S15B)

Curli is a proteinaceous extracellular matrix associated with attachment and biofilm formation, and it plays a major role in bacterial pathogenesis [100]. Most importantly, biofilm formation has been associated with oxidative stress and antibiotic resistance [101-103]. The expression of the curli associated genes *csgCDEFG* and the *pgaABCD* operon encoding poly-beta -1, 6 N-acetyl-D-glucosamine (PGA) was significantly higher at 0.5 h in N-

DOMW compared to PBW for *E. coli* (Fig. 5.7E). For *E. faecalis*, the LytSR regulator proteins were differentially expressed. These two component-regulatory protein interacts with multiple genetic networks including the *lrgAB* genes in *Staphyloccus aureus* and it is required for biofilm formation[104]. A Δ*lytS* mutant strain of *S. aureus* was shown to form a more adherent biofilm[105]. The *lytST* genes were upregulated in I-DOMW compared to PBW at 6 and 12 h while the *lrgAB* genes were upregulated in PBW compared to I-DOMW at 0.5, 3, and 6 h (Fig. 5S15B_4).

The tryptophan operon is a repressor operon that is turned-on or turned-off based on the levels of tryptophan in the environment. In addition, tryptophan is the primary source of indole production in *E. coli*, an organic compound that plays a role in quorum sensing, biofilm formation and antibiotic resistance [106, 107]. Expression of *trpDBCA* transcripts for tryptophan biosynthesis significantly increased with time and bacteria concentration in I-DOMW and N-DOMW relative to PBW, supporting their role as quorum sensors (Fig. 5.7D, Fig. 5S15A_2). Metabolomics also showed intracellular tryptophan levels to be significantly higher in I-DOMW at 0.5 h but lower at 3, 6, and 12 h when compared to N-DOMW, implying indole was being used for survival under HOOH exposure (Fig. 5.2A). Extracellular HOOH in our study was >15 μM and ~9 μM at 0.5 h in I-DOMW and N-DOMW, respectively (Fig. 5.1A and B). Tryptophan biosynthesis was also observed in mono-culture experiments with *E. coli* O157:H7 where *trpEDCBA* increased significantly following inoculation (0.5 h) into I-DOMW and after 6 h in N-DOMW. In addition, extracellular HOOH concentration in I-DOMW and N-DOMW at 0.5 h and 6 h was 15.4 ± 0.81 and 2.59 ± 1.26 (SE) μM, respectively (Oladeinde et al).

A major consequence of adaptive responses as displayed by both *E. coli* and *E. faecalis* in our study is severe DNA damage and mutations especially from antimicrobial exposure and horizontally transferred genes[71, 108]. Bacteria have evolved many DNA repair mechanisms to compensate for such substitutions, insertions or deletions. As expected, we found multiple DNA repair systems to be differentially expressed including endonucleases (*uvr*), bacteria recombination proteins (Rec) and mutation (*mut*) genes (Fig. 8). The *mut* genes *mutSHL* were upregulated in all treatments at differing time points for *E. coli* (Fig. 5S17A). These genes are required for methyl – directed mismatch repair which is vital during DNA recombination and replication[109, 110]. For *E. faecalis*, only the *mutL* gene was significantly upregulated in I-DOMW compared to PBW at 12 h (Fig. 5S17B).

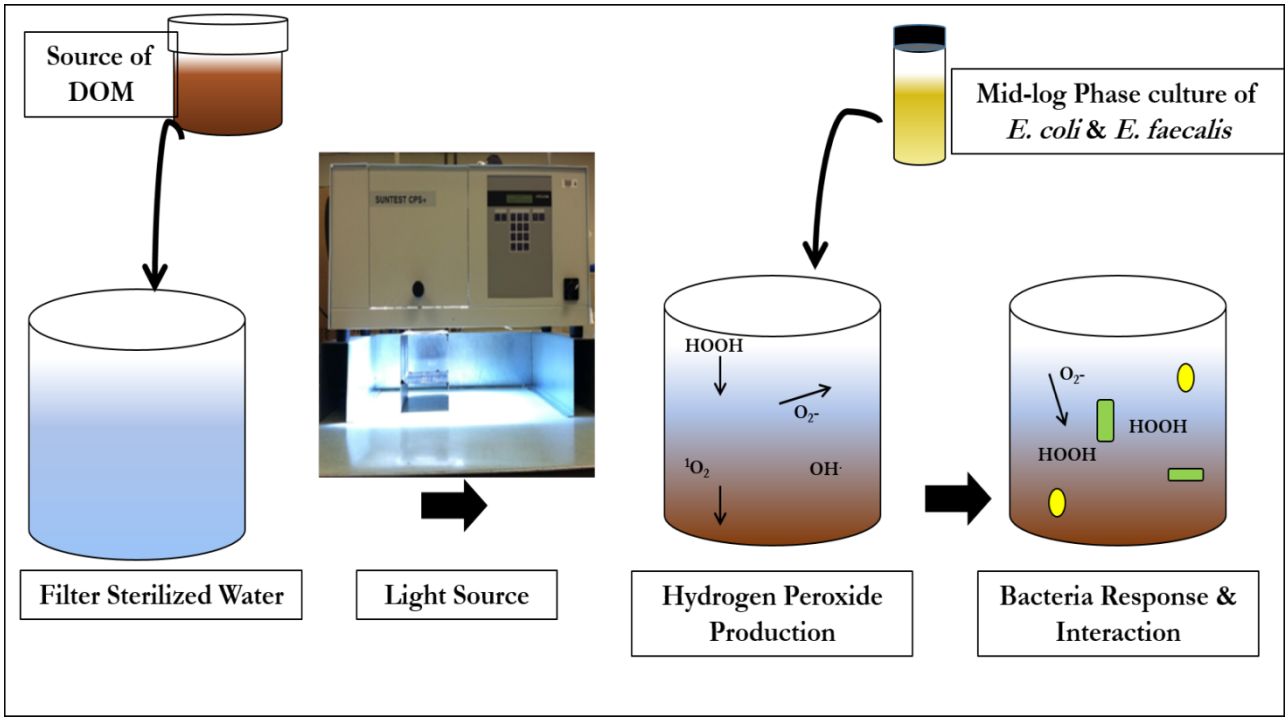

Figure 5S1. Schematic of co-culture indoor microcosm experiments. Fresh fecal samples were collected from 5 individual cattle from a commercial farm in Northeast Georgia. Fecal samples were composited, homogenized and made into 1:10 fecal slurry in 0.85% KCl and shook for 1hr in a hand wrist shaker. The fecal slurry was then centrifuged twice at 6000 rpm for 10 min and the resulting supernatant was termed cattle fecal extract (CFE). CFE was sequentially filtered through 1.2µm, 0.45µm and 0.2µm membrane filters. CFE was used as a source of DOM throughout the experiment. Solar irradiation was performed in an Atlas SunTest CPS/CPS+ solar simulator (Atlas Materials Testing Technology, Chicago, IL) equipped with a 1kW xenon arc lamp. Irradiance of the simulator in the UV spectral region was similar to mid-summer, midday natural sunlight at 33.95^{o}N, 83.33^{o}W (Athens, GA)

A

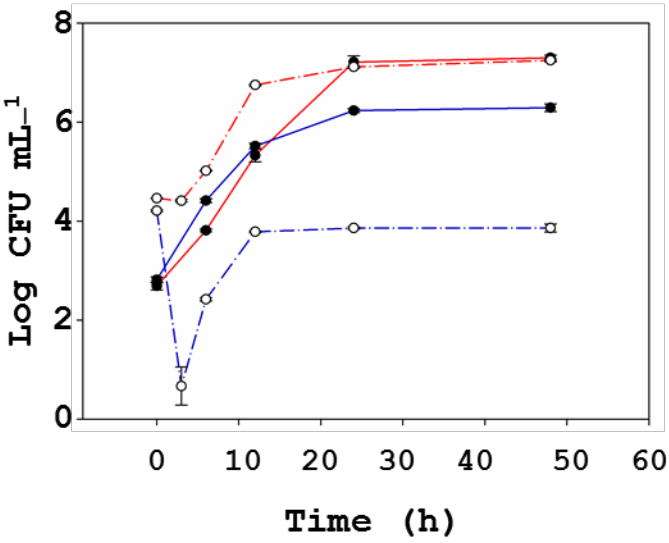
Log CFU mL-1
0
2
4
6
8
0
10
20
30
40
50
60
Time (h)

B

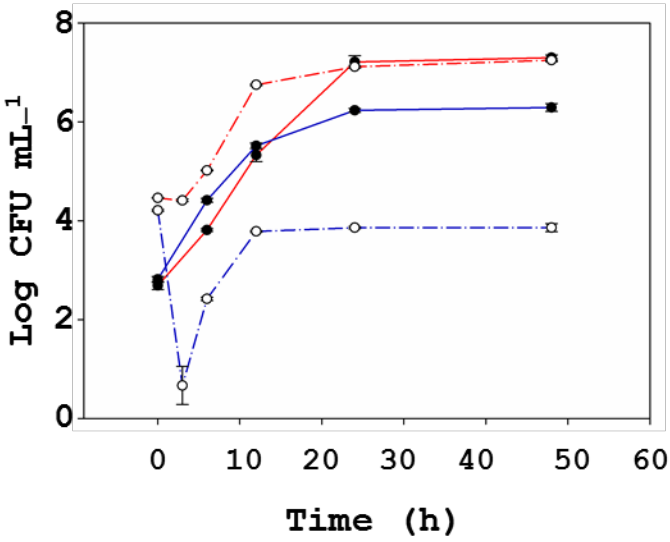
Log CFU mL-1
0
2
4
6
8
0
10
20
30
40
50
60
Time (h)

C

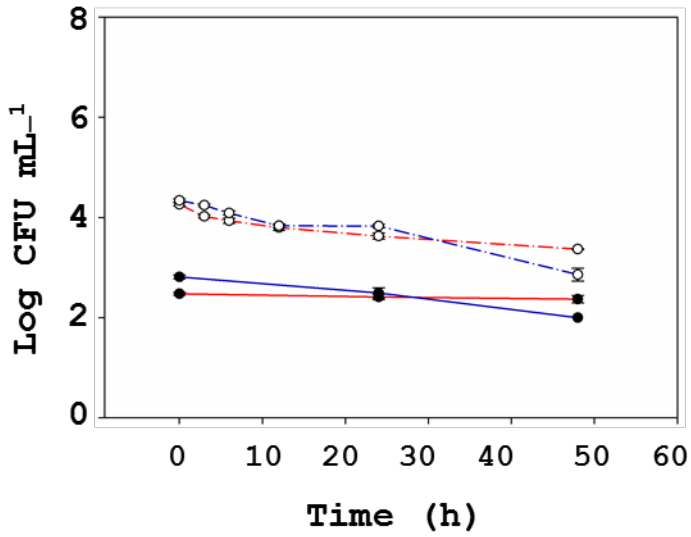

Figure 5S2. Growth comparison between *E. coli* and *E. faecalis* when grown as mono-culture or in co-culture. Fecal bacteria were quantified at 0.5, 3, 6, 12, 24, 48 h (n = 3 per group). Growth curve of *E. coli* and *E. faecalis* in **(A**) I-DOMW**, (B**) N-DOMW and (**C**) PBW. Concentration is reported in colony forming units (CFU) on the left y- axis. Solid and open circles represent mono-culture and co-culture experiments respectively. Red and blue lines represent *E. coli* and *E. faecalis*. Error bars represent standard error

A

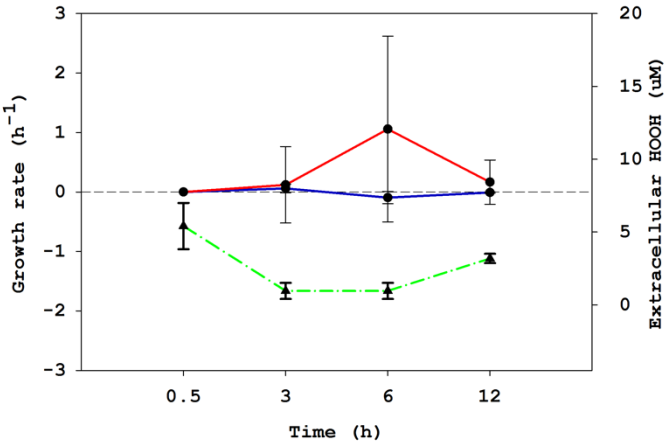

B

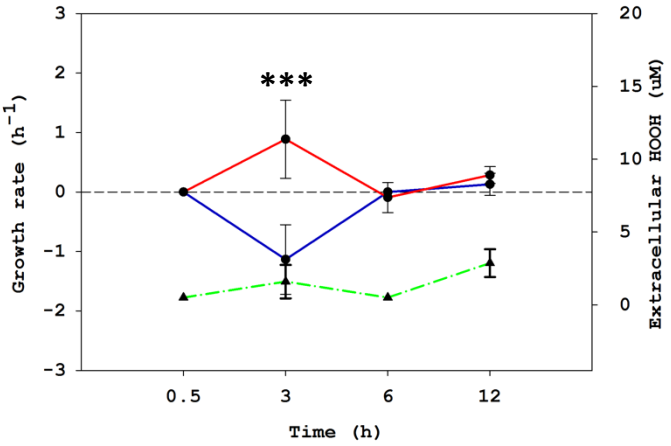

Figure 5S3. Bacteria growth rate and extracellular HOOH in co-culture microcosms used for metabolomics experiment. *E. coli* and *E. faecalis* concentration were determined at 0.5, 3, 6, and 12 h during dark incubation and filter sterilized with a 0.22µm syringe filter for extracellular HOOH determination (n = 6 per group). Green dashed lines represent extracellular HOOH concentration during dark incubation in **(A)** I-DOMW and **(B)** N-DOMW in the presence of both *E. coli* (red solid line) and *E. faecalis* (blue solid line). Growth rates per time point per group are plotted on the y-axis (dark circles). Error bars represent standard errors. *denotes significant difference in growth rate between *E. coli* and *E. faecalis* per time point (*P* value ***<0.001).

A

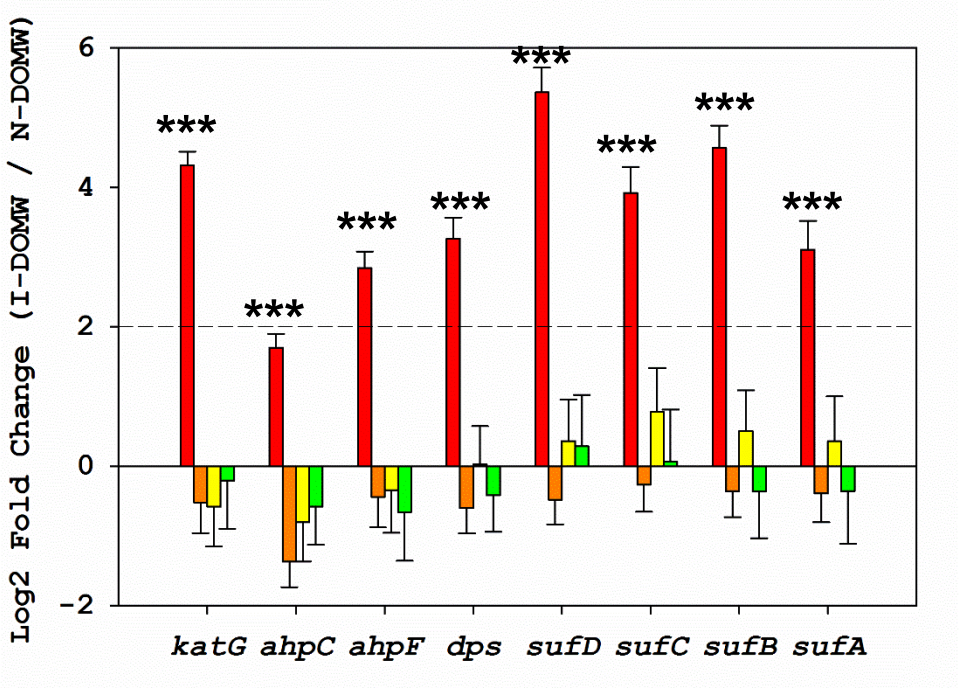

B

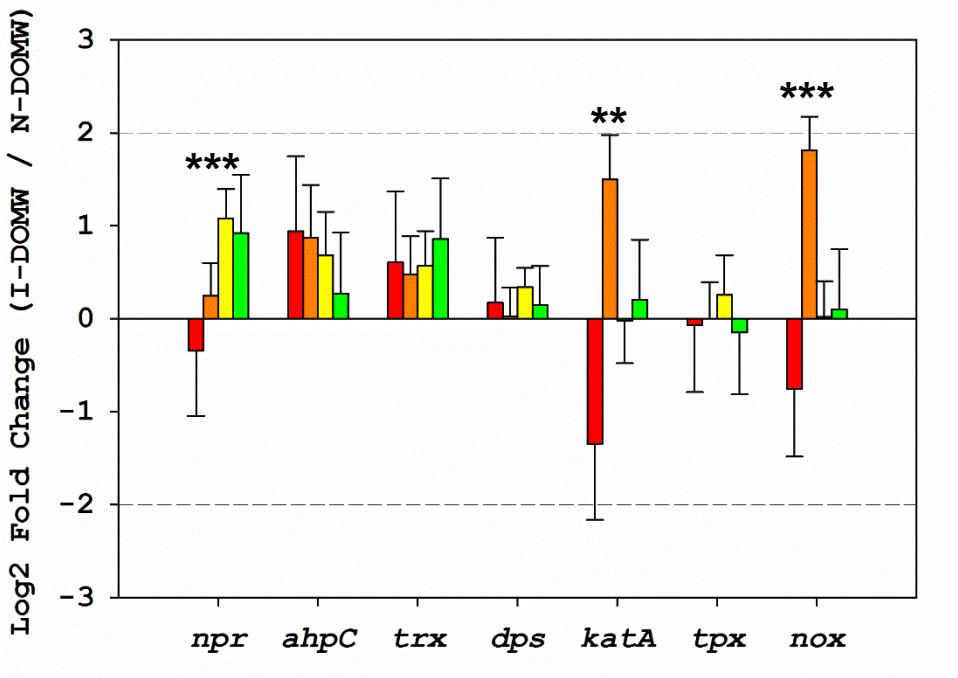

Figure 5S4. Fold-change of selected oxidative stress genes in I-DOMW compared to N-DOMW in mono-culture experiment. Total RNA was extracted from bacteria collected

at 0.5, 6, 12 and 24 h and used for WTS (n=2 per group). (**A**) *E. coli* (**B**) *E. faecalis*. Error bars represent standard errors. (**P* value <0.05, **<0.01, ***<0.001).

A1

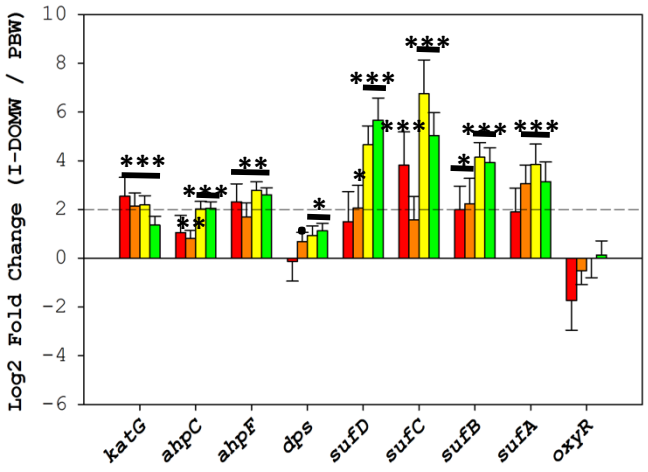
Log2 Fold Change (I-DOMW / PBW)
10
8
6
4
2
0
-2
-4
-6
katG
ahpC
ahpF
dps
sufD
sufC
sufB
sufA
oxyR

A2

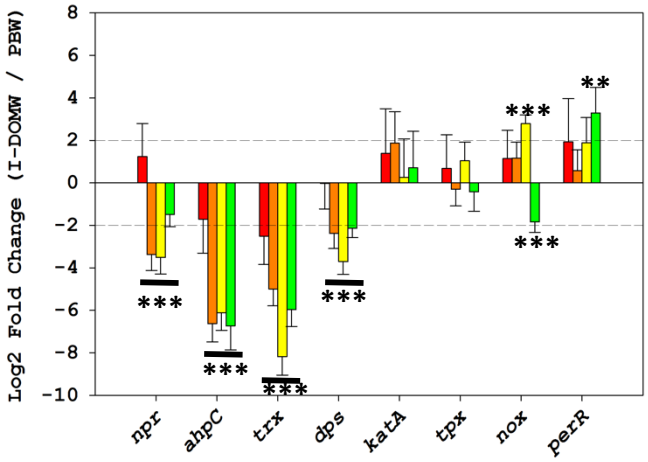
Log2 Fold Change (I-DOMW / PBW)
8
6
4
2
0
-2
-4
-6
-8
-10
npr
ahpC
trx
dps
katA
tpx
nox
perR

B1

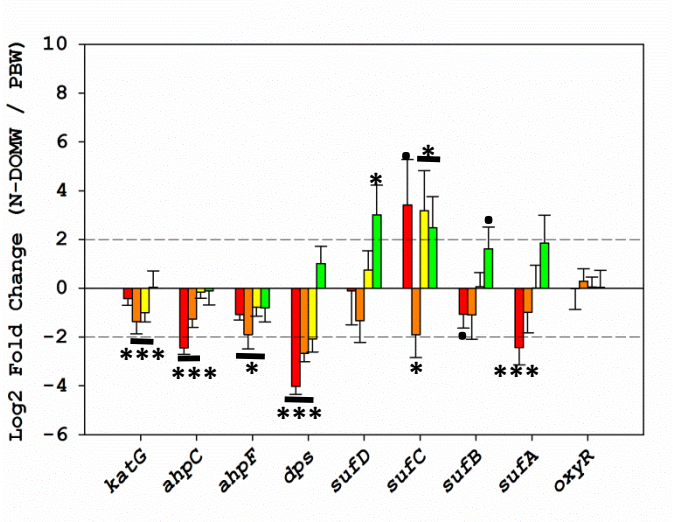
Log2 Fold Change (N-DOMW / PBW)
10
8
6
4
2
0
-2
-4
-6
katG
ahpC
ahpF
dps
sufD
sufC
sufB
sufA
oxyR

B_2

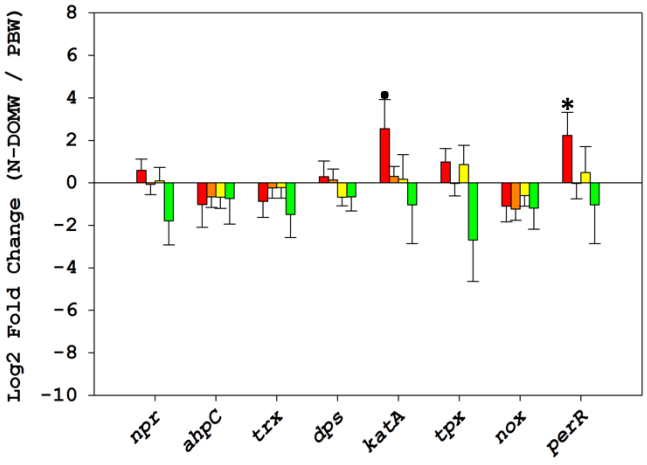

Figure 5S5. Fold-change of selected oxidative stress genes in co-culture experiment. Total RNA was extracted from co-cultures collected at 0.5, 3, 6 and 12 h and used for WTS (n=2 per group). (**A)** *E. coli* and **(B)** *E. faecalis* in (1) I-DOMW and (2) N-DOMW compared to PBW for the 12 h duration.
(*P. value ·<0.1· *<0.05, **<0.01, ***<0.001)

A

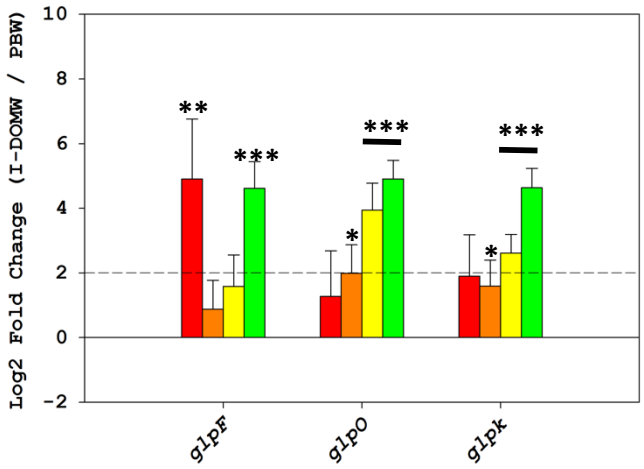

B

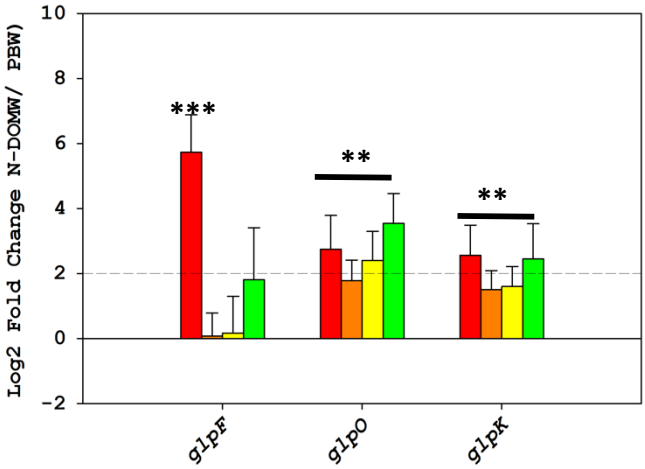

Figure 5S6. Fold-change of transcripts for aerobic metabolism of glycerol for *E. faecalis* in co-culture experiment. (A) I-DOMW compared to PBW (B) N-DOMW compared to PBW.
(**P*. value ·<0.1· *<0.05, **<0.01, ***<0.001)

A

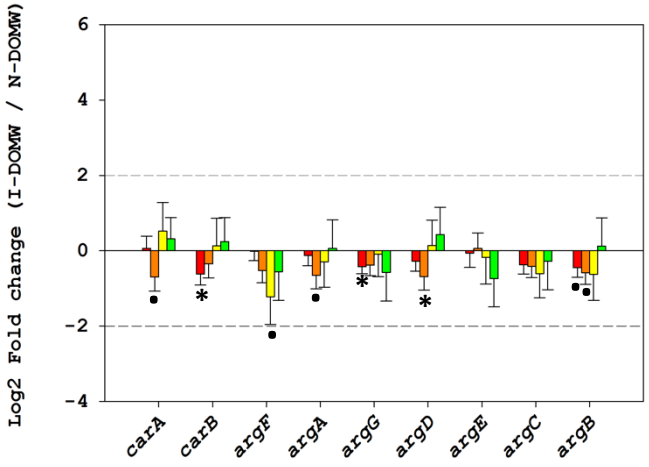
Log2 Fold change (I-DOMW / N-DOMW)
6
4
2
0
-2
-4
carA
carB
argF
argA
argG
argD
argE
argC
argB

B

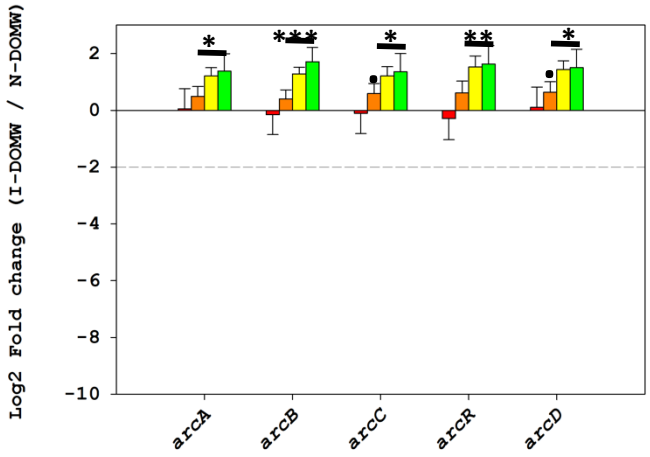
Log2 Fold change (I-DOMW / N-DOMW)
2
0
-2
-4
-6
-8
-10
arcA
arcB
arcC
arcR
arcD

C$_1$

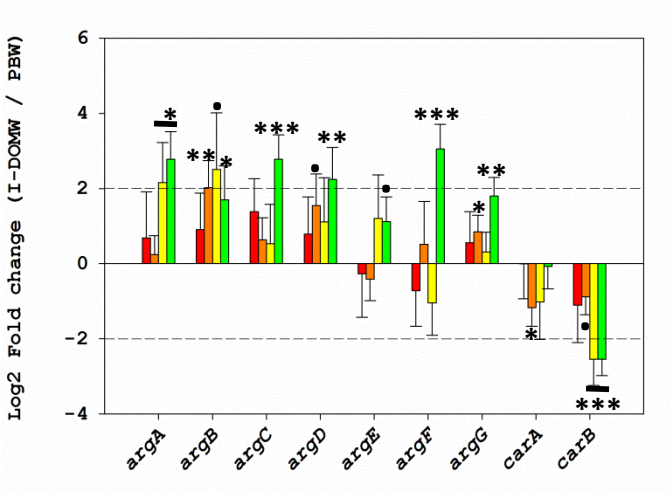
Log2 Fold change (I-DOMW / PBW)
6
4
2
0
-2
-4
argA
argB
argC
argD
argE
argF
argG
carA
carB

C2

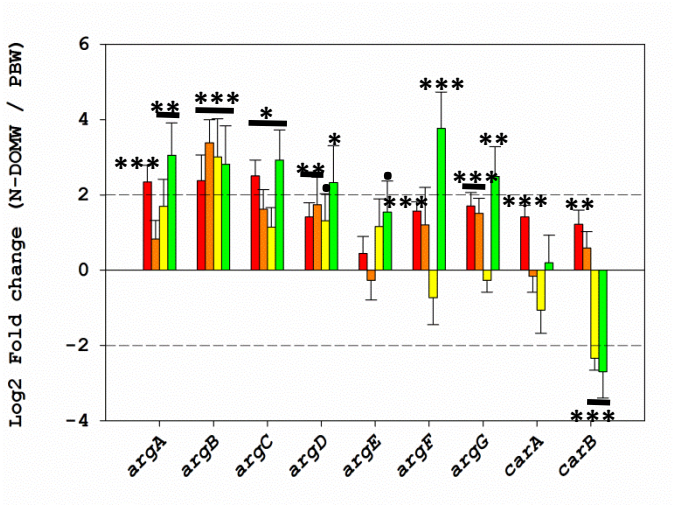
Log2 Fold change (N-DOMW / PBW)
6
4
2
0
-2
-4
argA
argB
argC
argD
argE
argF
argG
carA
carB

D1

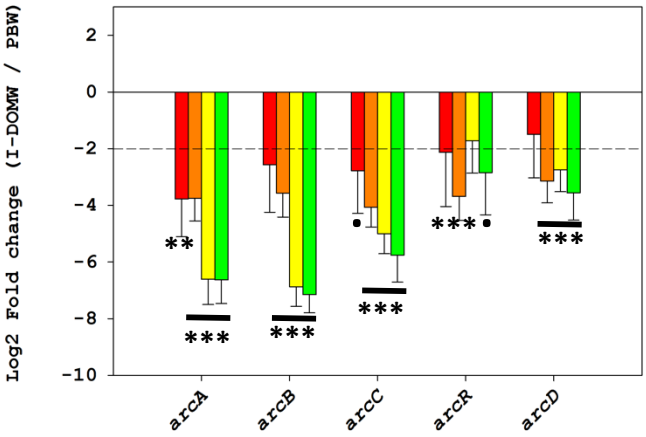
Log2 Fold change (I-DOMW / PBW)
2
0
-2
-4
-6
-8
-10
arcA
arcB
arcC
arcR
arcD

D2

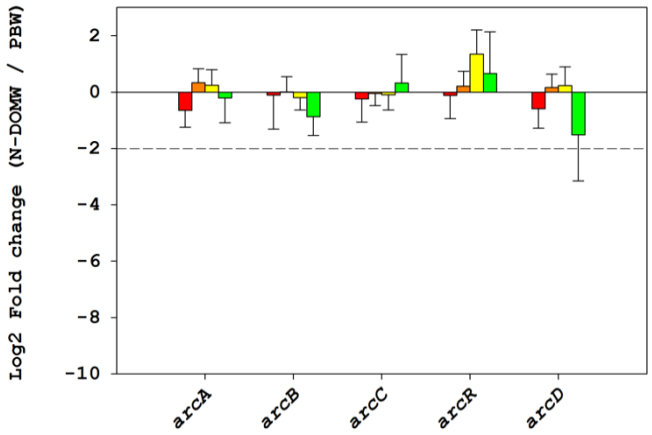
Log2 Fold change (N-DOMW / PBW)
2
0
-2
-4
-6
-8
-10
arcA
arcB
arcC
arcR
arcD

Figure 5S7. Fold-change of transcripts for arginine metabolism in mono and co-culture experiments. (**A**) *E. coli* and **(B)** *E. faecalis* in I-DOMW compared to N-DOMW for mono-culture; **(C)** *E. coli* and **(D**) *E. faecalis* in (1) I-DOMW and (2) N-DOMW compared to PBW for co-culture.
(**P*. value ·<0.1· *<0.05, **<0.01, ***<0.001)

A1

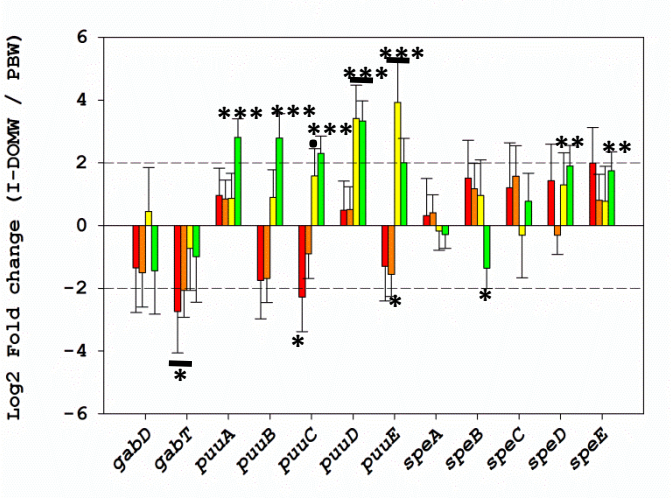
Log2 Fold change (I-DOMW / PBW)
6
4
2
0
-2
-4
-6
gabD
gabT
puuA
puuB
puuC
puuD
puuE
speA
speB
speC
speD
speE

A2

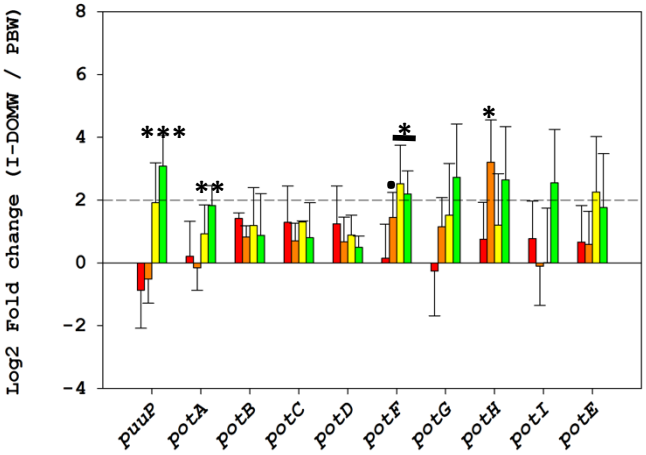
Log2 Fold change (I-DOMW / PBW)
8
6
4
2
0
-2
-4
puuP
potA
potB
potC
potD
potF
potG
potH
potI
potE

B1

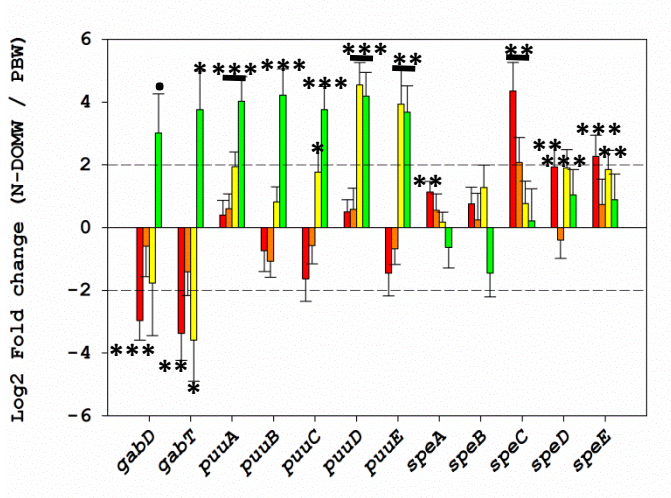
Log2 Fold change (N-DOMW / PBW)
6
4
2
0
-2
-4
-6
gabD
gabT
puuA
puuB
puuC
puuD
puuE
speA
speB
speC
speD
speE

B2

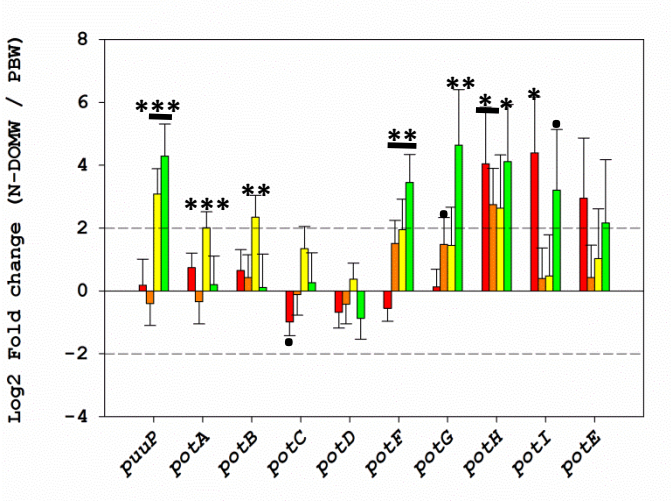
Log2 Fold change (N-DOMW / PBW)
8
6
4
2
0
-2
-4
***
***
**
**
**
**
*
puuP
potA
potB
potC
potD
potF
potG
potH
potI
potE

C1

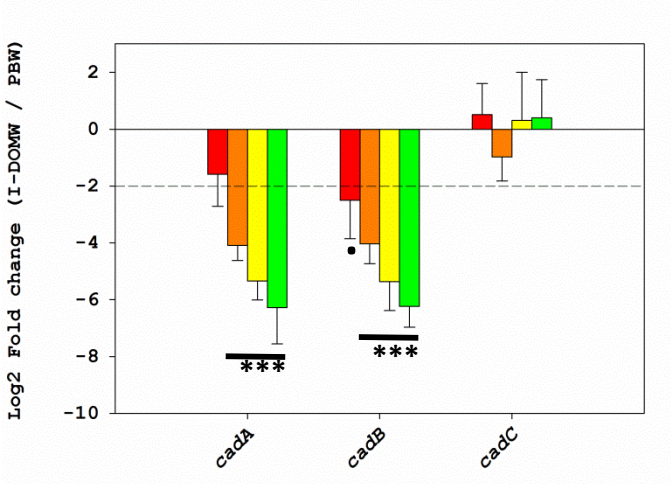
Log2 Fold change (I-DOMW / PBW)
2
0
-2
-4
-6
-8
-10
***
***
cadA
cadB
cadC

C2

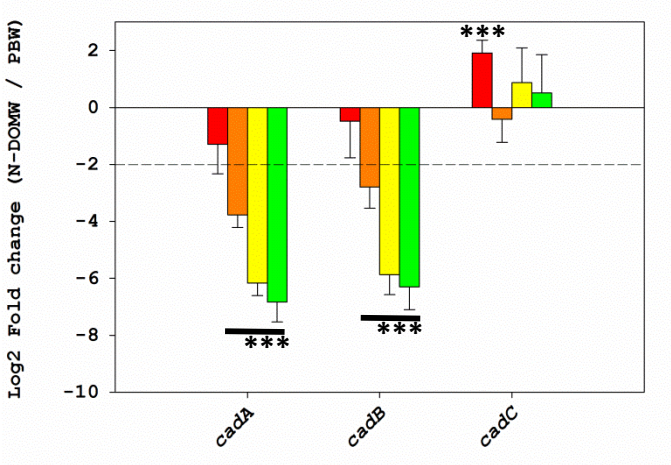
Log2 Fold change (N-DOMW / PBW)
2
0
-2
-4
-6
-8
-10
***
***
***
cadA
cadB
cadC

Figure 5S8. Fold-change of transcripts for polyamine metabolism and transport in co-culture experiment with *E. coli*. (**A**) Putrescine/spermidine metabolism and **(B)** transport in (1) I-DOMW and (2) N-DOMW compared to PBW for co-culture. (**C**) Cadaverine metabolism and transport in (1) I-DOMW and (2) N-DOMW compared to PBW. (**P*. value ·<0.1· *<0.05, **<0.01, ***<0.001)

A1

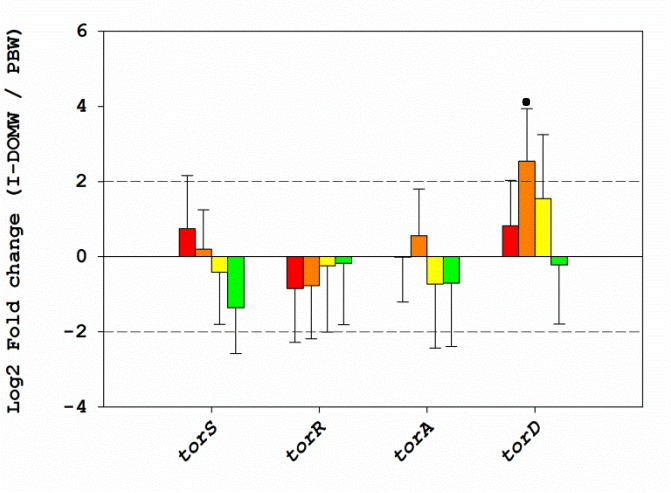
Log2 Fold change (I-DOMW / PBW)
6
4
2
0
-2
-4
torS
torR
torA
torD

A2

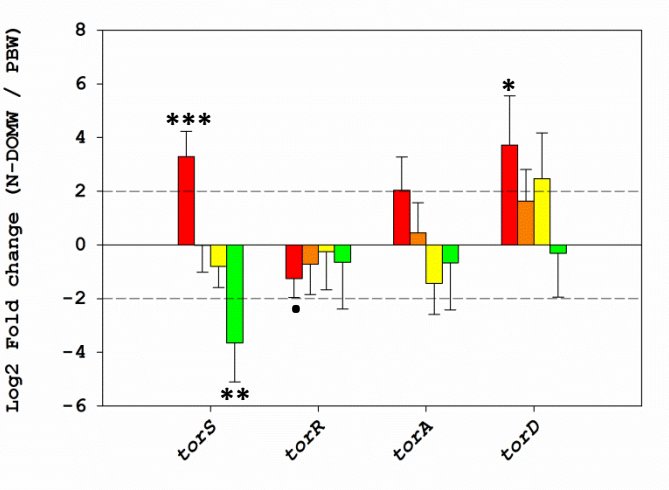
Log2 Fold change (N-DOMW / PBW)
8
6
4
2
0
-2
-4
-6
***
**
*
torS
torR
torA
torD

B

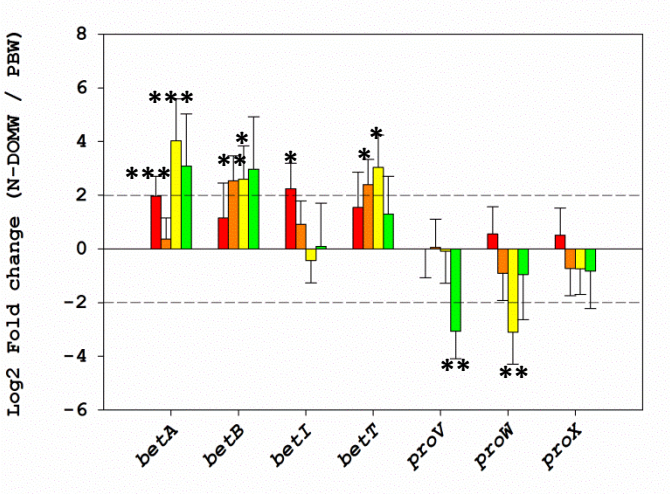

C

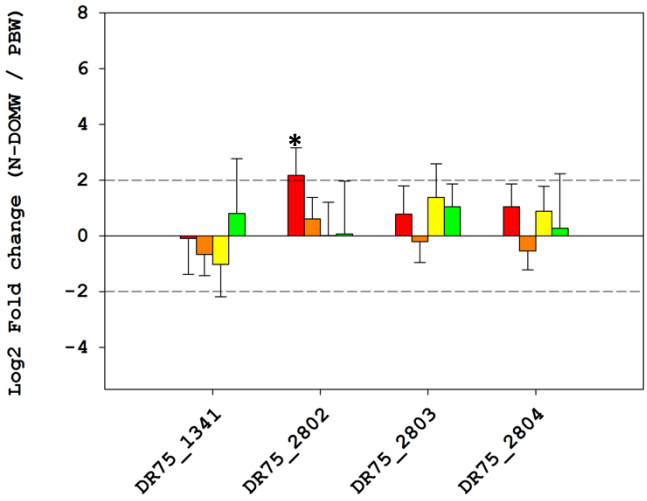

Figure 5S9. Fold-change of transcripts for methylamine metabolism and transport in co-culture experiment. (**A**) Trimethlyamine-N-oxide (TMAO) metabolism in (1) I-DOMW and (2) N-DOMW compared to PBW for *E. coli*; (**B and C**) Glycine betaine biosynthesis and transport for (B) *E. coli* and (C**)** *E. faecalis* in N-DOMW compared to PBW.
(*P. value ·<0.1· *<0.05, **<0.01, ***<0.001)

A_1

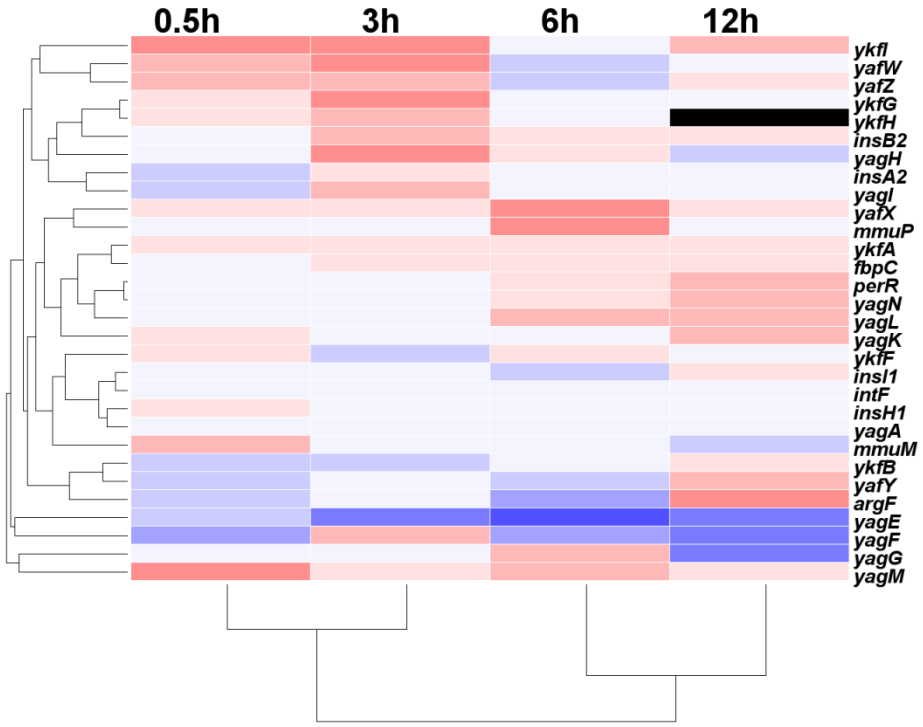
0.5h
3h
6h
12h
ykfI
yafW
yafZ
ykfG
ykfH
insB2
yagH
insA2
yagI
yafX
mmuP
ykfA
fbpC
perR
yagN
yagL
yagK
ykfF
insI1
intF
insH1
yagA
mmuM
ykfB
yafY
argF
yagE
yagF
yagG
yagM

A_2

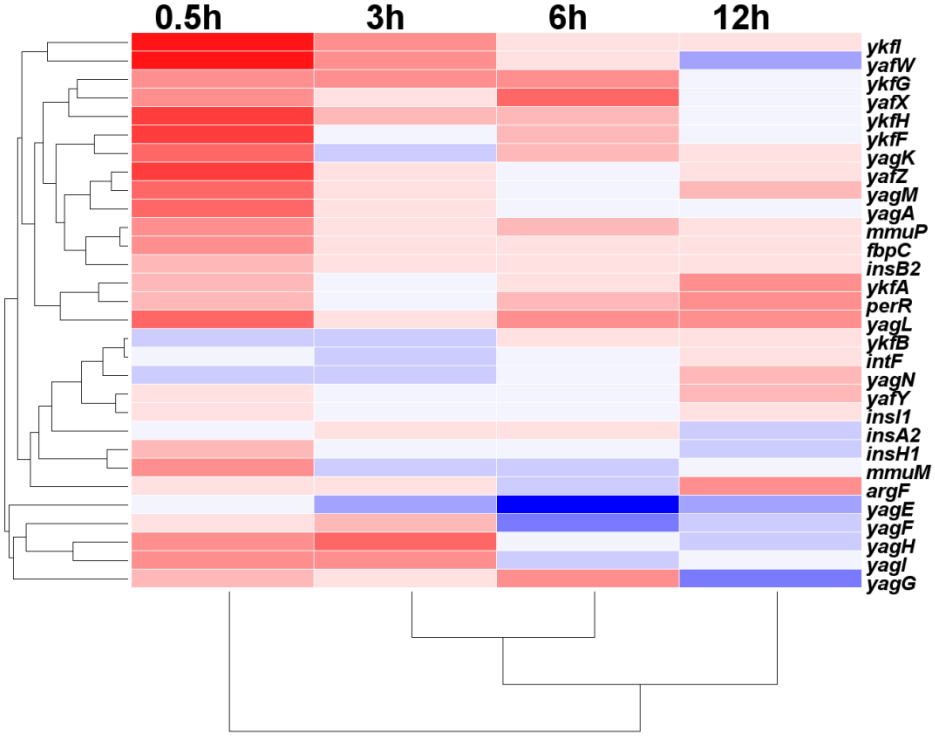
0.5h
3h
6h
12h
ykfI
yafW
ykfG
yafX
ykfH
ykfF
yagK
yafZ
yagM
yagA
mmuP
fbpC
insB2
ykfA
perR
yagL
ykfB
intF
yagN
yafY
insI1
insA2
insH1
mmuM
argF
yagE
yagF
yagH
yagI
yagG

B$_1$

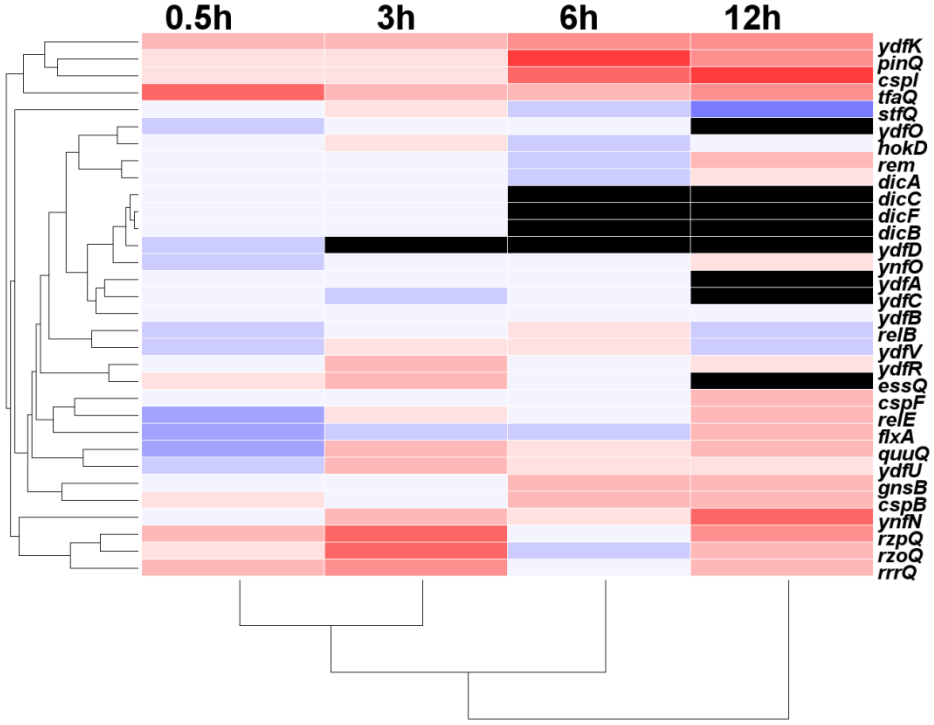
0.5h
3h
6h
12h
ydfK
pinQ
cspI
tfaQ
stfQ
ydfO
hokD
rem
dicA
dicC
dicF
dicB
ydfD
ynfO
ydfA
ydfC
ydfB
relB
ydfV
ydfR
essQ
cspF
relE
flxA
quuQ
ydfU
gnsB
cspB
ynfN
rzpQ
rzoQ
rrrQ

B$_2$

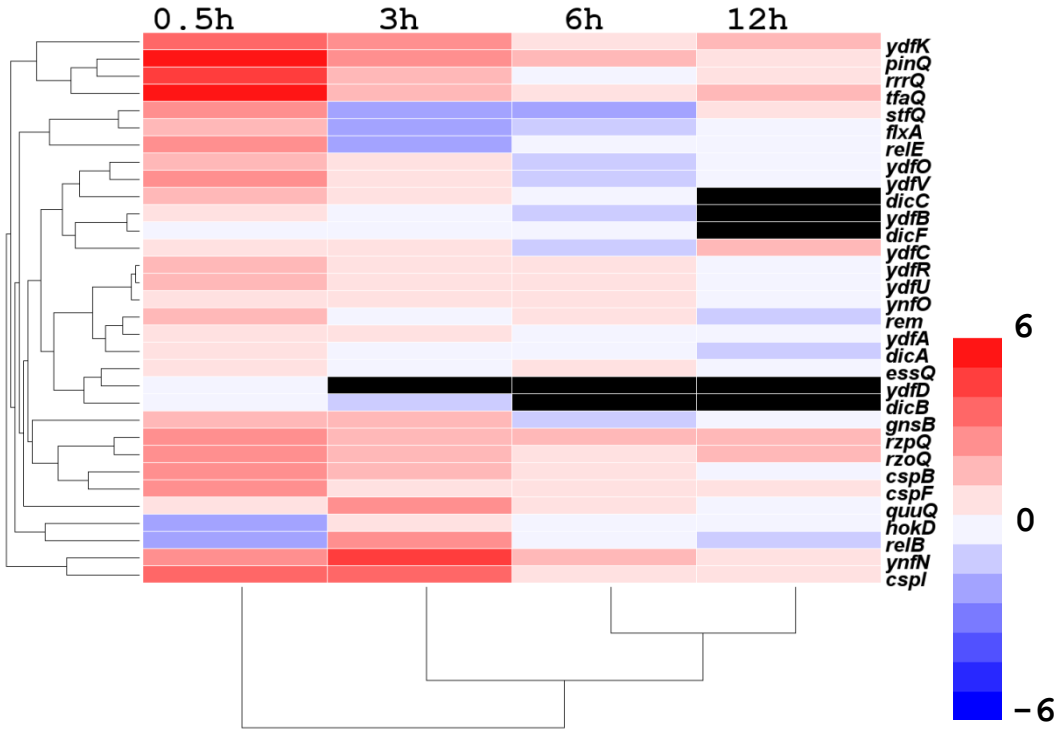
0.5h
3h
6h
12h
ydfK
pinQ
rrrQ
tfaQ
stfQ
flxA
relE
ydfO
ydfV
dicC
ydfB
dicF
ydfC
ydfR
ydfU
ynfO
rem
ydfA
dicA
essQ
ydfD
dicB
gnsB
rzpQ
rzoQ
cspB
cspF
quuQ
hokD
relB
ynfN
cspI
6
0
−6

Figure 5S10. Heatmap of significantly expressed transcripts of *E. coli* cryptic prophages in co-culture experiment. (A) CP4-6 and **(B**) Qin prophage in (1) I-DOMW and (2) N-DOMW compared to PBW for the 12 h duration. The color scale shows fold-change compared to PBW.

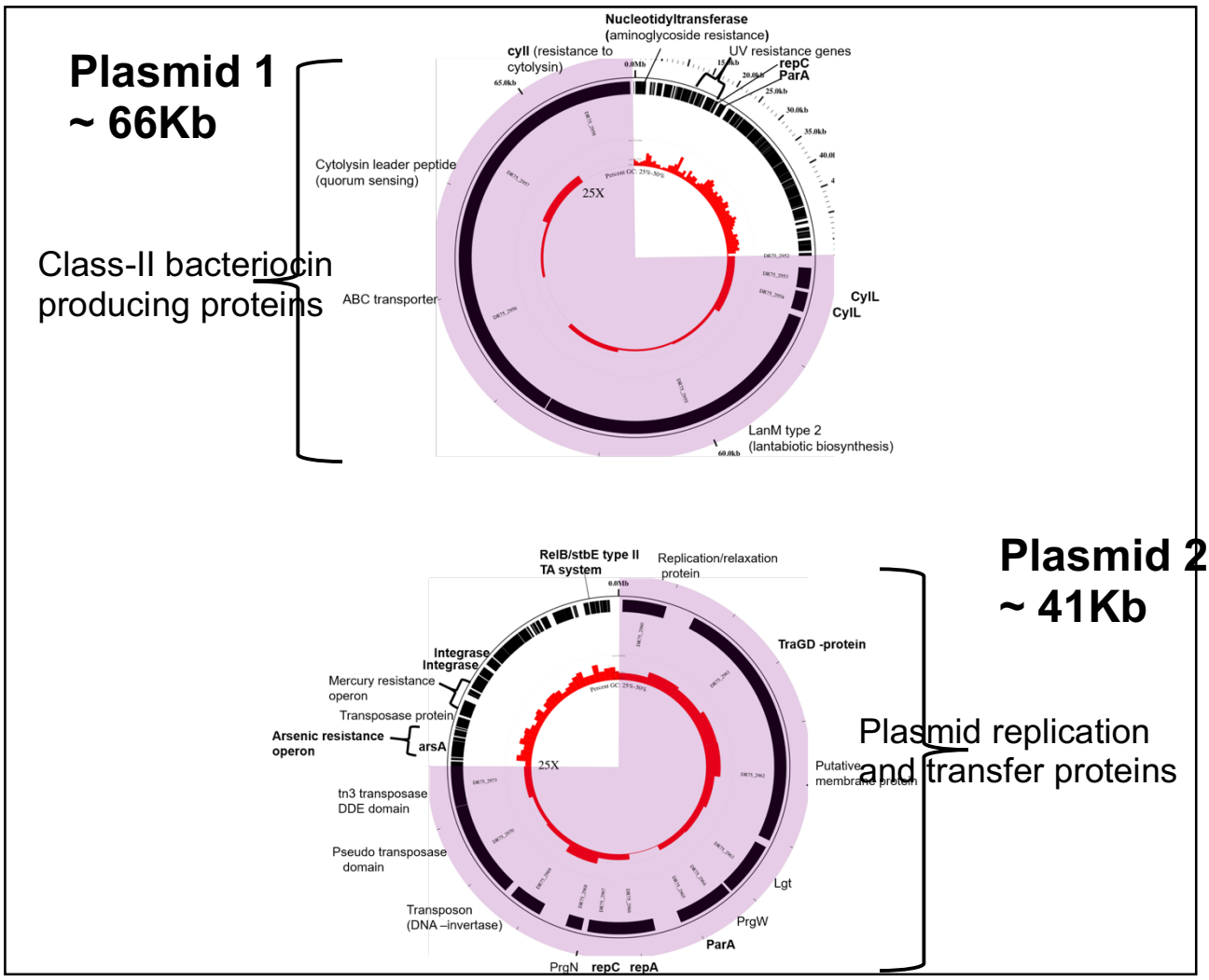

Figure 5S11. Circular map of plasmid 1 and plasmid 2 carried by *E. faecalis* strain ATCC 29212. Purple shading denotes 25X magnification of plasmid region. Bold gene/protein family name indicates gene was differentially expressed between treatments in our study. Map was generated using Circleator[119].

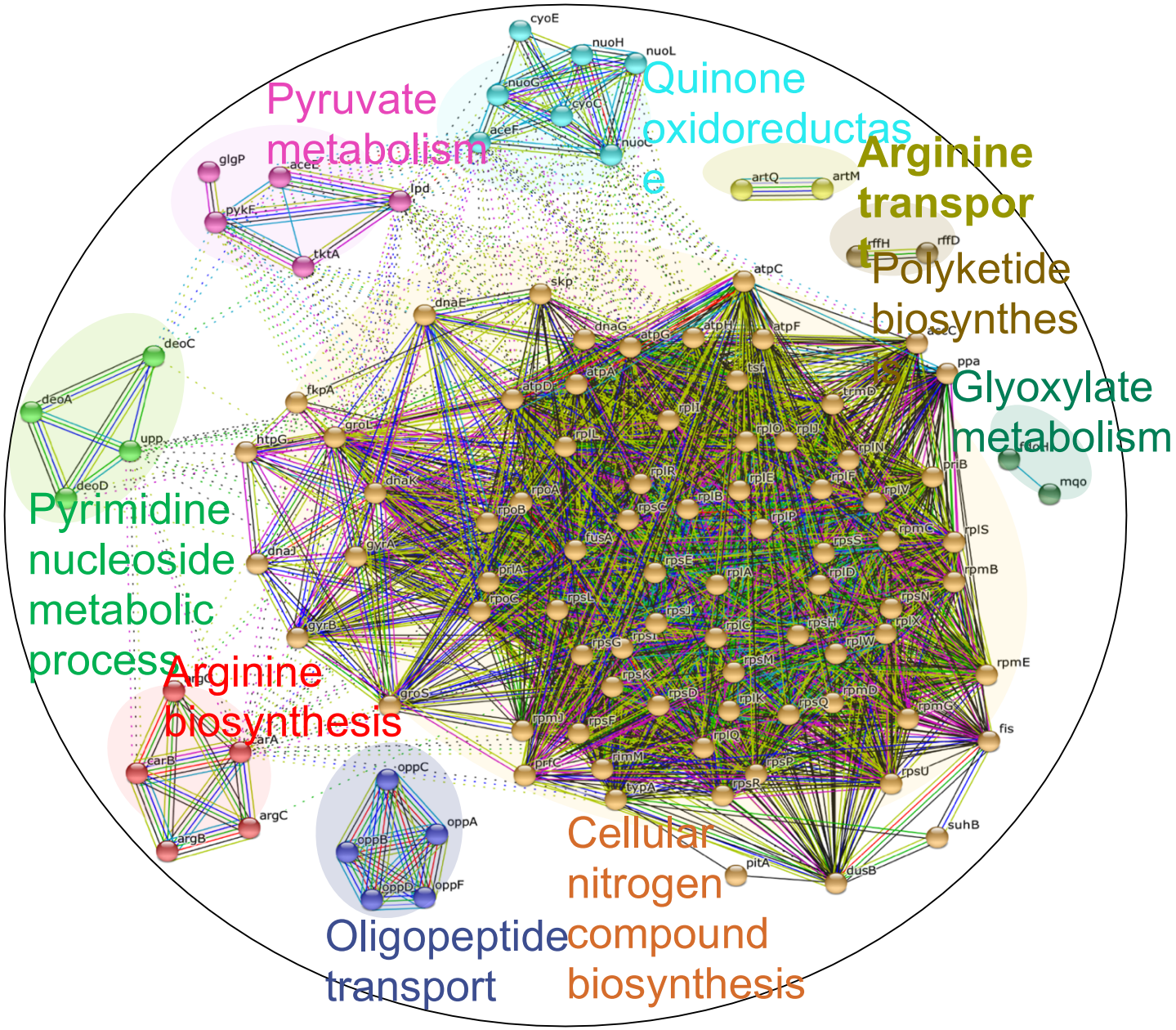
Pyruvate metabolism
Quinone oxidoreductase
Arginine transport
Polyketide biosynthes
Glyoxylate metabolism
Pyrimidine nucleoside metabolic process
Arginine biosynthesis
Cellular nitrogen compound biosynthesis
Oligopeptide transport
cyoE
nuoH
nuoL
nuoG
cyoC
aceF
nuoC
glgP
aceE
lpd
pykF
tktA
artQ
artM
rffH
rffD
atpC
skp
dnaE
dnaG
atpG
atpH
atpF
deoC
deoA
upp
deoD
fkpA
atpD
atpA
tsf
trmD
ppa
htpG
groL
rplJ
rplL
rplO
rplN
rplR
rplE
rplF
rplV
rpsC
rplB
rplP
rpsS
rpmC
rplS
dnaK
rpoA
rpoB
fusA
gyrA
dnaJ
rplA
rpsE
rplD
rpmB
rpoC
rpsL
rpsJ
rplC
rpsH
rplX
gyrB
rpsG
rpsI
rplW
rpsM
rpmE
rpsK
groS
rpsD
rplK
rpsQ
rpmD
rpmG
rpmJ
rpsF
rplQ
fis
prfC
rimM
rpsP
rpsU
typA
rpsR
suhB
pitA
dusB
carA
carB
argC
argB
oppC
oppA
oppB
oppD
oppF

Figure 5S12: STRING analysis for significantly altered transcripts in N-DOMW compared to l-DOMW at 3 h for *E. coli* in co-culture experiment. Total RNA was extracted from co-culture of *E. coli* and *E. faecalis* collected at 3 h and used for WTS (fold-change < 2; *P*. padj < 0.01).

A

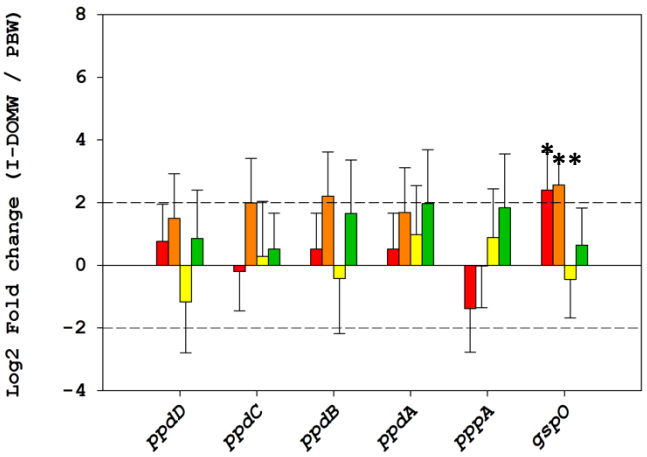

B

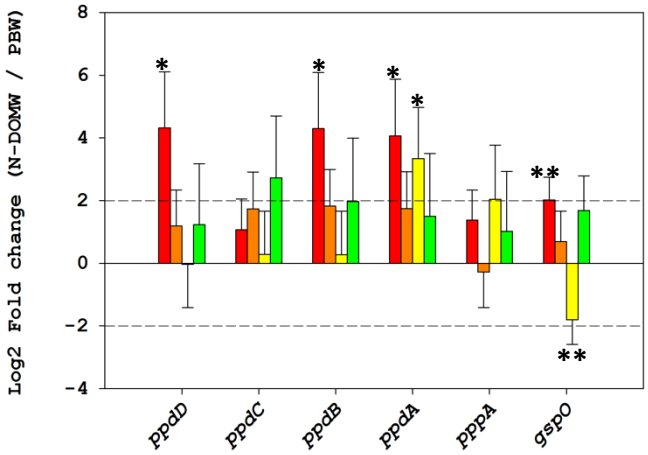

Figure 5S13: Fold-change of transcripts for type 4 prepilin pilin production for *E. coli* in co-culture experiment. (A) I-DOMW compared to PBW **(B)** N-DOMW compared to PBW.

A

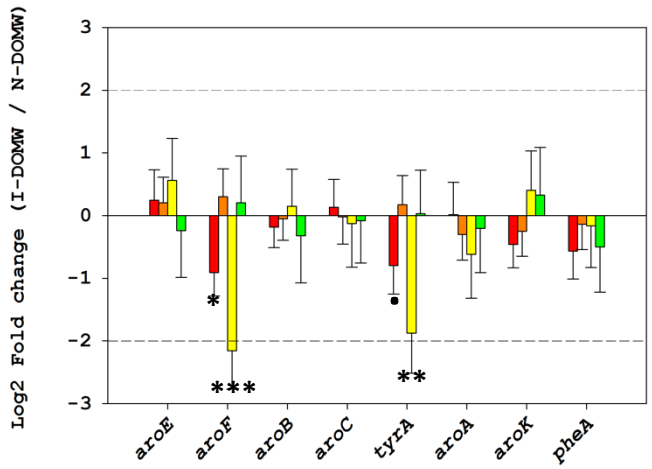
Log2 Fold change (I-DOMW / N-DOMW)
3
2
1
0
-1
-2
-3
*
***
**
aroE
aroF
aroB
aroC
tyrA
aroA
aroK
pheA

B

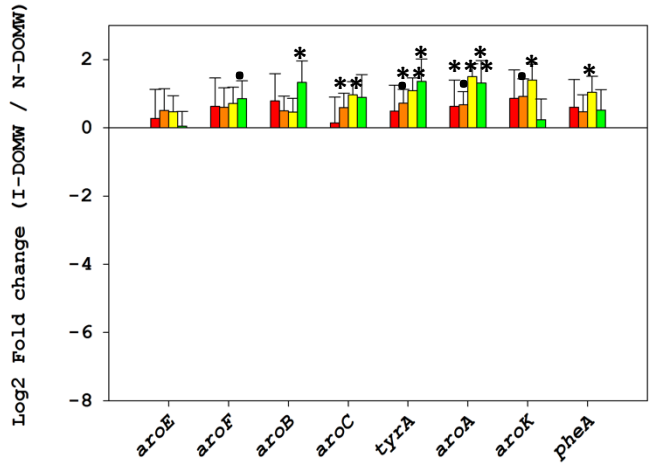
Log2 Fold change (I-DOMW / N-DOMW)
2
0
-2
-4
-6
-8
aroE
aroF
aroB
aroC
tyrA
aroA
aroK
pheA

C$_1$

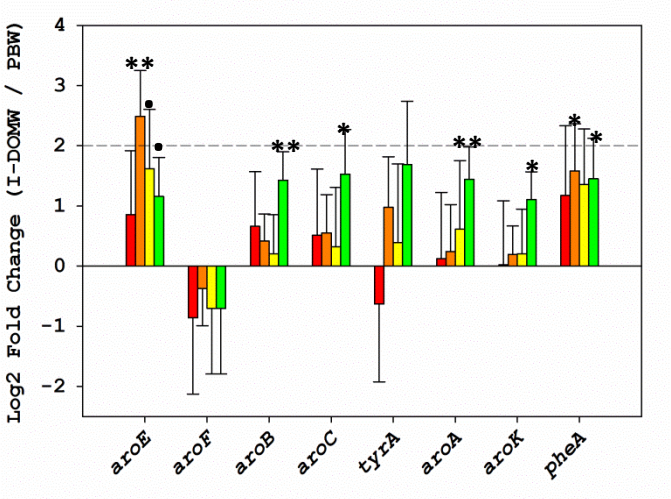
Log2 Fold Change (I-DOMW / PBW)
4
3
2
1
0
-1
-2
aroE
aroF
aroB
aroC
tyrA
aroA
aroK
pheA

C_2

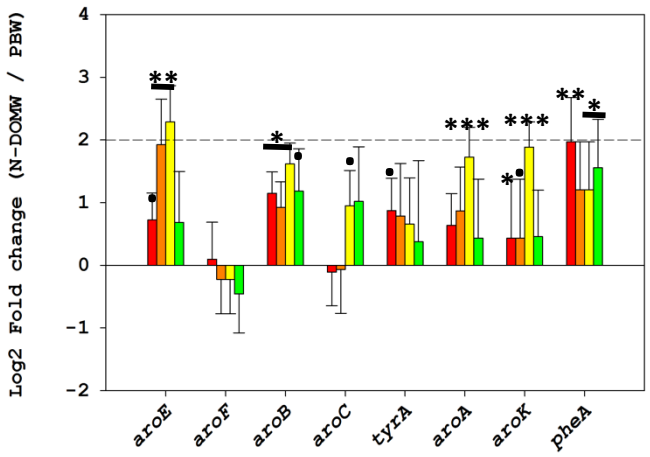
Log2 Fold change (N-DOMW / PBW)
4
3
2
1
0
−1
−2
aroE
aroF
aroB
aroC
tyrA
aroA
aroK
pheA

D_1

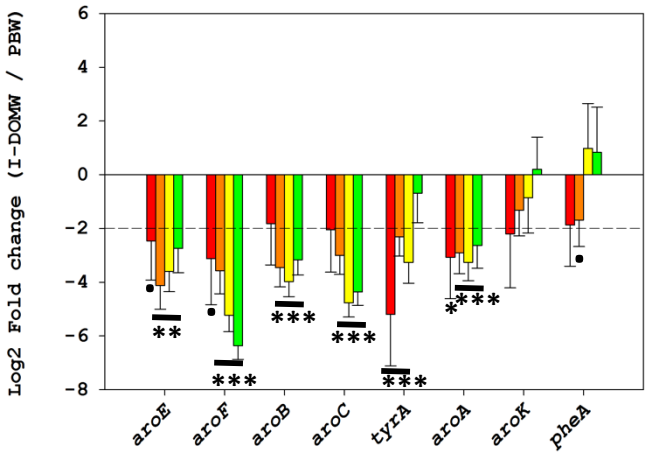
Log2 Fold change (I-DOMW / PBW)
6
4
2
0
−2
−4
−6
−8
aroE
aroF
aroB
aroC
tyrA
aroA
aroK
pheA

D_2

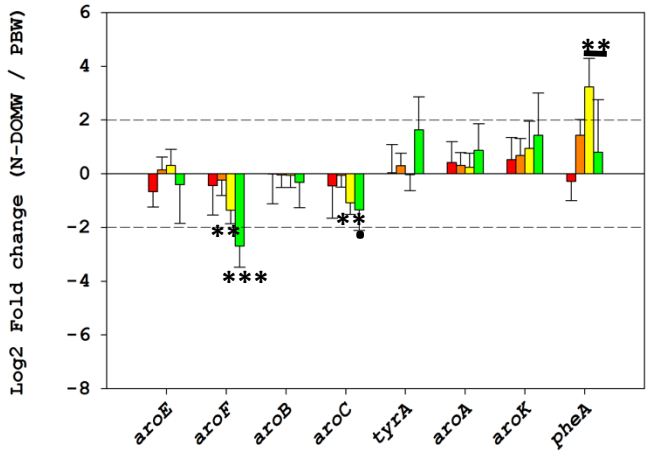
Log2 Fold change (N-DOMW / PBW)
6
4
2
0
−2
−4
−6
−8
aroE
aroF
aroB
aroC
tyrA
aroA
aroK
pheA

Figure 5S14. Fold-change of transcripts for chorismate biosynthesis in mono and co-culture experiments. (**A**) *E. coli* and **(B)** *E. faecalis* in I-DOMW compared to N-DOMW for mono-culture; **(C)** *E. coli* and **(D**) *E. faecalis* in (1) I-DOMW and (2) N-DOMW compared to PBW for co-culture.
(**P*. value ·<0.1· *<0.05, **<0.01, ***<0.001)

A

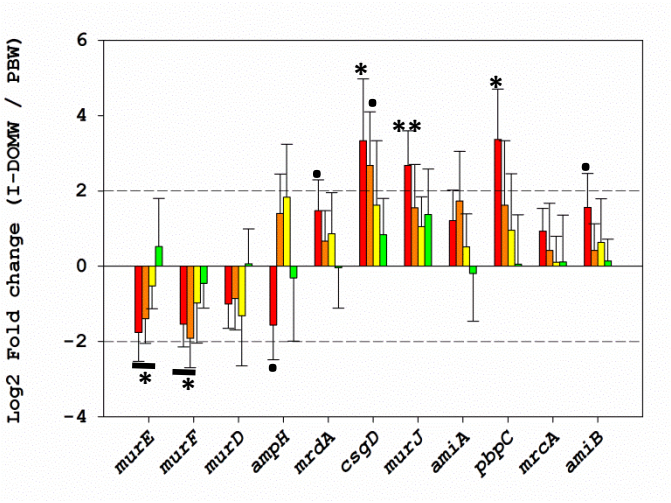
Log2 Fold change (I-DOMW / PBW)
6
4
2
0
-2
-4
murE
murF
murD
ampH
mrdA
csgD
murJ
amiA
pbpC
mrcA
amiB

B

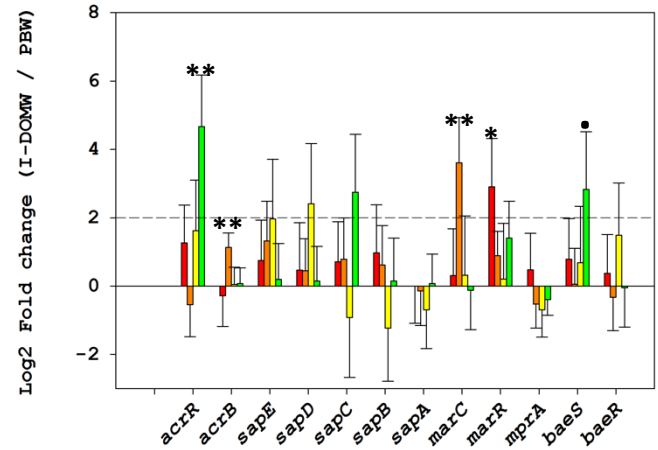
Log2 Fold change (I-DOMW / PBW)
8
6
4
2
0
-2
acrR
acrB
sapE
sapD
sapC
sapB
sapA
marC
marR
mprA
baeS
baeR

C

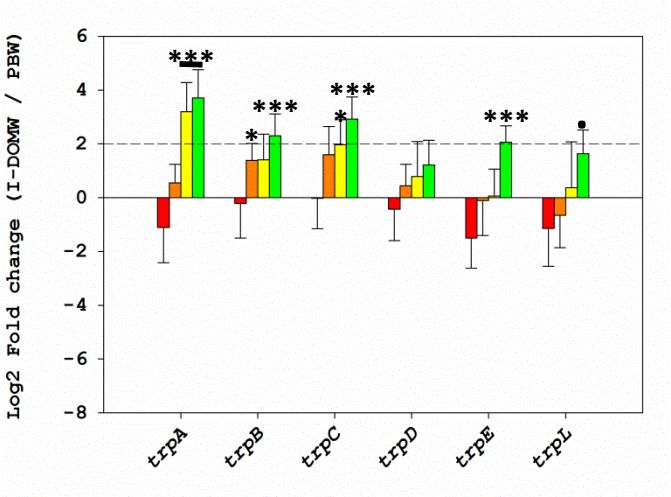
Log2 Fold change (I-DOMW / PBW)
6
4
2
0
-2
-4
-6
-8
trpA
trpB
trpC
trpD
trpE
trpL

D

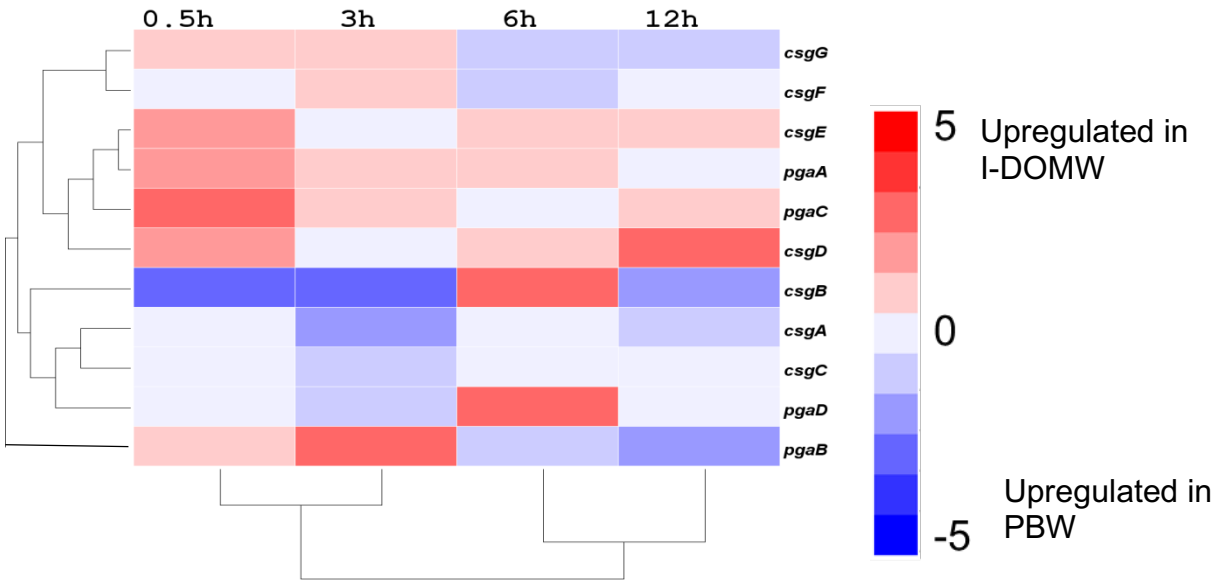

Figure 5S15. Fold-change in selected transcripts for (**A**) peptidoglycan/penicillin biosynthesis, (**B**) antimicrobial resistance/regulation and **(C**) tryptophan biosynthesis for *E. coli* in I-DOMW compared to PBW in co-culture experiment. **(D**) Heatmap for selected transcripts for biofilm formation for *E. coli* in I-DOMW compared to PBW in co-culture experiment. The color scale shows fold-change compared to PBW.

A1

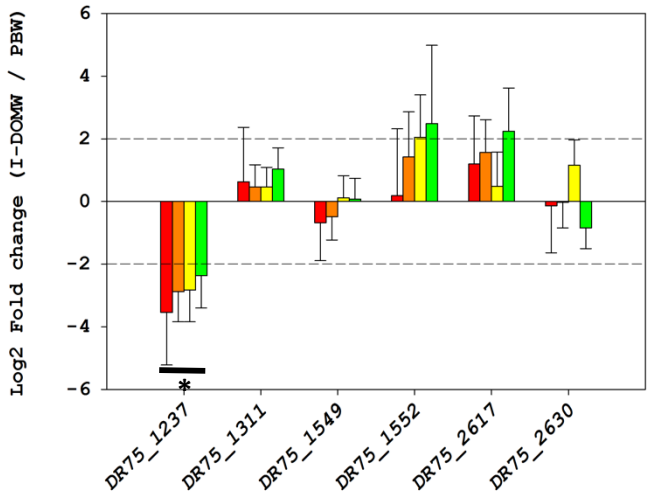
Log2 Fold change (I-DOMW / PBW)
6
4
2
0
-2
-4
-6
*
DR75_1237
DR75_1311
DR75_1549
DR75_1552
DR75_2617
DR75_2630

A2

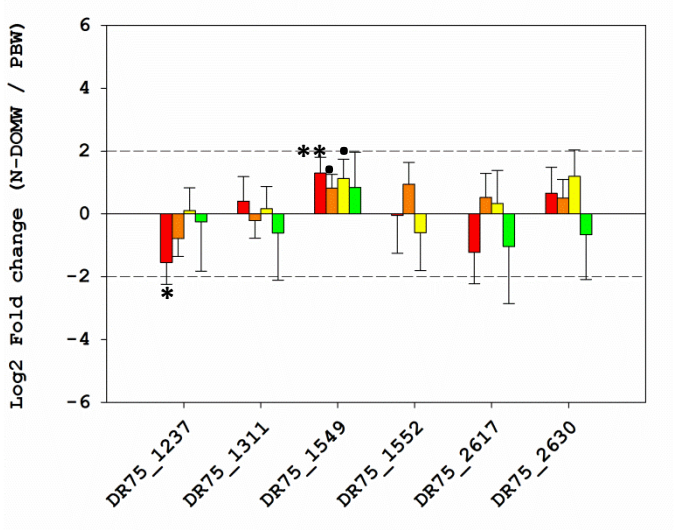
Log2 Fold change (N-DOMW / PBW)
6
4
2
0
-2
-4
-6
*
**
DR75_1237
DR75_1311
DR75_1549
DR75_1552
DR75_2617
DR75_2630

B1

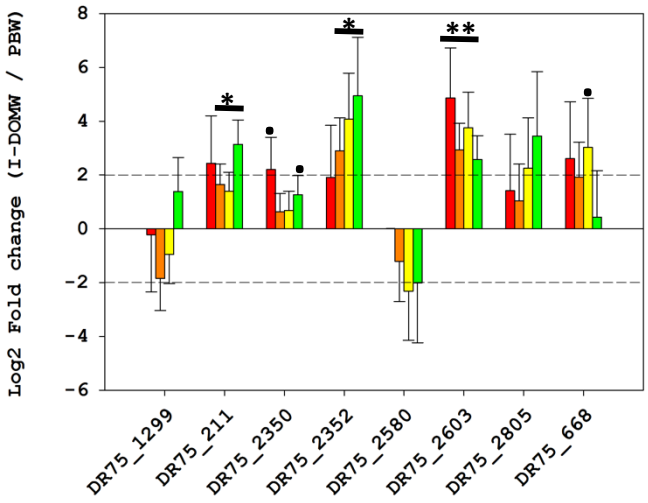
Log2 Fold change (I-DOMW / PBW)
8
6
4
2
0
-2
-4
-6
*
*
**
DR75_1299
DR75_211
DR75_2350
DR75_2352
DR75_2580
DR75_2603
DR75_2805
DR75_668

B_2

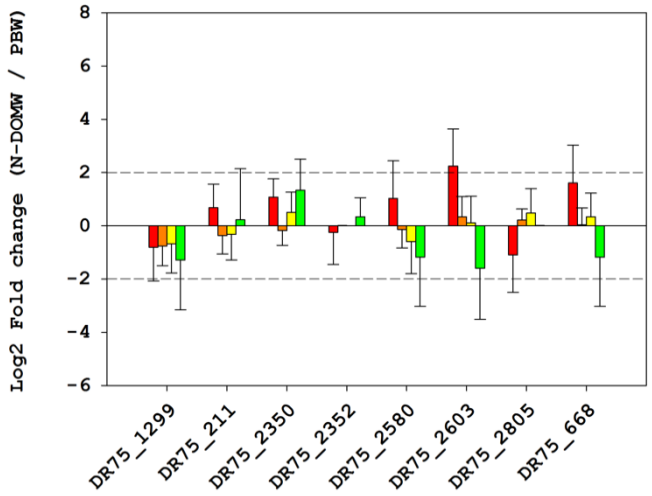
Log2 Fold change (N-DOMW / PBW)
8
6
4
2
0
-2
-4
-6
DR75_1299
DR75_211
DR75_2350
DR75_2352
DR75_2580
DR75_2603
DR75_2805
DR75_668

C_1

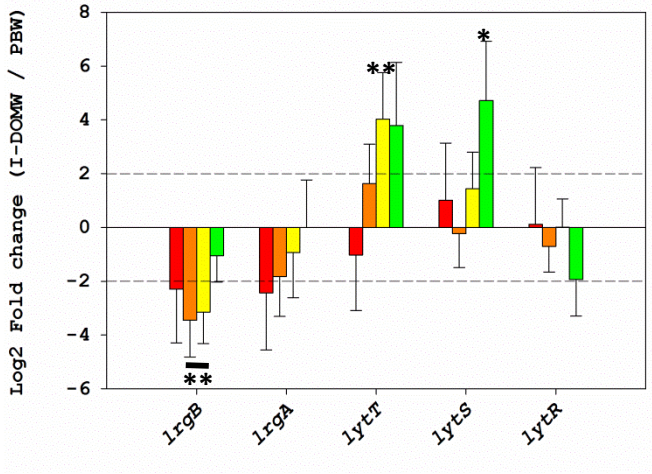
Log2 Fold change (I-DOMW / PBW)
8
6
4
2
0
-2
-4
-6
**
**
*
lrgB
lrgA
lytT
lytS
lytR

C_2

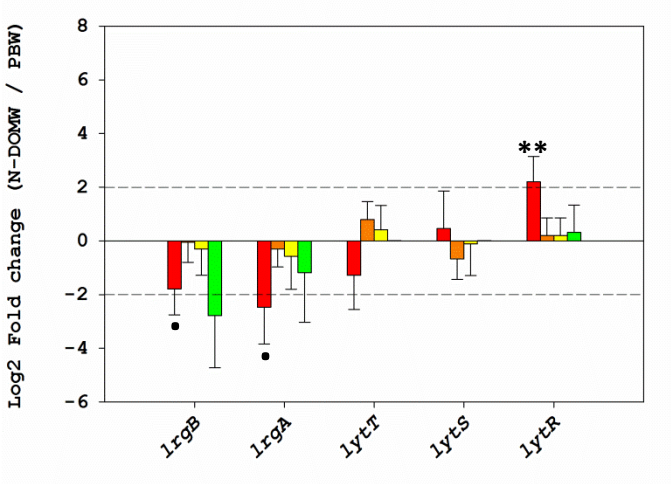
Log2 Fold change (N-DOMW / PBW)
8
6
4
2
0
-2
-4
-6
**
lrgB
lrgA
lytT
lytS
lytR

D

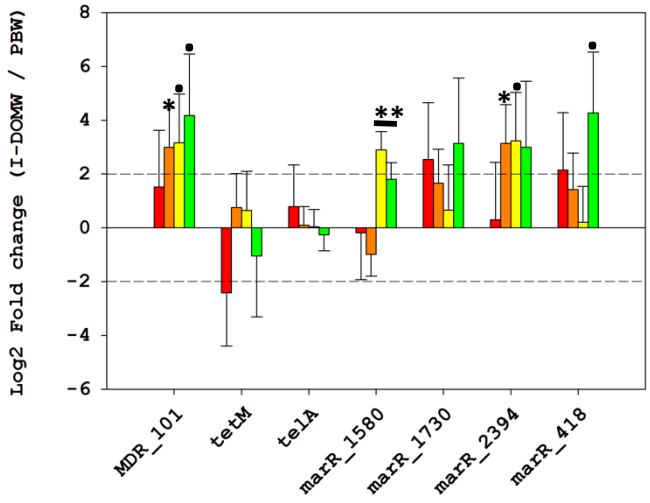

Figure 5S16. Fold-change in selected transcripts for (**A**) Peptidoglycan/penicillin biosynthesis, (**B**) Bleomycin/glyoxalases resistant and (**C**) Biofilm formation for *E. faecalis* in (1) I-DOMW and (2) N-DOMW compared to PBW in co-culture experiment. (**D**) Fold-change in selected transcripts for antimicrobial resistance/regulation in I-DOM compared to PBW for *E. faecalis*.
(**P* value ·<0.1· *<0.05, **<0.01, ***<0.001)

A_1

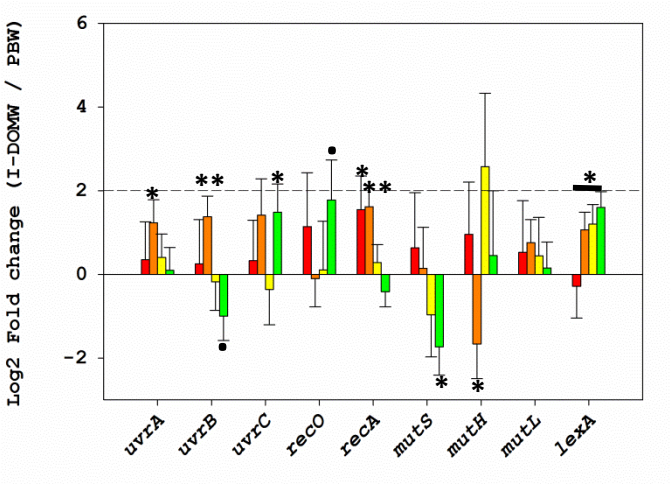
Log2 Fold change (I-DOMW / PBW)
6
4
2
0
−2
uvrA
uvrB
uvrC
recO
recA
mutS
mutH
mutL
lexA

A_2

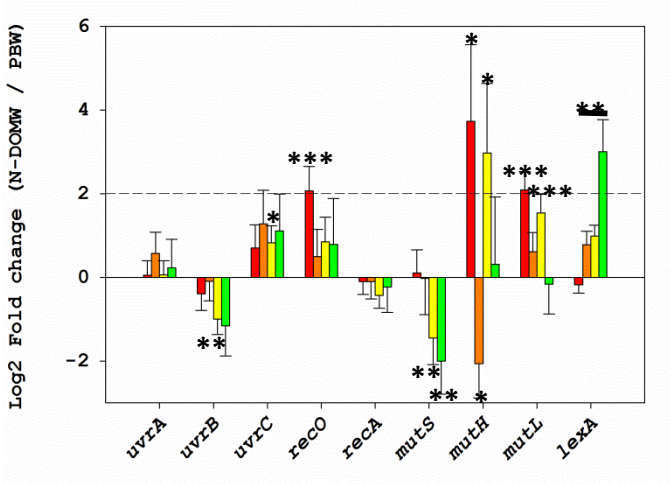
Log2 Fold change (N-DOMW / PBW)
6
4
2
0
−2
uvrA
uvrB
uvrC
recO
recA
mutS
mutH
mutL
lexA

B_1

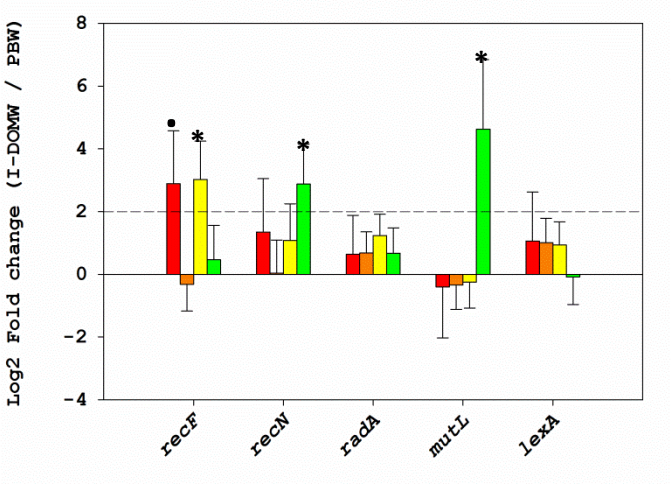
Log2 Fold change (I-DOMW / PBW)
8
6
4
2
0
−2
−4
recF
recN
radA
mutL
lexA

B_2

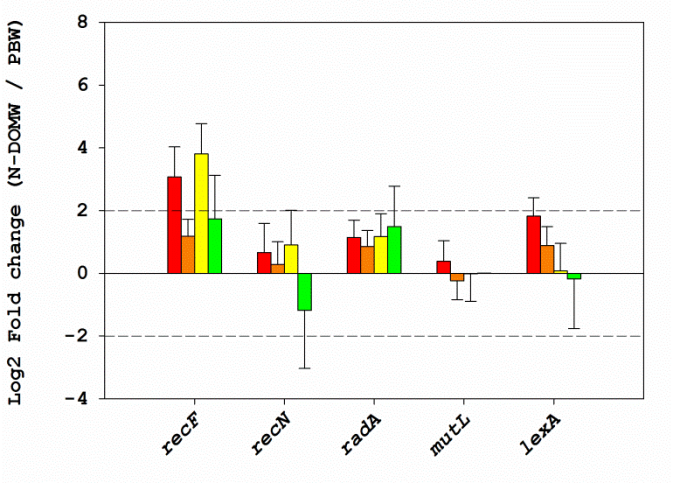

Figure 5S17: Differentially expressed DNA repair transcripts. Fold-change in selected DNA repair genes for (**A**) *E. coli* and (**B**) *Ent. feacalis* in (1) I-DOMW and N-DOMW when compared to PBW.
(**P* value ·<0.1· *<0.05, **<0.01, ***<0.001)

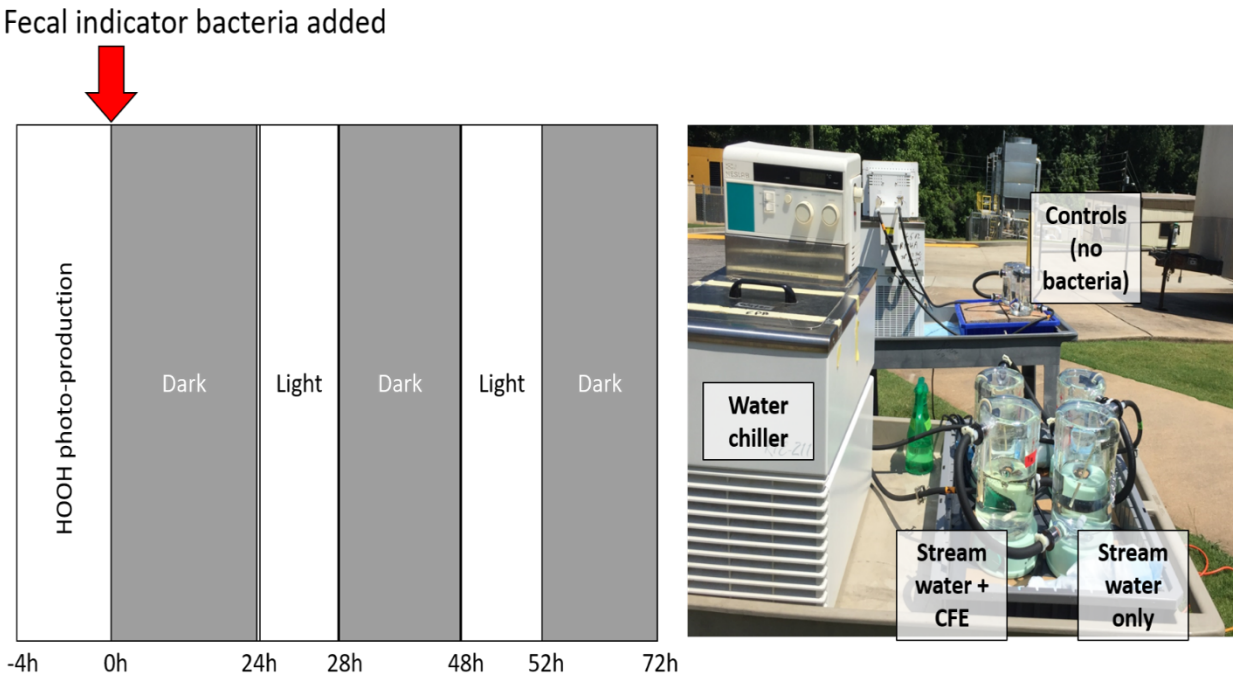

Figure 5S18: Schematic of outdoor mesocosm experiment. Filter sterilized stream water was spiked with cattle fecal extract (CFE) and exposed to natural sunlight for 4 h to initiate HOOH production prior to FIB co-culture inoculation in the dark. Following inoculation, mesocosms were incubated in the dark for 20 h before the next cycle of sunlight exposure and dark incubation.

A

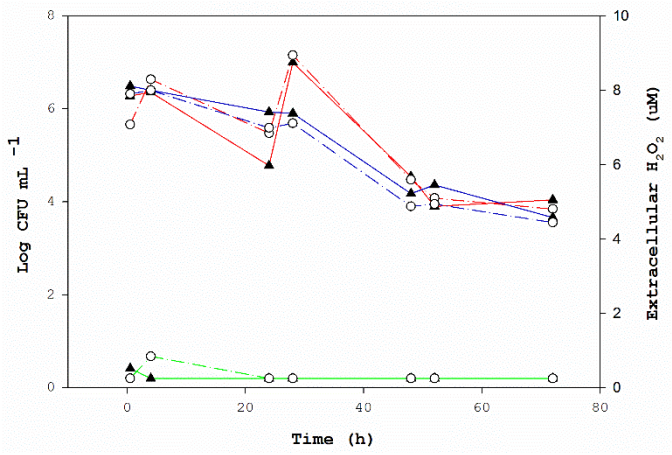
Log CFU mL -1
Extracellular H_2O_2 (uM)
Time (h)
0
20
40
60
80
0
2
4
6
8
10

B

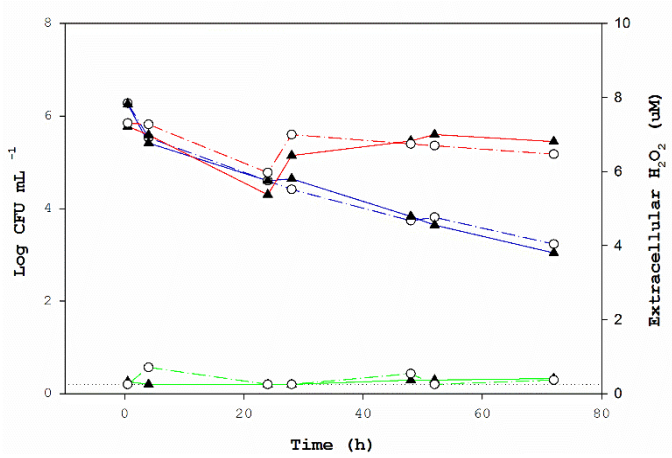
Log CFU mL -1
Extracellular H_2O_2 (uM)
Time (h)
0
20
40
60
80
0
2
4
6
8
10

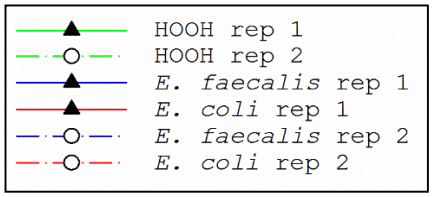
HOOH rep 1
HOOH rep 2
E. faecalis rep 1
E. coli rep 1
E. faecalis rep 2
E. coli rep 2

C

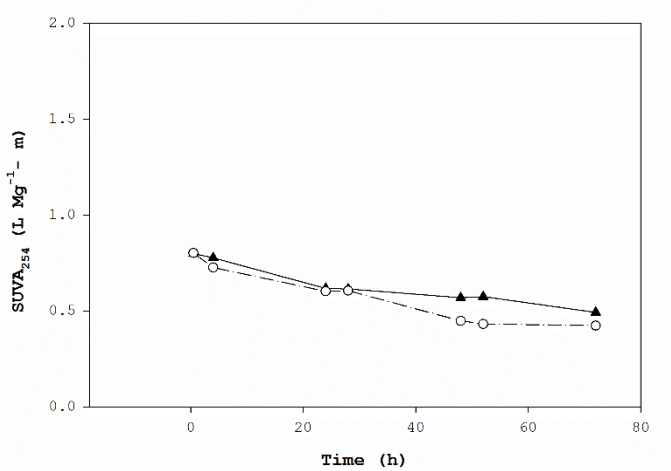

D

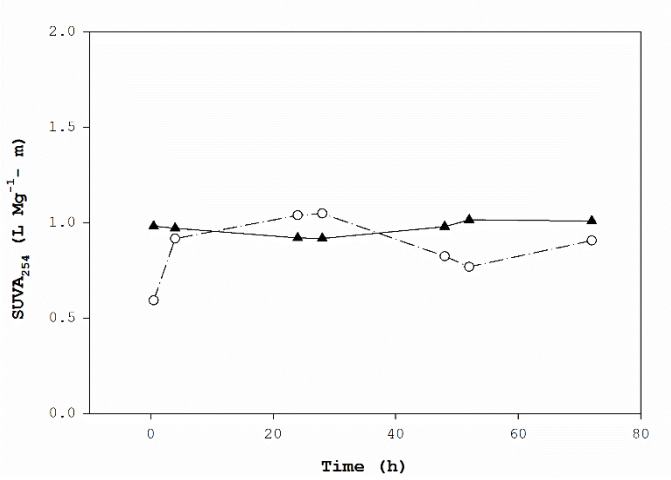

Figure 5S19: Fecal bacteria and extracellular HOOH concentration in unexposed mesocosms. Filter sterilized stream water was spiked with cattle fecal extract (CFE) and inoculated separately with a culture of *E. coli* and E. *faecalis* in mid-logarithm growth phase. Following inoculation, mesocosms were placed in an incubator shaker in the dark. Water samples were collected 0.5, 4, 24, 28, 48, 52 and 72 h for FIB concentration, extracellular HOOH, DOC, and UV-Vis measurement. (**A** and **B**) Green solid or dashed lines represent extracellular HOOH concentration in (A) DOM spiked mesocosm (no sunlight) (B) Unspiked mesocosm (unexposed control) in the presence of both *E. coli* (red solid or dashed line) and *E. faecalis* (blue solid or dashed line). Dotted black line represents HOOH method detection limit of 250nM. Concentration is reported in colony forming units (CFU) on the y- axis. (**C** and **D**) Specific Ultraviolet absorbance (SUVA) of DOM present post-inoculation, 4, 24, 28, 48, 52 and 72 h was determined by dividing their

absorption coefficient at 254nm by DOC concentration. (C) $SUVA_{254}$ (L Mg-C^{-1} m^{-1}) over time in treatment and (D) control.

A

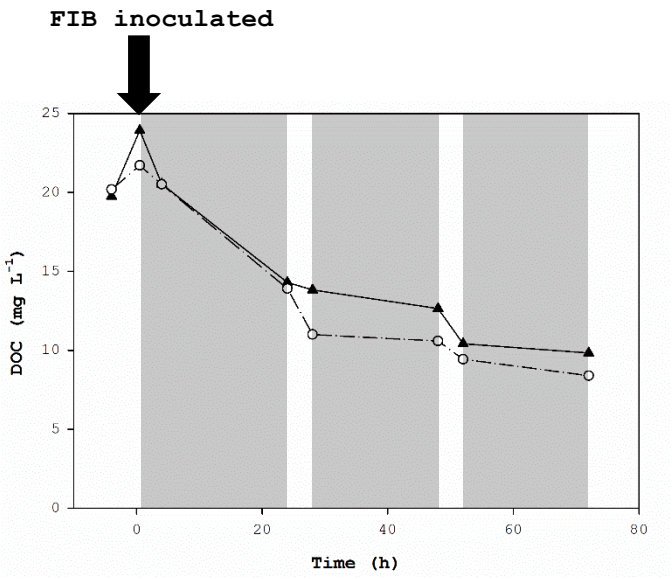

B

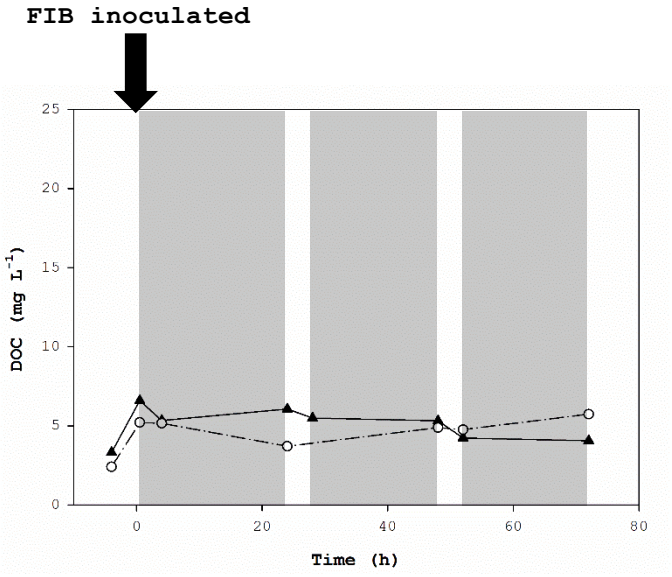

C

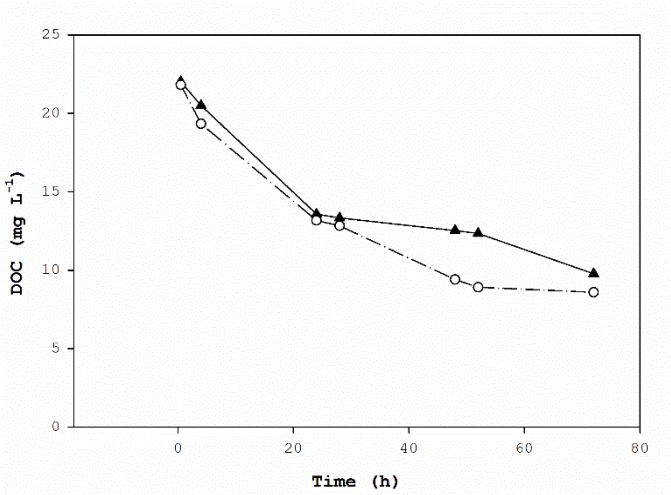

D

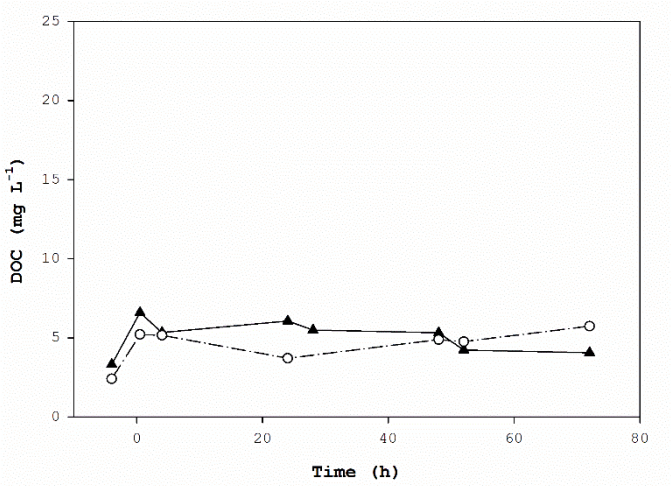

Figure 5S20. Dissolved organic carbon (DOC) concentration over time in mesocosms. (**A** and **B**) Following bacteria inoculation, exposed mesocosms were incubated in the dark for 20 h before the next cycle of sunlight exposure and dark incubation. Water samples were collected post irradiation, 0.5, 4, 24, 28, 48, 52 and 72 h and filter-sterilized before DOC determination. Grey shaded rectangles represent when the mesocosm was in the dark whereas white rectangles represent exposure to direct sunlight. DOC (mg L^{-1}) in (A) exposed treatments (B) exposed controls. DOC in (C) unexposed treatments and (D) unexposed controls was determined 0.5, 4, 24, 28, 48, 52 and 72 h.

A

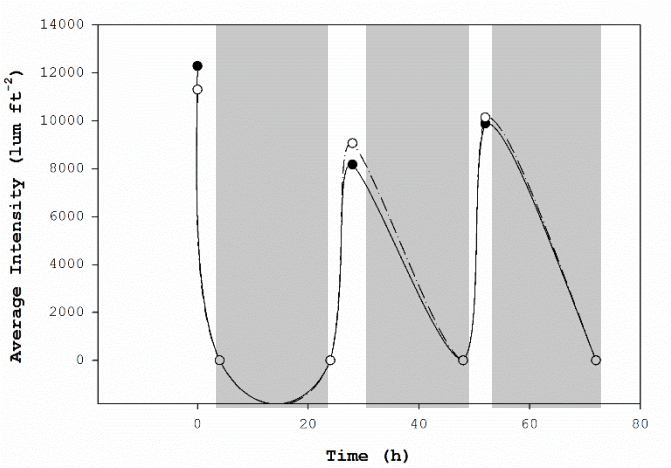

B

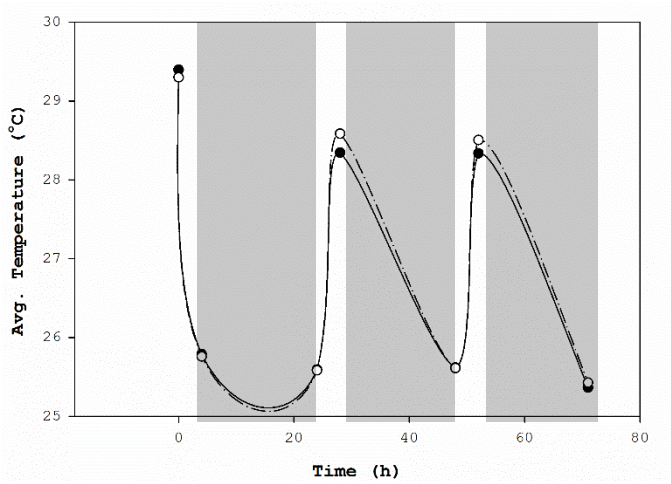

Figure 5S21. Average sunlight intensity and temperature values in exposed mesocosms. Two individual mesocosms with no bacteria inoculated was used to monitor for sunlight, temperature and extracellular HOOH. A HOBO data logger was placed in mesocosms and configured to record temperature and sunlight measurements every 15 min for 72 h. Reported are averages from each cycle of sunlight exposure or dark incubation. Solid circle represents exposed treatments and open circle represents exposed controls. Grey shaded rectangles represent when the mesocosm was in the dark whereas white rectangles represent exposure to direct sunlight (A) Sunlight intensity (lum ft $^{-2}$) and (B) Temperature (^{o}C) over time. Water samples were collected and filter-sterilized (0.22 µm) at post-irradiation, 4, 24, 28, 48, 52 and 72 h before HOOH measurement.

A

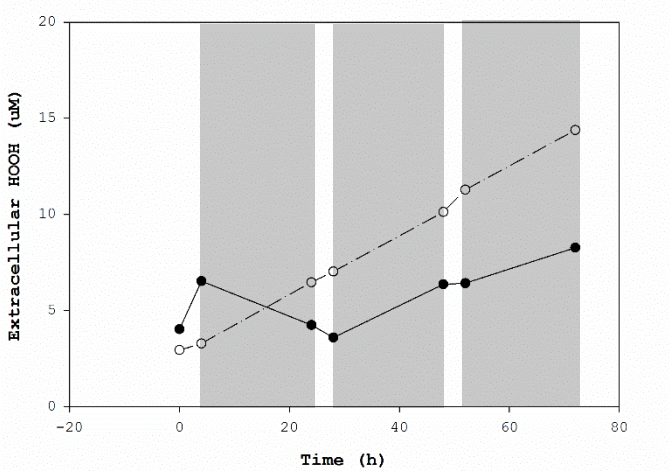

B

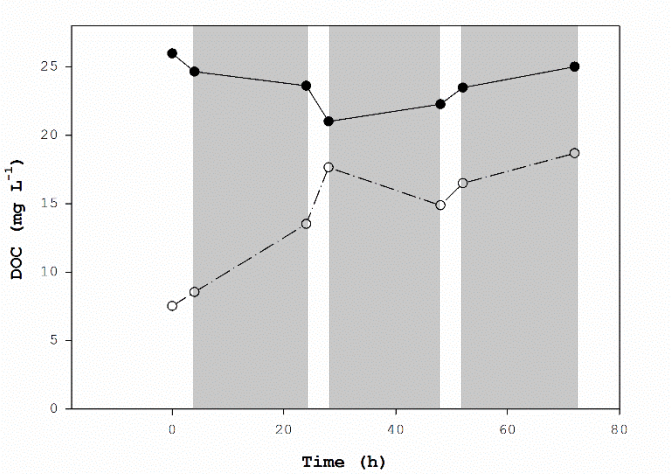

Figure 5S22. Extracellular HOOH and DOC concentration in the absence of bacteria. For HOOH and DOC measurements, we employed the same mesocosms used for determining temperature and sunlight intensity. Water samples were collected and filter-sterilized at post-irradiation, 4, 24, 28, 48, 52 and 72 h before HOOH or DOC measurement. Solid circle represents exposed treatments and open circle represents exposed controls. Grey shaded rectangles represent when the mesocosm was in the dark whereas white rectangles represent exposure to direct sunlight. Reported are averages of 3 measurements per time point. Dashed horizontal line represents HOOH method detection limit of 250nM (A) Hydrogen peroxide (μM) and (B) Dissolved organic carbon (mg L^{-1}) concentrations over time.

Table 5S1. Up-regulated genes in I-DOMW and N-DOMW compared to PBW at 0.5 h for *E. coli*

Locus Tag/Gene ID	Gene Name	Description	Function/ Role	I-DOMW Fold Change	N-DOMW Fold Change
b0073	leuB	3-isopropylmalate dehydrogenase	Oxidation catalyst	3.42	4.43
b3215	yhcA	Periplasmic chaperone protein	Cell wall organization	1.80	2.28
b0150	fhuA	Ferrichrome-iron receptor	Ferrichrome-iron ligand receptor	2.42	2.42
b1451	yncD	Probable TonB-dependent receptor	Iron-ion binding	2.83	4.30
b4290	fecB	KpLE2 phage-like element	Iron-ion transport	2.13	3.04
b4292	fecR	Protein FecR	Iron-ion transport	3.37	4.86
b1679	sufE	Cysteine desulfuration protein	Iron-sulfur cluster assembly	2.39	3.42
b3722	phoE	Outer membrane pore protein	Porin acitivity - ion transporter	2.71	4.01
b0847	ybjL	Putative transport protein	Potassium ion transporter	2.19	1.40
b2392	mntH	Divalent metal cation transporter	Membrane ion transporter	1.73	1.70
b3722	bglF	protein-N(PI)-phosphohistidine-sugar phosphotransferase	Carbohydrate transmembrane transporter	2.73	3.06
b3824	rhtB	Homoserine/homoserine lactone efflux protein	Homoserine transmembrane transporter	2.61	3.69
b3691	dgoT	D-galactonate transporter	Transmembrane transporter	2.79	5.27
b3523	yhjE	Inner membrane metabolite transport	Transmembrane transporter	2.83	5.03

		protein			
b3266	acrF	Multidrug export protein	Transporter activity	2.90	3.58
b2888	uacT	Uric acid transporter	Urate transmembrane transporter	3.36	5.38
b3006	exbB	Biopolymer transport protein	Protein stabilization and transport	3.05	4.30
b1691	ydiN	Putative MFS transporter protein	Substrate-specific membrane transporter	3.87	5.37
b0468	ybaN	Inner membrane protein	Integral membrane protein	3.06	4.60
b1353	sieB	Superinfection exclusion protein	Integral membrane component	3.61	4.88
b1828	yebQ	Transporter YebQ	Transmembrane transporter	2.82	2.15
b2308	hisQ	Histidine ABC transporter permease	Amino acid transmembrane transporter	2.26	2.73
b2019	hisG	ATP phosphoribosyltransferase	Histidine biosynthesis	3.07	4.43
b2020	hisD	Histidinol dehydrogenase	Histidine biosynthesis	2.38	1.96
b2023	hisH	Imidazole glycerol phosphate synthase	Histidine biosynthesis	2.71	2.98
b2024	hisA	N-(5'-phospho-L-ribosyl-formimino)-5-amino-1- (5'-phosphoribosyl)-4-imidazolecarboxamide isomerase	Histidine biosynthesis	3.89	5.48
b2218	rcsC	Sensor histidine kinase	Phosphorelay signal transduction system	2.50	3.14

b0674	asnB	Asparagine synthetase B	Asparagine synthesis	2.41	1.92
b0193	yaeF	Probable endopeptidase	Cysteine-type peptidase activity	2.92	4.94
b1704	aroH	3-deoxy-D-arabinoheptulosonate-7-phosphate (DAHP) synthase	Aromatic amino acid biosythesis	3.10	6.18
b3335	gspO	Type 4 prepilin-like proteins leader peptide-processing enzyme	Aspartic-type endopeptidase activity / transferase activity	2.92	4.94
b4114	eptA	Phosphoethanolamine transferase	Lipid biosynthesis	2.11	1.59
b2378	lpxP	Lipid A biosynthesis palmitoleoyltransferase	Lipid biosynthesis	3.71	4.77
b0175	cdsA	Phosphatidate cytidylyltransferase	CDP-diacylglycerol biosynthesis for Phospholipid metabolism	2.37	2.54
b3634	coaD	Phosphopantetheine adenylyltransferase	Coenzyme A biosynthesis	2.88	4.59
b2436	hemF	Oxygen-dependent coproporphyrinogen-III oxidase	Heme biosynthesis	3.20	4.65
b1047	mdoC	Glucans biosynthesis protein C	Glucan biosynthesis	3.46	3.95
b0403	malZ	Maltodextrin glucosidase	Alpha-glucan catabolic process	2.68	3.13
b1326	mpaA	Protein MpaA	Peptidoglycan catabolism	2.89	3.84
b3718	yieK	Glucosamine-6-phosphate deaminase	Carbohydrate metabolism/ N-acetylglucosamine catabolism	2.48	1.58
b1022	pgaC	Poly-beta-1,6-N-acetyl-D-	Cell adhesion in	3.94	6.48

		glucosamine synthase	biofilm formation		
b1024	pgaA	Poly-beta-1,6-N-acetyl-D-glucosamine export protein	Single species biofilm formation	2.91	4.73
b0461	tomB	Hha toxicity modulator	Attenuates Hha toxicity and regulates biofilm formation	2.36	2.42
b3717	cbrC	UPF0167 protein	Bacteriocin immunity	2.88	5.24
b0593	entC	Isochorismate synthase	Biosynthesis of the siderophore enterobactin	2.83	4.02
b0315	yahA	Cyclic di-GMP phosphodiesterase	Regulation of transcription	3.46	3.80
b0327	yahM	Uncharacterized protein	Control of transcriptional elongation	3.81	6.66
b0990	cspG	Cold shock-like protein	DNA-templated transcription regulation	2.18	1.46
b1594	mlc	Protein mlc	Transcriptional repression	2.58	2.67
b1916	sdiA	Regulatory protein SdiA	DNA-templated transcription regulation	3.12	5.01
b1987	cbl	HTH-type transcriptional regulator	DNA-templated transcription factor	2.17	1.97
b2364	dsdC	HTH-type transcriptional regulator	Transcription, DNA-templated	3.17	5.65
b4178	nsrR	HTH-type transcriptional repressor	DNA-templated transcription factor	2.99	5.31
b3170	rimP	Ribosome maturation factor	Ribosomal small subunit assembly	3.36	4.43
b3252	csrD	RNase E specificity factor	Regulation of RNA	2.85	4.46

			metabolism		
b1374	pinR	Putative DNA-invertase	DNA integration	3.68	4.38
b1403	insC2	Transposase InsC	DNA-mediated transposition	2.81	3.49
b2861	insC4	Transposase InsC for insertion element IS2H	DNA-mediated transposition	3.80	4.11
b3484	yhhI	H repeat-associated protein	DNA-mediated transposition	2.40	2.02
b3557	insJ	IS150 transposase A	Sequence-specific DNA binding	2.34	3.67
b3558	insK	Transposase InsK	DNA integration and transposition	3.36	6.65
b2698	recX	Regulatory protein	DNA repair	2.84	1.67
b3149	diaA	DnaA initiator-associating protein	DNA-dependent DNA relication initiation	2.02	1.06
b0457	ylaB	YlaB protein	Cyclic-guanylate-specific phosphodiesterase activity	2.98	4.57
b2420	yfeS	WGR domain protein	Unknown	1.98	2.43
b1191	cvrA	K(+)/H(+) antiporter NhaP2	Cell volume homeostasis	2.82	3.48
b0245	ykfI	Toxin ykfI	Negative regulation of cell growth	3.32	6.30
b4043	lexA	LexA repressor	SOS response repressor	3.27	4.13
b0459	maa	Maltose O-acetyltransferase	Maltose acetylation	3.21	3.96
b1546	tfaQ	Qin prophage	Phage lambda tail fiber assembly	4.25	6.99
b2583	yfiP	DTW domain-containing protein	Unknown	2.69	2.27

b3944	yijF	DUF1287 family protein	Unknown	3.36	5.32
b4536	yobH	Uncharacterized protein	Unknown	4.39	5.04
b0279	yagM	CP4-6 putative prophage remnant	Unknown	3.39	4.24
b1666	valW	tRNA-Val	Aminoacyl-tRNA biosynthesis	2.38	3.42

Table 5S2. Up-regulated genes in I-DOMW and N-DOMW compared to PBW at 0.5 h for *E. faecalis*

Locus Tag/Gene ID	Gene Name/locus tag	Description	Function/ Role	I-DOMW Fold Change	N-DOMW Fold Change
DR75_516	EF_1513	Pheromone binding protein	Oligopeptide transport	5.03	5.55
DR75_2107	EF_0063	Pheromone binding protein, putative	Oligopeptide transport	5.15	5.49
DR75_2649	EF_1789	SPFH domain/Band 7 family protein	Transmembrane transport	4.54	3.74
DR75_784	DR75_784	SPFH domain / Band 7 family protein	Membrane protein	4.00	3.16
DR75_1405	EF_2708	Membrane protein, putative	Integral membrane component	4.06	2.71
DR75_2844	EF_0908	Uncharacterized	Integral membrane component	5.28	4.15
DR75_190	EF_1118	ABC transporter permease	Amino Acid Transport	5.55	3.90
DR75_1819	EF_3107	Peptide ABC transporter permease	Transporter	3.02	2.25
DR75_1822	EF_3110	Peptide ABC transporter ATP-binding protein	Peptide transport	2.98	2.60
DR75_514	EF_1511	Hydrophobic dipeptide epimerase	Amino Acid catabolism	4.73	5.45
DR75_2829	EF_0891	Aspartate aminotransferase	Oxaloacetate formation/ biosythetic process	5.10	3.51
DR75_893	glpF	glycerol uptake facilitator protein	Transporter	4.91	5.73

DR75_1034	EF_2203	TetR family transcriptional regulator	DNA-templated transcription regulation	3.03	2.87
DR75_1403	recX	Recombination regulator RecX	DNA strand exchange inhibitor	4.34	3.01
DR75_2372	EF_0379	Death-on-curing family protein	Toxin	4.41	3.01
DR75_1948	DR75_1948	TA system MazF toxin	Toxin	3.96	3.20
DR75_1949	DR75_1948	TA system MazE anti-toxin	Antitoxin	2.99	2.21
DR75_1399	EF_2701	Acetyltransferase, GNAT family	N-acetyltransferase activity	4.00	2.89
DR75_1292	EF_2583	HTH domain protein	DNA binding	5.82	3.64
DR75_2907	DR75_2907	CobQ/CobB/MinD/ParA nucleotide binding domain protein	Plasmid partitioning	4.99	3.28
DR75_898	EF_1933	Uncharacterized	Unknown	4.73	3.04

Table 5S3: Number of differentially expressed genes between DOMW and PBW treatment for co-culture experiment (*P*. value < 0.05).

Bacteria	Time (h)	I-DOMW / PBW	PBW / I-DOMW	N-DOMW / PBW	PBW/N-DOMW
E. coli	0.5	93	130	1082	533
	3	478	280	369	294
	6	242	351	740	577
	12	569	441	597	354
Total		**1,382**	**802**	**2,788**	**1,758**
E. faecalis	0.5	48	24	168	38
	3	97	105	46	18
	6	173	146	54	53
	12	338	167	42	46
Total		**656**	**442**	**310**	**155**

Table 5S4: Number of differentially expressed genes between l-DOMW and N-DOMW for mono-culture and co-culture experiments (*P*. value < 0.05).

Bacteria	Time (h)	l-DOMW / N-DOMW mono-culture	l-DOMW / N-DOMW co-culture	N-DOMW / l-DOMW mono-culture	N-DOMW / l-DOMW co-culture
E. coli	0.5	134	267	190	678
	3	ND	242	ND	355
	6	41	216	56	160
	12	50	117	18	410
	24	3	ND	2	ND
E. faecalis	0.5	36	72	21	170
	3	ND	180	ND	211
	6	213	164	229	180
	12	66	161	77	96
	24	25	ND	28	ND

ND= Not determined

Table 5S5. Growth rate comparison between *E. coli* and *E.faecalis*

Bacteria	Experiment	Treatment	Starting inoculum concentration (~CFU mL^{-1})	Growth rate (hr-1)	Maximum growth (LogCFU mL^{-1})
E. coli	Monoculture	I-DOMW	10^3	0.293	7.49
	Co-culture*	I-DOMW	10^4	0.274	6.94
	Monoculture	N-DOMW	10^3	0.235	7.30
	Co-culture	N-DOMW	10^4	0.276	7.25
	Monoculture	I-DOMW	10^6	0.135	7.56
	Co-culture	I-DOMW	10^6	0.141	6.94
	Monoculture	N-DOMW	10^6	0.167	7.49
	Co-culture	N-DOMW	10^6	0.390	7.05
E. faecalis	Monoculture	I-DOMW	10^3	0.089	5.31
	Co-culture	I-DOMW	10^4	0.172	5.95
	Monoculture	N-DOMW	10^3	0.279	6.29
	Co-culture*	N-DOMW	10^4	0.325	4.20
	Monoculture*	I-DOMW	10^6	0.03	6.55
	Co-culture	I-DOMW	10^6	SS	ND
	Monoculture	N-DOMW	10^6	SS	ND
	Co-culture*	N-DOMW	10^6	0.07	6.33

** Die-off was observed before growth started.*

SS = Steady state

CHAPTER 6

CONCLUSION

This work shows that *E. coli* and Enterococci differ in their survival and growth dynamics when exposed to photo-produced HOOH or when in competition with each other. More importantly, I demonstrate that this relationship is at times, exploitative and beneficial to both organisms. Further, we show that agriculturally derived DOM from cattle feces played an important role in their social behavior which poses several implications from a water quality monitoring perspective. These findings suggest that the behavior of FIB could differ in surface waters depending on the concentration of DOM present and its potential transformations in the presence of sunlight. *E. coli* demonstrated that it can grow under both high and low DOM inputs, which may suggest a potential for regrowth upon entry into eutrophic or meso-oligotrophic surface waters. On the other hand, *Ent. faecalis* regrowth potential may be limited to only eutrophic environments. In addition, the interacting role of sunlight from the production of exogenous HOOH from DOM photodegradation may further confound this dynamic. Our results suggests that while *E. coli* has a mechanism to efficiently scavenge exogenous HOOH, *E. faecalis* produces HOOH from glycerol metabolism, and struggles under toxic concentrations. Consequently, this could result in a overall limited regrowth potential for *Ent. faecalis* in ROS dominated water.